From the Institute for Anatomy I
at Heinrich Heine University Düsseldorf

Multimodal MRI, Lifestyle, and Cognition in Aging: Mechanisms and Predictive Models

Dissertation

to obtain the academic title of “Doctor of Philosophy” (PhD) in Medical Sciences
from the Faculty of Medicine at Heinrich Heine University Düsseldorf

submitted by

Mingxian Zhang

(2026)

As an inaugural dissertation printed by permission of the

Faculty of Medicine at Heinrich Heine University Düsseldorf

signed:

Dean: Prof. Dr. med. Nikolaj Klöcker

Examiners: Prof. Dr. Dr. Svenja Caspers, Prof. Dr. Nico Dragano

In memory of my grandmother, and to the uniqueness of every human mind.

Sections of this dissertation have been published in:

Zhang, M., Moebus, S., Dragano, N., Bittner, N., & Caspers, S. (2025). Linking individual variability of multi-modal connectivity, lifestyle, psycho-social factors and cognition in older adults. *Aging and Disease, 17*(5). https://doi.org/10.14336/AD.2025.0428.

Summary (German)

Kognitives Altern ist durch eine erhebliche interindividuelle Variabilität gekennzeichnet, die sich in Unterschieden der Hirnorganisation sowie gesundheitsbezogenen und psychosozialen Faktoren widerspiegelt. Diese Dissertation untersucht systematisch die Zusammenhänge zwischen Gehirnmerkmalen, Lebensstil-/psychosozialen Faktoren und Kognition in drei komplementären Studien, die Assoziation, Mechanismus und Vorhersage adressieren.

Die erste Studie untersuchte, wie interindividuelle Variabilität (inter-IV) der strukturellen (SC) und funktionellen Konnektivität (FC) mit Lebensstil-/psychosozialen Faktoren und kognitiver Leistung bei älteren Erwachsenen zusammenhängt. Die Ergebnisse zeigten, dass eine höhere inter-IV der Konnektivität mit ungesünderen Lebensstilmustern und geringerer kognitiver Leistung – einschließlich episodischem Gedächtnis und exekutiver Kontrolle – assoziiert war, wobei sich unterschiedliche Muster über das Altersspektrum hinweg zeigten, was mit der revidierten Scaffolding Theory of Aging and Cognition (STAC-r) vereinbar ist. Aufbauend auf diesen Befunden prüfte die zweite Studie, ob inter- und intraindividuelle Variabilität (inter- und intra-IV) den Zusammenhang zwischen der Segregation von Hirnnetzwerken und exekutiver Kontrolle vermittelt. Indirekte Effekte unter Einbezug von inter-IV variierten über Netzwerke hinweg und in Abhängigkeit vom Alter, insbesondere in der strukturellen Konnektivität, während intra-IV in der funktionellen Konnektivität schwächere und stärker netzwerkspezifische Zusammenhänge aufwies. Diese Befunde präzisieren unser Verständnis der Netzwerkreorganisation im Alter und sind grundsätzlich mit der Dedifferenzierungshypothese der Alterung vereinbar. Die dritte Studie untersuchte, ob Gehirnmerkmale, die kombinierte Lebensstil- und psychosoziale Muster abbilden, die Vorhersage kognitiver Leistung verbessern. Modelle, die mehrere solcher Faktoren integrierten, übertrafen solche mit einzelnen Faktoren, blieben jedoch hinter einem vollständig datengetriebenen auf einer Hauptkomponentenanalyse basierenden Modell zurück. Dies deutet auf einen moderaten prädiktiven Mehrwert, der extern validiert werden muss, hin.

Aus der Perspektive individueller Unterschiede entwickeln diese Studien gemeinsam ein kohärentes Rahmenkonzept zur Verknüpfung neuronaler, nicht-neuronaler und kognitiver Faktoren und legen ein vorläufiges Modell zur Vorhersage spezifischer kognitiver Funktionen vor, das Ansatzpunkte für zukünftige Forschung zur personalisierten kognitiven Gesundheit bietet.

Summary (English)

Cognitive aging is characterized by substantial individual variability, reflected in differences in brain organization as well as health-related and psychosocial factors. This dissertation systematically examines the relationships among brain characteristics, lifestyle/psychosocial factors, and cognition through three complementary studies addressing association, mechanism, and prediction.

The first study examined how inter-individual variability (inter-IV) in structural (SC) and functional connectivity (FC) relates to lifestyle/psychosocial factors and cognitive performance in older adults. Results showed that greater inter-IV of connectivity is associated with less healthy lifestyle patterns and poorer cognitive performance, including episodic memory and executive control, with distinct patterns across age subgroups, supporting the Scaffolding Theory of Aging and Cognition – revised (STAC-r). Building on these findings, the second study investigated whether inter- and intra-individual variability (inter- and intra-IV) mediate the relationship between large-scale network segregation and executive control. Indirect effects involving inter-IV were not uniform across networks and varied as a function of age within the sample, particularly in structural connectivity, whereas intra-IV exhibited weak and network-restricted associations in functional connectivity. These findings refine our understanding of age-related network reorganization and are broadly consistent with the Dedifferentiation Hypothesis. The third study evaluated whether MRI features reflecting composite lifestyle and psychosocial patterns improve the prediction of cognitive performance. We found that brain models incorporating multiple such factors outperformed brain features based solely on the effects of individual factors but did not surpass a fully data-driven model that reduces brain features using principal component analysis. This suggests that integrating diverse lifestyle and psychosocial information and multimodal brain features yields modest predictive value and requires external validation.

From the perspective of individual differences, these studies collectively construct a coherent framework linking multiple factors, including brain, non-brain, and cognitive factors, while preliminarily establishing an integrated model for predicting specific cognitive functions, and provide important insights for future personalized cognitive health research.

Table of contents

List of abbreviations

AD	Axial diffusivity
ALC	Alcohol consumption
ANCOVA	Analysis of covariance
APMs	Anisotropic power maps
AROMA	Automatic removal of motion artifacts
Asso	Association fiber tract
BF-Life$_{multi}$	Multiple lifestyle-informed brain features
BF-Life$_{single}$	Single lifestyle-informed brain features
BOLD	Blood oxygen level dependent
BS	Brainstem fiber tract
CAT	Computational anatomy toolbox
Cereb	Cerebellar network
CI	Confidence intervals
Comm	Commissural fiber tract
CSD	Constrained spherical deconvolution
CT	Cortical thickness
DAN	Dorsal attention network
DBI	Davies–Bouldin Index
DMN	Default mode network
DWI	Diffusion weighted imaging
+dem	Includes demographic data
+dem+life	Includes demographic and lifestyle data
ENR	Elastic net regression
EPI	Gradient-echo planar imaging
FA	Fractional anisotropy
FC	Functional connectivity
FDR	False discovery rate
FoV	Field of view
FPN	Frontoparietal control network
GMV	Gray matter volume
ICVF	Intracellular volume fraction
inter-IV	Inter-individual variability
intra-IV	Intra-individual variability
k	Number of clusters
Lasso	Least absolute shrinkage and selection operator
LIN	Limbic network
LOOCV	Leave-one-out cross-validation
LV	Latent variable
MAE	Mean absolute error
MD	Mean diffusivity
MET	Metabolic equivalent of the task
ML	Machine learning
MNI	Montreal neurological institute coordinate system
MPRAGE	Magnetization-prepared rapid acquisition gradient-echo
MRI	Magnetic resonance imaging
NODDI	Neurite orientation dispersion and density imaging
net FC	Network-wise functional connectivity metrics
node FC	Node-wise functional segregation
ODI	Orientation dispersion index
PA	Physical activity
PCA	Principal component analysis
PLSC	Partial least squares correlation
Proj	Projection fiber tract
R^2	Coefficient of determination
RD	Radial diffusivity
Ridge	Ridge regression
RVRlin	Relevance vector regression with linear kernel
SA	Surface area
SAN	Salience/ventral attention network
SC	Structural connectivity
SD	Standard deviation
SI	Social integration
SMN	Somatomotor network
SMO	Smoking
Sub	Subcortical network
SVRrbf	Support vector regression with radial basis function kernel
TE	Echo time
TMT	Trail Making Test
TPMs	Tissue probability maps
TR	Repetition time
VIN	Visual network
WM	Working memory

Chapter 1: Introduction

1.1 General Background

With the global population aging rapidly, understanding the neural mechanisms underlying brain and cognitive aging has become a major scientific and societal challenge. A key challenge in this field lies in the pronounced individual differences observed in cognitive and brain aging: older adults differ substantially in how their brains change structurally and functionally, and in how these changes relate to cognitive performance. Evidence suggests that age-related differences in brain structure and function, as well as cognition, do not follow a uniform pattern but instead vary widely across individuals, yet the factors contributing to this heterogeneity remain incompletely understood (Cox, 2024; Perez et al., 2025).

Neuroimaging studies across adulthood have demonstrated that cognitive performance is associated with age-related differences in gray matter morphology, white matter microstructure (e.g., fractional anisotropy and neurite density), and functional connectivity (FC) (Groh & Simons, 2025; MacDonald & Pike, 2021; Ranasinghe & Mapa, 2024). In parallel, research adopting a brain network and graph theory perspective has shown that aging is accompanied by large-scale reorganization of functional brain networks, including increased communication between brain networks, and decreased network segregation, reflecting reduced functional specialization within networks and greater integration across networks, which are in turn related to cognitive performance (Nolin et al., 2025; Stumme et al., 2020). Despite these advances, much of the existing literature remains modality-specific, with structural, diffusion, and functional imaging markers often examined in isolation, thereby capturing only a subset of brain tissue properties or organizational levels (e.g., gray matter morphology and white matter microstructure). As such, unimodal approaches can provide only a partial account of individual differences in brain aging rather than capturing common or distinct representational patterns across modalities that jointly contribute to cognitive outcomes (Jirsaraie et al., 2023). A multimodal brain network perspective, which integrates complementary information from different imaging modalities, therefore offers a promising framework for characterizing heterogeneity in brain aging and cognitive outcomes.

Importantly, individual differences in multimodal brain organization are not only driven by demographic or genetic factors but may also be influenced by interactions between complex environmental factors and modifiable life-course experiences. Lifestyle factors, such as physical, cognitive, and social engagement, have been associated with brain connectivity and structural integrity in older adults (Anaturk et al., 2018; Rolls et al., 2023). Although these influences are typically smaller than those attributable to age or genetics, lifestyle factors represent modifiable influences that may be associated with cumulative or interactive effects on brain aging trajectories. As such, they offer a potential explanatory framework for understanding how individuals of similar chronological age may exhibit markedly different brain and cognitive outcomes.

Despite growing evidence linking lifestyle factors to brain structure and function, most related research remains confined to specific modalities and is fragmented. Few studies have integrated lifestyle with multimodal neuroimaging biomarkers within an integrative framework. Consequently, it remains unclear how individual differences in structural and functional connectivity jointly relate to lifestyle factors and cognitive performance, and how these individual differences are associated with large-scale network reorganization. Moreover, it remains to be determined whether integrating lifestyle information and multimodal brain features can improve the prediction of cognitive outcomes.

Addressing these gaps, the present dissertation systematically investigates how lifestyle factors and individual differences in multimodal neuroimaging markers relate to cognitive aging. To provide a theoretical foundation for these investigations, Chapter 1.2 reviews major theoretical models of cognitive aging that inform the study's conceptual framework.

1.2 Neurocognitive Theories of Aging and the Role of Lifestyle in the Aging Brain

Aging is accompanied by progressive structural and functional changes in the brain that contribute to declines across multiple cognitive domains. Early neurocognitive theories primarily emphasized structural deterioration. Among these, the Frontal Aging Hypothesis proposes that the prefrontal cortex (PFC) is disproportionately vulnerable to normal aging, leading to greater decline in frontal-dependent cognitive functions such as executive control (West, 1996). Complementing this regional perspective, the "first-in-last-out" (FILO) hypothesis suggests that brain regions that myelinate later in development, particularly frontal areas, tend to be more vulnerable to age-related deterioration (Wallace et al., 1980). In addition, the white matter disconnection theory posits that degeneration of long-range white matter pathways disrupts interregional communication, contributing to cognitive decline (Madden et al., 2009; O'Sullivan et al., 2001).

Structural decline is accompanied by functional reorganization, which has given rise to several influential theories of functional aging. The Neural Dedifferentiation hypothesis proposes that aging reduces neural selectivity, resulting in broader and less specialized activation patterns (Koen et al., 2020; Li et al., 2001). In addition, the Right Hemisphere Aging Hypothesis emphasizes the selective vulnerability of right-hemisphere functions, which may underlie age-related declines in visuospatial processing and attention (Brown & Jaffe, 1975; Dolcos et al., 2002). More global mechanisms have also been proposed. The General Slowing hypothesis attributes widespread deficits to age-related reductions in processing speed (Choi & Feng, 2015; Salthouse, 1996), whereas the Inhibitory Deficit theory highlights impaired suppression of task-irrelevant information, which may contribute to age-related changes in attention and working memory (Hasher & Zacks, 1988; McDowd, 1997).

Beyond decline-focused accounts, several models emphasize compensatory mechanisms that may help maintain cognitive performance in later life. The atrophy–compensation perspective posits that increased functional recruitment in remaining or contralateral regions may partially offset age-related neural loss. Within this framework, the Hemispheric Asymmetry Reduction in Older Adults (HAROLD) model describes more bilateral prefrontal recruitment in older adults during cognitive tasks (Cabeza, 2002). In contrast, the Posterior – Anterior Shift in Aging (PASA)

characterizes increased frontal activation coupled with reduced posterior activity as a potential adaptive pattern (Craik & Salthouse, 2011; Grady et al., 1994). The Compensation-Related Utilization of Neural Circuits Hypothesis (CRUNCH) further proposes that older adults progressively recruit additional neural resources as task demands rise. However, compensatory capacity may be limited under high cognitive load (Reuter-Lorenz & Cappell, 2008). Importantly, not all age-related increases in activation necessarily reflect successful compensation, as similar patterns may also arise from neural inefficiency or dedifferentiation.

Beyond task-specific compensatory models, the Cognitive Reserve (CR) Hypothesis highlights that lifetime experiences, such as education, intellectual engagement, and complex occupations, buffer the impact of brain aging on cognition without necessarily altering the rate of neural decline (Stern, 2002, 2012). Complementing these frameworks, the Scaffolding Theory of Aging (STAC) and its revision (STAC-r) conceptualize cognitive aging as a dynamic balance between age-related neural decline and compensatory scaffolding processes, with STAC-r further emphasizing that these processes are shaped by experiences accumulated across the lifespan (Goh & Park, 2009; Reuter-Lorenz & Park, 2014, 2024). Critically, STAC-r emphasizes that positive life-course experiences, including education, physical fitness, and social engagement, can strengthen neural scaffolding, whereas negative factors such as brain disease, mental illness, and toxin exposure may deplete neural resources and undermine compensatory capacity.

Within the STAC-r framework, modifiable life-course influences may differentially enrich or deplete neural resources across the lifespan (Reuter-Lorenz & Park, 2024). For example, stair climbing and higher educational attainment have been linked to younger-appearing brain age (Steffener et al., 2016), whereas smoking and high alcohol intake are associated with structural brain changes indicative of accelerated aging (Bittner et al., 2021; Topiwala et al., 2022). Psychosocial factors, such as social support and perceived social support, have also been associated with larger gray matter volumes and enhanced connectivity in key brain networks (Schurz et al., 2021; van der Velpen et al., 2022). Together, these findings suggest that modifiable lifestyle and psychosocial factors may modulate neural scaffolding and compensatory mechanisms, and may help explain individual differences in cognitive aging, though further empirical support is still needed.

To provide a structured overview, Table 1.1 summarizes the core assumptions, empirical support, strengths, and key limitations of major neurocognitive aging theories. Importantly, multiple

patterns of brain aging—including neural dedifferentiation, brain maintenance, and compensatory recruitment—can coexist within the same individual, highlighting the complexity of individual differences (McDonough et al., 2022). This complexity underscores the need for studies that examine individual variability in brain networks and their relation to cognitive outcomes, particularly with respect to modifiable lifestyle and psychosocial factors that are associated with such variability.

Table 1.1 Summary of neurocognitive aging theory.

Theory	Core assumption	Key neural evidence	Strengths	Limitations / Challenges
Frontal Lobe Hypothesis of Aging	Age-related cognitive decline arises primarily from early structural deterioration in the prefrontal cortex (PFC) (West, 1996).	Selective decline in executive functions and pronounced age-related changes in prefrontal structure, connectivity, and dopamine function (Cabeza & Dennis, 2012).	Simple and intuitive.	Age-related cognitive and neural changes extend beyond the frontal lobes, involving posterior regions and large-scale brain networks (Greenwood, 2000).
First-in-Last-out Hypothesis	Brain regions that develop later (e.g., frontal areas) are the first to decline with age (Wallace et al., 1980).	Later-myelinating white matter tracts show earlier age-related decline (Bender et al., 2016; Mendez Colmenares et al., 2023).	Matching developmental sequences with aging sequences is logically straightforward and verifiable.	White matter aging patterns are inconsistent across regions and fiber types.
White Matter Disconnection Theories	Cognitive aging is driven by declines in white matter integrity, disrupting interregional communication (O'Sullivan et al., 2001).	DTI studies show age-related decreases in fractional anisotropy, which are linked to slower processing (Bennett & Madden, 2014; Madden et al., 2009).	It attributes age-related cognitive decline to disrupted white matter connectivity, linking brain structure, function, and behavior in a unified framework.	Its explanatory power is partial, and may not account for functional compensation.
Neural Dedifferentiation Hypothesis	Aging is associated with less selective neural responses, resulting in broader cortical activation patterns (Li et al., 2001).	fMRI evidence of reduced category selectivity in older adults (Koen & Rugg, 2019; Koen et al., 2020).	Neural dedifferentiation has cross-level empirical support.	Neural dedifferentiation does not always lead to age-related cognitive decline (Koen & Rugg, 2019).
Right Hemisphere Aging Hypothesis	Right hemisphere functions (e.g., visuospatial processing) decline more with age than the left (Brown & Jaffe, 1975).	Behavioral and imaging studies have shown greater right-hemisphere vulnerability (Dolcos et al., 2002).	It provides a simple, behaviorally supported framework for hemispheric asymmetry in aging.	Empirical evidence is mixed and less consistent than that for alternative models such as HAROLD.
General Slowing Hypothesis	Age-related cognitive decline reflects a general slowing of processing speed (Salthouse, 1996).	Behavioral studies consistently show that slower processing speed in older adults mediates age-related declines across a wide range of cognitive tasks (Choi & Feng, 2015).	It can explain the age effects commonly observed across various cognitive tasks.	It lacks specificity for specific domains and cannot account for compensatory mechanisms or underlying neural changes.
Inhibitory Deficit Theory	Older adults have reduced ability to suppress irrelevant information, leading to cognitive decline (Hasher & Zacks, 1988).	Supporting evidence includes ERP indicators and behavioral Stroop scores demonstrating age-related decline in inhibition (McDowd, 1997).	It provides a mechanistic explanation for age-related increases in distractibility and working memory interference, linking inhibitory control deficits to cognitive decline.	Neuroimaging evidence for this theory is limited and inconsistent, partly because observed effects can be confounded by task demands, motor slowing, or difficulty isolating inhibition-related neural activity.
HAROLD Model	Older adults show reduced hemispheric asymmetry, recruiting both hemispheres to support tasks (Cabeza, 2002).	Bilateral PFC activation during memory tasks in older adults (Cabeza, 2002).	It provides a clear compensatory explanation for the maintenance of cognitive performance.	It is PFC-centric, neglects whole-brain and network-level aging, and relies on a limited set of memory tasks.

Posterior–Anterior Shift in Aging (PASA)	Aging brains show increased anterior and reduced posterior activity (Craik & Salthouse, 2011).	Frontal increases and occipital decreases observed in PET and fMRI studies (Ansado et al., 2013).	It is supported by robust fMRI evidence across tasks and performance correlations.	It remains unclear which cognitive processes drive this shifting; enhanced prefrontal activity may not necessarily indicate compensation, but could also reflect inefficiency or dedifferentiation.
CRUNCH Model	Older adults recruit additional neural resources as task demands increase, up to a capacity limit (Reuter-Lorenz & Cappell, 2008).	Older adults recruit additional neural resources at low to moderate task demands (Kang et al., 2021).	CRUNCH uniquely predicts load-dependent compensation, falsifiably tested via parametric designs.	It has limited empirical support, with few studies testing its predictions and some reporting effects opposite to model expectations (Jamadar, 2020).
Cognitive Reserve Hypothesis	Lifelong experiences (education, occupation) buffer cognitive decline (Stern, 2002).	Reserve proxies correlate with better outcomes despite similar pathology (Stern, 2012; Whalley et al., 2004).	Explains individual differences in aging trajectories.	CR is difficult to measure directly, relies on indirect proxies, and faces challenges in establishing causality, separating it from brain reserve, and generalizing across populations.
STAC (Scaffolding Theory of Aging and Cognition)	The brain constructs compensatory scaffolds to maintain cognitive function in response to structural and functional decline (Goh & Park, 2009).	It is supported by neuroimaging evidence of increased recruitment despite structural decline (Goh & Park, 2009).	Provides an integrative framework linking structural decline, functional changes, and compensatory plasticity to cognitive outcomes.	Conceptually broad and difficult to falsify; mechanisms need further specification.
STAC-r (Revised STAC)	Expands STAC by incorporating life-course factors (e.g., lifestyle, engagement, health) affecting both scaffolding and neural maintenance (Reuter-Lorenz & Park, 2014).	Recent neuroimaging and longitudinal lifespan data show that life-course enriching and depleting factors (e.g., education, activity levels, health) influence both neural structure and compensatory scaffolding across adulthood (Reuter-Lorenz & Park, 2024).	Integrating structural degeneration, functional compensation, behavioral manifestations, and lifestyle factors into a unified framework provides a more comprehensive approach than the original STAC model.	Reliance on indirect measures, difficulty distinguishing compensation from inefficiency, and predominance of cross-sectional evidence.

1.3 Individual Variability of Brain Connectivity and Network Reorganization in Aging

The human brain is organized as a complex network of distributed regions that interact through functional and structural connectivity (Rubinov & Sporns, 2010). Functional connectivity (FC), reflecting the temporal coordination of neural activity, is measured with techniques such as resting-state or task-based functional magnetic resonance imaging (fMRI) and Electroencephalogram (EEG), while structural connectivity (SC), indicating anatomical pathways, is typically derived from diffusion MRI tractography (Babaeeghazvini et al., 2021). Together, they provide complementary perspectives on how information is dynamically exchanged and anatomically constrained across large-scale brain networks.

In recent years, there has been a growing interest in individual differences in brain connectomes, and an increasing number of studies have begun to examine how such variability manifests in older adults and across the aging process (e.g., Huang et al., 2025; Karahan et al., 2022; Ma et al., 2021; Sun et al., 2022). Functional connectivity has been shown to vary substantially across individuals, and such differences can serve as a neural "fingerprint" for predicting cognitive performance rather than noise (Finn et al., 2015; Van Horn et al., 2008). Mueller et al. (2013) systematically mapped the spatial distribution of inter-individual variability of FC (hereafter abbreviated as inter-IV_{FC}), showing that variability in associative cortices—particularly frontal and parietal regions—substantially exceeds that in primary sensorimotor areas. This pattern has been interpreted as compatible with the idea that higher-order association networks support more flexible, experience-dependent functional organization, although the study itself did not directly examine plasticity mechanisms. Subsequent diffusion MRI studies extended this framework to SC, revealing that while inter-individual variability of SC (hereafter abbreviated as inter-IV_{SC}) is generally lower than inter-IV_{FC}, systematic differences persist across brain networks (Chamberland et al., 2017; Huang et al., 2025; Sun et al., 2022). Moreover, evidence suggests that the amount of individual differences in both functional and structural connectivity increase with age in older adults (Huang et al., 2025; Ma et al., 2021) and are associated with worse cognitive performance (Ma et al., 2021), offering novel insights into the topic of brain heterogeneity in aging research. A summary of the

literature on individual variability in brain connectivity is presented in Table 1.2.

In addition to inter-individual differences, brain heterogeneity also encompasses intra-individual variability, referring to within-person changes in neural signals or network organization across time. While short-term fluctuations in blood-oxygen-level-dependent (BOLD) signals have been linked to cognitive flexibility and processing speed (e.g., Garrett, Kovacevic, et al., 2013; Goodman et al., 2024), cognitive aging unfolds over extended periods, making long-term within-person dynamics particularly relevant. Although structural connectivity is generally more stable than functional connectivity (Nakuci et al., 2023), this difference in temporal stability raises the question of whether long-term within-person variability in both modalities contributes meaningfully to cognitive aging. Examining long-term intra-individual variability (see Figure 1.1) alongside inter-individual differences may therefore provide a more comprehensive characterization of connectivity-related heterogeneity in cognitive aging.

Individual differences in brain connectivity may be associated with variability in the extent or pattern of age-related reorganization of large-scale networks across individuals. In healthy aging, network reorganization refers to systematic changes in network architecture across the adult lifespan, both between and within individuals (Bagarinao et al., 2019; Sala-Llonch et al., 2015; Wang et al., 2022). Graph-theoretical analysis provides a useful tool to quantify the properties of brain organization, reducing high-dimensional connectome data into interpretable systems-level measures (He & Evans, 2010). Among these measures, network segregation has emerged as an important index of age-related reorganization because it captures the balance between functional specialization and cross-network integration (see Chan et al., 2014; Wang et al., 2021; see also Figure 1.1). Higher segregation indicates greater functional specialization, whereas lower segregation—network dedifferentiation—is a prominent feature of aging, particularly in higher-order networks such as the default mode, frontoparietal, and salience/ventral attention networks, and is linked to declines in executive control and processing speed (Chan et al., 2014; Chong et al., 2019; Ng et al., 2016; Nolin et al., 2025). While age-related changes in functional network connectivity have been widely reported, age-related alterations in structural network segregation remain less well understood. In youth, higher structural network segregation was observed in older compared to younger individuals, consistent with cognitive development (Baum et al., 2017). Cross-sectional evidence suggests that, from adulthood to old age, structural modularity varies nonlinearly,

with lower values in mid-to-late adulthood and higher values in late old age (Puxeddu et al., 2020). Evidence on this pattern remains inconsistent (Khalilian et al., 2024; Rodriguez-Nieto et al., 2025).

As discussed above, age-related reorganization of brain connectivity networks is closely associated with cognitive outcomes, with cognitive aging showing pronounced domain-specific heterogeneity (Deary et al., 2009; Hedden & Gabrieli, 2004; Salthouse, 2004). Among cognitive domains, executive control functions are especially sensitive to aging-related neural changes and have been frequently reported to decline with age (Harada et al., 2013; Lacreuse et al., 2020). Executive control is a higher-order construct comprising partially dissociable components, including inhibitory control, working memory updating, and set shifting (Friedman & Miyake, 2017). These executive processes rely on coordinated activity across distributed brain networks, including the frontoparietal and salience systems, and are essential for successful daily functioning (Buckner, 2004; Xia et al., 2022). Importantly, age-related cognitive decline is characterized not only by domain specificity but also by substantial inter-individual variability. While some older adults maintain relatively preserved cognitive performance, others exhibit marked decline (Harada et al., 2013). We proposed that such cognitive heterogeneity may reflect individual differences in the reorganization of brain networks during aging. In this context, lifestyle and psychosocial factors, as discussed in Section 1.2, may contribute to brain variability, and empirical evidence is needed to address this gap.

Together, these considerations motivate the first two broad lines of investigation in the present study, focusing on inter-individual differences in brain connectivity in relation to cognition and lifestyle, as well as on how such differences link brain network reorganization to executive control. To address these questions at the systems level, resting-state fMRI is particularly well suited, as it captures intrinsic whole-brain coupling independent of task performance (Shen, 2015) and provides a representation of trait-like network organization in aging populations. In parallel, diffusion MRI tractography reconstructs probabilistic interregional pathways in vivo (Zhang et al., 2022), allowing the characterization of structural network architecture within the same connectome framework as functional connectivity.

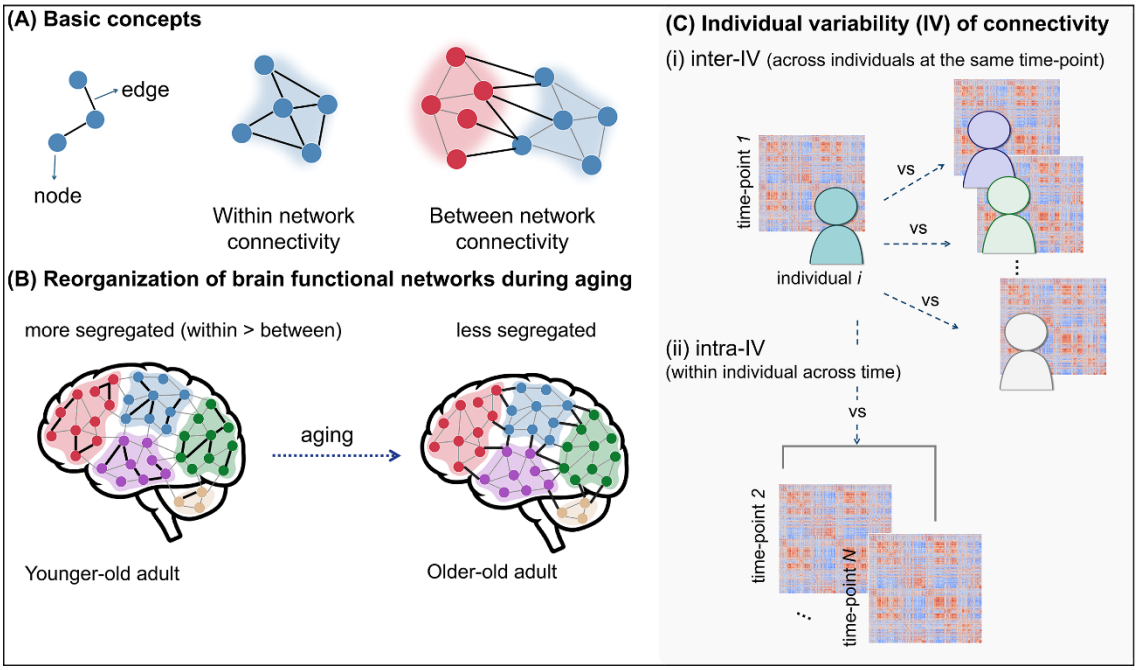

Figure 1.1 Conceptual framework of brain network, aging-related reorganization, and individual variability of brain connectivity. (A) Brain networks consist of nodes (brain regions) and edges (connections) representing functional or structural connectivity between regions. These connections can be classified as within-network or between-network. **(B)** Conceptual illustration of network segregation, reflecting the balance between within- and between-network connectivity and its age-related decrease (network dedifferentiation). **(C)** Illustrates a measurement framework for individual differences in connectivity.

Table 1.2 Literature review on research into inter-individual variability of brain connectivity.

Reference	Subjects	Age (range/mean years)	Sample size	Imaging modality	Definition of individual variability	Main findings
Mueller et al. (2013)	Healthy adults	**aged 51.8 ± 6.99 years**	*N* = 23	rs-fMRI	Inter-IV_{FC} was defined as the residual dissimilarity (1 − inter-subject correlation) of seed-based functional connectivity maps across subjects after regressing out intra-subject variance, reflecting subject-specific functional differences beyond measurement noise and within-subject fluctuations.	The inter-IV_{FC} is highest in heteromodal association cortex, which is linked to evolutionary cortical expansion, long-range connectivity, and individual differences in cognition.
Gao et al. (2014)	Infants	Birth to 2 years	*N* = 288	rs-fMRI	Similar to Mueller et al. (2013), without considering intra-individual variability.	Inter-IV_{FC} was higher in association cortices than in primary regions at birth, followed a U-shaped developmental trajectory during infancy, and showed dynamic, age-dependent genetic influences.
Chamberland et al. (2017)	Healthy young adults	21-30 years	*N* = 9	rs-fMRI dMRI	Similar to Mueller et al. (2013).	FC exhibited substantially greater inter-IV than SC, and the two were largely independent across brain regions.
Li et al. (2017)	Cognitively normal older adults	**60-80 years**	*N* = 108	rs-fMRI	Similar to Mueller et al. (2013), without considering intra-individual variability.	Inter-IV_{FC} increased from primary sensory networks to association, subcortical, and cerebellar regions, and regions with greater variability showed stronger associations with cognitive performance.
T. Xu et al. (2019)	Young adults; Rhesus macaque monkeys	Human: aged 29.03 ± 3.45 years; Monkey aged varied by cohort	Human: *n* = 177; Macaque: *n* = 2-19	rs-fMRI	Similar to Mueller et al. (2013).	Inter-IV_{FC} was lower in primary sensory and motor cortices than in association regions in awake macaques and was associated with long-distance connectivity and cortical microstructural properties.
Y. Xu et al. (2019)	Normal preterm and term infants	31.3–41.7 weeks	*N* = 40	rs-fMRI	Similar to Mueller et al. (2013), without considering intra-individual variability.	Inter-IV_{FC} emerged prenatally and resembled adult patterns, alongside age-dependent decreases in sensorimotor and visual networks and stronger distance-dependent connectivity constraints.
Stoecklein et al. (2020)	Healthy adults; Preterm-born infants	Healthy adults: aged 27.0 ± 3 0.8 years; Infants: 36.3 weeks ± 16.1 days; 37.1 weeks ± 10.2 days	Healthy adults: *n* = 25; Infants from two sites: *n* =25 & 25	rs-fMRI	Similar to Muller et al. (2013).	Inter-IV_{FC} was evident around term birth, with lower variability in unimodal regions and higher variability in association cortices; some regions showed adult-like shifts with cortical expansion and maturation.
Ma et al. (2021)	Healthy adults	**18-88 years**	*N* = 543	rs-fMRI	Similar to Mueller et al. (2013), without considering intra-individual variability.	Inter-IV_{FC} was higher in association than primary sensory cortices across adulthood, increased with age, negatively related to FC strength/number, and positively related to behavioral variability.
J. Li et al. (2021)	Young adults	Aged 23.67 ± 1.65 years	*N* = 45	rs-fMRI	Similar to Mueller et al. (2013).	White-matter FC exhibited spatially heterogeneous inter-IV, with greater variability in heteromodal regions linked to neuronal gene-expression profiles and lower variability in unimodal regions associated with glial gene-expression profiles.

L. Li et al. (2021)	Young adults	22-37 years	*N* = 339	rs-fMRI	Similar to Mueller et al. (2013) but considering intra-individual variability through linear subtraction.	Inter-IV_{FC} was highest in multimodal association cortices and lowest in unimodal and subcortical regions, and its spatial distribution was linked to human-accelerated genes and cerebral blood flow.
Sun et al. (2021)	Schizophrenia (SCZ); Healthy control (HC)	SCZ = 24.74 ± 9.03 years; HC = 26.62 ± 8.0 years	SCZ: *n* = 121 HC: *n* = 183	rs-fMRI	Similar to the study by Mueller et al. (2013). Removed intra-individual variability in validation analyses.	Schizophrenia patients showed elevated inter-IV_{FC} across sensorimotor, visual, auditory, and subcortical regions compared with healthy controls, and this altered variability was related to clinical heterogeneity.
Zhu and Qiu (2022)	Youth and young adults	8-23 years	*N* = 755	rs-fMRI	Inter-IV of FC quantifies the deviation of an individual's functional connectivity profile from a group-averaged reference by computing one minus the Pearson correlations between corresponding regional connectivity vectors.	Inter-IV_{FC} was highest in association and cerebellar networks during youth, decreased with age, and showed age-dependent relationships with cognition and psychopathology.
Sun et al. (2022)	Healthy adults	22-37 years	*N* = 42; validation dataset: *n* = 1012	rs-fMRI dMRI	Similar to Mueller et al. (2013).	Inter-IV_{FC} can be significantly predicted from a unified pattern of IV_{SC}, with prediction accuracy decreasing from primary to heteromodal cortical regions.
Karahan et al. (2022)	Young adults	18–35 years	Cohort 1: *n* = 51 Cohort 2: *n* = 35 Cam-CAN: *n* = 50	MEG dMRI	Inter-IV was defined as the average pairwise dissimilarity of regional connectivity profiles across subjects, quantified using cosine distance and further corrected for within-subject intersession variability.	Inter-IV of connectivity is higher in association than sensorimotor cortex, shows modality- and frequency-dependent patterns across structural and MEG connectivity, and is closely related to cortical myelin and white-matter microstructure.
Huang et al. (2025)	Healthy adults	**22-68 years**	*N* = 1,724 (from five cohorts)	dMRI	Similar to Mueller et al. (2013), with an intrasubject difference estimated in a retest dataset	The highest inter-IV_{SC} was observed in limbic regions and in unimodal sensorimotor regions, with minimal variability; it increased with age across most regions and was associated with cortical laminar differentiation and myelination.
Yang et al. (2025)	Adolescents and young adults	8-37 years	*N* = 761 (from two datasets); replication dataset: *n* = 218	rs-fMRI	Inter-IV of FC was quantified at the edge level by decomposing between-subject and within-subject variance using linear mixed-effects models, with adjusted interindividual variability estimated via intraclass correlation.	Inter-IV_{FC} edges were organized along a within-to-between-network axis, aligned with SC variability, flattened across youth development, and positively associated with higher-order cognition.

Note: Literature search was conducted using PubMed, Web of Science, and Scopus with keyword combinations (e.g., "inter-individual variability", "functional connectivity", "structural connectivity"). The search covered studies published in each database from its inception through January 1, 2026. Studies authored by the present author were not included in the literature search results to avoid potential self-citation bias. Although terminology for inter-individual variability in structural or functional connectivity varies across the literature, for brevity, it is uniformly abbreviated as inter-$IV_{SC/FC}$. Here, intra-individual variability refers to within-subject fluctuations over short time intervals (e.g., repeated scans conducted a few days apart, scans conducted within a single day, or split-half sessions within a single session).

1.4 Machine Learning for Predicting Cognitive Function

Given the pronounced heterogeneity of cognitive aging across individuals and cognitive domains (Harada et al., 2013; Mungas et al., 2010), no single neuroimaging modality can fully capture the variability underlying cognitive function. Multimodal neuroimaging approaches — integrating structural, diffusion, and functional MRI—provide a more comprehensive characterization of brain organization and its relationship to cognition (Ma et al., 2025; Pagnotta et al., 2024). However, the high dimensionality and complexity of these data have made it difficult to delineate consistent brain–behavior associations using traditional univariate analytic approaches.

Machine learning (ML) methods offer a powerful alternative by identifying multivariate patterns of brain connectivity that jointly explain inter-individual differences in cognitive performance (Kramer et al., 2024; Rasero et al., 2021; Schulz et al., 2024). Rather than focusing on isolated regions or single connections, ML models learn distributed representations of cognitive function across multiple spatial scales and imaging modalities. This framework has enabled the prediction of diverse cognitive traits—including intelligence, memory capacity, and executive control—and has demonstrated potential to identify neuroimaging-based markers of cognitive aging and neurodegeneration. Notably, in the ML context, prediction broadly refers to the out-of-sample estimation of target phenotypes, such as cognitive performance or clinical status, from neuroimaging features, encompassing both cross-sectional and longitudinal applications.

Despite these advances, predictive performance remains modest. In healthy populations, the proportion of explained variance (R^2) in cognitive outcomes rarely exceeds 10–15% (Hilger et al., 2020; Jockwitz et al., 2024; Kramer et al., 2024; Rasero et al., 2021; Schulz et al., 2024). For example, Rasero et al. (2021) reported less than 10% explained variance for overall cognition in a large young adult cohort (HCP; $N \approx 1{,}000$, aged 22–37 years), whereas Jockwitz et al. (2024) achieved up to 12% when predicting nonverbal ability from gray-matter volume in older adults. Large-scale simulations further suggest that, even with substantial increases in sample size, prediction performance tends to plateau at relatively low levels, indicating that limited statistical power alone cannot account for these constraints (Schulz et al., 2024).

These modest results likely reflect systematic sources of inter-individual variability that are not fully captured by neuroimaging features alone. Cognitive aging is shaped by both neural and

non-neural influences, including genetic background, health status, and lifestyle-related factors (Smith et al., 2020). From a predictive standpoint, lifestyle and psychosocial factors are particularly relevant because they are associated with systematic heterogeneity: individuals with different behavioral and psychosocial profiles may rely on partially distinct neural resources to support comparable levels of cognitive performance, consistent with STAC-r models of aging.

Although prior research has examined univariate associations between individual lifestyle/psychosocial factors and brain aging (e.g., Erickson et al., 2011; Funk-White et al., 2023; Steffener et al., 2016; Topiwala et al., 2022), these variables are often interdependent, and their combined effects may differ from the sum of individual contributions. To address this, some studies have constructed composite lifestyle measures, including risk scores derived from linearly transformed variables (Bittner et al., 2021; Bittner et al., 2019) or indices based on the frequency of health-related behaviors (Franz et al., 2021; Rolls et al., 2023). However, such approaches typically assume equal and independent contributions of lifestyle components, potentially overlooking meaningful interactions. In contrast, data-driven clustering methods can identify naturally occurring multidimensional lifestyle patterns—such as individuals who smoke but remain physically and socially active—that may exert opposing or compensatory effects on brain reserve, offering a more ecologically valid representation of real-world lifestyle configurations (Rodrigues et al., 2024). Importantly, predictive models that emphasize biologically and behaviorally meaningful individual differences may not only support predictions of baseline cognitive levels but also aid in anticipating subsequent cognitive outcomes—though this remains to be confirmed.

In summary, integrating multimodal brain parameters with composite lifestyle-related information within ML frameworks represents a potentially valuable approach for improving cognitive prediction. Such methods may modestly enhance predictive performance and offer preliminary insights into the neural and behavioral factors that may support cognitive resilience in aging, motivating the third line of investigation in the present study.

1.5 Aims of the Thesis

In short, although previous studies have documented widespread alterations in brain structure and function during aging, the contribution of individual variability of brain connectivity (hereafter, IV of connectivity) to the heterogeneity of cognitive aging remains unclear. Building on this research gap, the present dissertation examines how IV of connectivity relates to lifestyle and psychosocial factors, brain reorganization, and cognitive performance. Moreover, it further investigates whether integrating multimodal brain indicators with these lifestyle and psychosocial factors can enhance the prediction of cognitive outcomes. Through this work, we aim to provide theoretical insights into the neural underpinnings of cognitive aging. In addition, we seek to provide empirical evidence for how lifestyle and psychosocial factors, together with multimodal brain features, can inform individualized predictions of cognitive function.

Study 1: Multivariate Associations between Inter-Individual Variability in Brain Connectivity, Lifestyle/Psychosocial Factors, and Cognitive Function

This study examines multivariate associations between inter-individual variability of structural and functional connectivity, lifestyle and psychosocial factors (e.g., physical activity, smoking, social integration), and cognitive performance using Partial Least Squares Correlation (PLSC) at both the network and regional levels. Age-stratified analyses further assess whether these associations differ across age groups among healthy older adults. By adopting an individual-differences perspective, this study provides empirical support for cognitive aging frameworks, such as the STAC-r model, and delineates candidate lifestyle–brain pathways that warrant testing in intervention frameworks aimed at promoting brain and cognitive health in later life.

Study 2: Individual Variability of Brain Connectivity as a Mediator between Network Segregation and Executive Control

Building on findings from Study 1, this study investigates whether inter-individual variability of structural and functional connectivity constitutes a potential pathway linking age-related network dedifferentiation to decline in executive control. Specifically, we test whether IV of connectivity mediates the association between network segregation and executive control, with a primary focus on its set-shifting component, operationalized as performance on the Trail Making Test Part B minus Part A (TMT B–A), and whether these mediating pathways are moderated by age. To address these

aims, mediation and age-moderated mediation models are applied across large-scale brain networks. The IV of connectivity was assessed both as dissimilarity from group-level patterns across individuals (inter-IV) and as within-person dissimilarity across longitudinal connectivity profiles over approximately four years (intra-IV). By jointly modeling inter- and intra-individual variability, this study evaluates whether IV of connectivity explains individual differences in the relationship between network segregation and executive control, thereby informing mechanistic accounts of brain network dedifferentiation in cognitive aging.

Study 3: Lifestyle-Informed Multimodal Brain Features for Predicting Cognitive Function

This study shifts the analytical focus toward prediction, adopting an exploratory framework to examine whether brain features that vary systematically across composite lifestyle and psychosocial patterns contain predictive information for cognitive performance. Clustering procedures are first applied to combined lifestyle and psychosocial measures to identify subgroups of individuals characterized by distinct composite lifestyle and psychosocial patterns. Brain features that differentiate these subgroups are subsequently used as inputs for predictive models of baseline and follow-up cognitive outcomes. Critically, models based on brain features associated with these composite lifestyle and psychosocial patterns are compared against models based on a single lifestyle/psychosocial factor as well as fully data-driven neuroimaging features. The primary goal is to evaluate the predictive value of this multivariate, behaviorally informed neural profile. This provides an initial assessment of its applicability for modeling individual differences in cognitive aging.

In summary, this dissertation adopts the lens of individual variability to systematically interrogate the brain–lifestyle–cognition triad. It progresses through three complementary analytical perspectives: multivariate association between inter-IV of connectivity, lifestyle, and psychosocial factors, and cognition (Study 1); mechanistic insights into how network segregation relates to executive control via IV of connectivity (Study 2); and integrative prediction of cognitive performance using behaviorally informed multimodal brain features (Study 3). Together, these studies provide a coherent framework for understanding heterogeneity in cognitive aging, advancing from explanatory insights to predictive evaluation, and offering methodological implications for future research on personalized cognitive health.

Chapter 2: Data and Methods

2.1 Overall Cohort

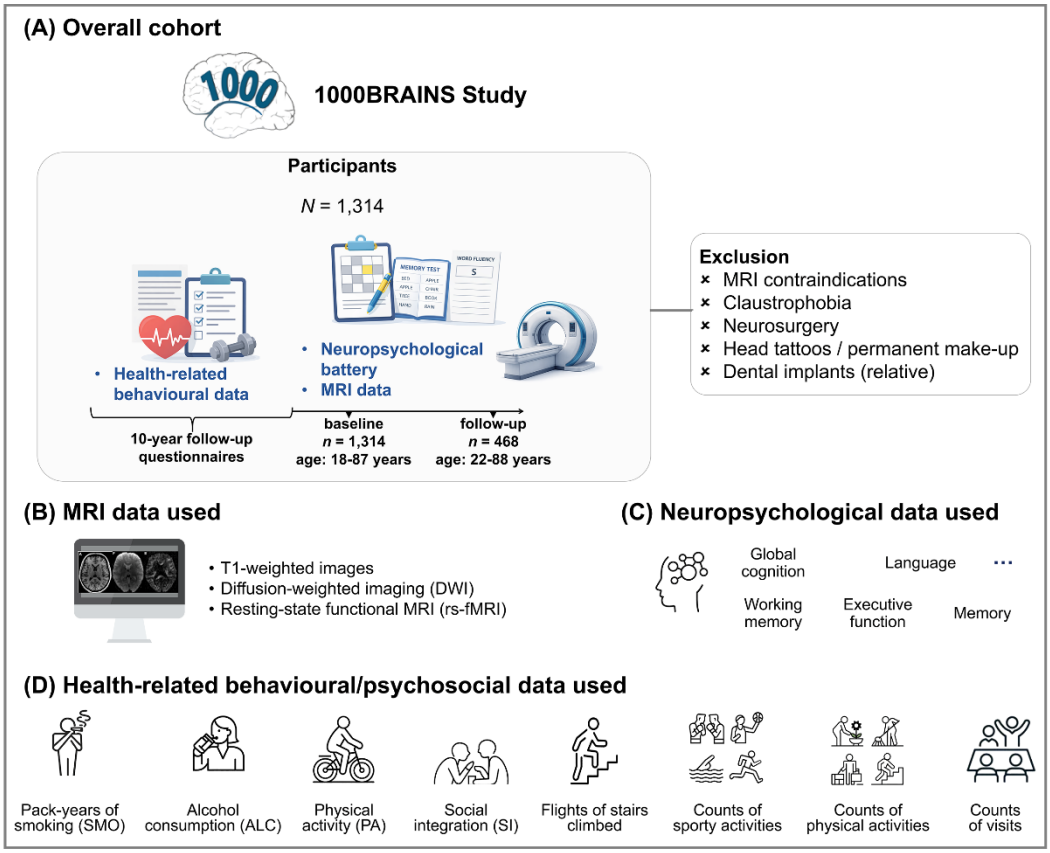

Figure 2.1 Overview of the cohort and data used. (A) 1000BRAINS cohort overview, including participant characteristics, collected data, and exclusion criteria. **Panels B–D** summarize the MRI, neuropsychological, and health-related behavioral/psychosocial data included in the current dissertation.

Participants were drawn from the population-based 1000BRAINS project, a large-scale neuroimaging study in Germany embedded in the Heinz Nixdorf Recall Study (HNR) and its offspring cohort. A total of 1,314 adults (582 women; aged 18–87 years at baseline) completed MRI and neuropsychological assessments at baseline, of whom 468 (204 women) were re-examined approximately four years later. Eligibility followed standard MRI safety criteria; detailed inclusion/exclusion procedures have been reported previously (Caspers et al., 2014; see also Figure 2.1). Health-related behavioral measures were collected across three examination waves (Schmermund et al., 2002) preceding the first MRI session.

2.2 Lifestyle/Psychosocial and Neuropsychological Assessments

Lifestyle/psychosocial measures

The lifestyle/psychosocial data used in this analysis were drawn from the third wave of the 10-year follow-up of the Heinz Nixdorf Recall Study (HNR), completed within 1 year prior to MRI scanning and cognitive assessments (Caspers et al., 2014; Schmermund et al., 2002). Eight lifestyle/psychosocial variables, including smoking and alcohol consumption, were included based on prior work and extended to capture more fine-grained aspects of daily behavior (see Table 2.1 and also Bittner et al., 2021; Bittner et al., 2019). Missing values were replaced using the participant-specific mean scores from the first and second examinations (Jahangiri et al., 2023).

Together, these indicators allow for a more comprehensive assessment of lifestyle and psychosocial behaviors. Other lifestyle factors, such as sleep and diet, were excluded because they involve distinct physiological regulatory processes beyond the behavioral scope of this study.

Table 2.1 Description of lifestyle/psychosocial factors.

Domains	Variables	Operational definitions	Time frame	Unit / Scale
Lifestyle behavior	**Pack-years of smoking** (SMO) (Bittner et al., 2021; Duriez et al., 2014)	Years of smoking × cigarettes per day.	Lifetime	years
Lifestyle behavior	**Alcohol consumption** (ALC) (Bittner et al., 2021)	The total amount of pure alcohol is weighted by beverage type and frequency.	Past 4 weeks	g/month
Lifestyle behavior	**Physical activity** (PA) (Ainsworth et al., 2000)	Sum of metabolic equivalents of task (METs) derived from the reported duration of sports and daily physical activities.	Past month	/
Psychosocial	**Social integration** index (SI) (Berkman et al., 2004; Bittner et al., 2019)	A composite score of marital status, close ties, and organizational membership.	Current	/
Lifestyle behavior	**Flights of stairs climbed** (Ghosal & Chandrasekaran, 2024; Steffener et al., 2016)	The self-reported number of stair flights climbed per day serves as a simple proxy for cardiovascular fitness and potentially for brain health.	Daily	Flights/day
Lifestyle behavior	**Count of sports activities**	The number of distinct sports practiced reflects the diversity of intentional exercise behaviors.	Past month	Count
Lifestyle behavior	**Count of physical activities**	The number of non-sport physical activities provides insight into everyday movement beyond formal exercise.	Past month	Count
Psychosocial	**Count of visits**	Total visits from children, relatives, and friends. It indexes the frequency of social interactions and informal support.	Past month	Count

Neuropsychological tests

In the 1000BRAINS project, participants' cognitive abilities were profiled using a comprehensive neuropsychological battery. The objective of the present study was to examine brain-cognition associations specific to individual domains. To this end, we selected 13 cognitive tasks intended to predominantly reflect specific cognitive constructs, with minimal overlap between domains. The assessed domains included measures of global cognitive status (via the dementia detection test, DemTect), episodic and long-term memory, working memory (WM), and executive control (see Table 2.2). Where executive control was indexed via the Trail Making Test, the specific metric used (B–A difference vs. B/A ratio) is specified per study (Chapters 3–5).

Table 2.2 Description of neuropsychological measurements.

Variables	Test (References)	Cognitive domain	Description
Cognitive status	DemTect (Kalbe et al., 2004)	Global cognition	The sum of the scores from a digit span memory test, a number conversion task, and a verbal fluency task (sum score).
Language comprehension	Wortschatztest (Word-Hoard-test) (Schmidt & Metzler, 1992)	General language comprehension, vocabulary	Total number of target words correctly identified among interfering words (sum score).
Nomination	Boston Naming Test (from CERAD; short form) (Morris et al., 1989)	Nomination	The number of correct answers on an object-naming task (using frequent, medium-frequent, and rare items) (sum score).
Figural memory	Benton-Test (Benton et al., 2009)	Visual memory, figural memory	Total number of correctly freely recalled figures from 20 previously presented figures (sum score).
Verbal WM	Zahlennachsprechen (from Nürnberger Alters-Inventar) (Oswald & Fleischmann, 1997)	Verbal working memory	Total number of correctly recalled digits given in a backward sequence (sum score).
Phonemic fluency	Regensburger Wortflüssigkeitstest (Aschenbrenner et al., 2000)	Phonemic verbal fluency	Total number of produced words beginning with a given letter B in 2 minutes (sum score).
Phonemic switch		Phonemic verbal switch	Total number of produced words beginning with a given letter G–R in 2 minutes (sum score).
Semantic fluency		Semantic verbal fluency	Total number of produced words in the category “Berufe (job)” in 2 minutes (sum score).
Semantic switch		Semantic switch	Total number of produced words in the category “sports–fruits” in 2 minutes (sum score).
Visuospatial WM	Corsi block tapping task (CBT) (Schelling, 1997)	Visuospatial working memory	The number of correct answers on a backward block sequence recall task (with gradually increasing sequence length) (sum score).
Episodic memory	Bielefelder Kategorielle Wortlisten (BKW) (Lux et al., 2012)	Verbal learning (episodic encoding)	The average of the relative proportions of reproduced free recalls across five runs.
Long-term memory		Delayed verbal memory	Total number of correctly freely recalled words from a list of 15 words in delayed run across 5 trials (sum score).
Executive control [a]	Trail making test (TMT) A and B (taken from CERAD-Plus) (Morris et al., 1989)	Set shifting / cognitive flexibility	Time difference between the completion time (seconds) of TMT Part B and TMT Part A (i.e., TMT B–A).
Executive control [b]		Set-shifting/ executive efficiency	Calculated by dividing the completion time (seconds) of TMT Part B by the completion time of TMT Part A (i.e., TMT B/A).

Note: [a] Variable used in studies 1 and 2. b Variable used in study 3. Further descriptions are provided in Caspers et al. (2014).

2.3 MRI Acquisition

All MRI data were collected on a 3T Siemens Tim-TRIO scanner equipped with a 32-channel head coil (Erlangen, Germany). Scans were acquired on the same day as the neuropsychological assessments. Detailed acquisition parameters are provided in Table 2.3 and have been described previously (Caspers et al., 2014).

During the resting-state scan, participants were instructed to remain still with eyes closed and stay awake. An experienced radiologist visually inspected all MRI datasets to identify pathological or incidental findings.

Table 2.3 MRI acquisition parameters.

Parameter	T1-weighted	Diffusion-weighted imaging (DWI)		rs-fMRI
		Low *b* value (60 directions)	High *b* value (120 directions)	
Sequence	3D magnetization-prepared rapid gradient-echo (MPRAGE)	Echo-planar imaging (EPI)	High-angular-resolution diffusion imaging (HARDI)	BOLD gradient-EPI
TR (ms)	2,250	6,300	8,000	2,200
TE (ms)	3.03	81	112	30
TI (ms)	900	–	–	–
Flip angle (°)	9	–	–	90
FoV (mm²)	256 × 256	–	–	200 × 200
Voxel size (mm³)	1 × 1 × 1	2.4 × 2.4 × 2.4	2.4 × 2.4 × 2.4	3.1 × 3.1 × 3.1
Slices	176	–	–	36
Directions	–	60	120	–
b value (s/mm²)	–	1,000	2,700	–
*b*0 images (interleaved)	–	7	13	–
Duration	–	–	–	~11 min

2.4 MRI Preprocessing

2.4.1 Structural MRI

To assess fine-grained cortical morphology, individual cortical surfaces were parcellated into 400 regions using the functionally defined Schaefer atlas (Schaefer et al., 2018). Parcels from the left and right hemispheres were treated as separate features, yielding a total of 400 cortical regions for subsequent analyses. Structural MRI data were processed using FreeSurfer (v7.1.0) with a customized recon-all pipeline, following procedures described in Kramer et al. (2024). Analyses included participants with T1-weighted images suitable for cortical surface reconstruction (see Chapter 5.1). For each parcel, cortical thickness (CT), surface area (SA), and gray matter volume (GMV) were extracted using standard FreeSurfer procedures. These measures capture complementary aspects of cortical morphology (Fjell & Walhovd, 2010; Panizzon et al., 2009).

2.4.2 Diffusion MRI

Diffusion MRI (dMRI) data were prepared for quantitative modeling following standard preprocessing procedures (Stumme et al., 2022). Tissue segmentation of the T1-weighted images was performed using the CAT12 toolbox (Gaser et al., 2024), which generated tissue probability maps (TPMs) of gray matter (GM), white matter, and cerebrospinal fluid (CSF) to assist later registration and to minimize partial volume bias. Preprocessing of the dMRI data included correction for eddy-current distortions and participant motion. Susceptibility-related geometric deformation was compensated by computing anisotropic power maps (APMs; Dell'Acqua et al., 2014) from the high *b*-value (b = 2700 s/mm^2) data and aligning them nonlinearly to the structural images via Advanced Normalization Tools (ANTs; https://github.com/ANTsX/ANTs). This procedure corrected geometric distortions caused by magnetic field inhomogeneities, particularly near air–tissue interfaces. For accurate spatial correspondence, representative $b0$ volumes from both diffusion shells ($b1000$ and $b2700$) were aligned to the T1-weighted image using rigid-body registration. These preprocessed datasets were then combined and harmonized to account for echo-time variations, preparing the data for subsequent neurite orientation dispersion and density imaging (NODDI) modeling and tractography.

Tensor fitting for diffusion tensor imaging (DTI) was carried out on the preprocessed $b1000$ shell using *dtifit* in FSL v6.0 (https://fsl.fmrib.ox.ac.uk/fsl) to obtain fractional anisotropy (FA),

mean diffusivity (MD = ($\lambda_1 + \lambda_2 + \lambda_3$)/3), radial diffusivity (RD = ($\lambda_2 + \lambda_3$)/2), and axial diffusivity (AD = λ_1) maps. Microstructural modeling was further refined using the NODDI framework implemented in the Microstructure Diffusion Toolbox (MDT; https://mdt-toolbox.readthedocs.io), producing estimates of intracellular volume fraction (ICVF) and orientation dispersion index (ODI) (Deligianni et al., 2016).

To reconstruct white matter architecture, we applied a multi-tissue constrained spherical deconvolution (CSD) approach (Jeurissen et al., 2014; Tournier et al., 2012) in MRtrix v0.3.15 (https://www.mrtrix.org), which separates tissue compartments and resolves complex fiber configurations. TPMs were used to construct a five-tissue-type (5TT) segmentation, enabling anatomically constrained tractography (ACT; Smith et al., 2012). Whole-brain probabilistic tractography was then generated using the iFOD2 algorithm with ACT, initiating streamlines dynamically from the gray–white matter interface. Each participant's connectome comprised ten million streamlines, with a maximum length threshold of 250 mm and a minimum cutoff of 0.06 to suppress anatomically implausible tracks. Streamline weights were subsequently estimated using the SIFT2 algorithm for subsequent connectome quantification.

2.4.3 Resting-State Functional MRI

Resting-state fMRI data were preprocessed using an established pipeline (Stumme et al., 2022). The initial four volumes of each run were removed to allow for magnetic field stabilization. To mitigate the effects of head motion, we first applied a two-pass affine registration procedure, aligning all volumes first to the initial volume and then to the mean image. To register fMRI data to the Montreal Neurological Institute (MNI) 152 standard space, we carried out a unified segmentation method in SPM12 (Ashburner & Friston, 2005). This approach was selected for its documented advantage in registration precision over traditional methods that depend exclusively on T1-weighted images (e.g., Dohmatob et al., 2018). For additional noise reduction, we employed ICA-based Automatic Removal Of Motion Artifacts (ICA-AROMA) (Pruim et al., 2015), which automatically detects and removes independent components that are correlated with motion. Consistent with contemporary guidelines for mitigating motion confounds in functional connectivity (Ciric et al., 2017; Parkes et al., 2018), global signal regression was also performed. Finally, a temporal band-pass filter (0.01–0.1 Hz) was applied to isolate low-frequency BOLD fluctuations.

2.5 Ethics Approval

The 1000BRAINS study received ethical approval from the Ethics Committee of the University of Duisburg-Essen (approval numbers 11-4678 and 12-5199-BO). All study procedures were conducted in accordance with the Declaration of Helsinki. All participants voluntarily agreed to take part after being fully informed about the study, and this agreement was documented in writing before the study began.

Chapter 3: Multivariate Associations between Inter-Individual Variability of Brain Connectivity, Lifestyle/Psychosocial Factors, and Cognitive Function

Study 1 aimed to examine the relationships among inter-individual variability (inter-IV) of brain connectivity, lifestyle/psychosocial factors, and multiple cognitive domains in healthy older adults. Specifically, it addressed two research questions: (1) Are inter-IV of functional and structural connectivity associated with lifestyle/psychosocial factors as well as cognitive performance in healthy older adults? (2) Do these associations differ across age subgroups in late adulthood? Based on prior theoretical and empirical evidence, we hypothesized that higher inter-individual variability (IV) of connectivity would be associated with less healthy lifestyle profiles and poorer cognitive performance. We also expected these associations to vary across age groups, reflecting increasing heterogeneity in brain–behavior relationships with advancing age.

Inter-individual variability of functional and structural connectivity was measured as the dissimilarity between each individual's connectivity profile and the connectivity profiles of other individuals within the corresponding group (Mueller et al., 2013; Sun et al., 2022). See Chapter 3.1.2 for a detailed description.

To examine multivariate relationships among lifestyle/psychosocial factors, cognitive performance, and neural measures, we used partial least squares correlation (PLSC), which identifies shared covariance patterns between two sets of variables. PLSC is well-suited to high-dimensional data with multicollinearity and can reveal distributed brain–behavior associations that may not be detectable with univariate approaches (Krishnan et al., 2011; see Chapter 3.1.3).

This chapter is based on Zhang et al. (2025), published in *Aging and Disease* under a CC-BY license. For the purposes of this dissertation, the manuscript has been structurally reorganized and revised, including modifications to the methods, results, and discussion.

3.1 Methods

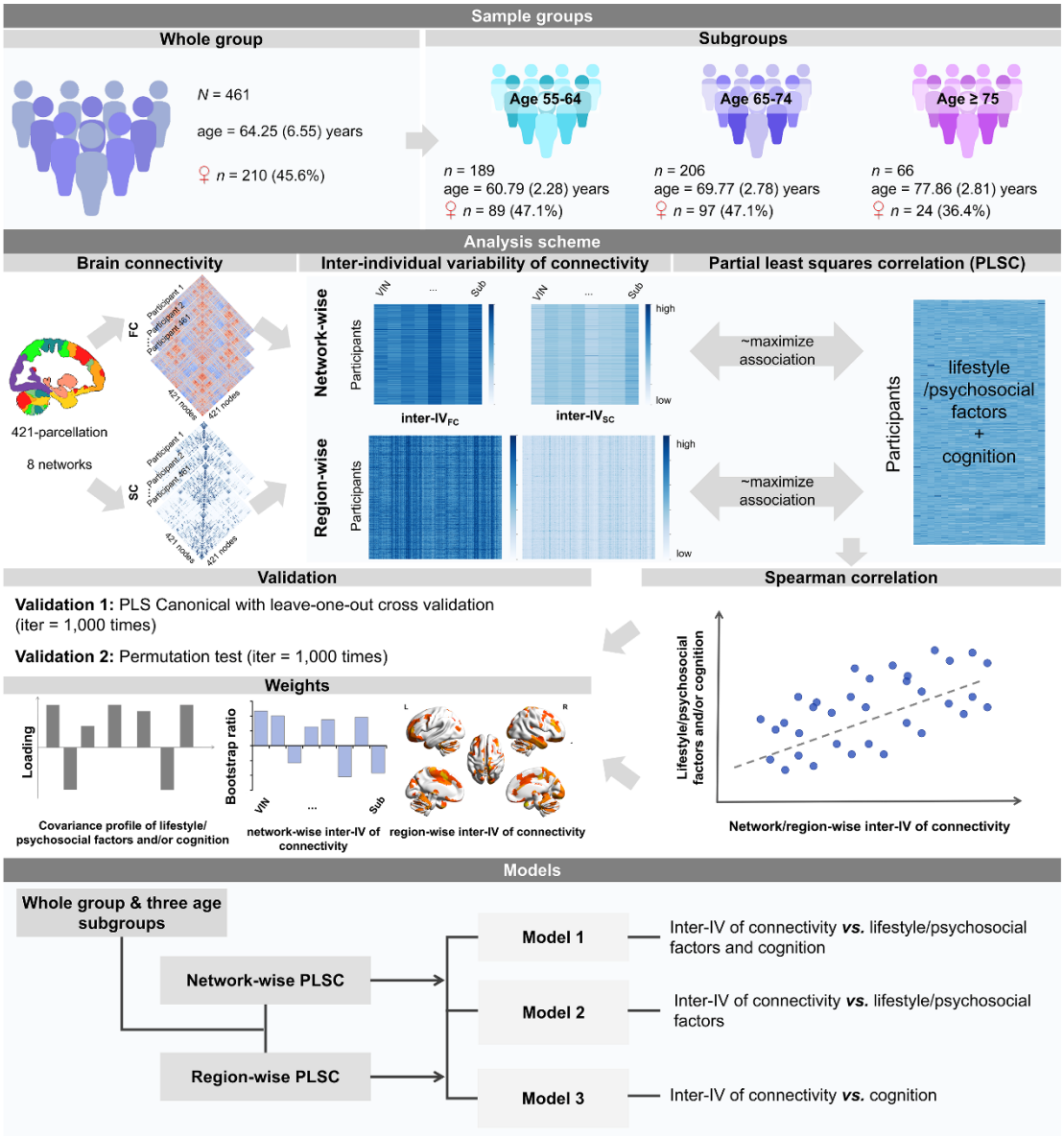

Figure 3.1.1 Overview of the PLSC framework and analysis design. **Top:** Full sample divided into three age groups. **Middle:** Brain connectivity from 421 regions (assigned to 8 networks); inter-IV calculated at network and region levels. Brain measures, lifestyle/psychosocial variables, and cognitive variables are input to PLSC to extract latent variables (with a focus on the first latent variable). Associations were tested using Spearman's rank correlation and two validation methods. Results shown as factor loadings and contributions of inter-IV in connectivity (bar charts for network-wise; brain maps for region-wise). **Bottom:** Three models with different input features applied to the whole group and age subgroups, separately for network- and region-wise analyses. Figure adapted and modified from Zhang et al. (2025) (CC-BY).

3.1.1 Sample and Data

From the initial 1,314 participants in the 1000BRAINS study, 345 participants younger than 55 or

missing the age information were excluded, leaving 969 older adults (≥55 years) eligible. Participants were further excluded if they showed potential cognitive impairment based on the dementia screening test (DemTect score ⩽ 8 or missing; $n = 31$; Kalbe et al., 2004), which ensured that the sample represented cognitively healthy older adults, leaving 938 participants. Of these, 851 participants had available structural MRI, diffusion MRI, and rs-fMRI. From this eligible sample, 692 participants had both structural and functional connectivity measures available for analysis. Additionally, participants missing lifestyle or psychosocial measurements at more than two time points ($n = 193$) or any of the 13 cognitive assessments of interest ($n = 38$) were excluded. The final sample comprised 461 participants (aged 67.3 ± 6.6 years; 210 females; see Table 3.2.1). See also Zhang et al. (2025).

Lifestyle/psychosocial measures

We focused on five lifestyle and psychosocial factors, that is, pack-years of smoking, alcohol consumption, physical activity, flights of stairs climbed, and social integration. These factors were included based on prior studies linking them to brain structure, function, and cognition (e.g., Bittner et al., 2021; Schurz et al., 2021; Topiwala et al., 2022; van der Velpen et al., 2022), as they represent both risk and protective domains.

Neuropsychological performance tests

For the current analysis, 13 cognitive measures from the 1000BRAINS dataset (described in Chapter 2.2) were included to investigate domain-specific associations. Executive control was represented by the TMT B–A score. Participants with any missing data in these 13 cognitive tests were excluded.

MRI brain data

This study focused on individual differences in brain connectivity, specifically structural and functional networks. To this end, we utilized diffusion MRI (dMRI) to assess structural connectivity and resting-state functional MRI (rsfMRI) to examine functional connectivity. Detailed information on data acquisition and preprocessing is provided in Chapters 2.3 and 2.4.

3.1.2 Brain Connectivity and Inter-Individual Variability

Brain atlas

We used a combined brain atlas comprising 421 regions to capture cortical, subcortical, and cerebellar structures.

The cortical component consisted of 400 parcels based on the Schaefer et al. (2018) parcellation, which provides a fine-grained functional organization aligned with Yeo's seven large-scale functional networks (Yeo et al., 2011). To ensure coverage of key non-cortical structures, 14 subcortical regions were included based on the FreeSurfer atlas ("Atlas_ROIs.2.nii.gz", version 5.3.0; Glasser et al., 2013). These regions were treated as a single subcortical network, consistent with previous network-level analyses (Liegeois et al., 2019; Nelson et al., 2023). Cerebellar regions were incorporated using the functional parcellation proposed by Buckner et al. (2011), with cerebellar voxels assigned to Yeo's seven networks with which they showed the strongest functional connectivity.

This approach resulted in 421 parcels organized into eight networks: seven cortical networks, including both cortical and cerebellar parcels, and one subcortical network.

Functional connectivity (FC)

Resting-state functional connectivity (RSFC) was computed from preprocessed resting-state fMRI data. Hereafter, we use FC to refer to RSFC. For each of the 421 brain regions, the average time series of all voxels within the region was extracted using *fslmeants* in FSL (Smith et al., 2004), capturing the overall activity of each region over time. Pearson correlation coefficients were then calculated between the time series of every pair of regions, resulting in a 421 × 421 FC matrix. Each matrix element reflects the degree to which the activities of two regions co-fluctuate, thereby indicating their functional relationship.

To reduce spurious correlations from noise or random fluctuations, a permutation test with 1,000 iterations was performed for each region pair (Stumme et al., 2020; Zalesky et al., 2012). Correlations not reaching statistical significance ($p \geqslant 0.05$) were set to zero, effectively removing unreliable connections. Finally, all remaining correlation coefficients were transformed using Fisher's *r*-to-*z* transformation to stabilize variance and allow more accurate statistical comparisons across participants.

Structural connectivity (SC)

For structural connectivity (SC) analysis, we first aligned the 421-region parcellation template to each participant's individual diffusion space. Since the original 400-region Schaefer template primarily covers cortical gray matter, we dilated the boundaries of each region by 5 voxels, following a previous study (Stumme et al., 2022), to ensure that each region includes the gray-white

matter interface, which is critical for initiating tractography. This step ensures that the regions serve as reliable seed points for tracking white matter pathways.

Next, we performed probabilistic streamline tractography to estimate the white matter connections between all pairs of regions using MRtrix v0.3.15. To improve the biological accuracy of these estimates, we applied SIFT-2 (Smith et al., 2015), which adjusts the raw streamline counts using a cross-sectional area multiplier, making the connectivity weights more representative of actual white matter fiber densities. Finally, the resulting 421 × 421 structural connectivity matrix was logarithmically transformed (log10) to reduce skewness and better handle the wide range of connection strengths across the brain following a previous study (Conrad et al., 2023).

Measuring the inter-individual variability of connectivity

To quantify inter-individual variability of connectivity, we operationalized inter-IV as one minus the mean correlation between a participant's connectivity profile and those of all other participants in the group. This approach aligns with the conceptual framework of Mueller et al. (2013) and builds upon the individual-level decomposition method introduced by Sun et al. (2022). In this study, the procedure was adapted from Sun et al. (2022) without regressing out intra-individual variability, thereby capturing each participant's overall deviation from the group mean (see Figure 3.1.2).

For each participant m and brain region (node) i, the connectivity profile of node i (i.e., the vector of connections between node i and all other nodes) was correlated with the corresponding profiles of all other participants $n \neq m$. The mean correlation across these participants was defined as the inter-individual similarity of functional connectivity (inter-IS_{FC}):

$$\text{inter-IS}_{FCi\_m} = \frac{\sum \mathbf{corr}(\mathbf{FC}_{i\_m}, \mathbf{FC}_{i\_n})}{N-1}$$

The inter-individual variability of functional connectivity (IV_{FC}) was then calculated as one minus the IS_{FC}:

$$\text{inter-IV}_{FCi\_}\text{m} = 1 - \text{IS}_{FCi\_}\text{m}$$

Higher inter-IV_{FC} values indicate greater deviation from the connectivity patterns of other participants. The same procedure was applied to structural connectivity to obtain inter-IV_{SC}, yielding a participant-by-region matrix of FC- and SC-based inter-variability estimates used in all subsequent analyses. Additional group-level inter-variability measures are reported in Table 3.2.2.

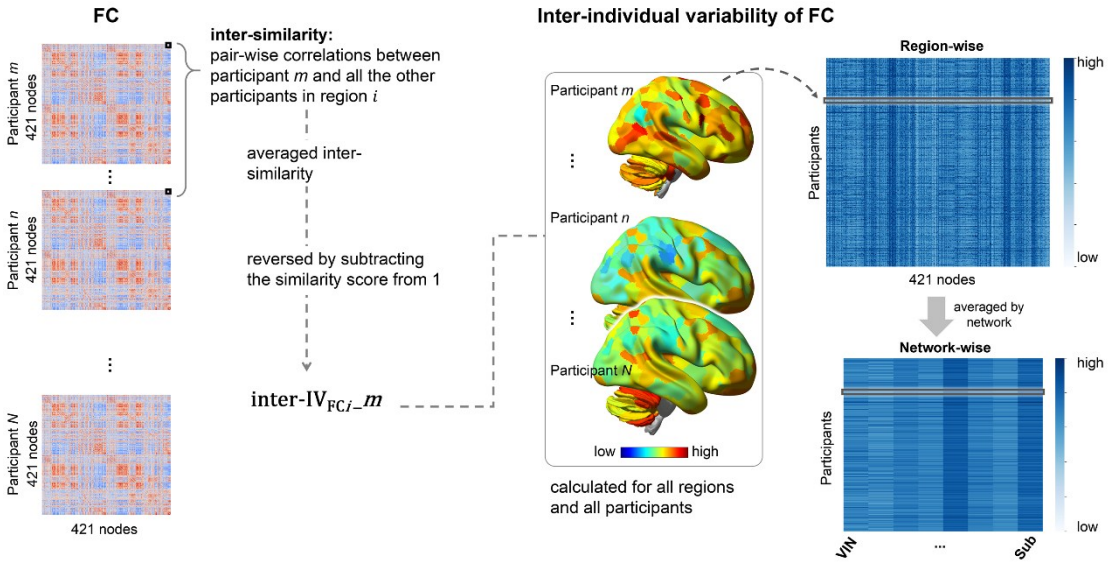

Figure 3.1.2 Calculation of inter-individual variability (IV) of connectivity. This figure illustrates the computation of IV using functional connectivity (FC) as an example. For each participant, the connectivity profile of each brain region was correlated with the profiles of all other participants, and the resulting correlations were averaged to obtain the inter-individual similarity of FC, which was then converted into dissimilarity measures (IV_{FC}), with higher values indicating greater variability from the group-average pattern. IV_{FC} was calculated for all regions and participants, resulting in a participant-by-region matrix, and network-wise IV_{FC} was obtained by averaging regional values within each functional network. The same procedure was applied to structural connectivity (SC) to obtain inter-IV_{SC}. Figure adapted and modified from Zhang et al. (2025) (CC-BY).

3.1.3 Partial Least Squares Correlation (PLSC) and Models

To explore associations between inter-IV of connectivity, lifestyle/psychosocial factors, and cognitive functions, we performed a partial least squares correlation analysis (pypyls package; https://github.com/netneurolab/pypyls; see Figure 3.1.1). PLSC identifies latent patterns of covariation between two sets of variables, the *X* matrix and *Y* matrix, by deriving latent variables (LVs) that maximize the covariance between linear combinations of the original variables (Abdi & Williams, 2013). This multivariate approach is robust against multicollinearity, can capture complex relationships, and is increasingly applied to explore brain-behavior associations (Hoagey et al., 2019; Mihalik et al., 2022; Petersen et al., 2024). In our study, each LV represents a pattern of covariation linking brain connectivity with lifestyle/psychosocial factors and cognition, summarizing the most prominent linear relationships in the data. This multivariate approach allows detection of associations that might be missed by univariate analyses. The PLSC analysis code was adapted from Petersen et al. (2024).

PLSC Models

To examine both large-scale network effects and more fine-grained regional contributions, we conducted PLSC analyses at two levels for the whole sample:

(i) Network-wise analysis: connectivity features aggregated by network (461 participants×8 networks).

(ii) Region-wise analysis: inter-$IV_{SC/FC}$ from 421 regions forming the *X* matrix (461 participants×842 features).

We constructed three types of PLSC models to address complementary research questions:

a) Model 1 (Combined model):

The *Y* matrix included five lifestyle/psychosocial variables and thirteen cognitive tests. This model captures the overall pattern linking inter-IV of connectivity with both lifestyle behaviors and cognitive functions, reflecting their shared and combined associations with individual variability of connectivity.

b) Model 2 (Lifestyle/psychosocial-only model):

The *Y* matrix included only the eight lifestyle and psychosocial variables. This model focuses on associations between inter-IV of connectivity and lifestyle/psychosocial variables by excluding cognitive variables from the covariance space, ensuring that their associations with brain connectivity are estimated without competition from cognitive variation.

c) Model 3 (Cognition-only model):

The *Y* matrix included only thirteen cognitive tests. This model focuses on inter-IV of connectivity–cognition associations by excluding lifestyle/psychosocial variables from the covariance space, ensuring that cognitive variables contribute uniquely to the derived latent pattern without competition from cognitive variation.

Model 1 reveals the joint brain–behavior pattern, while Models 2 and 3 assess whether lifestyle and cognitive measures relate to overlapping or distinct brain features. The same model structure was applied at both the network and region levels. Before performing PLSC, all *X* and *Y* matrices were normalized and residualized for age, sex, and education. Analyses were additionally repeated within three age subgroups, resulting in a total of 24 models (2 levels × 3 models × 4 sample sets: whole sample plus three age subgroups). In all cases, we focused on the first latent

variable, which accounted for the largest proportion of the covariance. For anatomical interpretation, brain regions were labeled by functional network, Schaefer parcel, and Juelich atlas (e.g., SAN_FrOperIns_2, area Id6; Amunts et al., 2020).

PLSC Procedure

Partial least squares correlation (PLSC) was used to identify multivariate patterns of covariation between brain (i.e., IV of connectivity, namely *X*) and behavioral variables (e.g., lifestyle/psychosocial and cognitive variables, namely *Y*). First, a correlation matrix between *X* and *Y* was computed. The number of latent variables (LVs) corresponded to the smaller dimension of this matrix.

To identify the main patterns linking brain connectivity and behavior, PLSC applies singular value decomposition (SVD). Specifically, SVD splits the correlation matrix into three parts. Each LV consisted of a set of brain weights (*U*) and behavioral weights (*V*), together with a singular value reflecting the amount of covariance explained by that LV.

Each LV identifies a brain-behavior pattern in which specific brain regions and behavioral traits exhibit the strongest coordinated differences across individuals. The explained variance of each LV was calculated as the squared singular value divided by the sum of squared singular values across all LVs. Statistical significance was assessed using permutation testing (5,000 permutations), with LVs considered significant at $p < 0.05$.

Subject-specific *covariance scores* of brain and behavior were obtained by projecting individual *X* and *Y* data onto the corresponding singular vectors. These scores quantify the degree to which each participant expresses the identified brain–behavior pattern.

Bootstrap resampling (5,000 iterations with replacement) was used to assess the reliability of variable contributions to the PLSC models. Singular value decomposition was recomputed for each resample, yielding distributions of singular vector weights. For behavioral variables in the *Y* matrix, these distributions were used to estimate 95% confidence intervals (CI). For brain features in the *X* matrix, bootstrap ratios were computed as the ratio of the singular vector weight to its bootstrap-estimated standard error (DuPre & Spreng, 2017; Petersen et al., 2024):

$$\text{Bootstrap ratio} = \frac{\text{Singular vector weight } U_{i,j}}{\text{Standard error estimated from bootstrapping}}$$

where *i* represents a brain feature; *j* represents a latent variable.

Post PLSC analyses

Following the primary PLSC analysis, Spearman correlations were computed between the participant-level covariance scores derived from the *X* and *Y* matrices. A high correlation coefficient (rho) indicates consistent expression of the latent variables linking brain measures with behavioral and cognitive measures.

The robustness of these correlations was evaluated using two approaches. First, a resampling-based repeated leave-one-out cross-validation (LOOCV) procedure implemented with PLSCanonical (Petersen et al., 2024) was applied solely as a validation framework. Across 1,000 resampling iterations, latent scores were recomputed and correlated to generate empirical distributions of correlation coefficients and associated *p*-values. Statistical significance was assessed at $p < 0.05$ and corrected for multiple comparisons using false discovery rate (FDR; $q < 0.05$; Benjamini & Hochberg, 1995).

Second, permutation testing (1,000 iterations) was conducted to assess whether the observed correlations exceeded chance levels.

3.1.4 Statistics and Sensitivity Analyses

We first compared demographic and neuropsychological variables across the whole group and three age subgroups to characterize the sample. Because age stratification naturally leads to differences in behavior, cognition, and brain measures, these variations were expected and not considered confounds. Instead, these comparisons served to document age-related profiles and to confirm that non-age variables—especially sex—were not unevenly distributed across samples.

"For normally distributed variables, we used Analysis of Variance (ANOVA) to compare differences among the three subgroups" (Zhang et al., 2025, page 8). For sex, between-group differences were assessed using Chi-Square tests, which are appropriate for categorical distributions. For non-normally distributed variables, the non-parametric Kruskal–Wallis test was applied to provide a robust comparison without assuming normality.

To provide a comprehensive characterization of individual variability in brain connectivity, we also summarized group-level inter-IV of connectivity and performed ANOVA to compare differences across the three age subgroups at the network level. These analyses served as descriptive assessments to characterize how intrinsic connectivity varies with age, complementing the

multivariate findings. All univariate statistical analyses were conducted using IBM SPSS Statistics 29.0.

The PLSC, Spearman correlation analysis, validation analyses, and visualization were performed in Python (version 3.10.9) using established scientific computing and machine learning libraries (pandas, NumPy, pyls, pingouin, seaborn, scipy, scikit-learn, and matplotlib).

The network-wise and region-wise PLSC analyses for Model 1 in the whole group were rerun after removing participants who were outliers on any lifestyle, psychosocial, or cognitive variable. Outliers were defined as scores exceeding ±3 standard deviations (*SD*) from the mean for each variable. This procedure retained 403 participants (mean age = 67.4 ± 6.5 years; 192 females) for the sensitivity analysis and was used to assess the robustness of the PLSC results to extreme values.

3.2 Results

3.2.1 Sample Characteristics

Descriptive statistics for the full sample (N = 461; mean age = 67.3 ± 6.6 years; mean education level = 6.39 ± 1.95) and for the three age subgroups are presented in Table 3.2.1. As expected, older age was accompanied by significant variations in several variables, including physical activity, number of flights of stairs climbed, and 12 cognitive domains—except for phonemic fluency.

The characteristics of group-level individual variability of connectivity for the whole group and three age subgroups are listed in Table 3.2.2. Except for the inter-IV_{SC} of the dorsal attention (DAN), salience/ventral attention (SAN), and subcortical networks, inter-IV of connectivity differed significantly among the three age subgroups.

Table 3.2.1 Basic information about participants.

	Mean (*SD*)				Statistic	
	Whole group	**Age 55-64**	**Age 65-74**	**Age ≥ 75**	**χ^2/*F*-value**	***p*-value**
Demographic variables						
Age (years)	67.3 (6.6)	60.8 (2.3)	69.8 (2.8)	77.9 (2.8)	/	/
Females (*n*, %) [a]	210, 45.6%	89, 47.1%	97, 47.1%	24, 36.4%	2.623	.269
Education (ISCED) [b]	6.39 (1.95)	6.54 (1.91)	6.46 (1.95)	5.79 (1.98)	8.428	**.015**
Lifestyle/psychosocial factors						
Packyears (of smoking) [b]	12.85 (20.99)	12.45 (21.29)	14.01 (21.23)	10.41 (19.37)	1.817	.403
Alcohol (in g/week) [b]	10.36 (17.72)	11.68 (18.27)	9.16 (17.57)	10.32 (16.58)	4.248	.120
MET (per week) [b]	46.19 (51.84)	44.77 (60.05)	48.46 (45.71)	43.14 (44.39)	6.064	**.048**
Stairs (number per day) [b]	6.75 (9.22)	8.04 (11.25)	6.62 (8.02)	3.48 (4.13)	14.879	**<.001**
Social integration (as social integration index) [b]	12.74 (6.38)	12.59 (5.81)	12.98 (6.66)	12.42 (7.10)	2.212	.331
Cognitive variables						
Cognitive status (sum) [b]	14.86 (2.34)	15.24 (2.36)	14.88 (2.26)	13.73 (2.24)	17.411	**.001**
Language comprehension [b]	30.95 (4.79)	31.47 (4.22)	31.13 (4.86)	28.92 (5.58)	13.133	**.001**
Nomination [b]	14.53 (0.76)	14.69 (0.61)	14.53 (0.78)	14.09 (0.91)	30.336	**<.001**
Figural memory [b]	8.70 (4.06)	10.36 (3.67)	8.00 (3.98)	6.09 (3.40)	66.762	**<.001**
Verbal WM [b]	4.70 (1.07)	4.87 (1.16)	4.61 (1.00)	4.52 (0.93)	9.604	**.008**
Phonemic fluency [c]	18.97 (6.20)	19.36 (6.13)	18.80 (5.86)	18.39 (7.39)	1.627	.443
Phonemic switch [b]	18.63 (5.96)	19.29 (5.46)	18.50 (5.94)	17.15 (7.08)	3.259	**.039**
Semantic fluency [b]	23.21 (6.90)	23.99 (6.73)	23.25 (6.94)	20.83 (6.77)	9.254	**.010**
Semantic switch [b]	19.66 (4.67)	20.29 (4.34)	19.66 (4.62)	17.88 (5.33)	15.112	**<.001**
Visuospatial WM [b]	4.70 (1.08)	4.92 (1.05)	4.52 (1.09)	4.61 (1.05)	13.173	**.001**
Episodic memory [c]	60.11 (11.69)	64.11 (10.52)	58.36 (11.31)	54.08 (12.30)	24.39	**<.001**
Long-term memory [b]	10.74 (2.68)	11.4 (2.51)	10.60 (2.55)	9.30 (2.93)	32.678	**<.001**
Executive control [b]	54.31 (38.59)	43.39 (25.18)	55.57 (36.03)	81.67 (59.16)	50.619	**<.001**

Note: The mean value and standard deviation are represented as mean (*SD*). Statistical analysis was performed among three age subgroups. Adapted and modified from Zhang et al. (2025) (CC-BY).

[a] Chi-Square Test

[b] Independent-Samples Kruskal-Wallis Test

[c] One-way ANOVA

Abbreviations: ISCED, International Standard Classification of Education; Packyears, pack-years of smoking; Alcohol, alcohol consumption; MET, metabolic equivalent of the task; Stairs, flights of stairs climbed; WM, working memory

Table 3.2.2 Characteristics of group-level inter-IV of connectivity.

Network	*Mean (SD)*				Statistic	
	Whole group (N = 461)	Age 55-64 (n = 189)	Age 65-74 (n = 206)	Age ≥ 75 (n = 66)	F-value	p-value
inter-IV$_{FC}$						
whole brain	0.71 (0.08)	0.69 (0.09)	0.70 (0.09)	0.77 (0.07)	115.103	**<.001**
VIN	0.70 (0.06)	0.67 (0.07)	0.70 (0.07)	0.75 (0.05)	26.083	**<.001**
SMN	0.67 (0.05)	0.65 (0.05)	0.66 (0.06)	0.75 (0.04)	98.363	**<.001**
DAN	0.73 (0.07)	0.71 (0.07)	0.72 (0.07)	0.78 (0.06)	17.245	**<.001**
SAN	0.69 (0.08)	0.68 (0.08)	0.68 (0.09)	0.75 (0.06)	13.157	**<.001**
LIN	0.83 (0.05)	0.83 (0.05)	0.83 (0.05)	0.86 (0.03)	4.688	**.012**
FPN	0.72 (0.06)	0.71 (0.06)	0.71 (0.06)	0.77 (0.06)	17.530	**<.001**
DMN	0.67 (0.09)	0.66 (0.09)	0.66 (0.10)	0.74 (0.08)	25.035	**<.001**
Sub	0.81 (0.05)	0.80 (0.05)	0.81 (0.05)	0.85 (0.06)	4.346	**.020**
inter-IV$_{SC}$						
whole brain	0.37 (0.09)	0.35 (0.09)	0.36 (0.09)	0.40 (0.10)	29.509	**<.001**
VIN	0.32 (0.07)	0.31 (0.07)	0.32 (0.07)	0.36 (0.09)	6.627	**.002**
SMN	0.40 (0.06)	0.38 (0.06)	0.39 (0.06)	0.42 (0.08)	4.795	**.009**
DAN	0.37 (0.07)	0.35 (0.06)	0.37 (0.07)	0.39 (0.08)	2.343	.100
SAN	0.41 (0.11)	0.39 (0.11)	0.41 (0.11)	0.45 (0.13)	2.950	.056
LIN	0.31 (0.06)	0.29 (0.06)	0.31 (0.06)	0.35 (0.06)	7.981	**<.001**
FPN	0.35 (0.07)	0.33 (0.07)	0.35 (0.07)	0.38 (0.09)	6.718	**.002**
DMN	0.36 (0.10)	0.34 (0.10)	0.36 (0.10)	0.39 (0.10)	7.330	**<.001**
Sub	0.47 (0.13)	0.44 (0.12)	0.47 (0.13)	0.51 (0.14)	1.176	.319

Note: The mean value and standard deviation are represented as mean (*SD*). The between-group differences among age subgroups were examined by one-way ANOVA. A significant p-value is marked in bold. Adapted and modified from Zhang et al. (2025) (CC-BY). Abbreviations: inter-IV$_{FC}$/IV$_{SC}$, inter-individual variability of functional/ structural connectivity; VIN, visual network; SMN, somatomotor network; DAN, dorsal attention network; SAN, salience/ventral attention network; LIN, limbic network; FPN, frontoparietal control network; DMN, default mode network; Sub, subcortical network

3.2.2 PLSC Analyses for the Whole Group

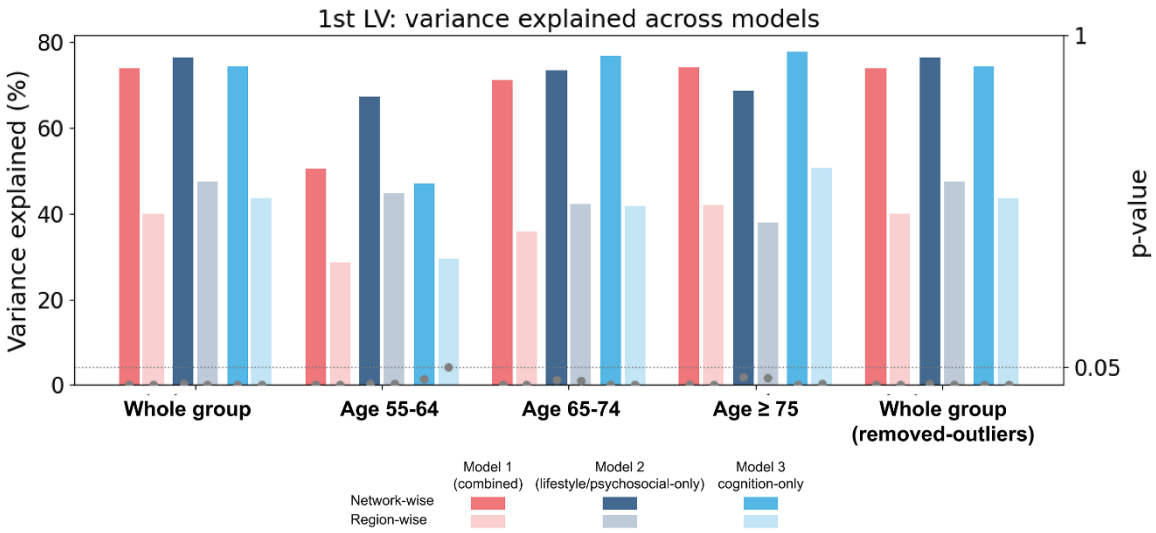

Figure 3.2.1 Explained variance and *p*-values of the first latent variable (LV1) in the whole group and three age subgroups. Gray dots represent the corresponding permutation-based *p*-values. The dotted horizontal line marks the significance threshold ($p = 0.05$).

Model 1 (combined model)

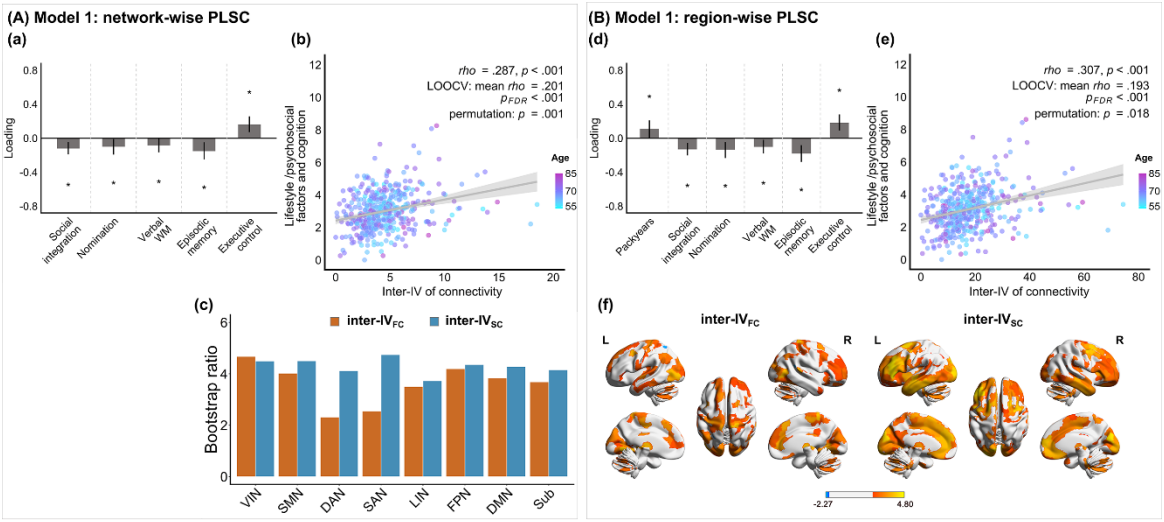

Figure 3.2.2 Network-wise (A) and region-wise (B) PLSC results for Model 1 in the whole group (*N* = 461). The first latent variable was used to examine latent relationships. **(a, d)** Loadings of lifestyle/psychosocial and cognitive variables with 95% confidence intervals (bootstrap). Only significant variables (*) are shown. **(b, e)** Scatterplots of covariance scores: inter-individual variability (inter-IV) of connectivity (*X*-axis) vs. lifestyle/psychosocial and cognitive scores (*Y*-axis), colored by age (55 – 85 years, light blue – pink). **(c)** Bootstrap ratio bar chart for network-wise inter-IV of functional (red) and structural connectivity (blue). **(f)** Brain maps of region-wise inter-IV of functional (left) and structural connectivity (right). Warm = positive, cool = negative; only significant regions (|ratio| > 1.96) are shown. Confounders (age, sex, education) were regressed out prior to PLSC. Figure adapted and modified from Zhang et al. (2025) (CC-BY). Abbreviations: rho, Spearman correlation coefficient; *ns*, non-significant contributions; Packyears, pack-years of smoking; WM, working memory

In Model 1, both network-wise and region-wise PLSC analyses identified a significant latent variable (LV1) reflecting shared variance between inter-IV of connectivity and lifestyle/psychosocial and cognitive functions. At the network level, the LV1 explained 73.89% of the variance ($p < .001$; Figure 3.2.1), with inter-IV of connectivity scores positively correlated with lifestyle/psychosocial and cognitive scores (rho = .287, $p < .001$). This effect remained robust after PLSCanonical with repeated LOOCV (mean rho = .201, $p_{FDR} < .001$) and permutation testing ($p = .001$). Variable loadings indicated a coherent behavioral pattern: greater inter-IV of connectivity was associated with lower social integration and poorer performance across multiple cognitive domains, including nomination, verbal working memory, episodic memory, and executive control (note that higher executive control scores indicate worse performance). Among connectivity measures, inter-IV_{SC} within the SAN showed the strongest contribution (bootstrap ratio = 4.745; panel A-C in Figure 3.2.2, Tables 3.2.3 and 3.2.4).

Region-wise analysis revealed a similar pattern, with LV1 explaining 40.1% of the variance ($p < .001$) and a positive correlation between region-wise inter-IV of connectivity and behavioral scores (rho = .307, $p < .001$; LOOCV: mean rho = .193, $p_{FDR} < .001$; permutation $p = .018$). Higher inter-IV of connectivity was linked to higher pack-years of smoking and lower social integration, along with lower performance across executive control, episodic memory, nomination, and verbal working memory domains. Positive inter- IV_{FC} contributions were observed in regions of the visual network (VIN), including the left fusiform gyrus (area FG3), left visual cortex (area hOc2/V2), and left subiculum. Inter-IV_{SC} contributions involved bilateral anterior cingulate cortex (area 33), the left inferior frontal gyrus (area 45), left frontal operculum (area OP9), and right visual cortex (area hOc2 and area hOc3d). In contrast, one lateral occipital region showed a negative inter-IV_{FC} contribution, indicating an inverse regional association pattern (panel D-F in Figure 3.2.2, Table 3.2.5).

Model 2 (lifestyle/psychosocial-only model)

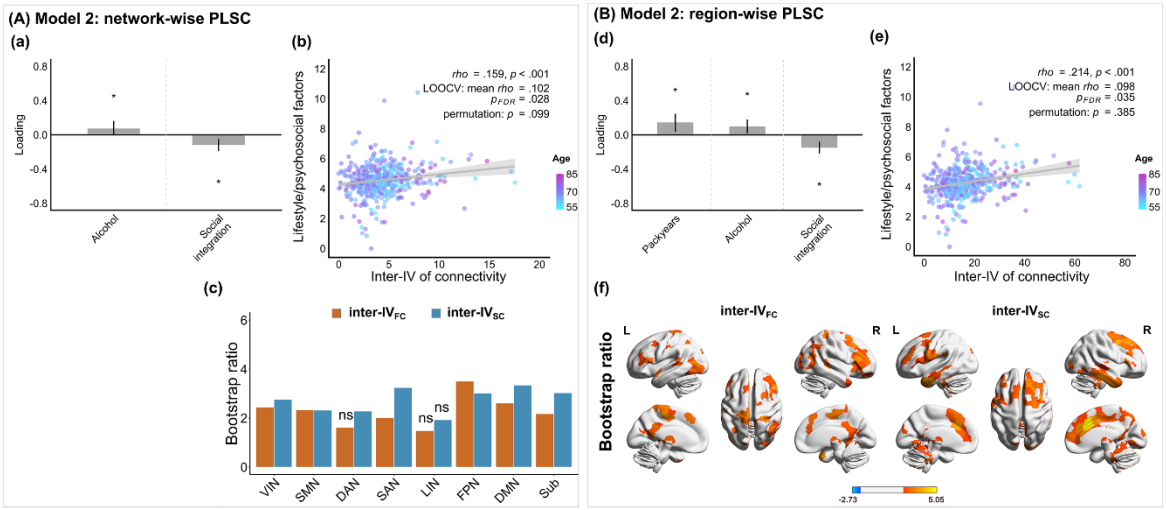

Figure 3.2.3 Network-wise (A) and region-wise (B) PLSC results for Model 2 in the whole group. The first latent variable was used to examine latent relationships. **(a, d)** Loadings of lifestyle/psychosocial variables with 95% confidence intervals (bootstrap). Only significant variables (*) are shown. **(b, e)** Scatterplots of covariance scores: inter-individual variability (inter-IV) of connectivity (*X*-axis) vs. lifestyle/psychosocial scores (*Y*-axis), colored by age (55–85 years, light blue–pink). **(c)** Bootstrap ratio bar chart for network-wise inter-IV of functional (red) and structural connectivity (blue). **(f)** Brain maps of region-wise inter-IV of functional (left) and structural connectivity (right). Warm = positive, cool = negative; only significant regions (|ratio| > 1.96) are shown. Confounders (age, sex, education) were regressed out prior to PLSC. Figure adapted and modified from Zhang et al. (2025) (CC-BY). Abbreviations: rho, Spearman correlation coefficient; ns, non-significant contributions; Packyears, pack-years of smoking

In Model 2, network-wise and region-wise analyses revealed convergent findings. At the network level, the LV1 explained 76.5% of the variance (p = .002), linking higher alcohol consumption and lower social integration to higher inter-IV_{FC} across six networks—most prominently the frontoparietal control network (FPN)—and higher inter-IV_{SC} across seven networks, especially the SAN, partially consistent with Model 1 (rho = .159, p < .001; LOOCV: mean rho = .102, p_{FDR} = .028; permutation p = .099) (panel A in Figure 3.2.3, Tables 3.2.3 and 3.2.4).

Region-wise analysis further showed that higher pack-years of smoking, greater alcohol consumption, and lower social integration were associated with increased inter-IV of connectivity in regions within somatomotor network (SMN) and FPN (rho = .214, p < .001; LOOCV: mean rho = .098, p_{FDR} = .035; permutation p = .385), including the right inferior frontal gyrus (area 45), medial prefrontal cortex, anterior cingulate cortex (area 33), left precentral gyrus (area 4a), right postcentral gyrus (area 1), and the precuneus (panel B in Figure 3.2.3, Table 3.2.5).

Model 3 (cognition-only model)

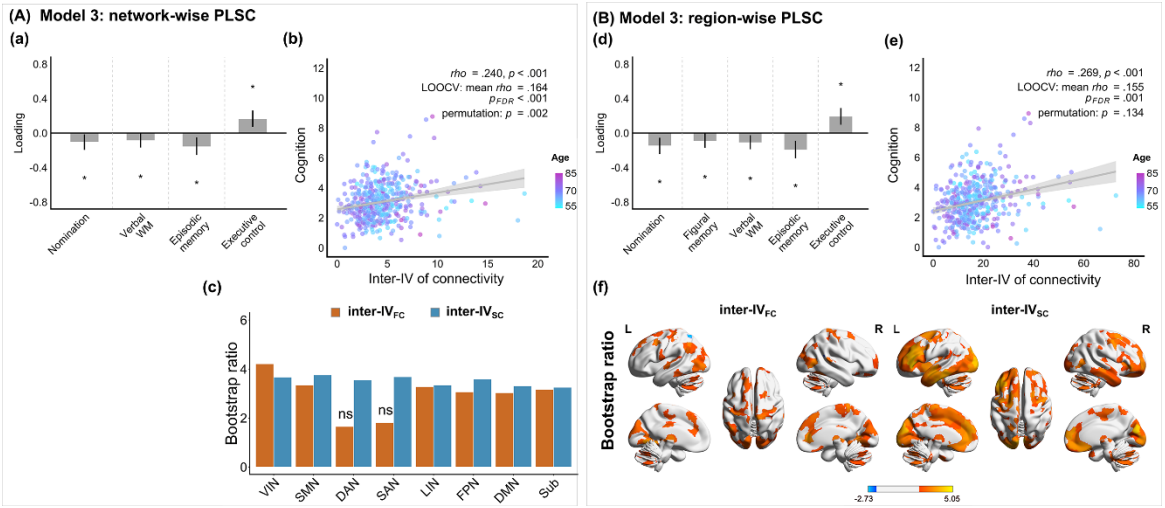

Figure 3.2.4 Network-wise (A) and region-wise (B) PLSC results for Model 3 in the whole group. The first latent variable was used to examine latent relationships. **(a, d)** Loadings of cognitive variables with 95% confidence intervals (bootstrap). Only significant variables (*) are shown. **(b, e)** Scatterplots of covariance scores: inter-individual variability (inter-IV) of connectivity (*X*-axis) vs. cognitive scores (*Y*-axis), colored by age (55 – 85 years, light blue – pink). **(c)** Bootstrap ratio bar chart for network-wise inter-IV of functional (red) and structural connectivity (blue). **(f)** Brain maps of region-wise inter-IV of functional (left) and structural connectivity (right). Warm = positive, cool = negative; only significant regions (|ratio| > 1.96) are shown. Confounders (age, sex, education) were regressed out prior to PLSC. Figure adapted and modified from Zhang et al. (2025) (CC-BY). Abbreviations: rho, Spearman correlation coefficient; ns, non-significant contributions; WM, working memory

In Model 3, both network-wise and region-wise analyses partially replicated the pattern observed in Model 1. In terms of network-wise analysis, higher inter-IV of connectivity was associated with poorer performance across nomination, verbal working memory, episodic memory, and executive control (rho = .240, $p < .001$; LOOCV: mean rho = .164, $p_{FDR} < .001$; permutation $p = .002$). The latent variable largely mirrored the inter-IV of connectivity pattern from Model 1, except for inter-IV_{FC} within the DAN and SAN (Figure 3.2.4; Tables 3.2.3 and 3.2.4).

Consistently, region-wise analysis showed that lower cognitive performance correlated with higher inter-IV of connectivity across widespread brain regions overlapping those identified in Model 1 (rho = .269, $p < .001$; LOOCV: mean rho = .155, $p_{FDR} = .001$; permutation $p = .134$; Figure 3.2.4; Table 3.2.5).

Overlapping regions

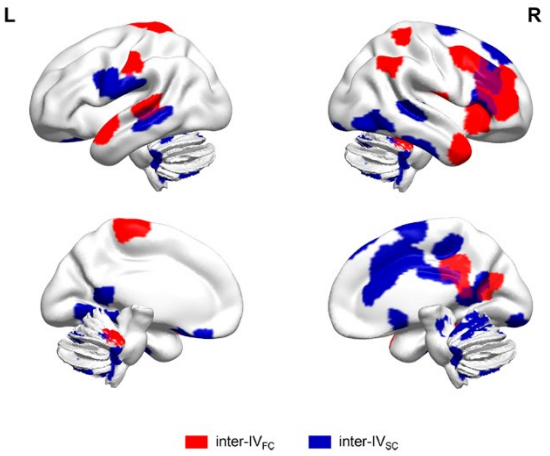

Figure 3.2.5 The overlapping regions of significant contributions from Model 1 (combined model) and Model 2 (lifestyle/psychosocial-only model) in the whole group. The red color signifies inter-IV of functional connectivity (inter-IV_{FC}), and the blue color represents inter-IV of structural connectivity (inter-IV_{SC}).

We overlaid the bootstrap-ratio brain maps from Models 1 and 2 to identify regions contributing to the relationship between inter-IV of connectivity and lifestyle/psychosocial factors. Although these regions may also support specific cognitive functions, the overlay primarily identifies brain areas shared between inter-IV of connectivity and lifestyle/psychosocial factors (Figure 3.2.5). The bootstrap ratio maps showed that inter-IV_{FC} contributions were mainly located in regions within the SMN, FPN, and default mode network (DMN), including the right frontal operculum and posterior opercular cortex (areas OP9/OP4), left superior and inferior parietal lobules (areas 5L/PFt), postcentral gyrus, and right lateral occipital cortex (area hOc5). In contrast, inter-IV_{SC} contributions were primarily observed in regions within the VIN, SAN, and DMN, such as the bilateral inferior frontal gyrus (area 44), left orbitofrontal cortex (area Fo2), right medial superior frontal gyrus (area 6ma), left posterior opercular cortex (area OP1), right superior parietal lobule (areas 5Ci/5M), right precentral gyrus (areas 4a/6d2), and right anterior cingulate cortex (area 33).

Table 3.2.3 Loading of the lifestyle/psychosocial factors, and/or cognition covariance pattern of the network-wise PLSC analysis in the whole group.

Variables	Model 1		Model 2		Model 3	
	Loading	CI (lower, upper)	Loading	CI (lower, upper)	Loading	CI (lower, upper)
Packyears	0.09	-0.01, 0.18	0.10	-0.01, 0.19	/	/
Alcohol	0.07	-0.01, 0.15	**0.07**	**4.65×10^{-5}, 0.16**	/	/
MET	-0.03	-0.12, 0.07	-0.03	-0.11, 0.07	/	/
Stairs	0.01	-0.06, 0.10	0.02	-0.06, 0.10	/	/
Social integration	**-0.12**	**-0.19, -0.05**	**-0.12**	**-0.19, -0.05**	/	/
Cognitive status	-0.01	-0.11, 0.09	/	/	-0.01	-0.11, 0.08
Language comprehension	-0.07	-0.18, 0.03	/	/	-0.07	-0.18, 0.03
Nomination	**-0.10**	**-0.19, -0.01**	/	/	**-0.10**	**-0.19, -0.02**
Figural memory	-0.06	-0.15, 0.03	/	/	-0.06	-0.14, 0.02
Verbal WM	**-0.09**	**-0.17, -1.33×10^{-3}**	/	/	**-0.08**	**-0.17, -9.20×10^{-4}**
Phonemic fluency	4.15×10^{-3}	-0.09, 0.09	/	/	3.79×10^{-3}	-0.09, 0.09
Phonemic switch	0.07	-0.03, 0.18	/	/	0.07	-0.03, 0.18
Semantic fluency	-0.02	-0.11, 0.07	/	/	-0.02	-0.11, 0.07
Semantic switch	0.03	-0.05, 0.12	/	/	0.03	-0.05, 0.11
Visuospatial WM	-0.02	-0.10, 0.07	/	/	-0.01	-0.10, 0.08
Episodic memory	**-0.15**	**-0.25, -0.05**	/	/	**-0.15**	**-0.26, -0.05**
Long-term memory	-0.04	-0.14, 0.05	/	/	-0.04	-0.14, 0.06
Executive control	**0.16**	**0.07, 0.26**	/	/	**0.16**	**0.07, 0.26**

Note: A significant loading is marked in bold. Adapted and modified from Zhang et al. (2025) (CC-BY). Abbreviations: CI, 95% confidence intervals; Packyears, pack-years of smoking; Alcohol, alcohol consumption; MET, metabolic equivalent of the task; Stairs, flights of stairs climbed; WM, working memory

Table 3.2.4 Bootstrap ratio of network-wise PLSC analysis in the whole group.

	inter-IV_{FC}			inter-IV_{SC}		
	Model 1	Model 2	Model 3	Model 1	Model 2	Model 3
VIN	**4.674**	**2.444**	**4.207**	**4.496**	**2.756**	**3.665**
SMN	**4.019**	**2.330**	**3.334**	**4.503**	**2.321**	**3.759**
DAN	**2.316**			**4.116**	**2.282**	**3.546**
SAN	**2.551**	**2.012**		**4.745**	**3.245**	**3.68**
LIN	**3.506**		**3.275**	**3.726**		**3.34**
FPN	**4.199**	**3.501**	**3.057**	**4.361**	**3.016**	**3.586**
DMN	**3.832**	**2.612**	**3.023**	**4.285**	**3.348**	**3.303**
Sub	**3.685**	**2.175**	**3.16**	**4.155**	**3.029**	**3.251**

Note: Bootstrap ratios are reported for the first latent variable (LV1) of each model and are shown only for networks exceeding the significance threshold (|bootstrap ratio| > 1.96). Positive values (red) indicate positive contributions, and negative values (blue) indicate negative contributions to the latent pattern. Empty cells indicate non-significant bootstrap ratios. Adapted and modified from Zhang et al. (2025) (CC-BY). Abbreviations: inter-$IV_{FC/SC}$, individual variability of functional/ structural connectivity; VIN, visual network; SMN, somatomotor network; DAN, dorsal attention network; SAN, salience/ventral attention network; LIN, limbic network; FPN, frontoparietal control network; DMN, default mode network; Sub, subcortical network

Table 3.2.5 Loading of the lifestyle/psychosocial factors and/or cognition covariance pattern of the region-wise PLSC analysis in the whole group.

	Model 1		Model 2		Model 3	
	Loading	**CI (lower, upper)**	**Loading**	**CI (lower, upper)**	**Loading**	**CI (lower, upper)**
Packyears	**0.11**	**0.01, 0.21**	**0.15**	**0.03, 0.25**	/	/
Alcohol	0.06	-0.02, 0.13	**0.10**	**0.02, 0.18**	/	/
MET	-0.03	-0.11, 0.07	-0.04	-0.13, 0.05	/	/
Stairs	0.01	-0.07, 0.09	0.01	-0.07, 0.10	/	/
Social integration	**-0.13**	**-0.20, -0.06**	**-0.15**	**-0.22, -0.08**	/	/
Cognitive status	-0.02	-0.12, 0.08	/	/	-0.03	-0.12, 0.07
Language comprehension	-0.10	-0.21, 0.01	/	/	-0.11	-0.21, 6.80×10^{-4}
Nomination	**-0.14**	**-0.23, -0.05**	/	/	**-0.14**	**-0.24, -0.06**
Figural memory	-0.08	-0.16, 4.90×10^{-3}	/	/	**-0.09**	**-0.17, -3.99×10^{-3}**
Verbal WM	**-0.10**	**-0.18, -0.02**	/	/	**-0.11**	**-0.19, -0.03**
Phonemic fluency	-0.02	-0.11, 0.07	/	/	-0.02	-0.11, 0.07
Phonemic switch	0.05	-0.05, 0.15	/	/	0.05	-0.06, 0.15
Semantic fluency	-0.04	-0.13, 0.04	/	/	-0.05	-0.13, 0.04
Semantic switch	0.01	-0.07, 0.10	/	/	0.01	-0.07, 0.09
Visuospatial WM	-0.03	-0.12, 0.06	/	/	-0.03	-0.12, 0.05
Episodic memory	**-0.18**	**-0.28, -0.08**	/	/	**-0.19**	**-0.29, -0.09**
Long-term memory	-0.07	-0.18, 0.02	/	/	-0.08	-0.17, 0.02
Executive control	**0.18**	**0.09, 0.28**	/	/	**0.19**	**0.10, 0.29**

Note: A significant loading is marked in bold. Adapted and modified from Zhang et al. (2025) (CC-BY). Abbreviations: CI, 95% confidence intervals; Packyears, pack-years of smoking; Alcohol, alcohol consumption; MET, metabolic equivalent of the task; Stairs, flights of stairs climbed; WM, working memory

3.2.3 PLSC Analyses for Age Subgroups

Model 1 (combined model)

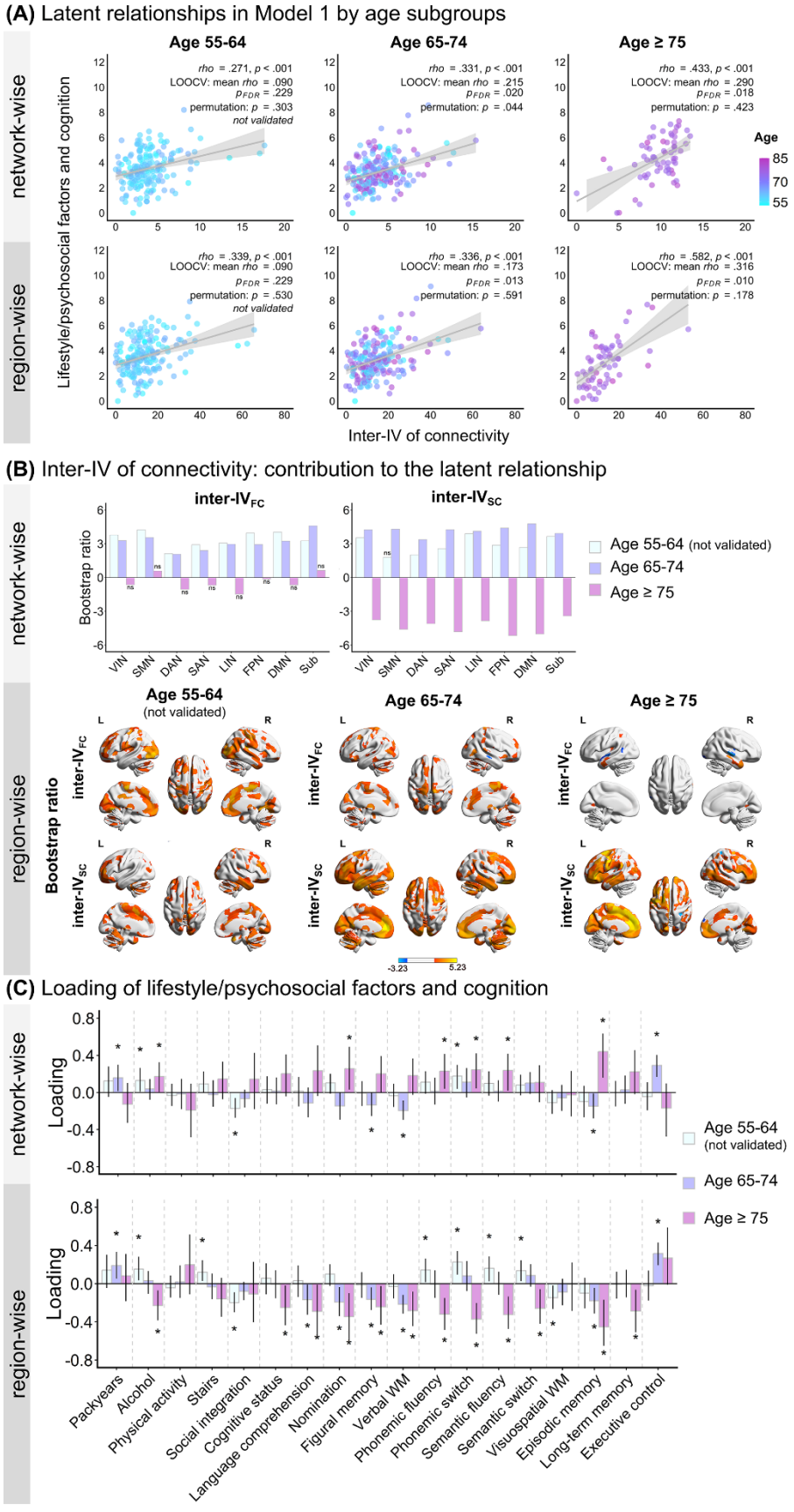

Figure 3.2.6 Network-wise and region-wise PLSC results (Model 1) across three age subgroups. (A) Scatterplots of covariance scores: inter-IV of connectivity (*X*-axis) versus lifestyle/psychosocial and cognitive scores (*Y*-axis) for ages 55–64, 65–74, and ⩾75. Colors indicate age subgroups, with darker shades representing older individuals within each subgroup. **(B)** Bootstrap ratio bar plots (up) for inter-IV of functional and structural connectivity. Brain maps (down) of region-wise inter-IV of functional (left) and structural connectivity (right). Warm = positive, cool = negative; only significant regions (|ratio| > 1.96) are shown. **(C)** Loadings of lifestyle/psychosocial and cognitive variables with 95% bootstrap confidence intervals. Significant variables are marked with *, and faded bars indicate effects not confirmed in validation analyses. Age, sex, and education were regressed out prior to PLSC. Figure adapted and modified from Zhang et al. (2025) (CC-BY). Abbreviations: IV, individual variability; rho, Spearman correlation coefficient; ns, non-significant contributions; Pack-years, pack-years of smoking; Alcohol, alcohol consumption; Physical activity, measured by metabolic equivalent of the task; Stairs, flights of stairs climbed; WM, working memory

Age-specific associations were observed between inter-IV of connectivity, lifestyle/psychosocial factors, and cognition in both network-wise and region-wise analyses. In the 55–64 age group, no validated associations were detected at either the network level or the regional level (Figure 3.2.6).

In the 65–74 age group, LV1 explained 73.9% of the variance ($p < .001$), with higher pack-years of smoking and poorer performance in figural memory, verbal working memory, episodic memory, and executive control associated with higher inter-IV of connectivity across eight networks, particularly inter-IV_{SC} of the DMN (Figure 3.2.6 and Table 3.2.6). Consistently, region-wise analyses showed that higher inter-IV_{SC} across widespread regions and inter-IV_{FC} in several regions were associated with greater smoking and poorer cognitive performance across six tests.

In participants aged 75 years and older, LV1 explained 74.1% of the variance at the network level ($p < .001$), indicating that higher alcohol consumption and better cognitive performance were both associated with lower inter-IV_{SC} across eight networks, especially within the FPN (Figure 3.2.6 and Table 3.2.6), while inter-IV_{FC} showed no significant contribution. Region-wise results further demonstrated that higher inter-IV of connectivity was linked to lower alcohol consumption and poorer performance across 11 cognitive tests, with key contributors including inter-IV_{FC} in the right superior temporal sulcus (area STS2) and inter-IV_{SC} of the left mesial superior frontal gyrus (area 6mp), frontal operculum (area OP9), precentral gyrus (area 6d2), and anterior cingulate cortex (area p32).

Model 2 (lifestyle/psychosocial-only model)

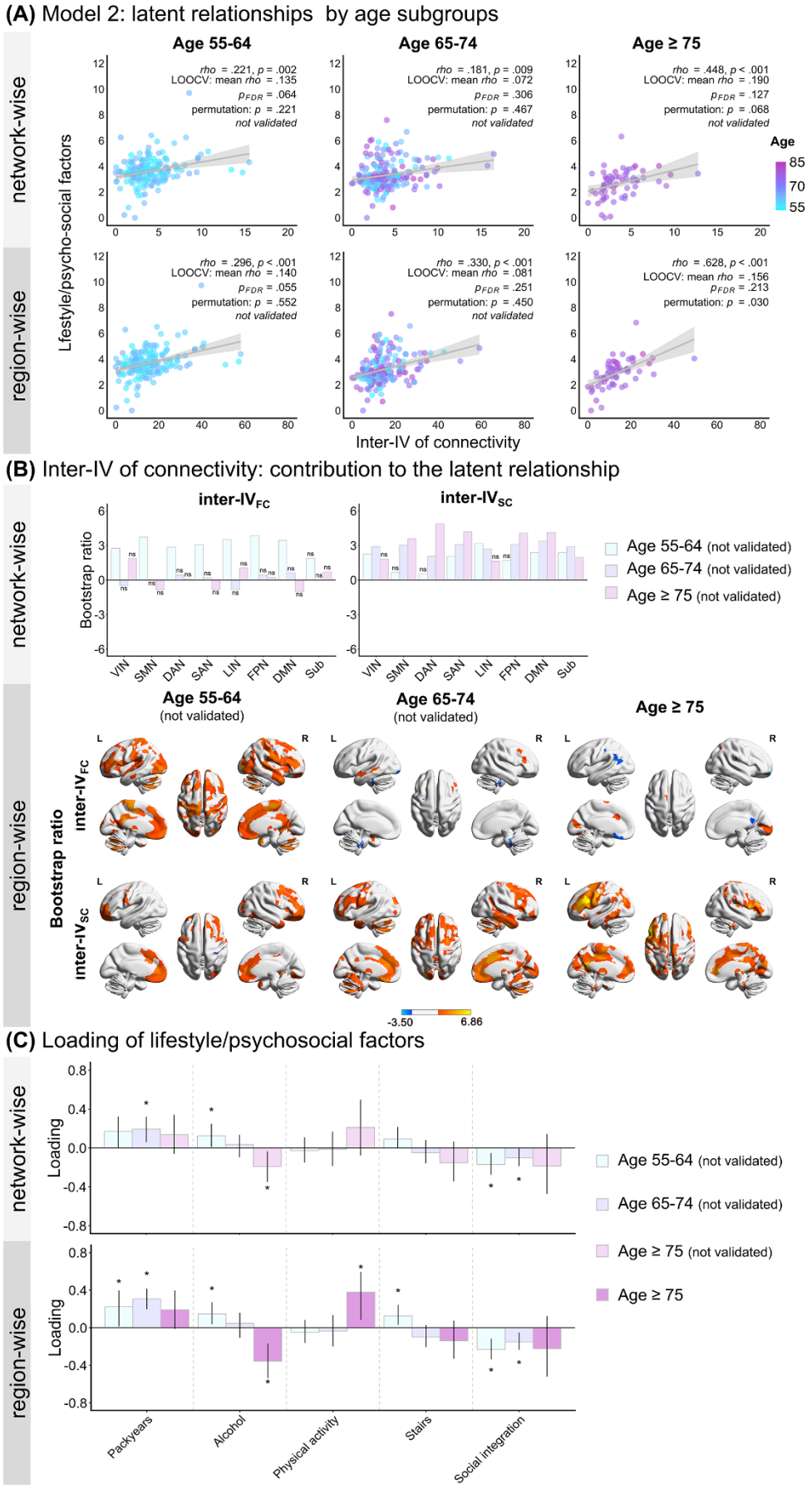

Figure 3.2.7 Network-wise and region-wise PLSC results (Model 2) across three age subgroups. (A) Scatterplots of covariance scores: inter-IV of connectivity (*X*-axis) versus lifestyle/psychosocial and cognitive scores (*Y*-axis) for ages 55–64, 65–74, and ≥75. Colors indicate age subgroups, with darker shades representing older individuals within each subgroup. **(B)** Bootstrap ratio bar plots (up) for inter-IV of functional and structural connectivity. Brain maps (down) of region-wise inter-IV of functional (left) and structural connectivity (right). Warm = positive, cool = negative; only significant regions (|ratio| > 1.96) are shown. **(C)** Loadings of lifestyle/psychosocial and cognitive variables with 95% bootstrap confidence intervals. Significant variables are marked with *, and faded bars indicate effects not confirmed in validation analyses. Age, sex, and education were regressed out prior to PLSC. Figure adapted and modified after Zhang et al. (2025). Abbreviations: IV, individual variability; rho, Spearman correlation coefficient; ns, non-significant contributions; Packyears, pack-years of smoking; Alcohol, alcohol consumption; Physical activity, measured by metabolic equivalent of the task; Stairs, flights of stairs climbed

In Model 2, no consistent network-wise associations were observed across age groups (Figure 3.2.7). At the region-wise level, however, significant effects emerged exclusively in participants aged 75 years and older, where lower alcohol consumption and higher physical activity were associated with higher inter-IV_{FC} in regions such as the right superior parietal lobule (area 7A), as well as increased inter-IV_{SC} across multiple regions, including the bilateral inferior frontal gyrus (areas 44 and 45).

Model 3 (cognition-only model)

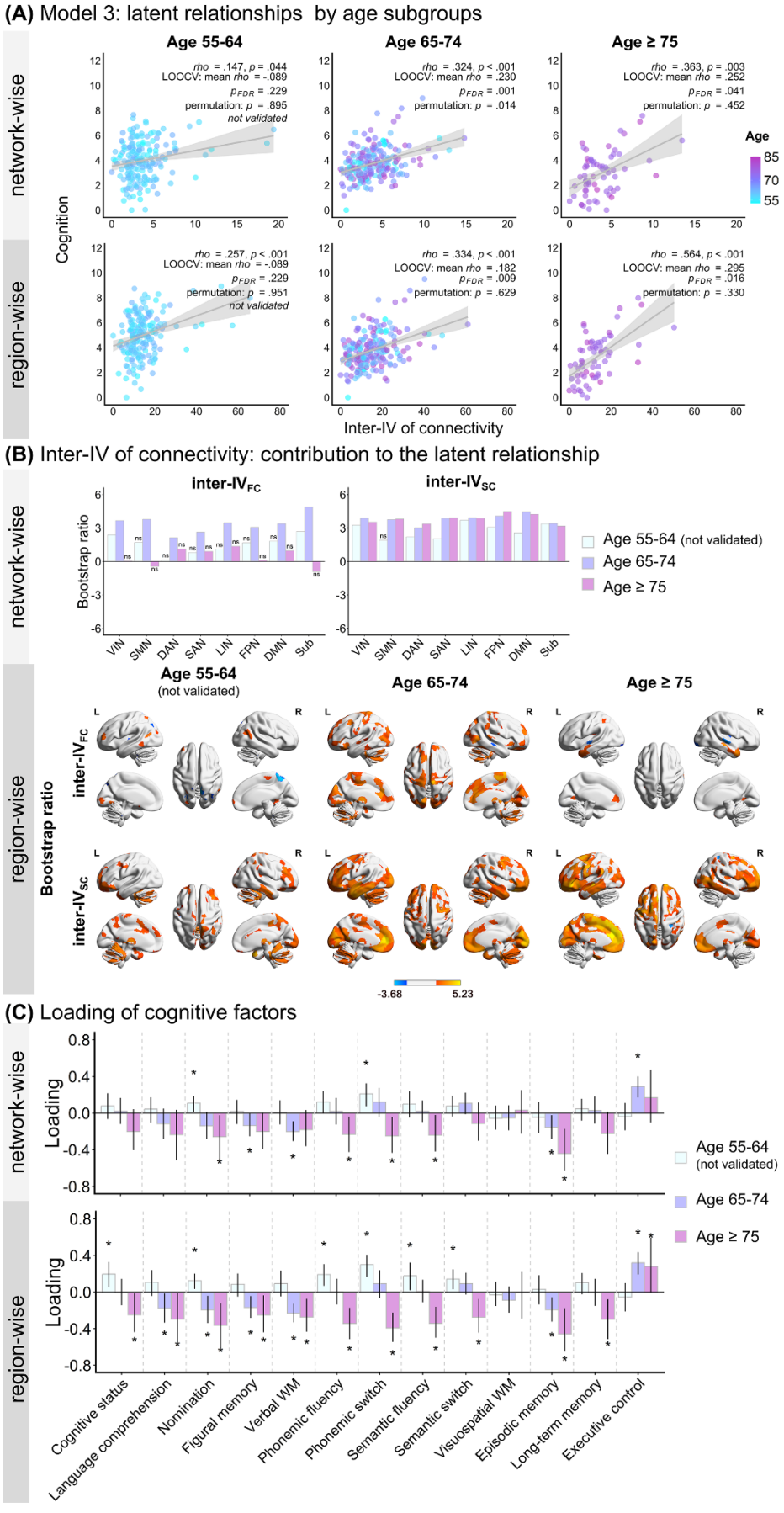

Figure 3.2.8 Network-wise and region-wise PLSC results (Model 3) across three age subgroups. (A) Scatterplots of covariance scores: inter-IV of connectivity (*X*-axis) versus lifestyle/psychosocial and cognitive scores (*Y*-axis) for ages 55–64, 65–74, and ⩾75. Colors indicate age subgroups, with darker shades representing older individuals within each subgroup. **(B)** Bootstrap ratio bar plots (up) for inter-IV of functional and structural connectivity. Brain maps (down) of region-wise inter-IV of functional (left) and structural connectivity (right). Warm = positive, cool = negative; only significant regions (|ratio| > 1.96) are shown. **(C)** Loadings of lifestyle/psychosocial and cognitive variables with 95% bootstrap confidence intervals. Significant variables are marked with *, and faded bars indicate effects not confirmed in validation analyses. Age, sex, and education were regressed out prior to PLSC. Figure adapted and modified from Zhang et al. (2025) (CC-BY). Abbreviations: IV, individual variability; rho, Spearman correlation coefficient; *ns*, non-significant contributions; WM, working memory

In Model 3, age-specific associations between inter-IV of connectivity and cognitive performance were observed in both network-wise and region-wise analyses. In the 55–64 age group, no validated associations were detected at either the network level or the regional level (Figure 3.2.8). Among participants aged 65–74 years, a robust pattern emerged: at the network level, both inter-IV_{FC} and inter-IV_{SC} were associated with poorer performance in figural memory, verbal working memory, episodic memory, and executive control (Figure 3.2.8 and Table 3.2.6). Consistently, region-wise analysis showed widespread inter-IV_{SC} contributions with less inter-IV_{FC} involvement.

Among participants aged 75 years and older, network-level effects were driven exclusively by inter-IV_{SC} and were primarily related to language-based cognitive measures (Figure 3.2.8 and Table 3.2.6). Region-wise results further revealed localized inter-IV_{FC} effects (e.g., the right superior temporal sulcus, area STS2) alongside inter-IV_{SC} contributions in the left orbitofrontal cortex (area Fo6) and anterior cingulate cortex (areas p24ab and p32), all of which were significantly associated with cognitive performance.

Table 3.2.6 Network-wise PLSC results showing bootstrap ratios of brain networks across three age subgroups.

Networks	inter-IV_{FC}			inter-IV_{SC}		
	Age 55-64	Age 65-74	Age ≥75	Age 55-64	Age 65-74	Age ≥75
Model 1						
VIN	3.781	3.291		3.537	4.244	-3.755
SMN	4.241	3.553			4.307	-4.6
DAN	2.117	2.076		2.011	3.374	-4.099
SAN	2.916	2.407		2.557	4.253	-4.82
LIN	3.069	2.963		3.905	4.128	-3.845
FPN	3.954	2.94		2.875	4.409	-5.159
DMN	4.036	3.238		2.683	4.786	-5.012
Sub	3.26	4.589		3.66	3.923	-3.412
Model 2						
VIN	2.76			2.261	2.906	
SMN	3.734				3.035	3.582
DAN	2.852				2.065	4.882
SAN	3.08			2.045	3.085	4.19
LIN	3.494			3.179	2.684	
FPN	3.849				3.103	4.073
DMN	3.436			2.385	3.376	4.129
Sub				2.374	2.882	1.973
Model 3						
VIN	2.395	3.669		3.256	3.888	3.532
SMN		3.788			3.758	3.81
DAN		2.141		2.204	3.009	3.369
SAN		2.637		2.043	3.866	3.915
LIN		3.47		3.711	3.918	3.866
FPN		3.079		3.072	4.083	4.48
DMN		3.399		2.574	4.452	4.237
Sub	2.688	4.889		3.375	3.42	3.18

Note: Bootstrap ratios are reported for the first latent variable (LV1) of each model and are shown only for networks exceeding the significance threshold (|bootstrap ratio| > 1.96). Positive values (red) indicate positive contributions, and negative values (blue) indicate negative contributions to the latent pattern. Empty cells indicate non-significant bootstrap ratios. Adapted and modified from Zhang et al. (2025) (CC-BY). Abbreviations: inter-$IV_{FC/SC}$, inter-individual variability of functional/ structural connectivity; VIN, visual network; SMN, somatomotor network; DAN, dorsal attention network; SAN, salience/ventral attention network; LIN, limbic network; FPN, frontoparietal control network; DMN, default mode network; Sub, subcortical network

3.2.4 Sensitivity Analyses

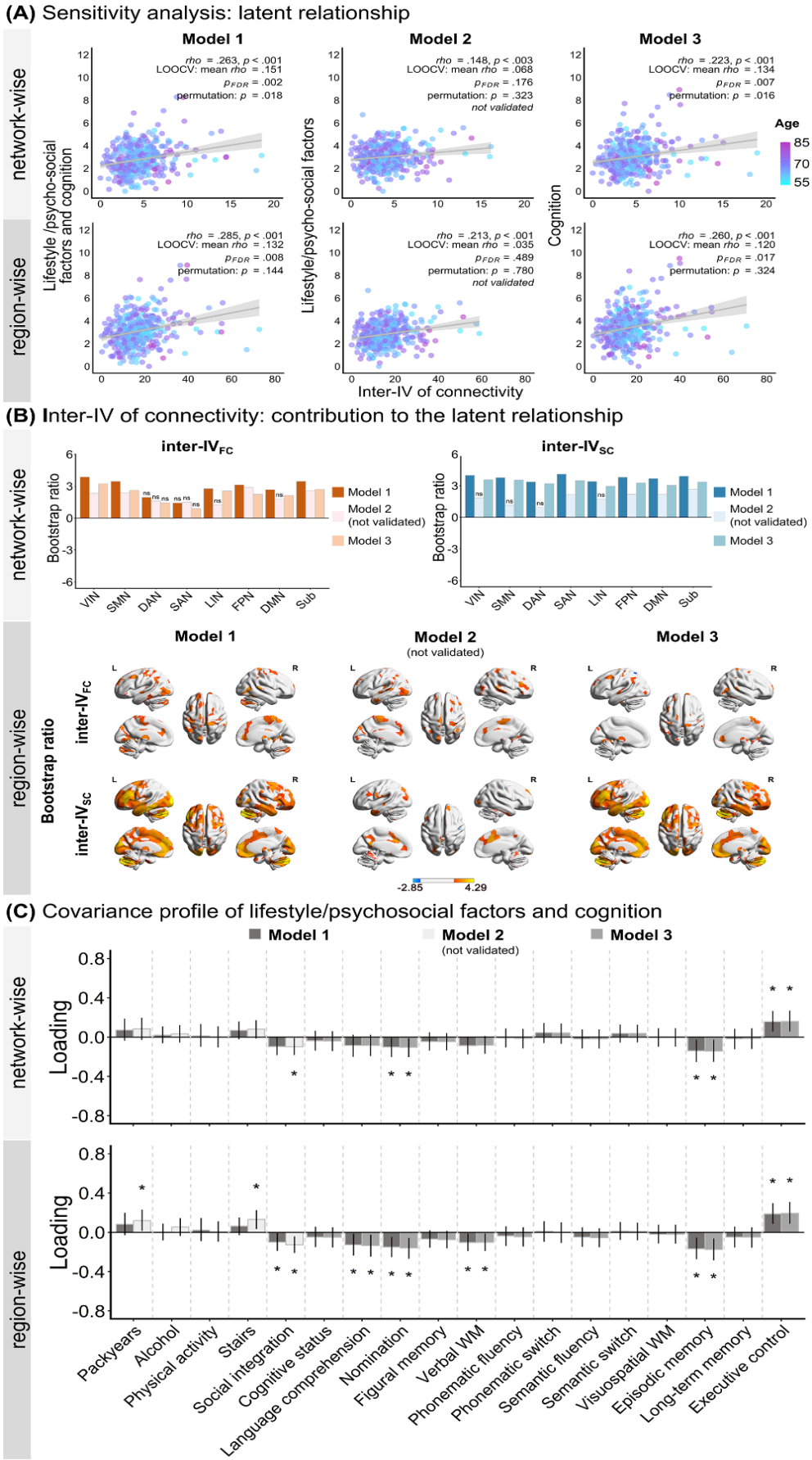

Figure 3.2.9 Sensitivity analysis: network-and region-wise PLSC analysis in 403 participants. **(A)** Covariance scatterplots showing inter-IV of connectivity (*X*-axis) versus lifestyle/psychosocial and cognitive scores (*Y*-axis). Colors indicate age subgroups, with darker shades representing older individuals. **(B)** Bootstrap ratio bar plots (up) for inter-IV of functional and structural connectivity. Brain maps (down) of region-wise inter-IV of functional (left) and structural connectivity (right). Warm = positive, cool = negative; only significant regions (|ratio| > 1.96) are shown. **(C)** Loadings of lifestyle/psychosocial and cognitive variables with 95% bootstrap confidence intervals. Significant variables are marked with *, and faded bars indicate effects not confirmed in validation analyses. Age, sex, and education were regressed out before PLSC. Figure adapted and modified from Zhang et al. (2025) (CC-BY). Abbreviations: IV, individual variability; rho, Spearman correlation coefficient; ns, non-significant contributions; Packyears, pack-years of smoking; Alcohol, alcohol consumption; Physical activity, measured by metabolic equivalent of the task; Stairs, flights of stairs climbed; WM, working memory

After excluding outliers, both network-wise and region-wise PLSC analyses were repeated. Overall patterns were qualitatively similar to the main analyses; however, at the network level, only the inter-IV of connectivity–cognition association in Model 3 remained consistent, whereas other network-wise associations were attenuated after outlier exclusion (Figure 3.2.9).

At the region-wise level, Model 1 continued to show that lower social integration and poorer performance in language comprehension, nomination, verbal working memory, episodic memory, and executive control were associated with higher inter-IV of connectivity; the inter-IV_{SC} distribution across significant brain regions was preserved, although inter-IV_{FC} effects were confined to the strongest contributors identified in the primary analysis. In Model 2, initial associations of higher pack-years, more flights of stairs, and lower social integration with inter-IV of connectivity were not validated following outlier removal. Consistent with the main results, Model 3 again demonstrated that poorer cognitive performance across several domains was associated with higher inter-IV of connectivity, with inter-IV_{SC} patterns closely matching the primary findings and inter-IV_{FC} contributions limited to the most robust regions.

3.3 Discussion

In this study, we used a multivariate approach to examine how inter-individual differences in functional and structural connectivity relate to lifestyle/psychosocial and cognitive factors in a large cohort of older adults. PLSC analyses at both the network and regional levels identified a latent variable linking higher smoking or lower social integration, poorer cognitive performance, and greater inter-individual variability of connectivity across the cohort. Analyses within age subgroups further clarified these relationships at different stages of late adulthood. The following discussion builds on the interpretation reported in Zhang et al. (2025).

3.3.1 Inter-Individual Variability of Brain Connectivity and Cognitive Functions

Emerging evidence suggests that associations between inter-individual variability of functional connectivity and cognition may differ across age groups, with negative associations reported in older adults (Ma et al., 2021). Our network-wise and region-wise analyses further demonstrated a negative association between cognitive performance and both inter-IV_{FC} and inter-IV_{SC} in older adults, extending previous findings. Importantly, this relationship appears to be age-heterogeneous in late life. Prior studies have shown higher inter-IV_{FC} in older than in younger adults (Ma et al., 2021) and an increasing inter-IV_{SC} with age (Sun et al., 2022). Consistent with this, we observed distinct inter-IV – cognition relationships across age subgroups, with the oldest subgroup showing the highest inter-individual variability, potentially reflecting deterioration in network efficiency and modularity (Damoiseaux, 2017; Deery et al., 2023; Ferreira & Busatto, 2013; Li et al., 2020; Ma et al., 2021) and less stability of inter-regional connections (Fu et al., 2023; Wise et al., 2017).

Region-wise analyses also indicated that widespread regions in frontal and occipital lobes contributed substantially to the inter-IV of connectivity – cognition relationship (see Figure 3.2.5). In the context of brain aging, such patterns may be associated with large-scale network reorganization. According to the Posterior-to-Anterior Shift in Aging (PASA) model, aging is accompanied by a compensatory redistribution of neural activity from posterior sensory regions toward anterior regions, particularly the prefrontal cortex (Davis et al., 2008; Perinelli et al., 2022; Zhang et al., 2017). However, our analysis does not allow inferences about the direction of connectivity changes. It may also be compatible with alternative frameworks, such as experience-

dependent compensatory reorganization involving anterior-to-posterior and subcortical shifts (Grundy et al., 2017). The specific directionality of these inter-individual differences and their underlying mechanisms remain unclear.

Finally, although inter-IV of connectivity could reflect unspecific noise, the observed associations with lower cognitive performance—particularly in episodic memory and executive control—suggest a link to neural inefficiency. Episodic memory relies on distributed systems, including the hippocampus and the default mode network (Nyberg, 2017), consistent with our findings. In contrast, studies reporting beneficial effects of higher BOLD signal variability focus on intra-individual temporal dynamics (Garrett, Kovacevic, et al., 2013; Goodman et al., 2024), which likely reflect compensatory processes (Spreng & Turner, 2019). By focusing on inter-individual variability, our results complement these approaches and underscore the importance of interpreting inter-IV of connectivity in relation to cognitive outcomes.

3.3.2 How Lifestyle/Psychosocial Factors Relate to Inter-IV in Aging

As discussed in the Introduction (Chapter 1.2), lifestyle and psychosocial factors may be an important source of increased brain heterogeneity in older adults. In the present study, lower social integration and poorer cognitive performance jointly contributed to a latent variable that covaried with higher network- and region-wise inter-IV of connectivity. This pattern is consistent with the revised scaffolding theory of aging and cognition (STAC-r), which posits that enriched environments, including social interaction, support the development and maintenance of compensatory neural scaffolding, whereas less engagement may compromise these mechanisms.

A growing body of evidence supports the protective role of social engagement for brain health during aging. Higher levels of social engagement have been linked to larger gray matter volumes, particularly in temporal and occipital regions (James et al., 2012), as well as increases in brain volume following social activity interventions (Mortimer et al., 2012). From a microstructural perspective, greater social engagement has been associated with lower mean diffusivity in the frontal and temporal regions, indicating greater gray matter integrity (Felix et al., 2021). Functional imaging studies further suggest that social engagement is associated with higher functional connectivity within the salience/ventral attention network, which partly mediates associations with

executive functioning and global cognition in non-demented older adults (Pruitt et al., 2022). However, despite this evidence, relatively few studies have examined social integration in relation to brain connectivity.

In addition to social integration, higher pack-years of smoking and lower cognitive performance jointly contributed to the latent variable that covaried with region-wise inter-IV of connectivity. Smoking may influence individual variability of brain connectivity through multiple pathways, including lower gray matter volume (Linli et al., 2023; Peng et al., 2018), white matter integrity (Gons et al., 2011), and accelerated brain aging (Bittner et al., 2021; Whitsel et al., 2022). Large-scale evidence from the UK Biobank (N = 19,415, age range: 45 – 78 years) indicates that smoking is associated with lower FC, particularly in frontal regions (Rolls et al., 2023). Longitudinal work further suggests that functional connectivity within frontal – insula circuits is related to smoking behavior, with connectivity between the anterior insula and ventromedial prefrontal cortex predicting long-term smoking reduction in older adults at risk for Alzheimer's disease (Thovinakere et al., 2024).

Within the STAC-r framework, smoking may be viewed as an adverse factor associated with reduced neural resources and less efficient compensatory scaffolding. However, the observed smoking-related effects in the present study were modest. Associations with pack-years of smoking were detected only in the region-wise PLSC analysis. They were not robust to sensitivity analyses excluding outliers, suggesting that these effects may be driven by extreme values rather than reflecting a strong population-wide association. This observation aligns with prior findings indicating that higher pack-years are primarily associated with accelerated brain aging in moderate to heavy smokers (Bittner et al., 2021).

Moreover, pack-years represent cumulative lifetime exposure and do not capture current smoking status; some participants with non-zero pack-years were no longer smokers, which may attenuate detrimental effects. Consequently, associations between smoking, cognition, and inter-IV of connectivity may be driven by both cumulative exposure and current behavior, which need to be further elucidated.

The STAC-r further emphasizes that aging outcomes reflect the combined influence of factors that either enrich or deplete neural resources. In this context, lower social integration and higher pack-years of smoking may exert additive or synergistic effects on compensatory scaffolding.

Consistent with this notion, large-scale studies have shown that healthier cardiovascular and lifestyle profiles are associated with lower dementia risk and better brain health, including larger brain volumes and less hippocampal atrophy (Sabia et al., 2019). Bittner et al. (2019) reported that social integration, together with smoking and alcohol consumption, contributed to higher FC in sensorimotor and prefrontal regions. Similarly, analyses of UK Biobank data identified brain aging components linked to modifiable risk factors such as smoking and alcohol consumption, which were also associated with poor cognitive performance (Smith et al., 2020). Extending these findings, our study highlights inter-IV of connectivity as an additional dimension of brain aging heterogeneity. Specifically, we identified a latent variable linking lower social integration, higher pack-years of smoking, and lower cognitive performance to higher inter-IV of connectivity, suggesting that accumulated modifiable risk factors may contribute not only to mean-level brain alterations but also to greater heterogeneity of brain reorganization. This interpretation is in line with evidence that cumulative lifestyle risks exert stronger effects on cognitive health than individual risk factors alone (Bittner et al., 2019; Kivipelto et al., 2001; Livingston et al., 2020).

Finally, to disentangle lifestyle-related effects from those driven primarily by cognition, we examined overlapping brain regions contributing to both the combined lifestyle – cognition model (Model 1) and the lifestyle-only model (Model 2). These overlapping regions may be particularly sensitive to factors associated with reduced neural resources, such as smoking and low social integration. Such sensitivity may reflect compromised compensatory scaffolding mechanisms, manifested as higher inter-individual variability of connectivity and lower cognitive performance. Nonetheless, given the cross-sectional design and the possibility of factors not included in the present analyses (e.g., socioeconomic status, vascular risk factors), these interpretations should be considered cautiously. Longitudinal studies are needed to clarify potential causal pathways linking lifestyle and psychosocial factors, inter-IV of connectivity, and cognition in older adulthood.

3.3.3 Age-Specific Patterns of Results

In the current study, we observed age-dependent differences in the contribution of inter-IV of connectivity to the relationship between lifestyle/psychosocial factors and cognition. Overall, with older age, the contribution of inter-IV of functional connectivity (inter-IV_{FC}) to the model became less important in older adults, involving fewer brain regions and smaller cluster sizes compared to

inter-IV of structural connectivity (inter-IV_{SC}) (Figure 3.2.6). This pattern suggests that individual variability of structural connectivity may better capture age-related differences in brain integrity, likely reflecting heterogeneity in the rate and spatial pattern of brain structural degeneration among older individuals. Consistent with previous studies showing reduced structural connectivity with age (Damoiseaux, 2017; Gong et al., 2009; Zhao et al., 2015), these changes appear to follow a more directionally consistent trajectory than functional connectivity.

Our findings align with Hebling Vieira et al. (2022), who demonstrated that combining baseline structural imaging with non-brain data improved prediction of cognitive decline, whereas adding FC did not provide additional benefit. Compared with SC, the relatively less contribution of FC in older age may be attributable to its non-linear, variable, and dynamic characteristics. In aging, functional connectivity may undergo adaptive reorganization to compensate for white matter degeneration, thereby supporting cognitive performance (Cabeza et al., 2018; Jauny et al., 2024). However, such compensatory changes can occur in different directions, including both increases and decreases in FC (Ferreira & Busatto, 2013; Geerligs et al., 2014; Jockwitz & Caspers, 2021; Stumme et al., 2022), making the relationship between inter-IV_{FC}, behavior, and cognition difficult to capture using linear models. For instance, FC tends to be lower with age in the default mode, cingulo-opercular, and frontoparietal control networks, but may remain stable or even higher in somatomotor and visual networks (Geerligs et al., 2015). In contrast, healthier lifestyle factors show a clearer association with larger brain volumes years later as reported in a recent work (Mulugeta et al., 2022). Similarly, the contribution of inter-IV_{SC} as a structural metric, which showed greater importance with older age in our models, is likely easier to interpret with a linear model than that of inter-IV_{FC}. Importantly, these findings do not negate the predictive value of FC; rather, they highlight the conditions under which FC becomes a more challenging predictor of cognition in aging.

Specifically, in the younger group (55–64 years), preliminary associations between inter-IV of connectivity, lifestyle/psychosocial factors, and cognition did not survive validation and should be considered exploratory. This may indicate that such relationships are either absent or too subtle to detect in this transitional age period. Increased heterogeneity related to retirement, physical health, psychosocial context, and environmental exposures not included in the present analyses may obscure early effects. Moreover, age-related changes in brain and behavior may follow nonlinear trajectories, with more pronounced and detectable effects emerging after age 65 and reflecting

accumulated lifestyle-related risk.

In the 65 – 74 group, higher pack-years of smoking, combined with lower cognitive performance (e.g., figural memory, verbal working memory, episodic memory, and executive control), were associated with higher network-wise and region-wise inter-IV of connectivity, consistent with results from the full sample. In contrast, social integration did not contribute significantly to this subgroup or to the oldest group, potentially due to reduced statistical power in smaller samples.

In participants aged ⩾75 years, negative associations between alcohol consumption and cognitive performance were primarily linked to inter-IV_{SC} rather than inter-IV_{FC}, highlighting increased vulnerability to structural connectivity decline in advanced age. Unlike younger-old participants, in whom functional connectivity may compensate for structural impairments, the oldest participants may exhibit reduced FC flexibility. They may no longer counteract SC decline, as suggested in previous studies (e.g., Lavanga et al., 2023).

Regarding alcohol consumption, although extensive literature indicates accelerated cognitive decline in older drinkers (Han & Jia, 2021; Listabarth et al., 2022; Sabia et al., 2014; Topiwala et al., 2017), we observed a counter-intuitive negative correlation between alcohol consumption, inter-IV of connectivity, and cognition in the oldest group. This effect was not explained by generally lower drinking levels in this group (Table 3.2.1). Potential explanations include selective survival, higher cognitive reserve (Zijlmans et al., 2022), or reverse directionality, whereby individuals experiencing cognitive decline tend to reduce alcohol intake under health recommendations. However, given the small sample size (n = 66) and potential confounding, this finding should not be interpreted as evidence of the beneficial effects of alcohol consumption. Indeed, prior work suggests that any level of drinking may increase cognitive risk in older adults (Hassing, 2018). Moreover, smaller samples are known to yield larger observed effects due to increased sampling variability (Slavin & Smith, 2009), which may partly explain the stronger effects observed in this age group. Larger samples are needed to validate these findings.

In summary, unlike previous large-scale studies focusing on single lifestyle factors or a composite lifestyle score (Gons et al., 2011; Linli et al., 2023; Mulugeta et al., 2022; Rolls et al., 2023; Whitsel et al., 2022), the present study provides a novel perspective by examining multimodal inter-IV of connectivity and its relationship with cognition and multiple lifestyle/psychosocial

factors. By extending evidence on inter-IV_{FC} and inter-IV_{SC} from younger populations to healthy adults aged $\geqslant 55$ years and refining age-specific patterns, we demonstrate that individual variability of connectivity captures meaningful associations that may be obscured in analyses of the whole sample. Linking multimodal inter-IV of connectivity to lifestyle and cognition offers empirical support for the STAC-r theory and provides a foundation for developing personalized interventions targeting cognitive aging.

However, when interpreting the research findings, it is important to note that we did not, as in previous studies, regress out intra-individual variability (intra-IV) of connectivity—typically estimated from multiple scans within a short time window—from inter-IV (Chamberland et al., 2017; Huang et al., 2025; Li et al., 2017; Ma et al., 2021; Sun et al., 2022). Although some studies split a single session into two halves to estimate intra-IV and remove it as noise (T. Xu et al., 2019; Y. Xu et al., 2019), we retained full scan durations to preserve signal-to-noise ratio and statistical power, as shorter time series reduce the reliability of functional connectivity estimates (Birn et al., 2013; Mueller et al., 2015). Consequently, the inter-IV distribution observed here cannot be directly compared with prior reports (see Table 3.2.2). Replication in external cohorts, such as the German National Cohort (NAKO) or the UK Biobank, is therefore warranted.

3.4 Conclusions

Overall, our study identified latent variables that link inter-individual differences of brain connectivity with lifestyle and psychosocial factors, as well as with cognitive functions. Specifically, greater inter-individual variability of connectivity—at both the network and regional levels—was associated with lower social integration and/or higher pack-years of smoking, as well as poorer cognitive performance across multiple domains, particularly episodic memory and executive control. The patterns of these associations varied across age subgroups. In the 65–74 age group, inter-IV of connectivity was positively correlated with smoking, whereas in the oldest age group, it was negatively correlated with alcohol consumption. With aging, inter-IV_{SC} tended to contribute more strongly to the latent associations than inter-IV_{FC}. These findings provide empirical support for the STAC-r theory, suggesting that unhealthier lifestyles may be associated with greater inter-individual variability of connectivity in older adults, potentially reflecting differences in neural resources and co-occur with poorer cognitive performance. However, these findings require replication in independent cohorts, and further research is needed to clarify the causal relationships among these factors.

Chapter 4: Individual Variability of Brain Connectivity as a Mediator between Network Segregation and Executive Control

Maintaining executive control, in later life, is critical for older adults' independence in daily functioning and quality of life. Age-related differences in executive control have been closely linked to functional and structural reorganization of large-scale brain networks (Gallen et al., 2016; Xia et al., 2022), particularly within association systems supporting executive processing, including the frontoparietal control network, the cingulo-opercular network, and the salience/ventral attention network (Gratton et al., 2018; Hausman et al., 2022). Within executive control, set shifting—often described as cognitive flexibility—is a core component that shows reliable age-related decline. Age-related alterations in functional network organization have been associated with reduced shifting performance (Xia et al., 2024). Network segregation, indexing the balance between within- and between-network connectivity, has emerged as a useful systems-level metric for quantifying these organizational changes and their impact on shifting performance (Chan et al., 2014).

Cross-sectional studies of functional connectivity consistently report age-related differences in network segregation, with older adults showing lower segregation compared to younger adults, which is often interpreted as reflecting neural dedifferentiation and has been associated with worse cognitive performance (see Koen et al., 2020; Rakesh et al., 2020, for reviews). However, findings within the domain of executive control remain mixed. While some studies report positive associations between functional network segregation and executive performance (e.g., Cohen & D'Esposito, 2016; M. Schulz et al., 2024), others suggest that network segregation mediates the association between age and executive control (e.g., Madden et al., 2020; Stumme et al., 2020), whereas still others report weak or non-significant relationships (e.g., Chong et al., 2019; Ng et al., 2016).

By contrast, emerging evidence regarding age-related patterns of structural network segregation is less consistent across studies. Although some work reports lower structural segregation in older relative to younger adults (e.g., Khalilian et al., 2024; Rodriguez-Nieto et al.,

2025), other studies describe more complex or non-monotonic age-related patterns, including findings consistent with higher structural segregation in later life, observed in both cross-sectional and longitudinal analyses (e.g., Coelho et al., 2021; Puxeddu et al., 2020). Notably, this heterogeneity may partially reflect methodological differences in how network segregation is operationalized in studies. Specifically, "segregation" has been quantified using graph-theoretical metrics, such as modularity and system segregation (Wig, 2017), while related measures, including participation coefficient (reflecting integration), hubs, and local efficiency, have also been used or interpreted in this context, as noted in prior methodological discussions (Rubinov & Sporns, 2010), potentially contributing to mixed findings.

Nevertheless, converging evidence indicates that age-related differences in white matter microstructure are closely associated with executive control in aging (see review in Bennett & Madden, 2014). Moreover, several recent studies across diverse populations, including typically developing samples and older adults, suggest that higher structural network segregation may be associated with better executive performance (e.g., Baum et al., 2017; Matyi et al., 2025; Rodriguez-Nieto et al., 2025), although further evidence is needed.

As described in Chapter 1.3, age-related network reorganization is also characterized by substantial variability in connectivity, which can be examined at both the inter-individual level (between-person dissimilarity) and the intra-individual level (within-person dissimilarity over time). However, it remains unclear how individual differences in connectivity relate to large-scale network segregation and executive control in healthy aging. To address this gap, the present study investigates whether inter- and intra-individual variability in brain connectivity mediate the relationship between large-scale network segregation and executive control in older adults, and whether this mediation is moderated by age. In the present study, executive control is operationalized via its set-shifting component, indexed by performance on the Trail Making Test Part B minus Part A (TMT B–A), a widely used measure of cognitive flexibility in aging research (Ashendorf et al., 2008).

4.1 Methods

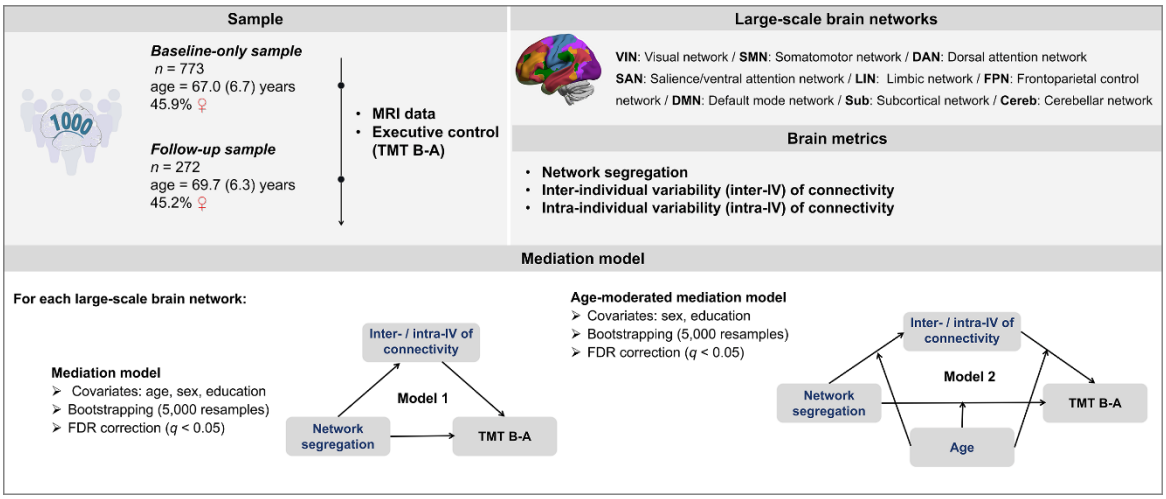

Figure 4.1.1 Overview of the study methodology. Top: Sample characteristics and construction of structural (SC) and functional (FC) connectivity matrices using 421 brain regions (400 cortical, 14 subcortical, 7 cerebellar). Middle: Calculation of brain metrics, including network segregation, inter- individual variability (inter-IV), and intra-individual variability (intra-IV) of connectivity within large-scale brain networks. Bottom: Mediation models (Model 1) and moderated mediation models were built for FC and SC separately within each network.

4.1.1 Sample and Data

Sample

At visit 1, participants younger than 55 years or with missing age information (n = 345) were excluded, resulting in 969 individuals aged ≥55 years. Participants with potential cognitive impairment were excluded (DemTect score ⩽ 8 or missing; n = 31; Kalbe et al., 2004), leaving 938 participants. Of these, 851 participants had available structural MRI, diffusion MRI, and rs-fMRI. Seventy-two participants were excluded because their imaging data did not yield usable connectivity measures. One participant with missing education information was excluded. Five participants missing the Trail Making Test (TMT) assessment were excluded. The final baseline sample comprised 773 participants (aged 67.0 ± 6.7 years, 355 females). At visit 2, 369 participants aged ⩾ 55 years at both visits were available. An additional 10 participants were excluded for potential cognitive impairment. Of this eligible sample, 295 participants had structural MRI, diffusion MRI, and rs-fMRI data available at both visits for connectivity analyses. Twenty-three participants were excluded because their imaging data did not yield usable connectivity measures. No missing values were observed for the TMT assessment at follow-up. The final study sample

comprised 272 participants with follow-up data (aged 69.7 ± 6.3 years, 123 females; see Table 4.2.1).

Trail Making Test

For the present analyses, executive control was operationalized as set-shifting ability measured using the Trail Making Test (TMT) B–A difference score (Ashendorf et al., 2008; Reitan, 1958), consistent with Study 1. The B–A score represents the difference in completion time (seconds) between TMT Part B and Part A and is commonly used to isolate set-shifting ability while reducing the influence of processing speed.

MRI brain data

Preprocessed rsfMRI was used to evaluate functional connectivity following the same procedure in the first study (see details in Chapter 3.1.2).

Compared to Study 1, the processing steps of the diffusion pipeline remained similar, despite the pipeline for the current study using a more recent Mrtrix (v3.0.4) with several refinements. First, Gibbs artifacts were reduced from the baseline images (b = 0 s/mm²) of both dMRI data sets using MRtrix3's *mrdegibbs* tool (Bautista et al., 2021; Kellner et al., 2016). Second, Motion and eddy-current correction were extended by incorporating slice-to-volume registration to improve motion correction at the slice level (Andersson et al., 2017). Third, non-linear registration was performed between the baseline images of the b = 1000 and b = 2700 s/mm² shells to account for geometric distortions arising from differences in the sequence parameters of the two diffusion shells. Linear and non-linear spatial transformations were combined and applied in a single reslicing step (1.25 mm³ isotropic resolution) to avoid repeated interpolation of the diffusion signal. Finally, an updated signal-normalization procedure was used to harmonize signal intensities between shells prior to their combination. Streamline tractography and structural connectivity reconstruction followed the procedures described in Study 1 (see Chapter 3.1.2 for details).

4.1.2 Network Segregation

For each large-scale brain network, we calculated network-wise within- and between-network connectivity, and network segregation for both FC and SC matrices. Calculations were performed separately for FC and SC. Specifically, FC matrices were first Fisher-z transformed, followed by taking the absolute value, to address the issue of positive and negative weights mutually inhibiting each other when estimating strength. SC matrices were log10 transformed (see Chapter 3.1.2).

Unlike the first study, cerebellar regions were treated as a separate network to additionally examine cerebellum-specific patterns, resulting in nine distinct networks in the present study.

(i) Within- and between network connectivity

Within-network connectivity was defined as the mean connectivity among nodes within a network, whereas between-network connectivity was defined as the mean connectivity between nodes of that network and all other networks.

(ii) Network segregation score

Network segregation quantifies the balance between within-network and between-network connectivity (Chan et al., 2014). We used the following general formula, applicable to both FC and SC:

$$\text{Segregation} = \frac{\overline{W} - \overline{B}}{\overline{W}}$$

where, $\overline{W}$ is the average connectivity of all within-network connections; $\overline{B}$ is the average connectivity of all between-network connections.

Positive segregation values (>0) indicate that within-network connections are stronger than between-network connections ("segregated"), whereas negative values indicate stronger between-network connections ("integrated"). A value of 1 occurs when there is no between-network connectivity. These calculations were performed using custom R scripts (R version 4.4.0; Glaubitz et al. (2022); Stumme et al. (2022)).

4.1.3 Individual Variability of Connectivity

Inter-individual variability (inter-IV)

Inter-IV of connectivity was computed following the procedure described in Chapter 3.1.2.

Intra-individual variability (intra-IV)

Intra-IV of connectivity was calculated following a logic similar to inter-IV of connectivity (Mueller et al., 2013; Sun et al., 2022), but quantified within-participant changes in connectivity across repeated scans. Each participant underwent two scans per modality, with an interval of approximately four years.

Take FC as an example, for each participant *m* and brain region (node) *i*, intra-IV_{FC} was defined as one minus the absolute correlation between the node's connectivity profiles across the two scans:

$$\text{intra} - \text{IV}_{FCi}\_m = 1 - \left| corr(FC_{i,1_m}, FC_{i,2}\_m) \right|$$

where $\text{FC}_{i,1}$ and $\text{FC}_{i,2}$ denote the connectivity profiles of node *i* at the first and second scans, respectively. The absolute value ensured that low similarity (regardless of direction) consistently corresponded to high variability. Raw intra-IV values were then regressed out scan interval for each node, retaining absolute residuals as time interval-adjusted intra-IV estimates. The same procedure was applied to structural connectivity to derive intra-IV_{SC}, yielding subject-by-region matrices used in subsequent analyses.

To assess the spatial distribution of inter- and intra-IV of connectivity, group-level inter- and intra- IV of connectivity estimates were derived (Figure 4.2.1).

4.1.4 Statistics and Sensitivity Analyses

Partial correlations were used to examine associations among key variables, controlling for sex and education; correlations involving age were computed without controlling for age. The significance threshold was set to $p < 0.05$ (two-tailed), with multiple comparison corrections applied across networks using the false discovery rate within each modality (FDR, $q < 0.05$).

Model 1 examined whether inter- and intra-IV of connectivity (inter/intra-IV_{SC} and inter/intra-IV_{FC}) mediate the association between network segregation and TMT B–A score within each large-scale brain network. Model 2 extended this framework by modeling age as a continuous moderator of the mediation pathways. In Model 1, age, sex, and education were included as covariates. In Model 2, sex and education were retained as covariates, and age was specified as a moderator through interaction terms for the respective mediation paths. Significant interaction effects were probed by estimating conditional path coefficients at the sample mean of age and at one standard deviation below and above the mean. For descriptive purposes, these reference points correspond to −1 SD (younger-old), the mean age (mean-age), and +1 SD (older-old). Moderated mediation was further evaluated by estimating conditional indirect effects of network segregation on TMT B–A score via IV of connectivity at these same reference values of age.

Mediation and moderated mediation analyses were conducted using the PROCESS macro (version 4.0; Model 4 and Model 59) for SPSS (Hayes, 2017), with 5,000 bias-corrected bootstrap resamples used to estimate indirect effects.

To facilitate interpretation, Trail Making Test B–A scores were multiplied by −1 so that

higher values indicated better set shifting in terms of executive control. Continuous predictors, mediators, outcomes, and education were z-standardized in all analyses. Age was z-standardized in Model 1 and mean-centered in Model 2, where it served as the moderator. Sex (0 = male, 1 = female) was included as a binary covariate. Indirect effects were considered statistically significant if their 95% bias-corrected bootstrap confidence intervals, derived from 5,000 resamples, did not include zero.

Correction for multiple comparisons was applied according to the structure of each analysis. FDR correction ($q < .05$) was applied across the nine networks for all effects in Model 1. For indirect effects, approximate two-sided *p*-values were computed based on the bootstrap standard error of the indirect effect estimate ($z = \text{indirect}/\text{BootSE}$; $p = 2 \times [1 - \Phi(|z|)]$) (MacKinnon, 2012) to enable FDR correction across networks. In Model 2, primary path effects (a, b, and c′) and age-moderated interaction terms were likewise FDR-corrected across networks. Simple slope analyses probing significant age-moderated paths were FDR-corrected across the three age levels within each network. Conditional indirect effects were FDR-corrected across networks separately at each reference value of age.

Sensitivity analyses were conducted by rerunning all models after excluding participants with TMT B–A scores exceeding three standard deviations from the sample mean; after outlier removal, the analytic samples included $n = 761$ for inter-individual variability of connectivity analyses (mean age = 66.9 ± 6.7 years; 45.5% female) and $n = 266$ for intra-individual variability of connectivity analyses (mean age = 69.1 ± 6.8 years; 43.0% female).

4.2 Results

4.2.1 Sample Characteristics: Demographic, Cognitive, and Brain Variables

Table 4.2.1 Sample characteristics of baseline and follow-up data.

	Baseline-only data	Follow-up data	
Full sample	**Baseline (*n* = 773)**	**Baseline (*n* = 272)**	**Follow-up (*n* = 272)**
Age (years)	67.0 (6.7)	66.0 (6.3)	69.7 (6.3)
Females (*n*, %)	355 (45.9%)	123 (45.2%)	123 (45.2%)
Education (ISCED)	6.49 (1.96)	6.74 (1.94)	6.75 (1.95)
TMT B–A score (seconds)	53.99 (40.75)	48.48 (33.18)	49.36 (31.34)
Outlier-removed sample	**Baseline (*n* = 763)**	**Baseline (*n* = 266)**	**Follow-up (*n* = 266)**
Age (years)	66.9 (6.7)	65.9 (6.4)	69.7 (6.3)
Females (*n*, %)	348 (45.7%)	120 (45.1%)	120 (45.1%)
Education (ISCED)	6.51 (1.96)	6.75 (1.94)	6.76 (1.95)
TMT B–A score (seconds)	50.70 (30.07)	46.09 (26.90)	46.48 (24.85)

Note: The mean value and standard deviation are represented as mean (SD).

Baseline-only sample included 773 participants (45.9% female; mean age = 67.0 ± 6.7 years). For the outlier-removed sample (n = 761), TMT B–A scores were slightly lower, while age and sex distribution remained comparable (Table 4.2.1).

The follow-up sample comprised 272 participants (45.2% female; baseline age = 66.0 ± 6.3 years; follow-up age = 69.7 ± 6.3 years). For the outlier-removed sample (n = 266), TMT B–A scores at baseline and follow-up were modestly reduced, with similar demographic characteristics (Table 4.2.1).

Network-level patterns of segregation and inter- and intra-IV of connectivity, together with their group-level spatial distributions projected onto the brain surface, are shown in Figure 4.2.1.

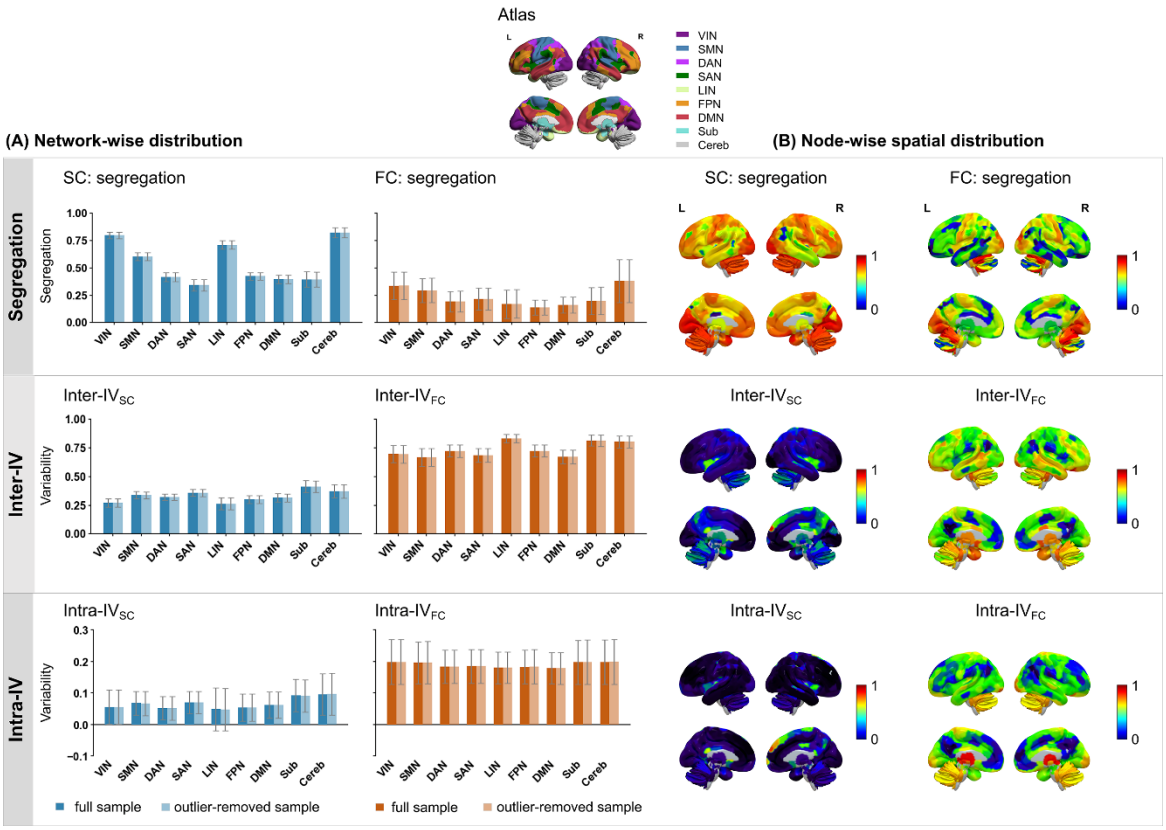

Figure 4.2.1 Network segregation and inter- and intra-individual variability of structural (SC) and functional connectivity (FC). (A) Network-wise distributions of SC and FC metrics across large-scale brain networks, including segregation, inter-individual variability (inter-IV), and intra-individual variability (intra-IV). Bars represent mean values for the full sample (dark colors) and the outlier-removed sample (light colors), with error bars indicating standard deviations. **(B)** Node-wise spatial distributions of SC and FC metrics displayed on brain surfaces. Color bars indicate normalized values ranging from 0 (blue) to 1 (red). Abbreviations: L / R, left and right hemispheres.

4.2.2 Partial Correlations Between Variables

In the baseline sample (n = 773), network segregation was consistently negatively associated with inter-IV across multiple networks for both structural and functional connectivity. Inter-IV_{SC} and inter-IV_{FC} were also positively associated with age, indicating greater variability in older participants. In contrast, greater inter-IV_{SC} was associated with poorer TMT B–A performance, whereas similar associations were observed for inter-IV_{FC} only in a few networks. In the follow-up sample (n = 272), network segregation remained negatively associated with intra-IV of connectivity across several networks, whereas associations with age and TMT B–A were generally weak or absent. Associations between network segregation and age were network-dependent and less consistent than those observed for IV of connectivity (Table 4.2.2).

Table 4.2.2 Partial correlations between brain metrics, age, and TMT B − A.

	Network	Structural connectivity					Functional connectivity				
		IV–age	Segregation – age	IV – Segregation	IV – TMT B − A	Segregation – TMT B − A	IV-age	Segregation – age	IV – Segregation	IV – TMT B − A	Segregation – TMT B − A
baseline-only sample (inter-IV)	VIN	**0.25**		**-0.60**	**-0.08**		**0.19**	**-0.09**	**-0.71**		
	SMN	**0.28**	**-0.11**	**-0.23**	**-0.09**		**0.19**	**-0.19**	**-0.74**		
	DAN	**0.28**	**0.09**		**-0.12**		**0.18**		**-0.56**		
	SAN	**0.37**		**-0.26**	**-0.09**		**0.18**	**-0.12**	**-0.65**		
	LIN	**0.20**		**-0.45**			**0.13**			**-0.10**	
	FPN	**0.32**	**-0.15**	**-0.39**	**-0.10**		**0.17**		**-0.35**		
	DMN	**0.31**		**-0.43**	**-0.08**		**0.17**		**-0.37**		
	Sub	**0.35**	**0.32**	**0.30**	**-0.16**	**-0.14**	**0.24**		**-0.15**	**-0.10**	
	Cereb	**0.21**		**-0.55**			**0.09**		**0.33**		
follow-up sample (intra-IV)	VIN			**-0.61**					**-0.19**		
	SMN			**-0.29**				**-0.19**			
	DAN										
	SAN			**-0.23**							
	LIN			**-0.31**					**-0.20**		
	FPN			**-0.41**					**-0.17**		
	DMN			**-0.39**					**-0.23**		
	Sub		**0.27**	**0.18**							
	Cereb			**-0.50**							

Note: Trail Making Test Part B–Part A difference score (TMT B–A) was reverse-coded (multiplied by −1) and normalized. Network segregation and inter-/intra-individual variability (IV) of connectivity were also normalized. Partial correlations controlled for sex and education, and additionally for age in all analyses except those involving age. Only correlations surviving false discovery rate (FDR) correction across the nine networks are shown; blank cells indicate non-significant correlations after FDR correction. Blue and red indicate negative and positive correlations, respectively. Abbreviations: VIN, visual network; SMN, somatomotor network; DAN, dorsal attention network; SAN, salience/ventral attention network; LIN, limbic network; FPN, frontoparietal control network; DMN, default mode network; Sub, subcortical network; Cereb, cerebellar network

4.2.3 Mediation Model (Model 1)

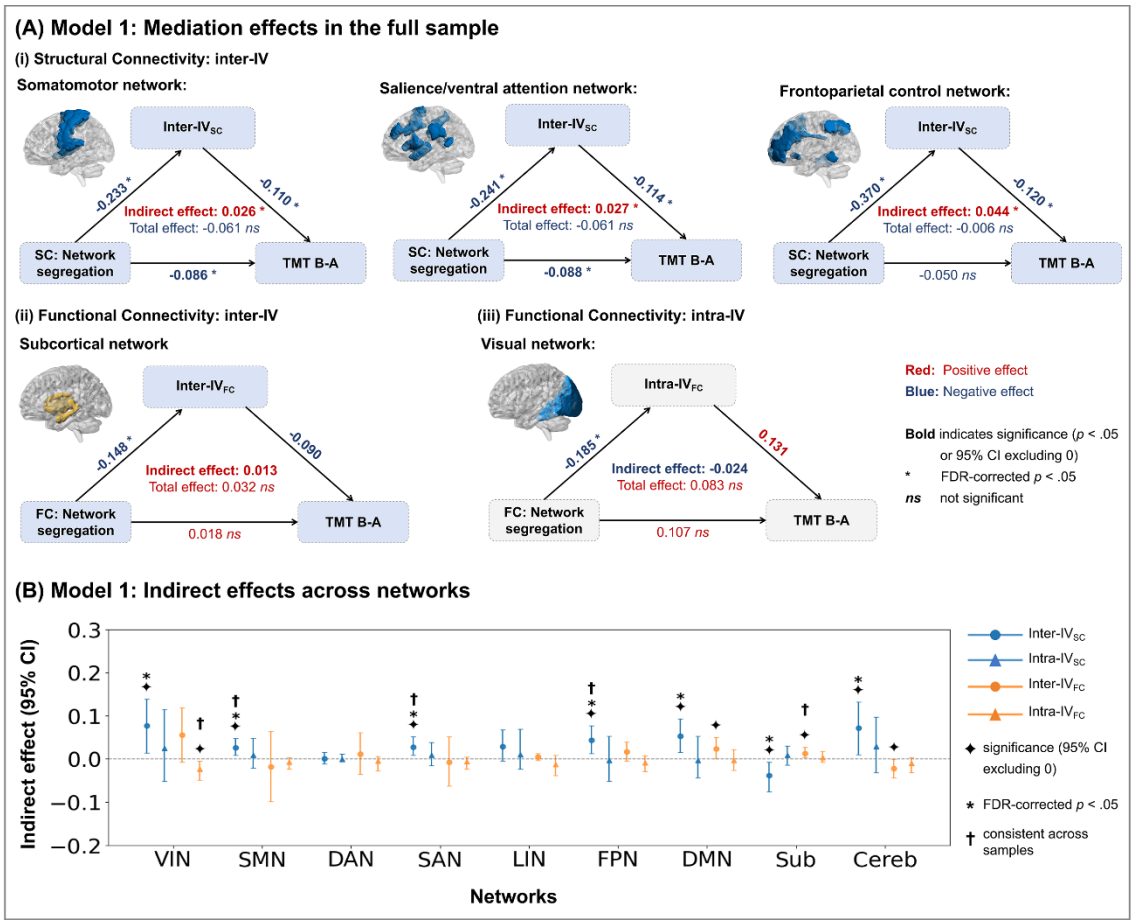

Figure 4.2.2 Mediation effects of individual variability (IV). (A) Network-specific mediation models illustrating the indirect effects of network segregation on TMT B–A via inter- or intra-individual variability (IV) of structural connectivity (SC) and functional connectivity (FC). Only representative networks with stable indirect effects after outlier removal are shown. Path effects (a, b, c′), total effects, and indirect effects were corrected for multiple comparisons across networks within each modality using false discovery rate (FDR). **(B)** Indirect effects across all networks with 95% confidence intervals (CI). ✦ indicates significant results; * indicates effects surviving false discovery rate (FDR) correction; † indicates that the mediation effect remained significant in the outlier-removed sample.

Indirect effects via inter-IV$_{SC}$

In structural networks (Model 1), inter-IV$_{SC}$ significantly mediated the association between network segregation and TMT B–A performance in seven of the nine networks (all $p_{FDR} < .05$), with no significant mediation observed in the dorsal attention (DAN) or limbic (LIN) networks (Figure 4.2.2; Table 4.2.3). Across these networks, lower network segregation was associated with greater inter-IV$_{SC}$, resulting in indirect effects indicating poorer TMT B–A performance (indirect effects = 0.026–0.077). These indirect effects were opposite in direction to the direct effects of segregation on TMT

B–A, thereby attenuating the total effects.

The subcortical network showed a distinct pattern in which higher network segregation was associated with greater inter-IV_{SC}, which in turn was related to poorer TMT B–A performance (indirect effect = -0.038), opposite to the direction observed in other networks.

Sensitivity analyses excluding outliers showed a similar overall pattern. Mediation effects remained evident in the somatomotor (SMN), salience/ventral attention (SAN), and frontoparietal control (FPN) networks, although these effects did not survive FDR correction (Figure 4.2.3; Table 4.2.5).

Indirect effects via inter-IV_{FC}

Mediation via inter-IV_{FC} was observed only in the default mode (DMN), subcortical and cerebellar networks (Figure 4.2.2; Table 4.2.3), but none of these effects survived FDR correction.

In the DMN and subcortical network, lower network segregation was indirectly associated with poorer TMT B–A performance via greater inter-IV_{FC} (indirect effects = 0.013–0.023). In contrast, in the cerebellar network, lower network segregation was associated with better TMT B–A performance via lower inter-IV_{FC} (indirect effect = -0.022). After excluding outliers, only the subcortical mediation effect remained significant (Figure 4.2.3; Table 4.2.5).

Indirect effects for intra-IV_{SC} and intra-IV_{FC}

No significant mediation effects were detected for intra-IV_{SC}. For functional connectivity, a mediation effect via intra-IV_{FC} was observed in the visual network (Figure 4.2.2; Table 4.2.4), where higher network segregation was indirectly associated with worse TMT B–A performance through lower intra-IV_{FC} (indirect effect = -0.024). This effect did not survive FDR correction but remained significant after excluding outliers (Figure 4.2.3; Table 4.2.6).

Table 4.2.3 Mediation analyses (full sample): Inter-individual variability of connectivity as a mediator between network segregation and TMT B–A.

Models					β (*p*-value)				Bootstrap effects and confidence intervals			
Modality	**Networks**	**X**	**M**	**Y**	***a* (*p*)**	***b* (*p*)**	***c'* (*p*)**	**Total**	**Indirect**	**BootSE**	**LLCI**	**ULCI**
Structural connectivity	VIN	SC: Network segregation	Inter-IV$_{SC}$	TMT B-A	**-0.592 (<.001)** ***	**-0.129 (0.003)** **	**-0.091 (0.034)** *	-0.015 (0.668)	**0.077** *	**0.032**	**0.014**	**0.139**
	SMN†				**-0.233 (<.001)** ***	**-0.110 (0.002)** **	**-0.086 (0.015)** *	-0.061 (0.081)	**0.026** *	**0.010**	**0.008**	**0.047**
	DAN				-0.012 (0.742)	**-0.113 (0.001)** **	-0.056 (0.099)	-0.054 (0.109)	0.001	0.006	-0.012	0.015
	SAN†				**-0.241 (<.001)** ***	**-0.114 (0.002)** **	**-0.088 (0.011)** *	-0.061 (0.071)	**0.027** *	**0.011**	**0.008**	**0.051**
	LIN				**-0.441 (<.001)** ***	-0.067 (0.082)	-0.06 (0.109)	-0.031 (0.359)	0.029	0.019	-0.005	0.067
	FPN†				**-0.370 (<.001)** ***	**-0.120 (0.002)** **	-0.050 (0.172)	-0.006 (0.865)	**0.044** *	**0.017**	**0.013**	**0.077**
	DMN				**-0.413 (<.001)** ***	**-0.128 (0.001)** **	**-0.104 (0.005)** *	-0.051 (0.130)	**0.053** *	**0.020**	**0.015**	**0.093**
	Sub				**0.298 (<.001)** ***	**-0.126 (0.001)** **	**-0.103 (0.005)** *	**-0.141 (<.001)** **	**-0.038** *	**0.018**	**-0.076**	**-0.007**
	Cereb				**-0.553 (<.001)** ***	**-0.129 (0.002)** **	**-0.121 (0.004)** *	-0.050 (0.153)	**0.071** *	**0.031**	**0.010**	**0.132**
Functional connectivity	VIN	FC: Network segregation	Inter-IV$_{FC}$	TMT B-A	**-0.699 (<.001)** ***	-0.080 (0.101)	-0.021 (0.661)	0.035 (0.301)	0.056	0.032	-0.008	0.118
	SMN				**-0.737 (<.001)** ***	0.024 (0.638)	0.057 (0.262)	0.039 (0.249)	-0.018	0.041	-0.099	0.064
	DAN				**-0.556 (<.001)** ***	-0.020 (0.637)	0.049 (0.229)	0.060 (0.075)	0.011	0.024	-0.035	0.061
	SAN				**-0.653 (<.001)** ***	0.010 (0.820)	0.060 (0.188)	0.053 (0.122)	-0.007	0.029	-0.062	0.052
	LIN				-0.045 (0.216)	**-0.091 (0.008)** *	0.009 (0.788)	0.013 (0.699)	0.004	0.004	-0.003	0.012
	FPN				**-0.346 (<.001)** ***	-0.046 (0.205)	0.023 (0.515)	0.039 (0.240)	0.016	0.011	-0.005	0.040
	DMN				**-0.368 (<.001)** ***	-0.063 (0.090)	-0.018 (0.628)	0.005 (0.871)	**0.023**	**0.013**	**3.71×10^{-4}**	**0.050**
	Sub†				**-0.148 (<.001)** ***	**-0.090 (0.010)** *	0.018 (0.592)	0.032 (0.349)	**0.013**	**0.006**	**0.003**	**0.027**
	Cereb				**0.326 (<.001)** ***	-0.067 (0.066)	0.017 (0.627)	-0.004 (0.896)	**-0.022**	**0.011**	**-0.044**	**-0.001**

Note: TMT B–A scores were reversed and normalized. Network segregation and inter-individual variability (inter-IV) of connectivity were normalized. Path coefficients (a, b, c′) and indirect effects are completely standardized. Indirect effects were estimated using bootstrap resampling (5,000 samples). Bold values indicate significant results. Asterisks denote effects surviving false discovery rate (FDR) correction (* $p_{FDR} < .05$; ** $p_{FDR} < .01$; *** $p_{FDR} < .001$). All models controlled for age, sex, and education. † indicates that the mediation effect remained significant in the outlier-removed sample. Colors indicate effect direction (blue = negative, red = positive).

Table 4.2.4 Mediation analyses (full sample): Intra-individual variability of connectivity as a mediator between network segregation and TMT B–A.

		Models			β (*p*-value)				Bootstrap effects and confidence intervals			
Modality	**Networks**	**X**	**M**	**Y**	***a* (*p*)**	***b* (*p*)**	***c'* (*p*)**	**Total**	**Indirect**	**BootSE**	**LLCI**	**ULCI**
Structural connectivity	VIN	SC: Network segregation	Intra-IV$_{SC}$	TMT B-A	**-0.610 (<.001)*****	-0.042 (0.576)	-0.042 (0.580)	-0.016 (0.786)	0.025	0.041	-0.051	0.115
	SMN				**-0.297 (<.001)*****	-0.026 (0.677)	-0.067 (0.281)	-0.06 (0.316)	0.008	0.017	-0.021	0.047
	DAN				-0.077 (0.203)	0.007 (0.908)	0.039 (0.502)	0.039 (0.506)	-0.001	0.004	-0.006	0.011
	SAN				**-0.229 (<.001)*****	-0.041 (0.505)	-0.106 (0.078)	-0.097 (0.098)	0.009	0.013	-0.015	0.038
	LIN				**-0.309 (<.001)*****	-0.034 (0.586)	**-0.079 (0.201)**	**-0.068 (0.242)**	0.010	0.023	-0.023	0.069
	FPN				**-0.405 (<.001)*****	0.009 (0.892)	0.054 (0.400)	0.05 (0.388)	-0.004	0.026	-0.052	0.053
	DMN				**-0.393 (<.001)*****	0.007 (0.908)	-0.06 (0.348)	-0.063 (0.284)	-0.003	0.024	-0.044	0.053
	Sub				**0.189 (0.003)****	0.047 (0.431)	**-0.122 (0.05)**	**-0.113 (0.064)**	0.009	0.011	-0.014	0.030
	Cereb				**-0.508 (<.001)*****	-0.057 (0.398)	-0.114 (0.099)	-0.085 (0.156)	0.029	0.032	-0.031	0.097
Functional connectivity	VIN†	FC: Network segregation	Intra-IV$_{FC}$	TMT B-A	**-0.185 (0.002)****	**0.131 (0.026)**	0.107 (0.069)	0.083 (0.155)	**-0.024**	**0.011**	**-0.049**	**-0.005**
	SMN				-0.093 (0.134)	0.088 (0.134)	0.086 (0.149)	0.077 (0.191)	-0.008	0.007	-0.023	0.003
	DAN				**-0.127 (0.038)**	0.042 (0.473)	0.090 (0.124)	0.085 (0.144)	-0.005	0.008	-0.027	0.006
	SAN				-0.088 (0.160)	0.066 (0.255)	0.019 (0.745)	0.014 (0.820)	-0.006	0.007	-0.024	0.004
	LIN				**-0.203 (0.001)****	0.063 (0.289)	-0.053 (0.369)	-0.066 (0.255)	-0.013	0.012	-0.038	0.009
	FPN				**-0.166 (0.006)***	0.057 (0.334)	0.017 (0.773)	0.008 (0.897)	-0.009	0.009	-0.029	0.007
	DMN				**-0.232 (<.001)****	0.014 (0.809)	0.006 (0.914)	0.003 (0.957)	-0.003	0.012	-0.026	0.022
	Sub				0.050 (0.416)	0.068 (0.248)	0.038 (0.524)	0.041 (0.487)	0.003	0.006	-0.007	0.018
	Cereb				-0.103 (0.093)	0.098 (0.096)	0.046 (0.433)	0.036 (0.538)	-0.010	0.009	-0.031	0.003

Note: TMT B–A scores were reversed and normalized. Network segregation and intra-individual variability (intra-IV) of connectivity were normalized. Path coefficients (a, b, c′) and indirect effects are completely standardized. Indirect effects were estimated using bootstrap resampling (5,000 samples). Bold values indicate significant results. Asterisks denote effects surviving false discovery rate (FDR) correction (* $p_{FDR} < .05$; ** $p_{FDR} < .01$; *** $p_{FDR} < .001$). All models controlled for age, sex, and education. † indicates that the mediation effect remained significant in the outlier-removed sample. Colors indicate effect direction (blue = negative, red = positive).

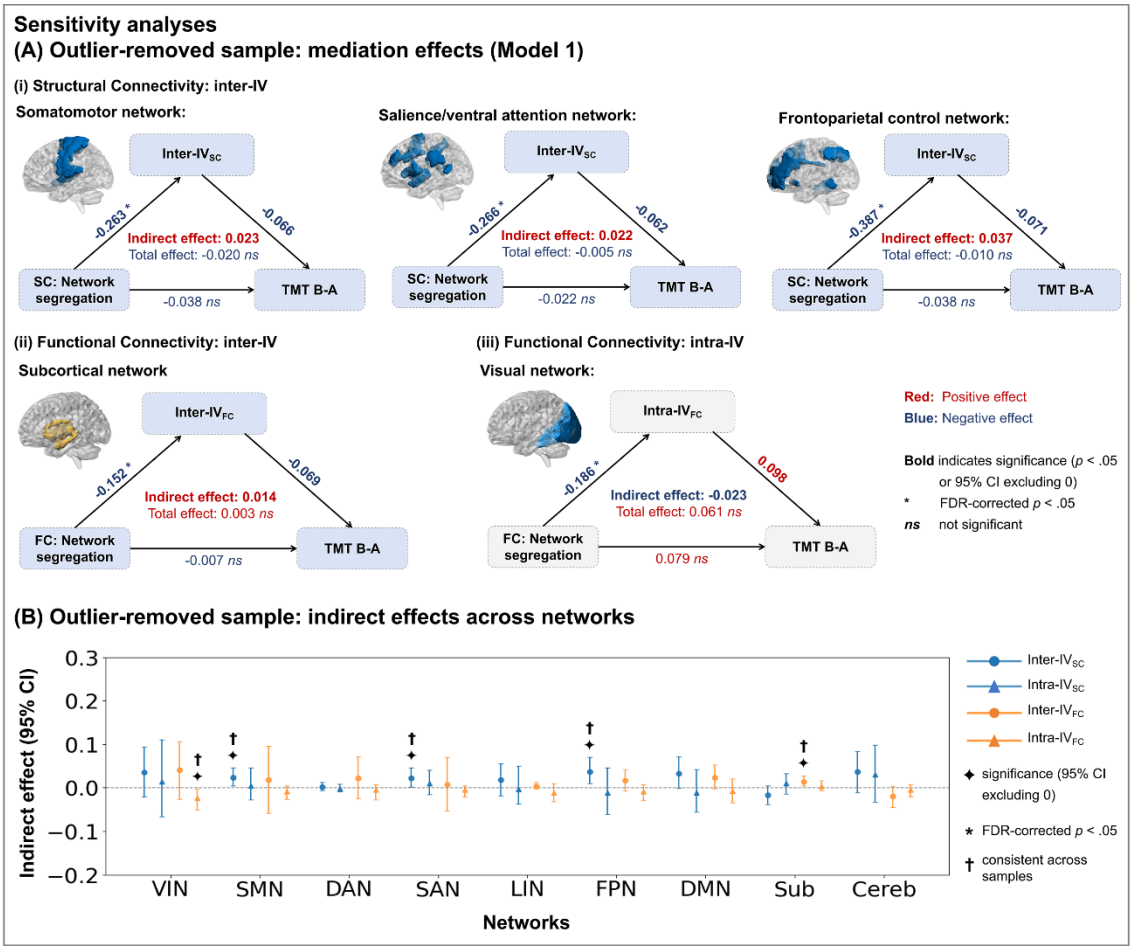

Figure 4.2.3 Mediation effects in the outlier-removed sample. (A) Network-specific mediation models illustrating the indirect effects of network segregation on TMT B–A via inter- or intra-individual variability (IV) of structural connectivity (SC) and functional connectivity (FC). Only representative networks with consistent indirect effects in the full sample are shown. Path effects (a, b, c′), total effects, and indirect effects were corrected for multiple comparisons across networks within each modality using false discovery rate (FDR). **(B)** Indirect effects across all networks with 95% confidence intervals (CI). ✦ indicates significant results (uncorrected); * indicates effects surviving false discovery rate (FDR) correction; † indicates that the mediation effect remained significant in the outlier-removed sample.

Table 4.2.5 Outlier-removed sample: Inter-individual variability of connectivity as a mediator between network segregation and TMT B–A.

		Models			β (*p*-value)				Bootstrap effects and confidence intervals			
Modality	**Networks**	**X**	**M**	**Y**	***a* (*p*)**	***b* (*p*)**	***c'* (*p*)**	**Total**	**Indirect**	**BootSE**	**LLCI**	**ULCI**
Structural connectivity	VIN	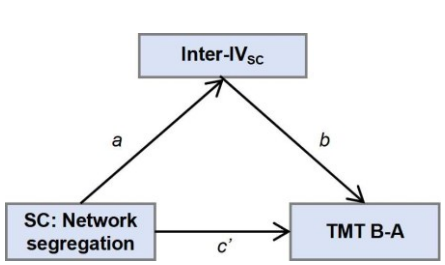			**-0.618 (<.001)*****	-0.044 (0.187)	0.003 (0.920)	0.030 (0.239)	0.036	0.03	-0.021	0.095
	SMN†				**-0.263 (<.001)*****	**-0.066 (0.013)**	-0.038 (0.161)	-0.020 (0.436)	**0.023**	**0.010**	**0.005**	**0.046**
	DAN				-0.031 (0.400)	**-0.058 (0.025)**	-0.008 (0.741)	-0.007 (0.794)	0.002	0.004	-0.006	0.012
	SAN†				**-0.266 (<.001)*****	**-0.062 (0.027)**	-0.022 (0.407)	-0.005 (0.833)	**0.022**	**0.011**	**0.002**	**0.046**
	LIN				**-0.455 (<.001)****	-0.029 (0.313)	-0.017 (0.536)	-0.004 (0.863)	0.018	0.019	-0.018	0.056
	FPN†				**-0.387 (<.001)*****	**-0.071 (0.012)**	-0.038 (0.173)	-0.010 (0.693)	**0.037**	**0.015**	**0.010**	**0.070**
	DMN				**-0.446 (<.001)*****	-0.056 (0.056)	-0.02 (0.484)	0.005 (0.841)	0.033	0.018	-0.001	0.072
	Sub				**0.269 (<.001)*****	-0.047 (0.089)	-0.052 (0.064)	**-0.064 (0.017)**	-0.017	0.010	-0.038	0.004
	Cereb				**0.578 (<.001)*****	-0.047 (0.131)	-0.044 (0.169)	-0.016 (0.531)	0.037	0.024	-0.012	0.084
Functional connectivity	VIN	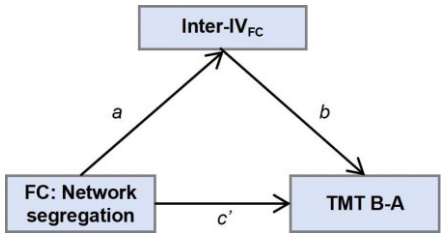			**-0.695 (<.001)*****	-0.044 (0.223)	-0.016 (0.654)	0.015 (0.558)	0.041	0.034	-0.026	0.107
	SMN				**-0.738 (<.001)*****	-0.018 (0.633)	0.002 (0.953)	0.016 (0.539)	0.018	0.039	-0.058	0.096
	DAN				**-0.559 (<.001)*****	-0.030 (0.335)	-0.008 (0.781)	0.008 (0.744)	0.022	0.025	-0.025	0.071
	SAN				**-0.653 (<.001)*****	-0.008 (0.810)	0.018 (0.593)	0.023 (0.359)	0.007	0.031	-0.053	0.070
	LIN				-0.044 (0.227)	**-0.058 (0.022)**	-0.012 (0.637)	-0.009 (0.711)	0.003	0.004	-0.002	0.012
	FPN				**-0.346 (<.001)*****	-0.035 (0.195)	0.001 (0.977)	0.013 (0.602)	0.017	0.013	-0.008	0.042
	DMN				**-0.363 (<.001)*****	-0.049 (0.075)	-0.027 (0.320)	-0.009 (0.721)	0.024	0.014	-0.002	0.053
	Sub†				**-0.152 (<.001)*****	**-0.069 (0.007)**	-0.007 (0.777)	0.003 (0.891)	**0.014**	**0.006**	**0.004**	**0.028**
	Cereb				**0.324 (<.001)*****	-0.044 (0.100)	0.003 (0.923)	-0.012 (0.637)	-0.019	0.012	-0.045	0.003

Note: TMT B–A scores were reversed and normalized. Network segregation and inter-individual variability (inter-IV) of connectivity were normalized. Path coefficients (a, b, c′) and indirect effects are completely standardized. Indirect effects were estimated using bootstrap resampling (5,000 samples). Bold values indicate significant results. Asterisks denote effects surviving false discovery rate (FDR) correction (* $p_{FDR} < .05$; ** $p_{FDR} < .01$; *** $p_{FDR} < .001$). All models controlled for age, sex, and education. † indicates that the mediation effect was consistent in the full sample. Colors indicate effect direction (blue = negative, red = positive).

Table 4.2.6 Outlier-removed sample: Intra-individual variability of connectivity as a mediator between network segregation and TMT B–A.

		Models			β (*p*-value)				Bootstrap effects and confidence intervals			
Modality	**Networks**	**X**	**M**	**Y**	***a* (*p*)**	***b* (*p*)**	***c'* (*p*)**	**Total**	**Indirect**	**BootSE**	**LLCI**	**ULCI**
Structural connectivity	VIN	SC: Network segregation	Intra-IV$_{SC}$	TMT B-A	**-0.617 (<.001)*****	-0.019 (0.753)	-0.029 (0.627)	-0.018 (0.709)	0.014	0.044	-0.066	0.111
	SMN				**-0.307 (<.001)*****	-0.014 (0.774)	-0.053 (0.289)	-0.049 (0.307)	0.005	0.018	-0.027	0.046
	DAN				-0.086 (0.182)	0.016 (0.730)	0.025 (0.607)	0.024 (0.626)	-0.002	0.004	-0.009	0.009
	SAN				**-0.228 (<.001)*****	-0.035 (0.462)	**-0.108 (0.023)**	**-0.100 (0.031)**	0.010	0.014	-0.016	0.041
	LIN				**-0.326 (<.001)*****	0.011 (0.833)	-0.009 (0.854)	-0.012 (0.788)	-0.004	0.021	-0.037	0.05
	FPN				**-0.414 (<.001)*****	0.021 (0.687)	0.036 (0.488)	0.027 (0.562)	-0.011	0.026	-0.061	0.046
	DMN				**-0.402 (<.001)*****	0.023 (0.649)	0.030 (0.562)	0.021 (0.664)	-0.012	0.024	-0.056	0.042
	Sub				**0.188 (0.003)****	0.040 (0.398)	-0.088 (0.076)	-0.08 (0.098)	0.010	0.012	-0.014	0.033
	Cereb				**-0.512 (<.001)*****	-0.047 (0.387)	-0.084 (0.127)	-0.06 (0.206)	0.030	0.034	-0.033	0.098
Functional connectivity	VIN†	FC: Network segregation	Intra-IV$_{FC}$	TMT B-A	**-0.186 (0.002)** **	**0.098 (0.036)**	0.079 (0.091)	0.061 (0.189)	**-0.023**	**0.012**	**-0.050**	**-0.002**
	SMN				-0.102 (0.103)	0.069 (0.136)	0.050 (0.292)	0.043 (0.364)	-0.009	0.008	-0.026	0.004
	DAN				**-0.129 (0.036)**	0.032 (0.488)	0.030 (0.526)	0.025 (0.583)	-0.005	0.009	-0.028	0.007
	SAN				-0.079 (0.215)	0.047 (0.310)	-0.003 (0.946)	-0.007 (0.884)	-0.005	0.007	-0.021	0.005
	LIN				**-0.211 (0.001)****	0.041 (0.393)	-0.027 (0.570)	-0.036 (0.444)	-0.011	0.011	-0.032	0.01
	FPN				**-0.155 (0.013)** *	0.049 (0.297)	0.055 (0.246)	0.047 (0.312)	-0.009	0.009	-0.029	0.007
	DMN				**-0.227 (<.001)****	0.026 (0.585)	-0.001 (0.983)	-0.007 (0.881)	-0.007	0.013	-0.034	0.021
	Sub				0.046 (0.454)	0.048 (0.309)	0.033 (0.480)	0.035 (0.451)	0.003	0.006	-0.006	0.017
	Cereb				-0.102 (0.100)	0.04 (0.396)	0.036 (0.435)	0.032 (0.484)	-0.005	0.007	-0.021	0.007

Note: TMT B–A scores were reversed and normalized. Network segregation and intra-individual variability (intra-IV) of connectivity were normalized. Path coefficients (a, b, c′) and indirect effects are completely standardized. Indirect effects were estimated using bootstrap resampling (5,000 samples). Bold values indicate significant results. Asterisks denote effects surviving false discovery rate (FDR) correction (* $p_{FDR} < .05$; ** $p_{FDR} < .01$; *** $p_{FDR} < .001$). All models controlled for age, sex, and education. † indicates that the mediation effect was consistent in the full sample. Colors indicate effect direction (blue = negative, red = positive).

4.2.4 Age-Moderated Mediation Model (Model 2)

Age-moderated path effects in the inter-IV_{SC} model

Age significantly moderated the association between network segregation and inter-IV_{SC} in the DAN (β = 0.017) and FPN (β = -0.017), with both effects surviving FDR correction and remaining significant after outlier exclusion (Figures 4.2.4 and 4.2.8; Table 4.2.7). In the DAN, lower network segregation was associated with higher inter-IV_{SC} at younger-old ages (−1 SD), whereas the association reversed at older-old ages (+1 SD). In the FPN, lower network segregation was associated with higher inter-IV_{SC}, and this association was stronger at higher age values.

Age also moderated the association between inter-IV_{SC} and TMT B–A in multiple structural networks, with negative associations between greater inter-IV_{SC} and lower TMT B–A evident primarily at higher age values (Figure 4.2.4; Table 4.2.7). Age additionally moderated the direct association between structural network segregation and TMT B–A in several networks.

Moderated mediation analyses showed that the conditional indirect effects of network segregation on TMT B–A via inter-IV_{SC} varied across probed age values (Figures 4.2.5 and 4.2.6; Table 4.2.7). No indirect effects were observed at younger-old ages. At the mean age values, positive indirect effects emerged in the SMN, SAN, FPN, and DMN. At older-old ages, indirect effects were evident in the visual (VIN), SMN, SAN, FPN, DMN, and cerebellar networks, surviving FDR correction. In these cortical and cerebellar networks, lower network segregation was associated with poorer TMT B–A performance via greater inter-IV_{SC}. In contrast, the subcortical network showed an opposite-direction conditional indirect effect, such that higher segregation was associated with poorer TMT B–A performance via greater inter-IV_{SC}.

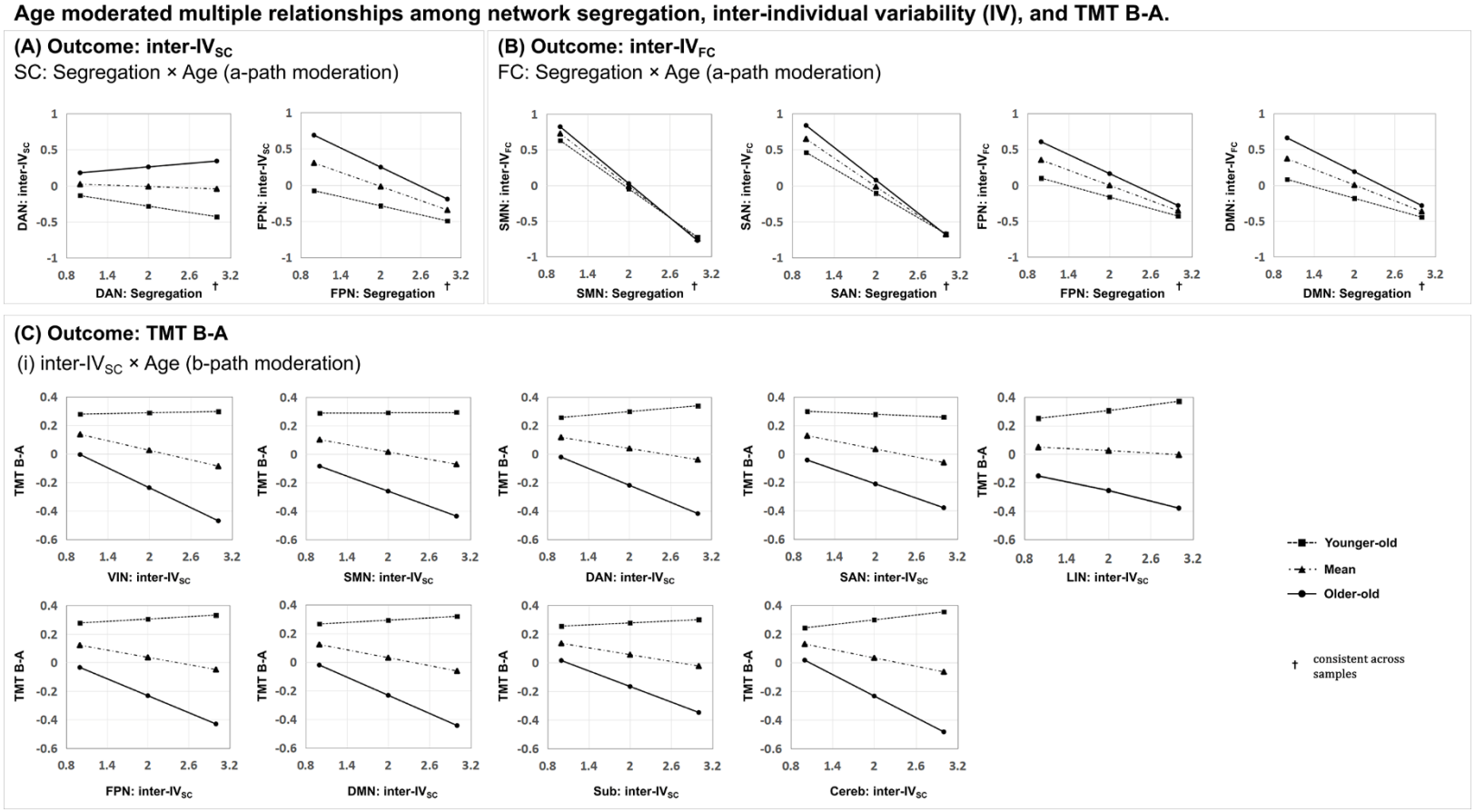

Figure 4.2.4 Age-moderated associations among network segregation, inter-individual variability (IV), and TMT B–A. (A) Simple slope plots illustrating age × network segregation of structural connectivity (SC) effects on inter-IV_{SC} (a-path moderation). **(B)** Simple slope plots illustrating age × network segregation of functional connectivity (FC) effects on inter-IV_{FC} in networks showing significant moderation. **(C)** Simple slope plots illustrating age-moderated associations between inter-IV_{SC} and TMT B–A (b-path moderation). Only effects surviving false discovery rate (FDR) correction across networks are shown. Age was modeled as a continuous variable; lines represent conditional effects estimated at mean − 1 SD (younger-old), mean, and mean + 1 SD (older-old) of age. † indicates results were consistent across samples.

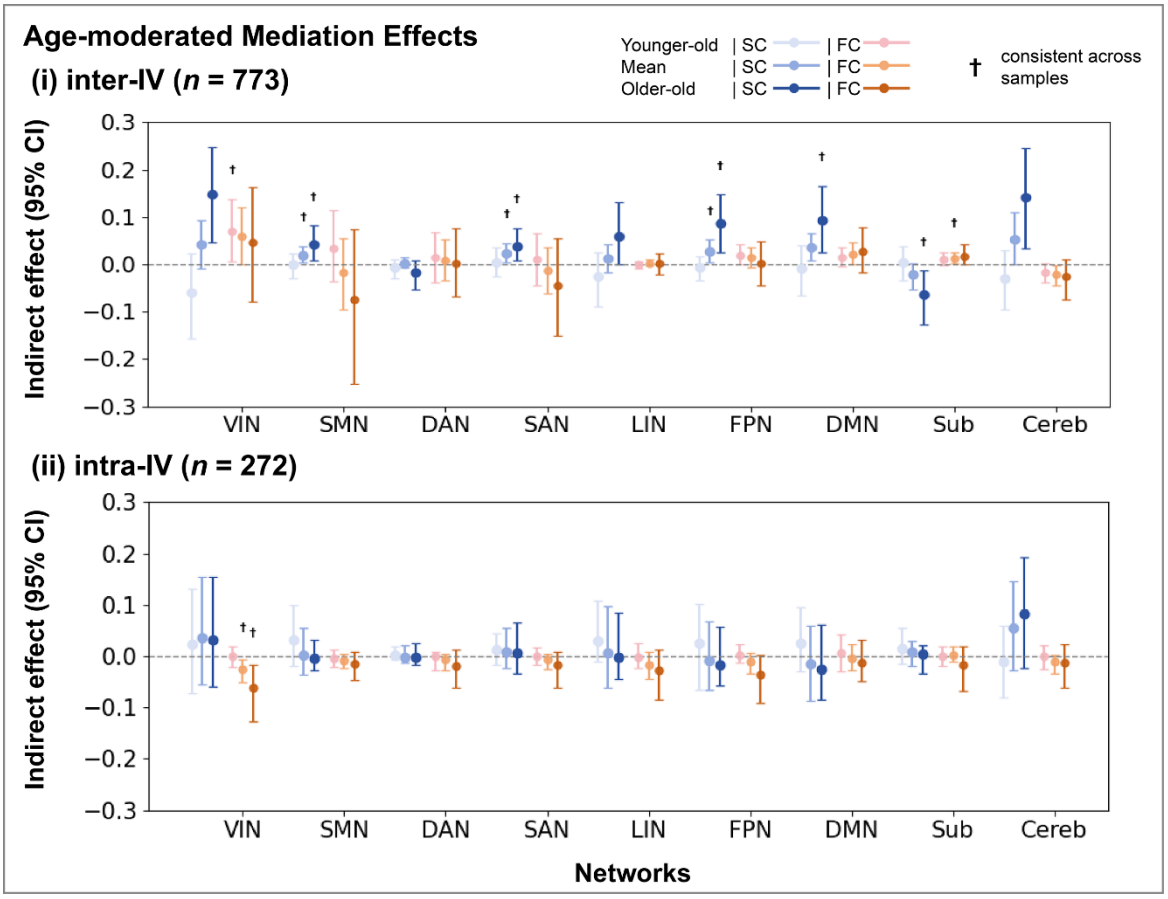

Figure 4.2.5 Age-moderated mediation effects of inter- (i) and intra- (ii) individual variability (IV) of connectivity across networks with 95% confidence intervals (CI). Age was modeled as a continuous variable; points represent conditional indirect effects estimated at mean − 1 SD (younger-old), mean, and mean + 1 SD (older-old) of age. † indicates effects that remained significant after outlier removal.

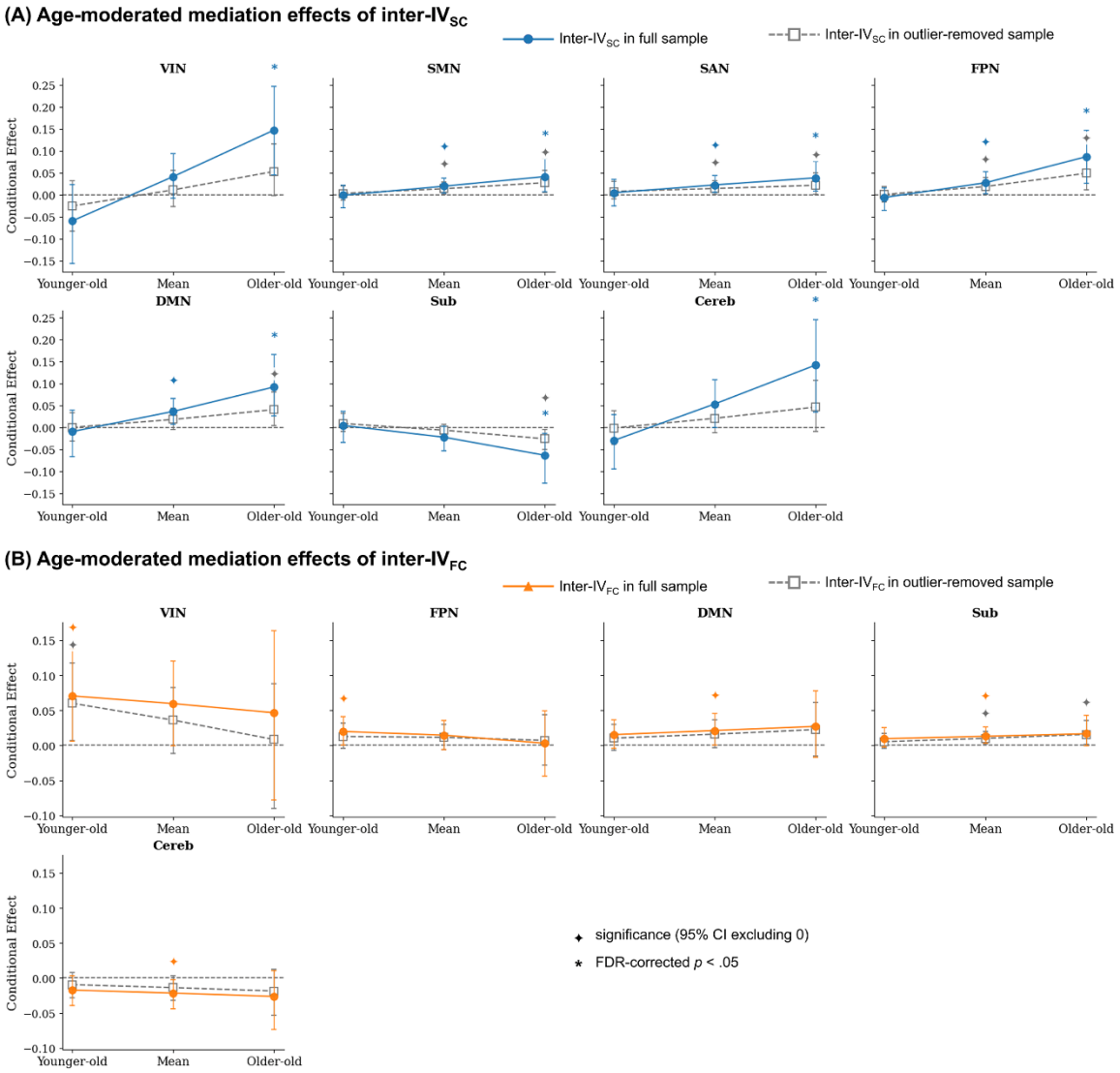

Figure 4.2.6 Age-moderated mediation effects via inter-individual variability (IV) of structural (A) and functional connectivity (B). Lines depict conditional indirect effects estimated at mean − 1 SD (younger-old), mean, and mean + 1 SD (older-old) of age. Colored lines represent estimates from the full sample, and gray lines represent estimates from the outlier-removed sample. ✦ indicates significant results (uncorrected); * indicates effects surviving false discovery rate (FDR) correction.

Age-moderated path effects in the inter-IV$_{FC}$ model

In functional networks, age significantly moderated the association between network segregation and inter-IV$_{FC}$ in several cortical networks (β = -0.009 to -0.015; Table 4.2.7), with all effects surviving FDR correction and remaining significant after outlier exclusion. Across these networks, lower network segregation was associated with higher inter-IV$_{FC}$, with stronger negative associations observed at older age values (Figures 4.2.4 and 4.2.8). Age-moderated associations involving inter-IV$_{FC}$ and TMT B–A scores, as well as network segregation and TMT B–A scores,

did not remain robust after outlier exclusion.

Conditional indirect effects of network segregation on TMT B–A via inter-IV_{FC} were detected in several networks, but remained consistent only in the visual and subcortical networks after outlier exclusion (Figures 4.2.5 and 4.2.6; Table 4.2.7). None of these conditional indirect effects survived FDR correction. In the visual network, a positive indirect effect was observed at younger-old age values, indicating that lower network segregation was associated with poorer TMT B–A performance via higher inter-IV_{FC}. A similar mediation pattern was observed at mean age values in the subcortical network.

Table 4.2.7 Age-moderated mediation model: Inter-individual variability of connectivity as mediator.

Modality	Network	Interaction β (p)			Indirect effect [95% CIs]		
		Segregation×Age → inter-IV	**inter-IV ×Age → TMT-B–A**	**Segregation×Age → TMT-B–A**	**−1 SD (younger-old)**	**Mean**	**+1 SD (older-old)**
Structural connectivity	VIN	-0.002 (0.604)	**-0.026 (<.001)** ***	**-0.016 (0.008)** *	-0.059 [-0.156,0.024]	0.042 [-0.007,0.094]	**0.148 [0.046,0.247]** *
	SMN†	-0.001 (0.859)	**-0.013 (0.006)** **	-0.010 (0.064)	-0.001 [-0.029,0.023]	**0.020 [0.004,0.038]**	**0.042 [0.008,0.082]** *
	DAN	**0.017 (0.002)** **	**-0.018 (<.001)** ***	**-0.010 (0.046)**	-0.006 [-0.029,0.01]	0.003 [-0.006,0.014]	-0.016 [-0.052,0.009]
	SAN†	0.002 (0.747)	**-0.011 (0.025)** *	**-0.014 (0.005)** *	0.005 [-0.025,0.036]	**0.023 [0.005,0.045]**	**0.039 [0.008,0.076]** *
	LIN	-0.007 (0.112)	**-0.014 (0.012)** *	**-0.011 (0.030)**	-0.025 [-0.088,0.026]	0.013 [-0.016,0.043]	0.059 [-8.77×10^{-5},0.13]
	FPN†	**-0.017 (<.001)** ***	**-0.017 (0.003)** **	-4.96×10^{-4} (0.923)	-0.006 [-0.035,0.016]	**0.028 [0.004,0.053]**	**0.087 [0.026,0.147]** *
	DMN†	-0.006 (0.140)	**-0.018 (0.001)** **	**-0.012 (0.020)** *	-0.009 [-0.066,0.039]	**0.037 [0.008,0.066]**	**0.092 [0.026,0.166]** *
	Sub†	**0.011 (0.033)**	**-0.015 (0.003)** **	-0.009 (0.096)	0.005 [-0.034,0.037]	-0.022 [-0.053,0.002]	**-0.063 [-0.127,-0.013]** *
	Cereb	-0.003 (0.535)	**-0.023 (<.001)** ***	**-0.021 (<.001)** **	-0.03 [-0.095,0.030]	0.054 [-2.83×10^{-4},0.109]	**0.142 [0.034,0.246]** *
Functional connectivity	VIN†	-0.007 (0.055)	0.003 (0.609)	-0.002 (0.813)	**0.071 [0.006,0.138]**	0.06 [-0.001,0.120]	0.047 [-0.078,0.164]
	SMN	**-0.009 (0.011)** *	0.011 (0.110)	**0.020 (0.006)** *	0.034 [-0.035,0.115]	-0.016 [-0.095,0.055]	-0.075 [-0.253,0.073]
	DAN	-0.005 (0.275)	0.002 (0.704)	**0.024 (<.001)** **	0.016 [-0.038,0.069]	0.009 [-0.034,0.052]	0.002 [-0.069,0.075]
	SAN	**-0.014 (<.001)** **	0.006 (0.328)	**0.024 (0.001)** **	0.01 [-0.044,0.065]	-0.013 [-0.062,0.036]	-0.044 [-0.151,0.054]
	LIN	0.003 (0.547)	**-0.012 (0.009)**	0.004 (0.408)	-0.001 [-0.008,0.006]	0.003 [-0.002,0.01]	0.003 [-0.021,0.023]
	FPN	**-0.013 (0.007)** *	0.005 (0.287)	**0.019 (0.001)** **	**0.02 [3.63×10^{-4},0.041]**	0.015 [-0.006,0.036]	0.003 [-0.044,0.049]
	DMN	**-0.015 (0.002)** **	5.46×10^{-5} (0.991)	0.006 (0.259)	0.015 [-0.004,0.037]	**0.021 [4.83×10^{-4},0.046]**	0.027 [-0.017,0.078]
	Sub†	-0.001 (0.789)	-0.003 (0.579)	0.005 (0.353)	0.01 [-0.002,0.025]	**0.013 [0.003,0.026]**	0.017 [-0.001,0.043]
	Cereb	0.004 (0.471)	-0.001 (0.779)	0.002 (0.666)	-0.017 [-0.039,0.003]	**-0.022 [-0.044,-0.002]**	-0.026 [-0.074,0.01]

Note: TMT B–A scores were reversed and normalized. Network segregation and inter-individual variability (inter-IV) were normalized. **Bold** values indicate statistically significant effects. Asterisks denote effects surviving false discovery rate (FDR) correction ($^{*}p_{FDR} < .05$; $^{**}p_{FDR} < .01$; $^{***}p_{FDR} < .001$). All models controlled for sex and education. Conditional effects are estimated at mean − 1 SD (younger-old), mean, and mean + 1 SD (older-old) of age. † indicates mediation effects that remained significant in the outlier-removed sample (see Figure 4.2.6).

Age-moderated path effects in the intra-IV$_{SC}$ model

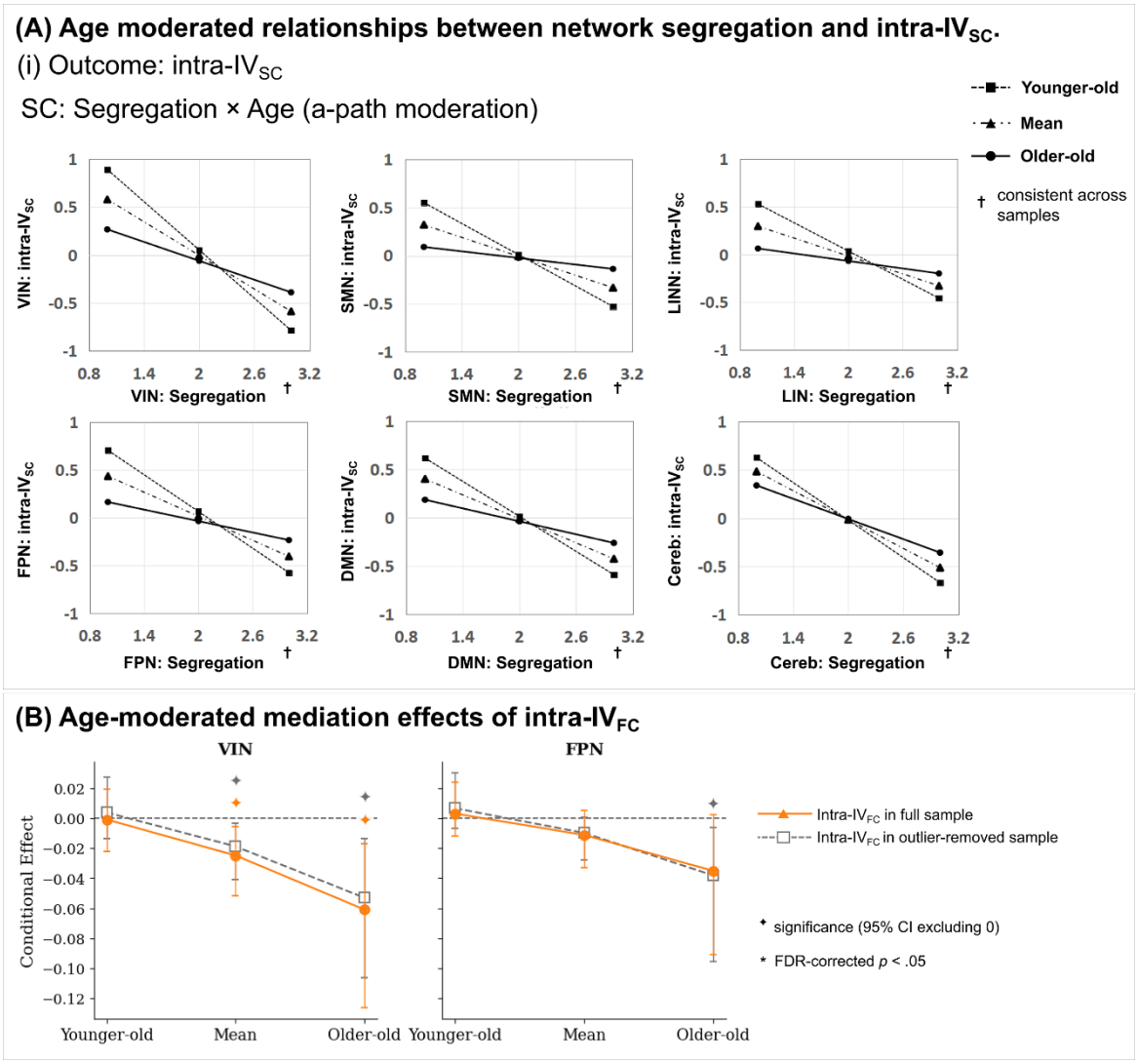

Figure 4.2.7 Age-moderated effects involving intra-individual variability (IV) of connectivity. **(A)** Simple slope plots illustrating age × network segregation of structural connectivity (SC) interactions on intra-IV$_{SC}$ (a-path moderation). Only effects surviving false discovery rate (FDR) correction across networks are shown. Lines depict conditional effects estimated at mean − 1 SD (younger-old), mean, and mean + 1 SD (older-old) of age. **(B)** Conditional indirect effects of network segregation on TMT B–A via intra-IV$_{FC}$ across age. Colored lines represent estimates from the full sample, and gray lines represent estimates from the outlier-removed sample. ✦ indicates significant results (uncorrected); * indicates effects surviving FDR correction. † indicates results were consistent across samples.

Age moderated the association between network segregation and intra-IV$_{SC}$ in several structural networks, including the VIN, SMN, LIN, FPN, DMN, and cerebellar networks (Figure 4.2.7; Table 4.2.8). All effects survived FDR correction and remained robust after outlier exclusion (Figure 4.2.8). Across these networks, higher network segregation was associated with lower intra-IV$_{SC}$, at

younger-old ages, with the negative association becoming weaker at higher age values.

Consistent with Model 1, intra-IV_{SC} was not associated with TMT B–A, and no conditional indirect effects of network segregation on TMT B–A via intra-IV_{SC} were observed (panel B in Figure 4.2.5).

Age-moderated path effects in the intra-IV_{FC} model

Age showed no consistent moderation of the paths linking functional network segregation, intra-IV_{FC}, and TMT B–A (Table 4.2.8).

Conditional indirect effects of network segregation on TMT B–A via intra-IV_{FC} were observed at mean and older-old ages in the visual network, indicating that higher network segregation was indirectly associated with worse TMT B–A performance through lower intra-IV_{FC}. This pattern remained consistent after outlier exclusion but did not survive FDR correction (Table 4.2.8; Figure 4.2.7). A similar but less stable conditional indirect effect was observed in the FPN in sensitivity analyses, but it did not survive multiple-comparison correction (Figure 4.2.7).

Table 4.2.8 Age-moderated mediation model: Intra-individual variability of connectivity as mediator.

Modality	Network	Interaction β (p)			Indirect effect [95% CIs]		
		Segregation×Age → intra-IV	**intra-IV ×Age → TMT-B–A**	**Segregation×Age → TMT-B–A**	**−1 SD (younger-old)**	**Mean**	**+1 SD (older-old)**
Structural connectivity	VIN	**0.041 (<.001)*****	-0.006 (0.661)	-0.001 (0.934)	0.023 [-0.072,0.132]	0.036 [-0.054,0.155]	0.032 [-0.06,0.154]
	SMN	**0.034 (<.001)*****	0.008 (0.446)	0.002 (0.873)	0.031 [-0.02,0.100]	0.003 [-0.036,0.056]	-0.004 [-0.028,0.032]
	DAN	0.007 (0.483)	0.005 (0.605)	0.009 (0.343)	0.002 [-0.005,0.019]	-0.002 [-0.012,0.02]	-0.002 [-0.016,0.026]
	SAN	0.010 (0.282)	3.21×10^{-4} (0.975)	-0.002 (0.792)	0.012 [-0.017,0.044]	0.009 [-0.024,0.055]	0.006 [-0.034,0.066]
	LIN	**0.029 (0.001)****	0.006 (0.653)	0.005 (0.563)	0.029 [-0.011,0.108]	0.006 [-0.062,0.097]	-0.003 [-0.045,0.084]
	FPN	**0.035 (<.001)*****	0.01 (0.389)	0.007 (0.449)	0.026 [-0.067,0.102]	-0.008 [-0.066,0.069]	-0.016 [-0.057,0.056]
	DMN	**0.030 (<.001)****	0.013 (0.299)	0.004 (0.671)	0.026 [-0.03,0.096]	-0.016 [-0.086,0.06]	-0.026 [-0.085,0.062]
	Sub	-0.013 (0.168)	-0.002 (0.836)	-0.009 (0.356)	0.015 [-0.014,0.055]	0.008 [-0.018,0.03]	0.003 [-0.033,0.021]
	Cereb	**0.024 (0.003)****	-0.020 (0.075)	-0.011 (0.299)	-0.011 [-0.08,0.060]	0.054 [-0.028,0.145]	0.082 [-0.023,0.193]
Functional connectivity	VIN†	-0.007 (0.443)	**0.021 (0.035)**	0.013 (0.172)	-0.001 [-0.022,0.019]	**-0.025 [-0.052,-0.006]**	**-0.061 [-0.126,-0.017]**
	SMN	-0.006 (0.497)	0.004 (0.710)	-0.001 (0.896)	-0.003 [-0.021,0.013]	-0.008 [-0.024,0.004]	-0.015 [-0.047,0.009]
	DAN	-0.008 (0.410)	0.008 (0.454)	0.015 (0.136)	-5.71×10^{-5} [-0.028,0.010]	-0.007 [-0.028,0.005]	-0.018 [-0.061,0.013]
	SAN	-0.003 (0.778)	0.014 (0.166)	0.001 (0.908)	0.001 [-0.018,0.017]	-0.007 [-0.026,0.004]	-0.017 [-0.061,0.009]
	LIN	0.004 (0.703)	0.011 (0.313)	-0.007 (0.451)	-0.002 [-0.024,0.025]	-0.016 [-0.045,0.009]	-0.026 [-0.086,0.013]
	FPN	-0.008 (0.431)	0.016 (0.124)	0.004 (0.639)	0.003 [-0.012,0.024]	-0.011 [-0.033,0.005]	-0.035 [-0.091,0.003]
	DMN	0.005 (0.643)	0.007 (0.485)	0.011 (0.275)	0.007 [-0.030,0.042]	-0.004 [-0.027,0.024]	-0.013 [-0.048,0.032]
	Sub	-0.021 (0.057)	0.013 (0.207)	-0.004 (0.707)	-2.32×10^{-4} [-0.020,0.019]	0.002 [-0.01,0.019]	-0.017 [-0.069,0.019]
	Cereb	0.005 (0.585)	0.015 (0.136)	0.012 (0.210)	-0.001 [-0.025,0.021]	-0.010 [-0.033,0.003]	-0.013 [-0.062,0.024]

Note: TMT B–A scores were reversed and normalized. Network segregation and intra-individual variability (intra-IV) were normalized. **Bold** values indicate statistically significant effects. Asterisks denote effects surviving false discovery rate (FDR) correction ($^{*}p_{FDR} < .05$; $^{**}p_{FDR} < .01$; $^{***}p_{FDR} < .001$). All models controlled for sex and education. Conditional effects are estimated at mean − 1 SD (younger-old), mean, and mean + 1 SD (older-old) of age. † indicates mediation effects that remained significant in the outlier-removed sample (see Figure 4.2.7).

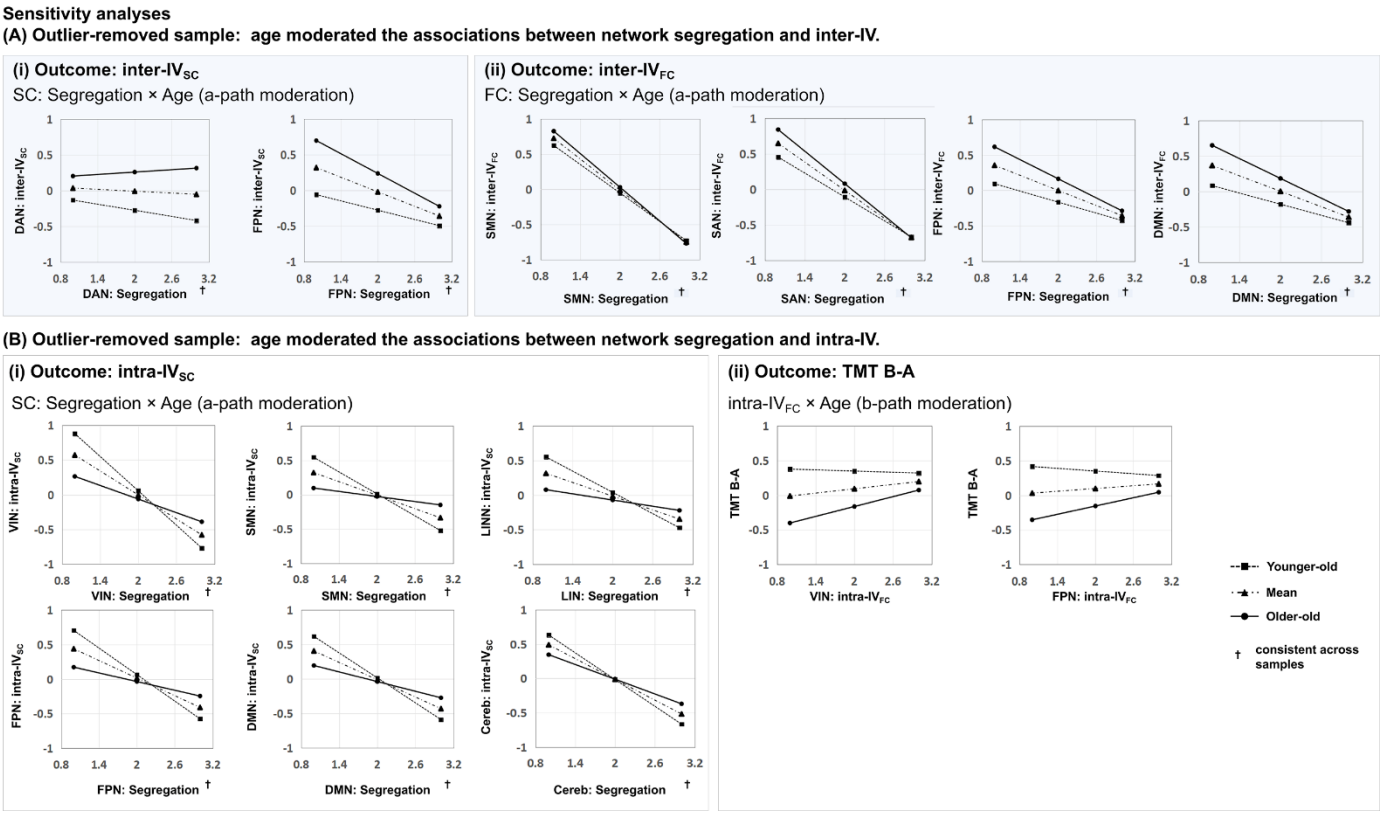

Figure 4.2.8 Sensitivity analyses in the outlier-removed sample: age-moderated associations involving network segregation and individual variability (IV) of connectivity. Only effects surviving false discovery rate (FDR) correction across networks are displayed. **(A)** Simple slope plots illustrating age × network segregation interactions on inter-individual variability of structural connectivity (inter-IV**sc**; **i**) and functional connectivity (inter-IV$_{FC}$; **ii**) (a-path moderation). **(B)** Age-moderated effects involving intra-individual variability (intra-IV). Left panels **(i)** show age × network segregation of structural connectivity (SC) interactions on intra-IV$_{SC}$ (a-path moderation). Right panels **(ii)** show age × intra-IV$_{FC}$ interactions on TMT B–A scores (b-path moderation). Lines represent conditional effects estimated at mean − 1 SD (younger-old), mean, and mean + 1 SD (older-old) of age. † indicates results were consistent across samples.

4.3 Discussion

This study advances understanding of age-related differences in large-scale brain network organization by explicitly modeling inter- and intra-individual variability in structural and functional connectivity as key variables within models examining associations between network segregation and executive control in healthy older adults. Rather than treating variability as noise, the findings indicate that inter-IV—particularly in SC—plays a prominent role in accounting for how network segregation relates to executive control, with this role differing as a function of age. Across networks and connectivity modalities, variability-related pathways showed distinct and context-dependent patterns, whereas intra-IV exhibited less involvement. Collectively, these results support a framework in which age-related differences in executive control are better characterized by considering interactions between network segregation and multiple sources of individual variability, rather than by focusing on network segregation or age effects in isolation.

4.3.1 Age-Related Network Segregation and Individual Variability of Connectivity

Network segregation, as a quantitative index of system separation or modular organization, has been consistently reported to decline with age in functional connectivity studies (Chan et al., 2014; Koen et al., 2020; Wang et al., 2021; Wig, 2017). Consistent with this literature, we observed correlations between lower functional network segregation and older age across several networks in the baseline sample, particularly in the somatomotor network, after controlling for sex and education (Table 4.2.2).

In contrast, age-related differences in structural network segregation were heterogeneous and network-dependent. Cortical systems, including the SMN and FPN, showed lower structural segregation at older ages, whereas the DAN and subcortical networks showed higher segregation at older ages. These findings align with previous reports that age-related changes in white matter integrity and connectivity are highly non-uniform across fiber systems and circuits (Poulakis et al., 2021; Vik et al., 2015). Importantly, greater structural segregation in the absence of corresponding behavioral benefits does not necessarily imply enhanced functional differentiation. In subcortical systems, in particular, higher segregation may reflect reduced cortico–subcortical integration, consistent with long-distance white-matter disconnection accounts of cognitive aging (Bennett & Madden, 2014).

Consistent with prior work (Huang et al., 2025; Ma et al., 2021), higher inter-IV of connectivity was associated with older age across systems without confounding of sex and education, indicating increased between-person heterogeneity in network organization with aging. However, the underlying mechanisms of age-related larger inter-IV_{SC} and inter-IV_{FC} may be distinct. The former may indicate the extent to which individuals diverge from age-expected population-level structural configurations, potentially reflecting heterogeneous trajectories of structural brain aging. Such heterogeneity may partly arise from asynchronous and regionally specific neurodegenerative changes, including demyelination and axonal degeneration, which unfold at different rates across individuals and fiber systems (Groh & Simons, 2025; Huang et al., 2025). Age-related greater inter-IV_{FC} likely reflects a mixture of neurobiological heterogeneity and non-neuronal contributions (e.g., vascular and motion-related factors) (Geerligs et al., 2017; Ma et al., 2021). These age-related increases in inter-IV may reflect reduced consistency in how large-scale network organization is expressed across individuals, potentially indexing greater divergence from a shared cross-sectional population-level network architecture in late life. In contrast, no robust association was observed between age and intra-IV of connectivity measured across an interval of approximately four years, supporting the notion that while cross-sectional individual differences may increase with age, within-person longitudinal variability does not necessarily do so (Salthouse, 2012).

These dissociable age-related patterns motivate an explicit examination of whether individual variability explains how network segregation relates to executive control.

4.3.2 Mediation Effects of Inter-Individual Variability of Connectivity

Across networks and modalities, significant mediation effects, when present, consistently pointed to an unfavorable role of higher inter-IV of connectivity for executive control—a pathway that held irrespective of the specific direction of the association between network segregation and inter-IV of connectivity. By explicitly incorporating inter-IV of connectivity within a framework centered on group-average network organization, the present analyses extend prior work on age-related differences in broader executive functions and large-scale network organization (e.g., Chong et al., 2019; Matyi et al., 2025; Ng et al., 2016).

Within cortical systems, the indirect effects through inter-IV_{SC} linking lower network

segregation to worse executive control were particularly robust in the SMN, SAN, and FPN networks—systems embedded in distributed white-matter circuits that have been associated with executive functions, particularly within frontoparietal and salience-related networks (see review in Ribeiro et al., 2024). A similar mediation effect involving inter-IV_{FC} was observed in the DMN.

Reduced structural segregation reflects an altered balance between within- and between-network connectivity (Chan et al., 2014), likely due to relatively greater declines in within-network connections, and is characterized by less distinct modular boundaries. Consistently, we observed that lower structural segregation was associated with higher inter-IV_{SC} within these cortical systems, suggesting that age-related alterations in white-matter organization may co-occur with increased heterogeneity in how structural networks are configured across individuals. In the context of aging, greater inter-IV_{SC} may be partly related to heterogeneous white-matter deterioration processes, including myelin and axonal changes, which have been associated with poor executive functions (Bennett & Madden, 2014; Madden et al., 2009).

A small number of studies have reported associations between lower white-matter network segregation and worse executive functions across different samples (Baum et al., 2017; Matyi et al., 2025; Rodriguez-Nieto et al., 2025). Findings for functional network segregation have been less consistent, with some studies reporting similar associations between functional segregation and executive functions and others observing no reliable relationship (Chong et al., 2019; Martin et al., 2023; Stumme et al., 2020). Although the direct correlation between network segregation and executive control was largely absent in the present study (Table 4.2.2), a similar pattern emerged in several cortical networks when inter-IV of connectivity was incorporated as a mediator, such that lower network segregation was indirectly associated with worse executive control via higher inter-IV of connectivity. These findings were broadly consistent with the framework of functional dedifferentiation, which proposes that aging is associated with reduced specialization and increased overlap between large-scale brain systems, and is related to cognitive declines (Chan et al., 2014; Koen et al., 2020). However, the indirect effect of inter-IV_{FC} was not robust in the sensitivity analyses, suggesting that between-person variability in structural, rather than functional, network organization may be more closely linked to executive control in these systems.

Within the subcortical and cerebellar networks, inter-IV_{SC} and inter-IV_{FC} exhibited heterogeneous mediation patterns, which may reflect modality-specific associations between

network segregation and inter-IV of connectivity. In the subcortical network, lower functional segregation was associated with higher inter-IV_{FC}, consistent with interpretations within cortical systems. However, higher structural network segregation co-occurred with higher inter-IV_{SC} in the subcortical network. As described in Section 4.3.1, higher structural network segregation in the subcortical network may be associated with altered cortico–subcortical connectivity during aging, which is inherently heterogeneous across individuals (Bennett & Madden, 2014). A similar structural–functional reversal relative to the subcortical network was observed in the cerebellar network, although the specific coupling directions differed. While recent studies increasingly examine large-scale subcortical and cerebellar connectivity using both functional and structural metrics (e.g., De Benedictis et al., 2022; Harrison et al., 2021), their network-level segregation—particularly in the structural domain—and its cognitive relevance remain less well characterized, limiting direct comparison with the present findings. These findings suggest that structural and functional segregation capture partially distinct aspects of network organization, consistent with evidence that structural and functional connectivity are only partly coupled (Honey et al., 2009). Accordingly, analyses confined to cortical systems may not fully capture the diversity of large-scale network reorganization during healthy aging.

Importantly, despite system- and modality-specific patterns, a general pattern emerges: inter-IV of connectivity consistently mediates the relationship between network segregation and executive control in an unfavorable direction. Conceptually, inter-IV captures the extent to which individual network configurations deviate from a shared group-common profile (Mueller et al., 2013). Greater inter-IV of connectivity, therefore, reflects reduced convergence or alignment in network organizations across individuals (Smith et al., 2023). In aging, such increased variability may arise from heterogeneous trajectories of structural decline and functional reconfiguration, both of which may weaken the consistency of network–behavior coupling at the population level. These findings highlight inter-IV of connectivity as an important dimension of brain aging that complements mean-level changes in connectivity or segregation. Traditional group-average metrics characterize how networks are organized on average, but not how consistently that organization is expressed across individuals. This interpretation is consistent with recent perspectives emphasizing the utility of individualized network approaches in aging research (Perez et al., 2025).

4.3.3 Age-Moderated Mediation Effects of Inter-Individual Variability of Connectivity

Age-moderated mediation analyses indicated that the indirect association between network segregation and executive control via inter-IV varied across the sampled age range.

For structural connectivity, conditional indirect effects were most evident at the mean and older-old age levels, particularly within the SAN, FPN, DMN, and subcortical networks. This cross-sectional pattern suggests that inter-individual heterogeneity in structural connectivity may play a greater role in explaining variability in executive control at older ages. One possible interpretation is that age-related increases in the dispersion of network organization amplify the behavioral relevance of such variability in later life. Consistent with this observation, our results showed greater inter-IV at older ages (see Section 4.3.1). Such increased variability may contribute to differences in cognitive performance across older adults, as prior work has linked greater connectivity variability to stronger brain–behavior associations (Li et al., 2017). Importantly, these findings reflect age-related differences in cross-sectional associations rather than evidence of within-person change (Salthouse, 2012).

In functional connectivity, age-moderated indirect effects via inter-IV_{FC} were more restricted than those observed for structural connectivity, robust only in the visual network in the younger-old (i.e., -1 SD of age) and the subcortical network at the mean age. These network-specific and age-related effects provide limited evidence for a generalized mediating role of inter-IV_{FC} in linking network segregation to executive control across older adults. The effect observed in the visual network, which lies outside core executive control systems (Gratton et al., 2018; Hausman et al., 2022), warrants particular caution and may reflect network- and age-specific associations or unmodeled methodological variability in functional connectivity estimates (Noble et al., 2019). Nevertheless, the association observed in the subcortical network may relate to age-sensitive cortico–subcortical circuits that support executive processes through interactions between prefrontal cortical regions and subcortical structures, particularly basal ganglia–thalamic loops implicated in cognitive control (Halassa & Kastner, 2017; Heyder et al., 2004). Overall, inter-IV in functional connectivity appears to play an unstable and context-dependent role in network segregation–executive control relationships, in contrast to the more consistent indirect effects observed for structural connectivity. Future longitudinal studies will be necessary to determine whether these cross-sectional patterns reflect cohort differences or within-person change (Raz &

Lindenberger, 2011; Salthouse, 2012).

4.3.4 The Role of Intra-Individual Differences

When extending the model to account for intra-individual variability, we found that intra-IV of connectivity played a much more limited role than inter-IV. Its associations with executive control and network segregation were largely absent, with the only exceptions being network-specific effects in functional connectivity. This contrast underscores the importance of distinguishing between between-person dispersion and multi-year within-person differences when examining network variability in aging.

In the present study, intra-IV was operationalized as the dissimilarity between baseline and approximately four-year follow-up scans, capturing long-term changes rather than short-term fluctuations examined in prior work (e.g., Mueller et al., 2013; Sun et al., 2022). Within the visual network, higher functional network segregation was indirectly associated with poorer TMT B–A performance through its association with lower intra-IV_{FC}. In the age-moderated mediation model, this indirect effect in the visual network was observed only in the mean age group. Although direct evidence linking multi-year intra-individual variability of functional connectivity to cognition remains limited, prior work on short-timescale neural dynamics provides a conceptual backdrop. For example, prior work on dynamic reconfiguration of functional connectivity has emphasized that learning performance is associated with dynamic changes in modular organization (Bassett et al., 2011). At a different level of analysis, resting-state BOLD signal variability—quantified at the regional time-series level—has also been associated with age and behavioral performance across the lifespan (e.g., Garrett, Samanez-Larkin, et al., 2013; Nomi et al., 2017). Importantly, such variability follows region-specific lifespan trajectories, with variability in sensory regions, including the visual cortex, decreasing with age (Nomi et al., 2017). Although these measures differ in temporal scale and operational definition from intra-IV_{FC}, they collectively suggest that adaptive cognitive functioning is associated with a balance between neural stability and flexibility. Extending this framework to a longitudinal timescale, one possible interpretation is that lower intra-IV_{FC} may reflect reduced functional reconfiguration across years, potentially limiting the system's capacity to adjust connectivity patterns over time. Notably, lower intra-IV_{FC} was associated with poorer executive control in the present sample, which makes interpretations in terms of beneficial stability

less likely; instead, it is more consistent with reduced capacity for functional reconfiguration. However, intra-IV_{FC} does not directly index stability or reconfiguration capacity, and the effect was restricted to a specific network and age group; thus, this interpretation remains tentative.

In contrast, intra-IV_{SC} showed minimal associations with executive control. The weak effects observed suggest that long-term within-person changes in structural connectivity do not substantially mediate the relationship between network segregation and executive control in healthy aging. This does not preclude a role for structural intra-individual variability in other contexts, such as development, pathology, or periods of rapid plasticity, but indicates that its contribution may be limited in the present sample.

In summary, the present findings suggest that long-term intra-IV_{FC} is associated with differences in network-level reconfiguration. Associations with executive control were limited to the visual network. In contrast, intra-IV_{SC} showed no robust associations with executive control in healthy older adults. Future research should further investigate how variability across different timescales and networks relates to cognitive functioning, thereby clarifying its relevance for both typical and atypical aging trajectories.

It should be noted that, although multiple-comparison correction was applied, several effects did not remain statistically significant after correction. Accordingly, the present discussion emphasizes consistency of patterns across networks, modalities, and models rather than the significance of individual effects in isolation. Findings not surviving correction are therefore interpreted as provisional and hypothesis-generating. In addition, interpretations of the observed triangular relationships should be considered only in light of the covariates (age, sex, and education) included in the current models; broader biological and contextual influences are discussed in detail in Chapter 6.2.

4.4 Conclusions

This study reveals that inter-individual variability (inter-IV) in brain connectivity plays a critical, yet highly specific, mediating role in the relationship between large-scale network segregation and executive control in healthy older adults. Inter-IV generally shows an unfavorable mediation role for the relationship between network segregation and executive control, which may complicate group-level interpretations of the association between brain network architecture and cognition. This effect was more robust and consistent across structural connectivity within cortical networks (e.g., SMN, FPN), whereas in functional connectivity, it was more dependent on specific systems and age groups. In contrast, long-term intra-individual variability showed isolated and unstable mediation effects, largely confined to functional connectivity of the visual network. Age-moderated mediation effects were observed more consistently in inter-IV_{SC} models and were stronger at higher age values, but there was no clear convergence between structural and functional pathways in their mediation effects. Overall, these findings suggest that interpretations of network segregation in aging should account for individual variability in connectivity, as such variability constitutes an integral pathway linking large-scale network organization to executive control.

Chapter 5: Lifestyle-Informed Multimodal Brain Features for Predicting Cognitive Function

While the previous chapters examined relationships between lifestyle factors, brain organization, and cognitive performance, the present study shifts the focus to a predictive modelling framework. As discussed in Chapter 1, cognitive aging is characterized by substantial inter-individual heterogeneity, and lifestyle and psychosocial factors may represent one source of such heterogeneity (Harada et al., 2013; Smith et al., 2020). From a predictive modelling perspective, this heterogeneity poses challenges for approaches that rely solely on neuroimaging features, as they may only partly explain individual differences in cognition (e.g., Mattoni, Smith, et al., 2025; Rasero et al., 2021; Wu et al., 2021). Non-neuroimaging information, such as behavioral or questionnaire-based measures, may also provide additional predictive value. Given that lifestyle and psychosocial factors may influence brain structure and function (Chapter 1.2), incorporating lifestyle information into the brain feature construction may provide a complementary strategy to better capture lifestyle-related variation embedded within neuroimaging data, in line with growing interest in multimodal approaches to individualized prediction (Sui et al., 2020). It remains unclear whether brain features reflecting composite lifestyle patterns—capturing the joint influence of multiple lifestyle dimensions (hereafter BF-Life$_{\mathbf{multi}}$)—can predict both baseline and follow-up cognitive performance in healthy older adults.

Specifically, we distinguish between brain features linked to individual lifestyle or psychosocial measures (BF-Life$_{\mathbf{single}}$) and those reflecting composite lifestyle and psychosocial patterns (BF-Life$_{\mathbf{multi}}$). BF-Life$_{\mathbf{single}}$ models isolate neural correlates associated with a single lifestyle or psychosocial measure at a time, whereas BF-Life$_{\mathbf{multi}}$ models aim to capture shared neural signatures emerging from multidimensional lifestyle and psychosocial configurations, without explicitly assuming additive or independent contributions. For brevity, the term "lifestyle" is used in the following sections of this chapter as a shorthand referring to both lifestyle behaviors and the psychosocial measures considered in this study. This information-guided feature construction differs from approaches that rely on predefined lifestyle indices or that derive brain features without reference to behavioral context. Rather than treating lifestyle variables as predictors or covariates,

lifestyle information is used to guide feature construction, allowing us to test whether lifestyle-informed brain patterns are informative for cognitive prediction.

In addition to comparing BF-Life$_{\mathbf{multi}}$ with BF-Life$_{\mathbf{single}}$ models, we further compare this information-guided approach with fully data-driven prediction models. A common example of such models is principal component analysis (PCA)-based feature compression, in which high-dimensional multimodal brain data are reduced to a certain number of orthogonal components derived solely from the statistical structure of the imaging data. PCA-based approaches are widely used in neuroimaging prediction because they address high dimensionality and multicollinearity while remaining agnostic to external phenotypic information (Mwangi et al., 2014). However, PCA components reflect distributed mixtures of brain regions, which limits model interpretation under certain circumstances (Wani, 2025).

Together, these comparisons allow us to evaluate whether a model integrating multiple lifestyle variables provides predictive value for cognitive outcomes beyond both models based on individual lifestyle measures and fully data-driven models.

5.1 Methods

5.1.1 Sample and Data

Sample

Following the same initial age criterion of 55 years or older as in Studies 1 and 2, a total of 969 participants from 1000BRAINS were available for this study (345 were excluded for being younger or missing age information). Participants with DemTect scores in the impairment-indicative range (<8) or missing values were excluded (n = 23; Kalbe et al., 2004). Of this eligible sample, 859 participants had available structural MRI, diffusion MRI, and functional rs-fMRI. An additional 79 participants did not yield usable imaging data and were excluded from further analyses. Additionally, participants missing more than three of the 13 cognitive assessments were excluded (n = 6), leaving 774 participants (mean age 67.0 ± 6.7 years, 46.1% females).

Subsample datasets

Participants were divided into three non-overlapping subsets:

(i) Main dataset: n = 453 (mean age 67.7 ± 6.6 years, 47.0% females), used for feature selection and model training/testing.

(ii) Holdout1 dataset: n = 211 (mean age 66.3 ± 7.1 years, 47.4% females), used to test the model's performance on a completely unseen dataset.

(iii) Holdout2 dataset: n = 110 (mean age 65.3 ± 6.2 years, 40.0% females), reserved for prediction of "future", i.e., follow-up cognitive performance.

Specifically, of the 774 participants, 563 had available lifestyle data (mean age 67.3 ± 6.8 years, 55.6% females). Participants without lifestyle data (n = 211) were assigned to the Holdout1 dataset. Among the 563 participants with lifestyle data, 252 had available follow-up cognitive assessments; from this subgroup, 110 participants (approximately 20%) were *randomly* assigned to the Holdout2 dataset, and the remaining 453 participants (approximately 80%) constituted the main dataset to form an independent prediction sample for follow-up cognitive performance while preserving sufficient statistical power for feature selection and model training.

Lifestyle/psychosocial measures

To provide a more comprehensive assessment of lifestyle and psychosocial factors, four additional variables were included in this study, compared with the first study, to capture finer-grained aspects

of daily behavior and social engagement. In total, eight lifestyle and psychosocial variables were included: pack-years of smoking, alcohol consumption, physical activity, social integration, flights of stairs climbed, number of sports activities, number of physical activities, and number of social visits. Detailed descriptions of these variables are provided in Chapter 2.2.

Neuropsychological performance tests

For this study, we included the same 13 cognitive tests as used in the first study. Executive control was assessed using the TMT B/A ratio rather than the TMT B–A score, as the ratio minimizes the influence of psychomotor demands and helps control for intrasubject variability (Tsiakiri et al., 2024; Waggestad et al., 2023). In the analytic sample (N = 774), a small proportion of cognitive scores remained missing (<3% of observations) and was imputed using the median score from the four participants closest in age to the individual (two younger and two older neighbors) (Beretta & Santaniello, 2016).

In addition to these domain-specific analyses, we included a global cognitive component score as an additional target to assess whether the predictive performance of the BF-Life$_{\mathbf{multi}}$ model generalizes beyond specific cognitive domains. This global score was directly adopted from prior 1000BRAINS studies (Jockwitz et al., 2024; Kramer et al., 2024; Kramer et al., 2023), which used overlapping cognitive measures to capture shared variance across domains and construct a comprehensive global component. Incorporating this established score enabled direct comparison with previous work and provided a reference point for evaluating the specificity of BF-Life$_{\mathbf{multi}}$ predictions.

MRI brain data

In this study, we applied three MRI modalities: structural MRI, diffusion MRI (dMRI), and resting-state fMRI (rsfMRI). Detailed information on data acquisition and preprocessing is provided in Chapters 2.3 and 2.4.1–2.4.3.

5.1.2 Brain Features

Across all modalities, a total of 1,936 whole-brain features were included as candidate predictors.

Structural MRI features

For structural MRI, we extracted gray matter volume, cortical thickness, and surface area for 400 regions (3 × 400 features) using the Schaefer 400 parcellation scheme (Schaefer et al., 2018; see

also Chapter 2.4.1).

Diffusion MRI features

We used the ICBM-DTI-81 white matter label atlas (Mori et al., 2008), which comprises 48 tracts. All metrics derived from both DTI and NODDI were first transformed into MNI space using ANTs. A region-of-interest (ROI) mask was created for each white matter region encompassing part of a fiber tract. Within each ROI, we computed and extracted the average values of FA, MD, RD, AD, ICVF, and ODI for each participant. These tract-wise DTI and NODDI metrics (6 metrics × 48 tracts) were then used as input features for subsequent analyses.

Functional graph theoretical parameters

Functional graph-theoretical parameters were computed as described in Study 2 (Chapter 4.1.2). In short, we used the same parcellation scheme (421 regions: 400 cortical, 14 subcortical, and 7 cerebellar) and network assignment (nine networks, with the cerebellar regions treated as a separate network) and preprocessing workflow, including Fisher-z transformation and absolute value conversion of connectivity matrices.

Graph-theoretical metrics (i.e., within- and between-network connectivity and network segregation) were computed following the definitions described in Study 2. The present analysis additionally included node-wise functional network segregation scores. In total, 421 node-wise functional segregation values and 27 network-wise metrics (9 networks × 3 metrics) were extracted.

.

5.1.3 Development of the BF-Life$_{multi}$ Model

A schematic overview of the machine learning workflow is provided in Figure 5.1.1.

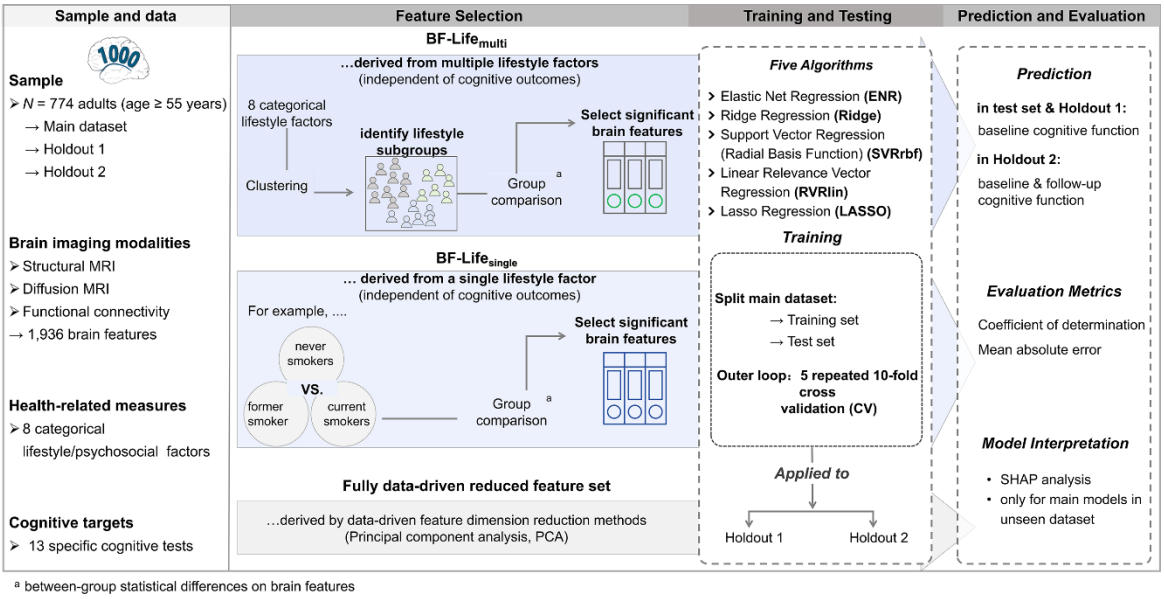

Figure 5.1.1 Overview of the workflow. Samples were split into a main dataset and two independent holdout sets, with 13 cognitive tests as prediction targets. From 1,936 brain features, feature extraction or dimensionality reduction was applied to construct machine-learning models. The primary analysis used an information-guided model based on optimal lifestyle clustering and derived multiple lifestyle-informed brain features (BF-Life$_{multi}$), while comparison models included single lifestyle-informed brain features (BF-Life$_{single}$) and fully data-driven principal component analysis (PCA)-based features. Models were trained using five repeats of nested cross-validation and evaluated using median coefficient of determination and mean absolute error. SHAP analysis was used for model interpretation.

Lifestyle clustering

To derive lifestyle-informed behavioral patterns and the corresponding brain features, participants were grouped into lifestyle-defined subgroups using a chosen set of eight lifestyle/psychosocial variables. Because these variables were originally continuous and prone to extreme values, they were transformed into ordinal categories to improve the robustness and stability of the clustering procedure:

(i) Pack-years of smoking (SMO): Smoking behavior was defined using self-reported number of smoked cigarettes per day (CigperDay) across three assessment points and was coded as never smoker (CigperDay = 0 at all assessments), former smoker (CigperDay = 0 at the final assessment but > 0 previously), or current smoker (CigperDay > 0 at the final assessment).

(ii) Alcohol consumption (ALC): It was classified into four groups based on self-reported daily intake (alc_gpday) and the consumption of spirits: never drinkers (alc_gpday = 0 at all time points), former drinkers (alc_gpday = 0 at the last measurement but > 0 earlier), current non-spirit drinkers (alc_gpday > 0 with no spirits consumption), and current spirit drinkers (alc_gpday > 0 with spirits consumption).

(iii) Physical activity (PA): It was quantified using metabolic equivalent of task (METs) scores, divided into quartiles, and reverse-coded from 3 (highest risk) to 0 (lowest risk) as follows: 3 = <25th percentile, 2 = 25th–50th percentile, 1 = 50th–75th percentile, 0 = ⩾75th percentile.

(iv) Social integration (SI): It was divided into four groups again using the quartiles approach.

Additionally, the same quartile-based approach was applied to flights of stairs climbed, counts of physical/sporty activities, and counts of visits. All variables were coded such that higher values indicated greater lifestyle-related health risks, for example, heavier smoking, higher alcohol intake, lower physical activity, or less social engagement.

Clustering was performed on the resulting categorical lifestyle dataset using the *k*-modes algorithm (version 0.12.2; Cao et al., 2009; Huang, 1998), which is specifically designed for categorical data and identifies clusters by minimizing Hamming distance between individual profiles and cluster modes. To reduce sensitivity to initialization, 1,000 random sets of initial centroids were evaluated, with cluster membership and modes iteratively updated until convergence or a maximum of 300 iterations was reached.

The optimal number of clusters (*k*) was determined by jointly considering quantitative cluster validity indices and substantive interpretability. Four evaluation metrics were used: the ratio of within- to between-cluster standard deviation (SW/SB), R-squared, the Silhouette coefficient (Rousseeuw, 1987), and the Davies–Bouldin Index (DBI) (Davies & Bouldin, 1979). Lower SW/SB and DBI values and higher R-squared and Silhouette scores were taken to indicate better clustering quality (Goh et al., 2024; Sofyan et al., 2021). Solutions with k ranging from 2 to 10 were examined. Because these indices tend to favor solutions with fewer clusters, the final selection of k was guided not only by statistical performance but also by biological and behavioral interpretability, in line with recommendations for clustering in applied research (Hennig, 2015).

Feature selection

Feature selection for constructing the BF-Life$_{multi}$ model was based on a systematic comparison of all 1,936 brain measures across the five lifestyle-defined subgroups. Univariate analyses of covariance (ANCOVAs) were performed for each brain feature while controlling for age, sex, education, and, in the case of morphometric indices, estimated total intracranial volume. Brain features showing significant differences between any pair of lifestyle subgroups were retained. Statistical significance was determined using a threshold of $p < .05$, followed by Bonferroni-adjusted post hoc comparisons ($q < .05$). When assumptions of homogeneity of variance were not met, the nonparametric Quade ANCOVA (Rae, 1985) was employed to ensure appropriate inference under violations of variance homogeneity.

This feature identification step was designed to select brain measures that differ across lifestyle-defined subgroups, rather than to test brain–lifestyle associations for statistical inference. Lifestyle information was therefore used only to define subgroups and identify candidate brain features, while cognitive outcomes were not involved at any stage of feature selection.

Because the purpose of this step was to construct a feature set for subsequent predictive modeling, no additional correction across the full set of neuroimaging variables was applied. Instead, all selected features were entered into the machine learning framework, where their utility was evaluated through nested cross-validation and independent holdout testing. Under this design, predictive performance reflects whether brain features carrying lifestyle-informed differences provide information relevant to cognitive function, rather than their univariate statistical significance alone.

Model setup

To estimate cognitive performance in older adults, a predictive model (BF-Life$_{multi}$) was constructed using brain features that differentiated the lifestyle-defined subgroups (see above). Five machine learning algorithms were implemented to assess model robustness and algorithmic variability: elastic net regression (ENR), ridge regression (Ridge), support vector regression with a radial basis function kernel (SVRrbf), relevance vector regression with a linear kernel (RVRlin), and least absolute shrinkage and selection operator (LASSO) regression (hereafter Lasso). Model development followed a nested cross-validation design, consisting of an outer loop with 10–fold cross-validation repeated five times to generate training and test datasets, and an inner 10–fold

cross-validation for hyperparameter tuning. For all algorithms, hyperparameters were optimized using predefined grid searches:

(i) ENR: *alpha* was sampled across eight logarithmic steps from 10^{-4} to 10^{3}, the L1 ratio varied from 0.1 to 0.9 in increments of 0.1, and maximum iterations were set to 1,000 to ensure convergence.

(ii) Ridge: *alpha* was sampled across the same logarithmic range (10^{-4} to 10^{3}), with the default solver selected automatically by the implementation, and a maximum of 1,000 iterations.

(iii) SVRrbf: the regularization parameter (*C*) was sampled across seven logarithmically spaced values between 10^{-3} and 10^{3}, and *gamma* was set to either *scale* or *auto*.

(iv) Lasso: *alpha* values were sampled logarithmically from 10^{-1} to 10^{5} using ten steps, with a maximum of 3,000 iterations.

(v) RVRlin: the precision parameters (*alpha* and *beta*) were tuned across values of 10^{-6}, 1, and 10^{3}, with a maximum of 1,000 iterations.

All features were standardized to a mean of zero and unit variance prior to model fitting. To mitigate overfitting and prevent information leakage, model performance was further evaluated on two independent holdout datasets. Holdout1 provided baseline cognitive measures, whereas Holdout2 included both baseline and follow-up assessments; in both cases, predictions relied exclusively on baseline MRI data. Although lifestyle information was not available for the Holdout1 sample, the full set of neuroimaging features was present, enabling the application of the trained models to estimate cognitive function at baseline.

Model evaluation

Model performance was assessed using the coefficient of determination (R^2) and the mean absolute error (*MAE*), where R^2 quantified the proportion of the variance in cognitive scores explained by the model. *MAE* provided a robust measure of average prediction error with intuitive interpretability, expressed in the same units as the cognitive scores (e.g., a *MAE* of 2 indicates an average prediction error of approximately two points) (Hodson, 2022).

Among the five algorithms evaluated, one was subsequently selected and fixed based on predictive performance, as quantified by R^2 and *MAE*, and all remaining models were constructed using the same algorithm (see Chapters 5.1.5 and 5.1.6).

Feature importance was evaluated using SHAP (SHapley Additive exPlanations; Lundberg & Lee, 2017) which estimates the contribution of individual predictors to model output. SHAP analyses were restricted to the optimal BF-Life$_{multi}$ model applied to a single independent holdout dataset, selected to provide stable out-of-sample predictions and to avoid overinterpretation across multiple test sets. Linear explainers were employed for ENR, Ridge, and LASSO, while kernel explainers were used for RVRlin and SVRrbf. For each feature, importance was quantified as the mean absolute SHAP value averaged over 50 cross-validation iterations (5 repeats × 10 folds).

For region-wise features, labels incorporated the functional network (e.g., SAN), the specific Schaefer parcellation region (e.g., FrOperIns_2), and the corresponding cytoarchitectonic area from the Juelich atlas (e.g., Id6; GapMap regions were omitted), enabling precise anatomical localization. To facilitate interpretation, given the high dimensionality of voxel- and region-level features, SHAP values were further aggregated into biologically meaningful categories (e.g., gray matter volume in the visual network, fractional anisotropy in association fiber tracts) according to established atlases or tractography references. Category-level importance was obtained by summing the SHAP values within each category and ranking them. All analyses were performed in Python (v3.10.9) using scikit-learn (v1.1.2).

5.1.4 Competitive Models for Comparison

Comparison with BF-Life$_{single}$ models

To evaluate whether combining multiple lifestyle-informed brain features enhances cognitive prediction, the BF-Life$_{multi}$ model was compared with four BF-Life$_{single}$ models, each derived from a single lifestyle or psychosocial measure (SMO, ALC, PA, and SI).

For each BF-Life$_{single}$ model, participants were grouped according to the categories defined for the corresponding measure (see Chapter 5.1.3). Feature selection was performed exclusively within the main dataset, following the same principles applied to the BF-Life$_{multi}$ model. Using the same ANCOVA framework, brain features associated with each measure were identified while adjusting for age, sex, education, estimated total intracranial volume (for morphometric measures), and the remaining three lifestyle/psychosocial measures. As in the BF-Life$_{multi}$ framework, cognitive outcomes were not involved in feature selection.

These identified features served as inputs for separate machine learning models. SHAP analyses were conducted for all BF-Life$_{single}$ models using the same procedures as for the BF-

$Life_{multi}$ model, ensuring consistent interpretation of feature importance.

Comparison with fully data-driven models

To evaluate the performance of the information-guided BF-$Life_{multi}$ model relative to the fully data-driven approaches, a set of models was developed using principal component analysis (PCA) to reduce dimensionality across all 1,936 brain features. PCA was applied either to the main dataset or solely to the training set, allowing assessment of potential information leakage and the robustness of data-driven dimensionality reduction. For each of these two settings, the number of components was determined using one of two strategies: **(a)** selecting components that cumulatively explained 80% of the total variance, and **(b)** selecting a number of components equal to the total features used in the BF-$Life_{multi}$ model. Combining these two PCA settings with the two component-selection strategies yielded four models: BF-PCAVar, BF-PCAVar(Train), BF-PCAMatch, and BF-PCAMatch(Train). This allowed assessment of how the number of components influenced predictive performance (see Figure 5.1.1).

All other modeling parameters, including algorithm selection and hyperparameter settings, were kept identical to those applied in the BF-$Life_{multi}$ model. Analyses focused on the algorithms and cognitive targets that demonstrated the highest predictive performance in the BF-$Life_{multi}$ framework, ensuring a fair comparison between information-guided and fully data-driven approaches.

5.1.5 Statistical and Supplementary Analyses

Statistical analyses

Descriptive statistics for the full sample, the main dataset, and the two holdout datasets are summarized in Tables 5.2.1 and 5.2.2. Comparisons between the main and holdout datasets were performed to assess their comparability in terms of demographic, lifestyle, and cognitive variables (Table 5.2.1). For normally distributed variables, one-way analyses of variance (ANOVA) were applied; sex differences were assessed using Chi-square tests, and non-normally distributed lifestyle variables were compared using Mann–Whitney U tests.

Differences among the lifestyle-defined subgroups identified in the main dataset were examined with respect to sex, demographic, lifestyle, and cognitive variables. Parametric ANCOVAs were used for normally distributed data, whereas nonparametric Quade ANCOVAs were applied when normality assumptions were violated.

To specifically assess the added predictive value of integrating multiple lifestyle-informed brain features, cross-validated predictive performance (R^2) of the BF-Life$_{\mathbf{multi}}$ model was compared with that of the four BF-Life$_{\mathbf{single}}$ models using ANOVA, followed by Bonferroni-corrected post hoc tests ($p < .05$; adjusted $q < .05$).

All statistical analyses were conducted using IBM SPSS Statistics version 29.0.

Supplementary Analyses

1. Role of adding non-brain data for model performance

To investigate the additional predictive value of non-brain factors, the BF-Life$_{\mathbf{multi}}$ model was extended in two steps. First, demographic variables (i.e., age, sex, education) were added to the original brain feature set, resulting in the BF-Life$_{\mathbf{multi}}$ + dem model. Second, the eight original continuous lifestyle variables were incorporated alongside demographic and brain features, yielding the BF-Life$_{\mathbf{multi}}$ + dem + life model.

Although these lifestyle variables had previously been transformed into categorical forms for clustering, they were not involved in the selection of brain features. In the extended models, lifestyle variables were treated solely as independent predictors, ensuring that their inclusion did not introduce circularity into the analysis.

All extended models were trained and evaluated using the same nested cross-validation and holdout procedures as the original BF-Life$_{\mathbf{multi}}$ model, allowing direct comparison of predictive performance.

2. Alternative lifestyle clustering

To examine the robustness of the BF-Life$_{\mathbf{multi}}$ framework with respect to different lifestyle subgroup definitions, alternative clustering solutions were evaluated. *K*-modes clustering was repeated for different values of *k*, excluding the optimal *k* identified in the primary analysis. Solutions with $k \geq 6$ were not considered due to excessive model complexity, reflected by small and unstable clusters that reduced interpretability and model robustness.

For each alternative *k*, lifestyle-informed brain features were identified using the same ANCOVA-based procedure as in the primary analysis and subsequently entered into machine learning models using identical hyperparameter settings.

3. Prediction of the global cognitive component

To determine whether the predictive performance of the BF-Life$_{\mathbf{multi}}$ model generalizes beyond

specific cognitive domains to overall cognitive function, a global cognitive component score was included as an additional outcome variable. Five participants lacking a global cognitive score were excluded, resulting in a sample of 769 individuals (mean age = 67.0 ± 6.7 years; 355 females), distributed across the main set (n = 449) and the two holdout datasets (Holdout1: n = 211; Holdout2: n = 109).

The models described above (14 models) were applied to predict the global cognitive component. This analysis assessed whether integrating multiple lifestyle-informed brain features added predictive value for overall cognition beyond domain-specific performance.

4. Comparison with target-dependent data-driven feature selection approaches

To evaluate whether the BF-Life$_{\mathbf{multi}}$ framework provided advantages over commonly used target-dependent, data-driven feature selection approaches (e.g., Kamalov et al., 2025), additional models were constructed using data-driven feature selection applied to the full set of brain features. In contrast to PCA-based models, which rely on unsupervised dimensionality reduction, these approaches selected features based solely on their association with cognitive outcomes. Four feature selection methods were implemented: mutual information regression, f-regression, ridge regression, and a hybrid filter–wrapper approach (Kraskov et al., 2004; Ross, 2014).

For each method, features were selected either by retaining the top 10% of variables or by matching the number of features used in the main BF-Life$_{\mathbf{multi}}$ model. All feature selection approaches were conducted exclusively within the training data of each cross-validation fold to prevent information leakage. All procedures were implemented in Python using the *mlxtend* package (Raschka, 2018). A complete overview of all evaluated models is provided in Table 5.1.1.

Table 5.1.1 Summary of machine learning models set up in this study.

Models	Feature count	Design	Description of feature selection
Main model and competitive models			
BF-Life$_{multi}$ models		Information-guided	Step1: clustering lifestyle subgroups using eight categorical lifestyle variables as input in the main set. Step2: performing univariate analyses of 1,936 brain features to identify intergroup differences among five identified lifestyle subgroups (main set).
k = 5	97		
BF-Life$_{single}$ models			Performing univariate analyses of 1,936 brain features separately for each lifestyle factor to identify intergroup differences among behavioral subgroups (main set).
SMO	117		
ALC	54		
PA	80		
SI	81		
Fully data-driven (reduction) models		Data-driven (unsupervised) feature reduction	
BF-PCAVar	166-167		Applying PCA to all 1,936 brain measures, with component number set either to explain 80% variance or to match the BF-Life$_{multi}$ feature size (main set). Applying PCA to all 1,936 brain measures, with component number set either to explain 80% variance or to match the BF-Life$_{multi}$ feature size (training set).
BF-PCAMatch	97		
BF-PCAVar(Train)	155-156		
BF-PCAMatch(Train)	97		
Supplementary analyses			
BF-Life$_{multi}$ models (alternative lifestyle clustering)		Information-guided	
k = 2	151		/
k = 3	102		/
k = 4	42		/
Incorporating non-brain data		mixed	
BF-Life$_{multi}$ +dem: k = 5	100		/
BF-Life$_{multi}$ +dem+life: k = 5	108		/
Data-driven feature selection approaches		Data-driven, target-dependent (supervised) feature selection	
BF-MI$_{unmatch}$	193		Mutual information regression: ranking features by their information with the target and selecting either the top 10% (unmatch) or top 5% (match) (training set). f_regression: ranking features by their F-test scores from univariate regressions with the target variable and retaining either the top 10% (unmatch) or top 5% (match) (training set). Ridge regression: ranking features by the magnitude of ridge-regularized coefficients and choosing either the top 10% (unmatch) or top 5% (match) (training set). Hybrid filter–wrapper approach: first filtering the top 50% of features using f_regression, then using a sequential forward floating selection with ridge regression to select either the top 193 features (unmatch) or the top 96 features (match) based on their rankings (training set).
BF-MI$_{match}$	96		
BF-f_regression$_{unmatch}$	193		
BF-f_regression$_{match}$	96		
BF-ridge$_{unmatch}$	193		
BF-ridge$_{match}$	96		
BF-hybrid$_{unmatch}$	193		
BF-hybrid$_{match}$	96		

Abbreviations: BF-Life$_{\mathbf{multi}}$, multiple lifestyle-informed brain features; *k*, cluster number; BF-Life$_{\mathbf{single}}$, single lifestyle-informed brain features; SMO/ALC/PA/SI, smoking- / alcohol consumption-/physical activity- / social integration-informed features; PCA, principal component analysis; BF-PCAVar / PCAVar(Train), PCA brain features from the main /training set, components explaining 80% variance; BF-PCAMatch / PCAMatch(Train), PCA brain features from the main /training set, components matched to the main BF-Life$_{\mathbf{multi}}$ model

5.2 Results

5.2.1 Demographic and Neuropsychological Measurements

Table 5.2.1 Basic information and baseline neuropsychological scores of participants.

	Mean (*SD*)				Statistic	
	Whole sample (*N* = 774)	**Main set (*n* = 453)**	**Holdout1 (*n* = 211)**	**Holdout2 (*n* = 110)**	**χ^2/*t*/*F*-value**	***p*-value**
Demographic variables						
Age [a]	67.0 (6.7)	67.7 (6.6)	66.3 (7.1)	65.3 (6.2)	7.020	**< .001**
Sex [b]	female, *n*= 357 (46.1%)	female, *n*= 213 (47.0%)	female, *n*= 100 (47.4%)	female, *n*= 44 (40.0%)	1.943	.378
Education [a]	6.48 (1.96)	6.32 (1.94)	6.71 (1.96)	6.72 (1.96)	3.807	**.023**
Lifestyle variables						
Packyears [c]	/	13.7 (20.64)	/	13.84 (20.43)	-0.832	.406
Alcohol [c]	/	10.57 (18.01)	/	11.47 (18.47)	-0.649	.516
Physical activity [c]	/	45.44 (53.77)	/	44.77 (41.24)	-0.961	.336
Stairs [c]	/	6.04 (8.03)	/	7.28 (11.14)	-1.846	.065
Social integration [c]	/	12.82 (6.09)	/	13.77 (7.13)	-1.299	.194
Visit_count [c]	/	6.10 (4.31)	/	6.76 (5.13)	-1.062	.288
Sporty_count [c]	/	2.53 (1.4)	/	2.48 (1.21)	-0.111	.911
Physical_count [c]	/	0.12 (0.42)	/	0.11 (0.37)	-0.005	.996
Cognitive variable						
Cognitive status [a]	14.82 (2.43)	14.76 (2.38)	14.89 (2.53)	14.93 (2.47)	0.326	.722
Language comprehension [a]	30.93 (4.93)	30.79 (5.14)	310 (4.93)	31.36 (4.02)	0.633	.531
Nomination [a]	14.51 (0.84)	14.51 (0.8)	14.46 (0.99)	14.59 (0.69)	0.814	.444
Figural memory [a]	8.72 (4.23)	8.17 (4.18)	9.26 (4.42)	9.94 (3.70)	10.35	**<.001**
Verbal WM [a]	4.70 (1.10)	4.64 (1.09)	4.86 (1.19)	4.65 (0.93)	3.088	**.046**
Phonemic fluency [a]	18.66 (6.01)	19.00 (6.12)	17.98 (5.59)	18.58 (6.26)	2.066	.127
Phonemic switch [a]	18.90 (5.96)	18.67 (5.88)	19.3 (6.12)	19.05 (5.99)	0.833	.435
Semantic fluency [a]	23.60 (6.74)	23.25 (6.62)	24.36 (6.78)	23.61 (7.06)	1.978	.139
Semantic switch [a]	19.86 (4.57)	19.47 (4.69)	20.7 (4.20)	19.86 (4.57)	5.281	**.005**
Visuospatial WM [a]	4.70 (1.05)	4.61 (1.06)	4.82 (1.01)	4.78 (1.10)	3.258	**.039**
Episodic memory [a]	60.76 (11.63)	59.86 (11.49)	61.8 (11.66)	62.49 (11.90)	3.431	**.033**
Long-term memory [a]	10.74 (2.63)	10.67 (2.62)	10.76 (2.55)	10.95 (2.80)	0.498	.608
Executive control [a]	2.40 (0.88)	2.46 (0.96)	2.30 (0.75)	2.38 (0.74)	2.375	.094

Note: Values are shown as mean (*SD*). Significant group differences are indicated in bold. Abbreviations: Packyears, packyears of smoking; Alcohol, alcohol consumption; Physical activity, measured by metabolic equivalent of the task; Stairs, flights of stairs climbed; Visit_count, count of visits from children, relatives, and friends; Sporty_count, count of sporty activities; Physical_count, count of physical activities

[a] Univariate Analysis of Variance

[b] Pearson Chi-Square

[c] Mann-Whitney U

Descriptive characteristics of the whole sample (N = 774; mean age = 67.0 ± 6.7 years) and the three sub-sample sets are summarized in Table 5.2.1. The three sub-sample sets did not differ in lifestyle factors. Significant differences, however, were observed in education level and several cognitive domains, including figural memory, verbal working memory, semantic switching, visuospatial working memory, and episodic memory. Table 5.2.2 lists the baseline and follow-up

neuropsychological scores of participants in Holdout2.

Table 5.2.2 Baseline and follow-up neuropsychological scores of participants in Holdout2.

	Holdout2 (*n* = 110)		***Statistic***	
	Baseline	**Follow-up**	***t*-value**	***p*-value**
Age	65.3 (6.2)	69.35 (6.0)	-58.373	**<.001**
Cognitive status	14.93 (2.47)	14.95 (2.43)	-0.126	0.900
Language comprehension	31.36 (4.02)	31.18 (3.91)	0.687	0.494
Nomination	14.59 (0.69)	14.5 (0.85)	1.234	0.220
Figural memory	9.94 (3.70)	9.96 (3.86)	-0.091	0.928
Verbal WM	4.65 (0.93)	4.61 (1.06)	0.360	0.720
Phonemic fluency	18.58 (6.26)	18.86 (6.50)	-0.364	0.717
Phonemic switch	19.05 (5.99)	18.5 (5.80)	0.700	0.486
Semantic fluency	23.61 (7.06)	24.15 (7.42)	-0.532	0.596
Semantic switch	19.86 (4.57)	20.33 (4.73)	-0.760	0.449
Visuospatial WM	4.78 (1.10)	4.71 (1.10)	0.619	0.537
Episodic memory	62.49 (11.90)	68.99 (10.26)	-5.224	**<.001**
Long-term memory	10.95 (2.80)	12.03 (2.39)	-4.811	**<.001**
Executive control	2.38 (0.74)	2.38 (0.76)	-0.061	0.952

Note: The mean value and standard deviation are represented as mean (*SD*). The statistical analysis employed a paired-samples *t*-test. Significant group differences are indicated in bold. Abbreviations: WM, working memory

5.2.2 Lifestyle Subgroups and Lifestyle-Informed Brain Features

Cluster evaluation (k = 2–10) showed that both k = 2 and k = 5 achieved similar clustering performance (see Table 5.2.3). The five-cluster solution was selected for the main analysis because it captured greater heterogeneity in lifestyle patterns; the predicted results of the other solutions are also provided.

Table 5.2.3 Optimal *k* value in *K*-Modes clustering.

Number of clusters (*k*)	*SW*/*SB* Ratio	*R*-Squared	Silhouette Score	Davies-Bouldin Index (DBI)
2	**0.029**	**0.972**	**0.111**	**2.438**
3	0.038	0.963	0.107	4.682
4	0.037	0.964	0.105	3.577
5	**0.035**	**0.967**	**0.107**	**3.117**
6	0.038	0.964	0.090	3.065
7	0.040	0.962	0.090	3.259
8	0.045	0.957	0.089	3.641
9	0.046	0.956	0.091	3.303
10	0.046	0.956	0.094	3.462

Note: A lower *SW*/*SB* ratio and DBI score indicate better clustering performance, while higher *R*-squared and Silhouette scores suggest better cluster separation. Bold indicates the optimal solution; italics indicate the suboptimal solution. Although k = 2 yields the best performance across all metrics, we selected k = 5 as the optimal number of clusters. This choice balances clustering quality and interpretability by providing finer subgroup differentiation, while still maintaining moderate *SW*/*SB* and *R*-squared values and relatively low DBI. Abbreviations: *SW*, standard deviation of the group; *SB*, standard deviation between groups

Figure 5.2.1 summarizes the brain, cognitive, and lifestyle characteristics of the five lifestyle subgroups. Lifestyle subgroups differed in figural and episodic memory, with subgroup 1 showing the lowest episodic memory, subgroup 3 the lowest figural memory, and subgroup 2 the highest scores. Lifestyle variables (pack-years of smoking, physical activity, social integration) varied significantly, with subgroup 1 presenting the least healthy lifestyle profile.

Feature selection identified 97 MRI measures that differed across at least one pair of subgroups (Figure 5.2.2). These features comprised gray matter morphometry (GMV, CT, SA), functional network segregation, and microstructural indices (e.g., ICVF). Most gray matter features were located in the visual (VIN) and default mode (DMN) networks, followed by salience/ventral attention (SAN), dorsal attention (DAN), and somatomotor (SMN) networks. White matter differences mainly involved association fibers (e.g., cingulum bundle) and projection fibers (e.g.,

corona radiata). These features served as input to the BF-Life$_{multi}$ model.

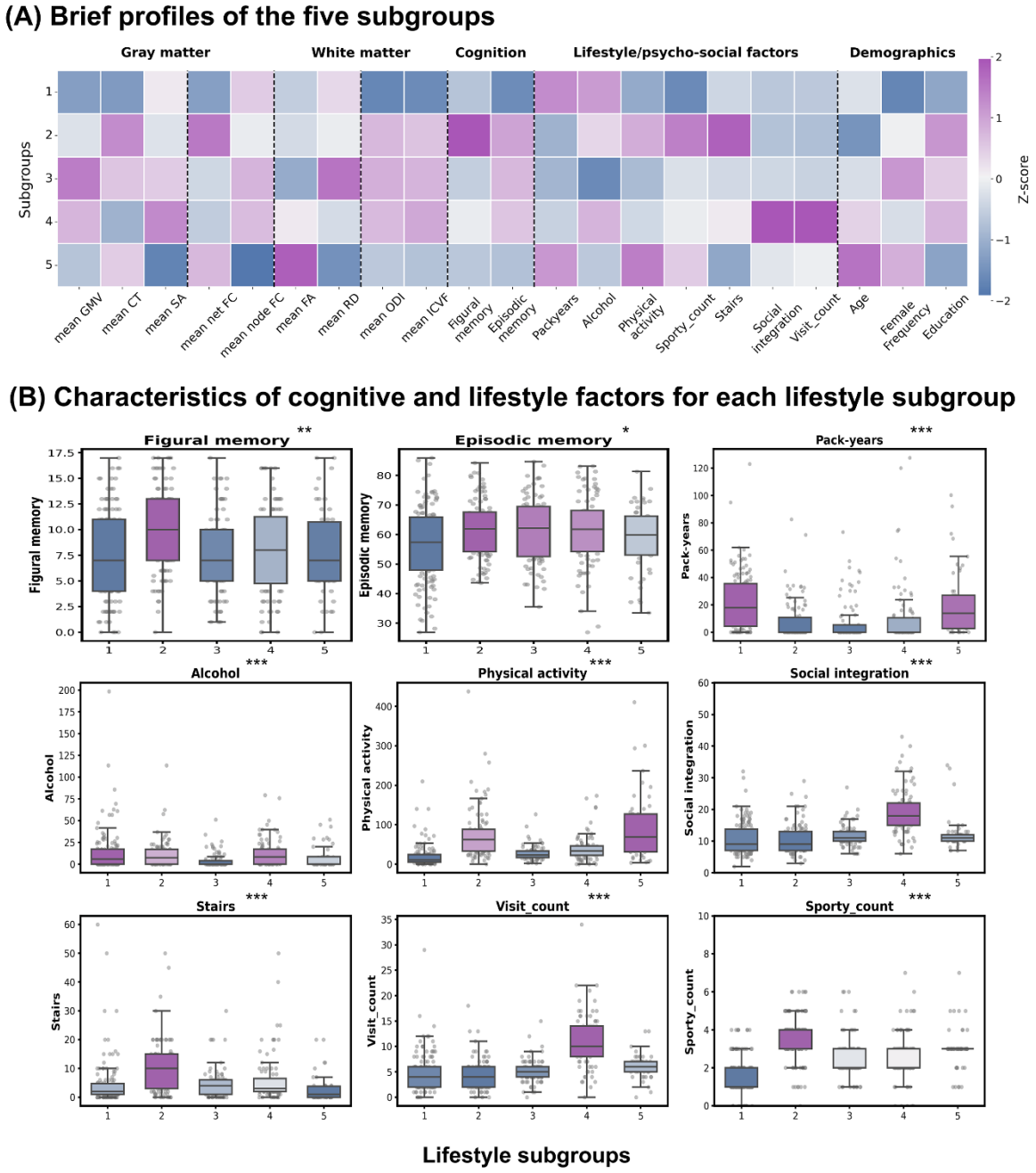

Figure 5.2.1 Characterization of the five lifestyle subgroups identified by clustering. Top: Variables were averaged within subgroups, normalized, and visualized as the colors ranging from purple (high) to blue (low). **Bottom:** Brief profiles of the five subgroups. Only variables with significant subgroup differences are shown. Abbreviations: GMV, gray matter volume; CT, cortical thickness; SA, surface area; FC, functional connectivity; net FC, network-wise FC metrics; node FC, node-wise functional segregation; FA, fractional anisotropy; RD, radial diffusivity; ICVF, intracellular volume fraction; ODI, orientation dispersion index; Stairs, flights of stairs; Visit_count, visits from children/relatives/friends; Sporty/physical_count, count of sporty/physical activities

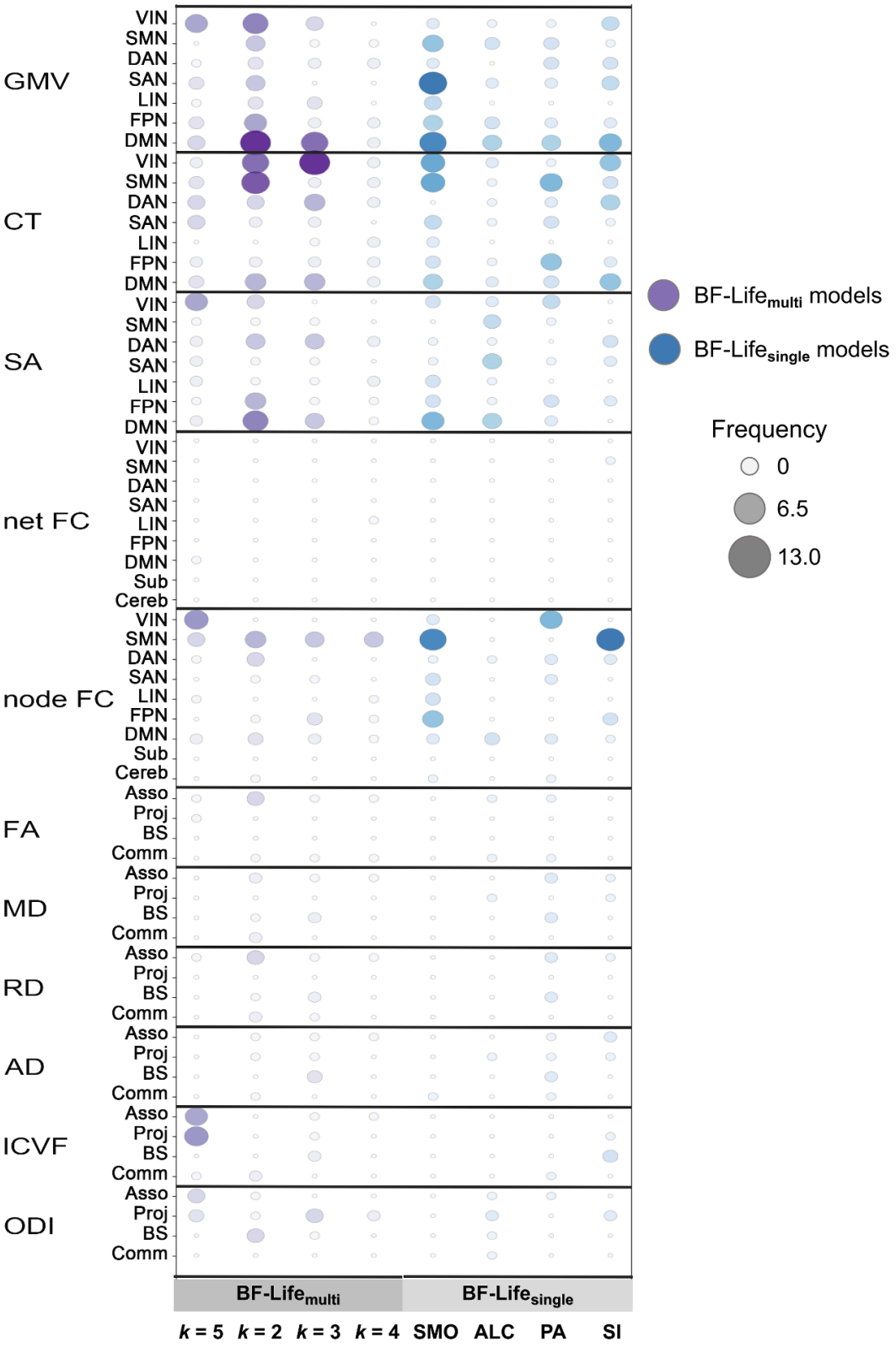

Figure 5.2.2 Frequency of each feature category in the BF-Life$_{multi}$ and BF-Life$_{single}$ models. Bubble color intensity and size correspond to feature frequency, with darker and larger bubbles indicating higher frequencies. Abbreviations: *k*, cluster number; BF-Life$_{multi}$, multiple lifestyle-informed brain features; BF-Life$_{single}$, single lifestyle-informed brain features; SMO/ALC/PA/SI, smoking-/alcohol-/physical activity-/social integration-informed brain features; GMV, gray matter volume; CT, cortical thickness; SA, surface area; FC, functional connectivity; net FC, network-wise

FC metrics; node FC, node-wise functional segregation; FA, fractional anisotropy; MD, mean diffusivity; AD, axial diffusivity; RD, radial diffusivity; ICVF, intracellular volume fraction; ODI, orientation dispersion index; Asso /Proj /BS /Comm, association /projection /brainstem /commissural fiber tract; VIN, visual network; SMN, somatomotor network; DAN, dorsal attention network; SAN, salience/ventral attention network; LIN, limbic network; FPN, frontoparietal control network; DMN, default mode network; Sub, subcortical network; Cereb, cerebellar network

5.2.3 Predictive Performance and Model Comparisons

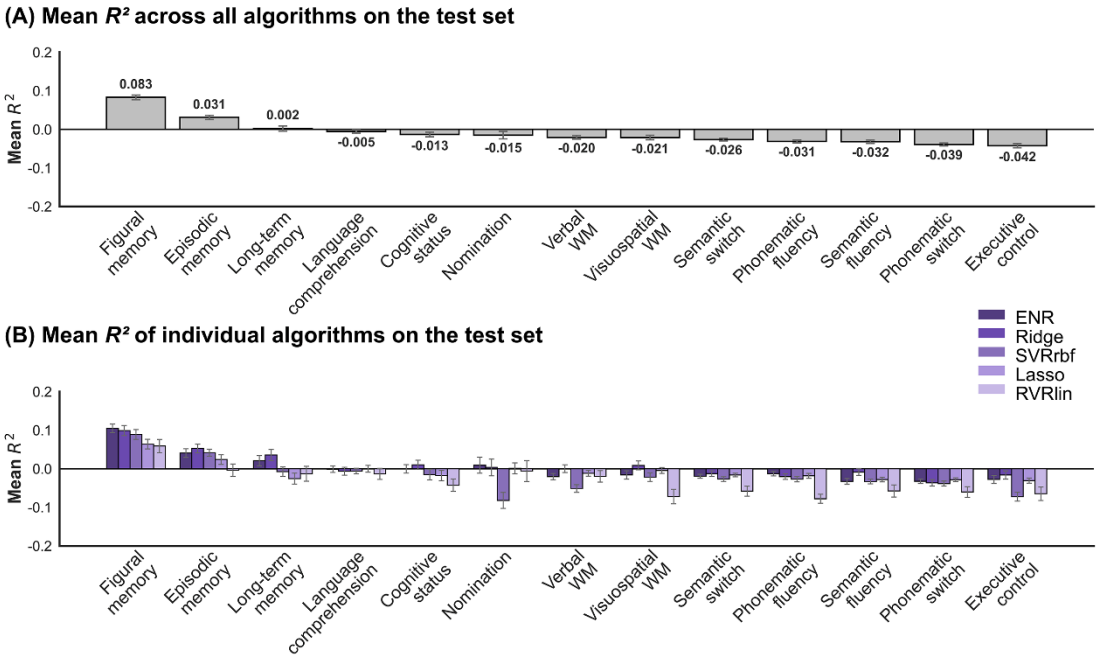

Figure 5.2.3 Overview of predictive performance of the BF-Life$_{multi}$ model (*k*=5) across cognitive outcomes. (A) Mean R^2 scores across five algorithms for each cognitive target, shown in descending order. **(B)** Mean R^2 scores of individual algorithms for the same 13 targets, displayed in the same order. Abbreviations: BF-Life$_{multi}$, multiple lifestyle-informed brain features; *k*, cluster number; WM, working memory; ENR, elastic net regression; Ridge, ridge regression; SVRrbf, support vector regression with RBF kernel; Lasso, least absolute shrinkage and selection operator regression; RVRlin, relevance vector regression with linear kernel

Figure 5.2.3 displays an overview of the predictive performance of the BF-Life$_{multi}$ model (k = 5) across cognitive outcomes, which was obtained by summarizing mean R^2 values across algorithms in the test set. Only figural and episodic memory demonstrated above-zero predictive performance across algorithms (mean R^2 = 0.083 and 0.031, respectively). Long-term memory showed negligible predictive power (mean R^2 = 0.002). In contrast, the remaining ten cognitive test scores exhibited negative mean R^2 values, indicating no reliable predictive performance, and were therefore not considered further.

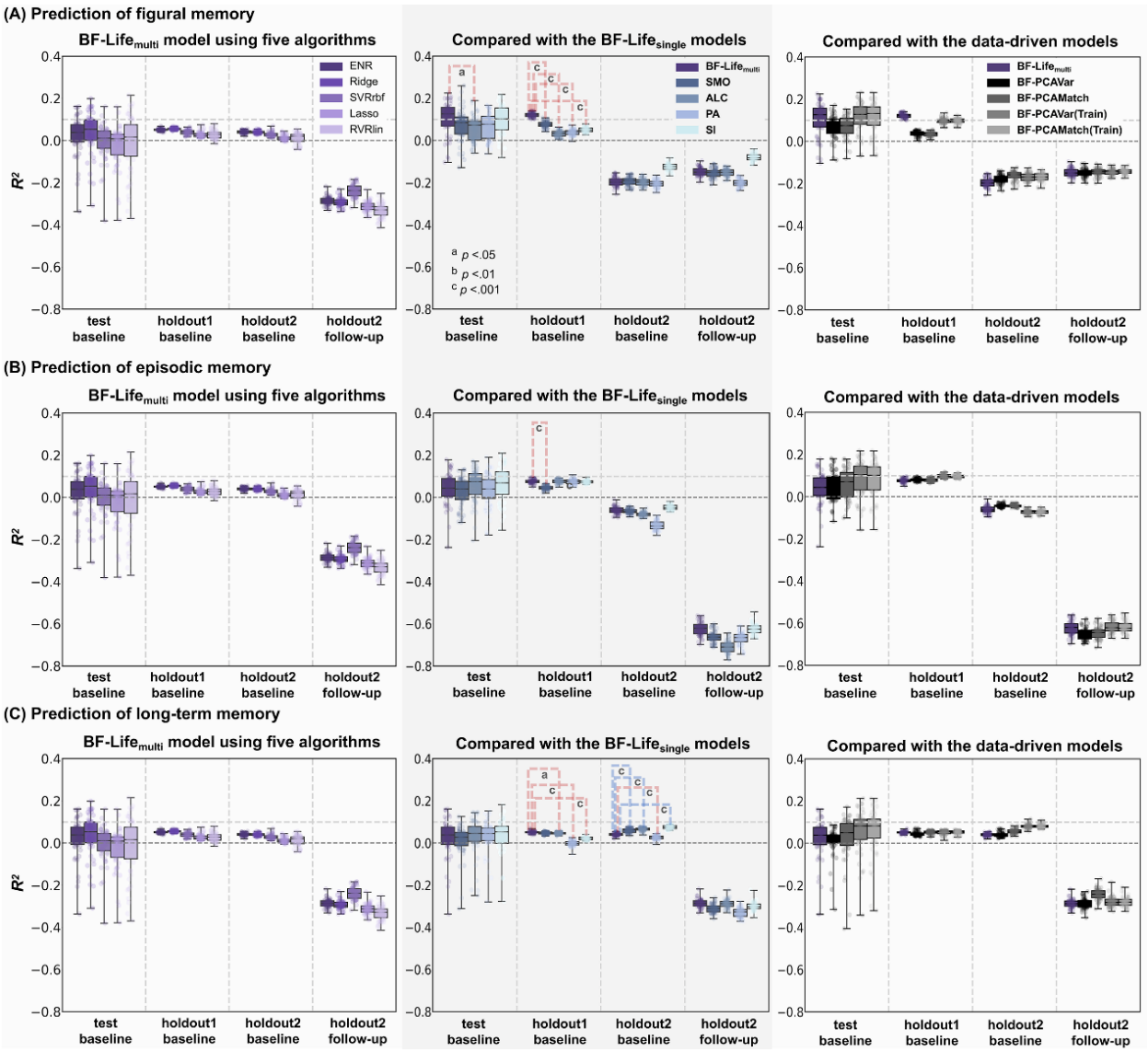

Figure 5.2.4 Performance of predictive models in predicting figural (A), episodic (B) and long-term memory (C). The first column shows the performance of the five algorithms. The second column compares the BF-Life$_{multi}$ model with four BF-Life$_{single}$ models using the elastic net regression (ENR) algorithm, with red dashed lines indicating higher R^2 for BF-Life$_{multi}$ and blue dashed lines indicating higher R^2 for the comparator. The third column compares BF-Life$_{multi}$ with four fully data-driven models. A light gray dashed line marks $R^2 = 0.10$ as a reference. Abbreviations: BF-Life$_{multi}$, multiple lifestyle-informed brain features; *k*, cluster number; BF-Life$_{single}$, single lifestyle-informed brain features; SMO/ALC/PA/SI, smoking-/alcohol-/physical activity-/social integration-informed brain features; PCA, Principal component analysis; BF-PCAVar / PCAVar(Train), PCA brain features from the train set, components explaining 80% variance; BF-PCAMatch / PCAMatch(Train), PCA brain features from the train set, components matched to the BF-Life$_{multi}$ model; +dem, includes demographic data

Figural memory

The BF-Life$_{multi}$ model showed the strongest predictive performance for figural memory across datasets. In the test set, the model explained up to 13% of the variance, with the ENR algorithm achieving the highest performance (median R^2 = 0.13, panel A in Figure 5.2.4; see Table 5.2.4 for median *MAE* value). Using ENR, the BF-Life$_{multi}$ model significantly outperformed the ALC model (median R^2 = 0.07, $p < 0.05$; Table 5.2.5) and performed comparably to the SMO, PA, and SI models (median R^2 = 0.08–0.10). Relative to the fully data-driven models BF-PCAVar and BF-PCAMatch, BF-Life$_{multi}$ showed slightly higher performance (median R^2 = 0.07 – 0.08) and performed comparably to BF-PCAVar(Train) and BF-PCAMatch(Train) (median R^2 = 0.13).

In Holdout1, BF-Life$_{multi}$ maintained comparable performance, explaining up to 12% of the variance (ENR: median R^2 = 0.12; Table 5.2.4). Using ENR, it significantly outperformed all four BF-Life$_{single}$ models (all $p < .001$; Table 5.2.5). It also surpassed BF-PCAVar and BF-PCAMatch (both median R^2 = 0.04) and slightly outperformed BF-PCAVar(Train) and BF-PCAMatch(Train) (median R^2 = 0.10).

In contrast, Holdout2 revealed a failure to generalize, with negative median R^2 values across all algorithms at both baseline and follow-up, and similarly, poor performance was observed in all comparison models (Tables 5.2.4 and 5.2.5).

Episodic memory

BF-Life$_{multi}$ showed modest predictive performance for episodic memory across datasets. In the test set, the model explained up to 6% of the variance, with the ENR algorithm achieving a median R^2 = 0.04 (panel B in Figure 5.2.4; Table 5.2.4). Using ENR, BF-Life$_{multi}$ performed comparably to BF-Life$_{single}$ models (median R^2 = 0.04–0.07, $p > 0.05$), but underperformed relative to all fully data-driven models (median R^2 = 0.06–0.10; Table 5.2.5).

In Holdout1, predictive performance slightly improved, explaining up to 8% of the variance (ENR: median R^2 = 0.07; Table 5.2.4). Using ENR, BF-Life$_{multi}$ outperformed the SMO model ($p < .001$) while performing comparably to the ALC, PA, and SI models (median R^2 = 0.07–0.08). Its performance was similar to BF-PCAVar and BF-PCAMatch (median R^2 = 0.08) but slightly lower than BF-PCAVar(Train) and BF-PCAMatch(Train) (median R^2 = 0.09–0.10; Table 5.2.5).

In Holdout2, none of the models, including BF-Life$_{multi}$, achieved meaningful prediction at baseline or follow-up (Table 5.2.5).

Long-term memory

BF-Life$_{multi}$ showed low but consistent predictive performance for long-term memory across datasets. In the test set, the model explained up to 5% of the variance, with ENR achieving a median R^2 = 0.04 (panel C in Figure 5.2.4; Table 5.2.4). Using ENR, BF-Life$_{multi}$ performed comparably to BF-Life$_{single}$ models (median R^2 = 0.03–0.05), and to BF-PCAVar and BF-PCAMatch (median R^2 = 0.03–0.05), but underperformed relative to the BF-PCAVar(Train) and BF-PCAMatch(Train) (median R^2 = 0.08; Table 5.2.5).

In Holdout1, BF-Life$_{multi}$ explained up to 6% of the variance (ENR: median R^2 = 0.05; Table 5.2.4). Using ENR, BF-Life$_{multi}$ outperformed ALC, PA, and SI models (all $p < .05$; median R^2 =-1.15×10^{-3} to 0.05) and performed comparably to SMO and all fully data-driven models (median R^2 = 0.04–0.05; Table 5.2.5).

In the Holdout2 baseline, BF-Life$_{multi}$ showed a weak positive predictive performance (median R^2 = 0.01–0.04, Table 5.2.4). Using ENR, it outperformed the PA model ($p < .001$; median R^2 = 0.03; Table 5.2.5) but underperformed relative to the SMO, ALC, and SI models ($p < 0.001$; median R^2 = 0.06–0.07). The BF-Life$_{multi}$ model performed comparably to both fully data-driven models (median R^2 = 0.04–0.06) but underperformed relative to those with features obtained in the training dataset (both median R^2 = 0.08). However, no model achieved meaningful prediction for follow-up long-term memory (Table 5.2.5).

Table 5.2.4 Performance of the BF-Life$_{multi}$ model in predicting figural, episodic, and long-term memory.

Models	Targets	Algorithms	Median R^2				Median *MAE*			
			Test baseline	Holdout1 baseline	Holdout2 baseline	Holdout2 follow-up	Test baseline	Holdout1 baseline	Holdout2 baseline	Holdout2 follow-up
BF-Life$_{multi}$ models	Figural memory	**ENR**	**0.13**	**0.12**	**-0.20**	**-0.15**	**3.16**	**3.35**	**3.30**	**3.32**
		Ridge	0.13	0.11	-0.20	-0.15	3.18	3.36	3.30	3.33
		SVRrbf	0.09	0.08	-0.24	-0.19	3.21	3.45	3.36	3.46
		Lasso	0.09	0.09	-0.19	-0.15	3.22	3.42	3.27	3.34
		RVRlin	0.07	0.09	-0.33	-0.26	3.22	3.41	3.50	3.44
	Episodic memory	**ENR**	**0.04**	**0.07**	**-0.06**	**-0.62**	**8.77**	**8.93**	**9.83**	**10.72**
		Ridge	0.06	0.08	-0.08	-0.64	8.67	8.92	9.92	10.79
		SVRrbf	0.05	0.05	-0.07	-0.68	8.65	9.10	9.80	10.97
		Lasso	0.03	0.07	-0.07	-0.63	8.79	8.89	9.88	10.70
		RVRlin	-2.46×10^{-3}	0.07	-0.11	-0.63	8.92	8.93	9.97	10.69
	Long-term memory	**ENR**	**0.04**	**0.05**	**0.04**	**-0.29**	**2.00**	**1.92**	**2.15**	**2.21**
		Ridge	0.05	0.06	0.04	-0.30	1.97	1.91	2.16	2.20
		SVRrbf	0.01	0.04	0.03	-0.24	2.03	1.88	2.13	2.11
		Lasso	0.01	0.02	0.01	-0.31	2.06	1.98	2.19	2.22
		RVRlin	0.02	0.03	0.02	-0.33	2.05	1.91	2.18	2.23

Abbreviations: R^2, coefficient of determination; *MAE*, mean absolute error; BF-Life$_{multi}$, multiple lifestyle-informed brain features; PCA, principal component analysis; BF-PCAVar / PCAVar(Train), PCA brain features from the main /training set, components explaining 80% variance; BF-PCAMatch / PCAMatch(Train), PCA brain features from the main /training set, components matched to the BF-Life$_{multi}$ model; ENR, elastic net regression; Ridge, ridge regression; SVRrbf, support vector regression with radial basis function kernel; Lasso, least absolute shrinkage and selection operator regression; RVRlin, relevance vector regression with the linear kernel

Table 5.2.5 Performance of 14 models predicting figural, episodic, and long-term memory using the elastic net regression algorithm.

Targets	Models	Median R^2				Median *MAE*			
		Test set baseline	Holdout1 baseline	Holdout2 baseline	Holdout2 follow-up	Test set baseline	Holdout1 baseline	Holdout2 baseline	Holdout2 follow-up
Figural memory	**BF-Life$_{multi}$ models**								
	k* = 5	**0.13**	**0.12**	**-0.20**	**-0.15**	**3.16**	**3.35**	**3.30**	**3.32**
	k = 2	0.06	0.09	-0.15	-0.10	3.23	3.39	3.27	3.29
	k = 3	0.08	0.04	-0.24	-0.17	3.22	3.49	3.33	3.42
	k = 4	0.08	0.02	-0.29	-0.25	3.29	3.49	3.41	3.51
	BF-Life$_{single}$ models								
	SMO	0.08	0.08	-0.19	-0.15	3.26	3.46	3.28	3.37
	ALC	0.07	0.03	-0.20	-0.15	3.25	3.50	3.33	3.40
	PA	0.08	0.04	-0.20	-0.20	3.25	3.52	3.29	3.46
	SI	0.10	0.05	-0.12	-0.08	3.17	3.49	3.24	3.32
	Data-driven models								
	BF-PCAVar	0.08	0.04	-0.18	-0.15	3.22	3.51	3.30	3.39
	BF-PCAMatch	0.07	0.04	-0.16	-0.14	3.26	3.51	3.29	3.38
	BF-PCAVar(Train)	0.13	0.10	-0.17	-0.14	3.15	3.37	3.28	3.36
	BF-PCAMatch(Train)	0.13	0.10	-0.17	-0.14	3.16	3.36	3.28	3.36
	Incorporating non-brain data								
	BF-Life$_{multi}$ +dem: *k* = 5	0.21	0.23	-0.07	3.42×10^{-3}	2.98	3.17	3.09	3.10
	BF-Life$_{multi}$ +dem+life: *k* = 5	0.22	/	-0.06	-5.74×10^{-4}	3.03	/	3.09	3.13
Episodic memory	BF-Life$_{multi}$ **models**								
	k* = 5	**0.04**	**0.07**	**-0.06**	**-0.62**	**8.77**	**8.93**	**9.83**	**10.72**
	k = 2	0.05	0.09	-0.11	-0.66	8.88	8.79	10.12	10.94
	k = 3	0.04	0.05	-0.07	-0.71	8.93	9.12	9.95	11.11
	k = 4	0.06	0.07	-0.07	-0.67	8.79	9.01	9.89	10.87
	BF-Life$_{single}$ models								
	SMO	0.04	0.04	-0.07	-0.66	8.89	9.14	9.89	10.98
	ALC	0.07	0.08	-0.08	-0.71	8.82	8.88	9.79	10.92
	PA	0.04	0.08	-0.14	-0.66	8.90	9.02	10.25	11.07
	SI	0.07	0.07	-0.05	-0.62	8.75	9.06	9.77	10.84
	Data-driven models								
	BF-PCAVar	0.06	0.08	-0.04	-0.65	8.91	8.95	9.80	10.88
	BF-PCAMatch	0.07	0.08	-0.04	-0.64	8.84	8.98	9.80	10.86

	BF-PCAVar(Train)	0.10	0.10	-0.07	-0.62	8.71	8.83	9.84	10.75
	BF-PCAMatch(Train)	0.10	0.09	-0.07	-0.62	8.71	8.84	9.83	10.76
	Incorporating non-brain data								
	BF-Life$_{\mathbf{multi}}$ +dem: k = 5	0.11	0.11	-0.02	-0.51	8.62	8.76	9.64	10.53
	BF-Life$_{\mathbf{multi}}$ +dem+life: k = 5	0.12	/	-0.01	-0.52	8.66	/	9.59	10.55
	BF-Life$_{\mathbf{multi}}$ models								
	k* = 5	**0.04**	**0.05**	**0.04**	**-0.29**	**2.00**	**1.92**	**2.15**	**2.21**
	k = 2	0.04	0.04	0.03	-0.31	2.03	1.96	2.16	2.21
	k = 3	0.02	0.04	0.07	-0.28	2.04	1.97	2.12	2.19
	k = 4	0.04	0.06	0.06	-0.29	2.04	1.95	2.10	2.18
	BF-Life$_{\mathbf{single}}$ models								
	SMO	0.03	0.05	0.06	-0.31	2.02	1.95	2.12	2.21
	ALC	0.05	0.05	0.07	-0.29	2.04	1.95	2.14	2.19
Long-term	PA	0.04	-1.15×10^{-3}	0.03	-0.33	2.02	1.99	2.17	2.23
memory	SI	0.05	0.02	0.07	-0.30	2.01	1.97	2.12	2.22
	Data-driven models								
	BF-PCAVar	0.03	0.04	0.04	-0.29	2.02	1.96	2.16	2.19
	BF-PCAMatch	0.05	0.05	0.06	-0.24	2.01	1.93	2.14	2.17
	BF-PCAVar(Train)	0.08	0.05	0.08	-0.28	1.97	1.92	2.12	2.19
	BF-PCAMatch(Train)	0.08	0.05	0.08	-0.28	2.00	1.92	2.12	2.19
	Incorporating non-brain data								
	BF-Life$_{\mathbf{multi}}$ +dem: k = 5	0.08	0.11	0.08	-0.24	1.96	1.86	2.09	2.17
	BF-Life$_{\mathbf{multi}}$ +dem+life: k = 5	0.09	/	0.09	-0.24	1.93	/	2.08	2.16

Note: (*) indicates the model used for the main analysis. Abbreviations: R^2, coefficient of determination; *MAE*, mean absolute error; *k*, cluster number; BF-Life$_{\mathbf{multi}}$, multiple lifestyle-informed brain features; BF-Life$_{\mathbf{single}}$, single lifestyle-informed brain features; SMO/ALC/PA/SI, smoking- / alcohol consumption- /physical activity- / social integration-informed features; BF-PCAVar / PCAVar(Train), brain features via PCA (main dataset/train set), components explain 80% variance; BF-PCAMatch / PCAMatch(Train), brain features via PCA (main dataset/train set), components matched to the BF-Life$_{\mathbf{multi}}$; +dem, includes demographic data; +dem+life, includes demographic and lifestyle data

5.2.4 Feature Importance for Predicting Figural Memory

Feature importance analysis via SHAP was focused on figural memory, specifically for the predictions based on Holdout1 with the ENR algorithm, as this prediction was the most reliable in terms of R^2 scores (see Chapter 5.2.3).

Summary of Feature Importance by Category (BF-Life$_{multi}$ vs BF-Life$_{single}$)

Analysis of the unseen Holdout1 dataset revealed distinct neuroanatomical predictors of figural memory performance across the BF-Life$_{multi}$ model and the four BF-Life$_{single}$ models using ENR. For the BF-Life$_{multi}$ model, the most influential feature categories included CT in the SAN and SMN, and GMV in the DMN, accounting for 8.5–9.6% of the BF-Life$_{multi}$ model's total contribution, respectively (see Figure 5.2.5).

In contrast, the four BF-Life$_{single}$ models (SMO, ALC, PA, and SI) showed distinct patterns of feature importance. The SMO model was mainly driven by CT and GMV in the SMN, as well as CT in the DMN. The ALC model was primarily driven by CT in the DMN and DAN, and GMV in the frontoparietal control network (FPN). In the PA model, key contributors included CT in the SAN, node-wise FC segregation in the VIN, and FA of commissural fiber tracts. Finally, the SI model relied on node-wise FC segregation and GMV in the SAN, and CT in the SMN. For all four single-lifestyle models, the most influential feature categories accounted for 9.3–11.6% of each model's overall contribution (see Figure 5.2.5).

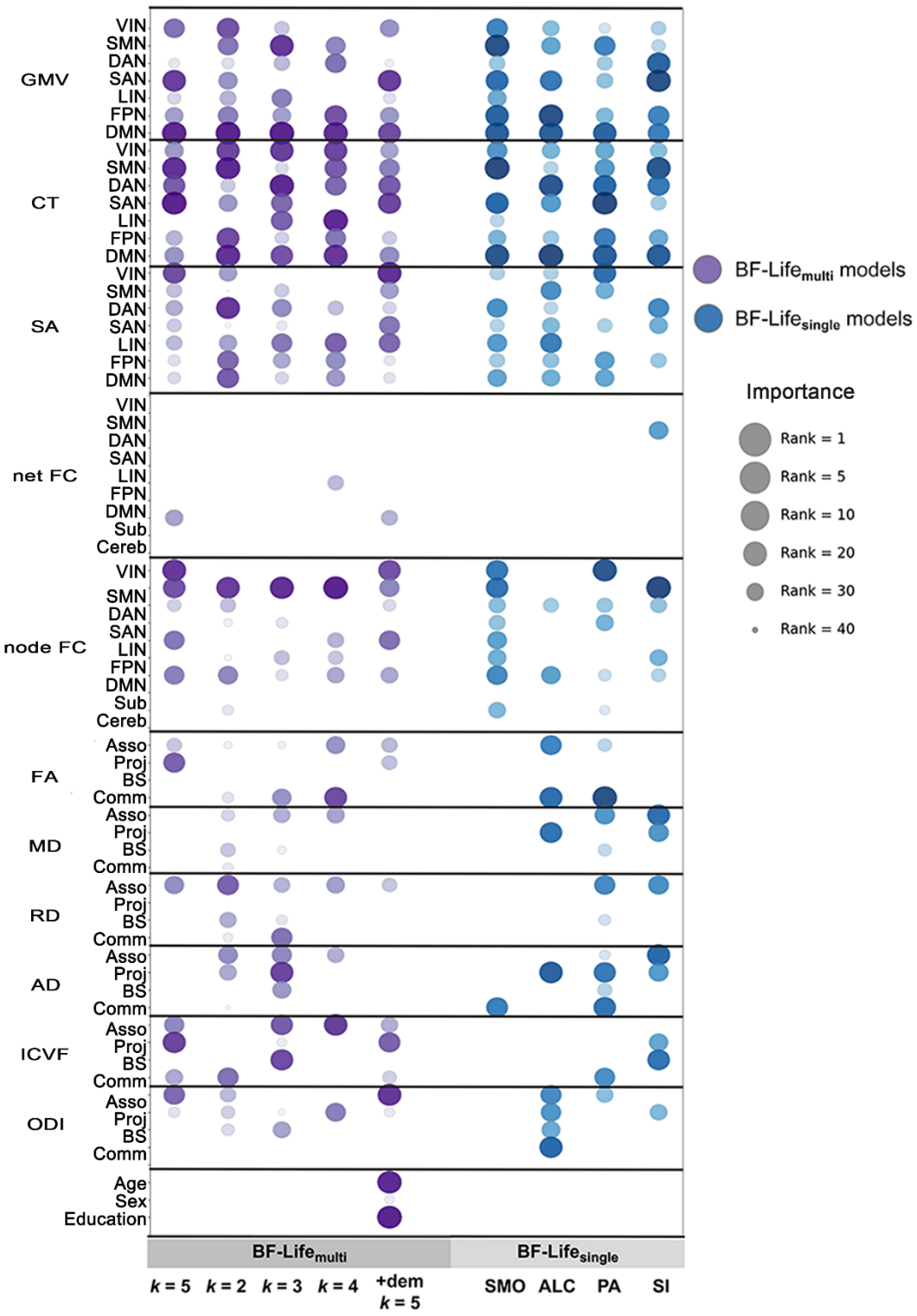

Figure 5.2.5 Importance of feature categories in nine models predicting figural memory using elastic net regression in Holdout1. Bubble color intensity and size correspond to feature importance, with darker and larger bubbles indicating higher contributions. Abbreviations: *k*, cluster number; BF-Life$_{multi}$, multiple lifestyle-informed brain features; BF-Life$_{single}$, single lifestyle-informed brain features; SMO/ALC/PA/SI, smoking-/alcohol-/physical activity-/social integration-informed brain features

Feature Importance of Individual Features (BF-Life$_{multi}$ vs BF-Life$_{single}$)

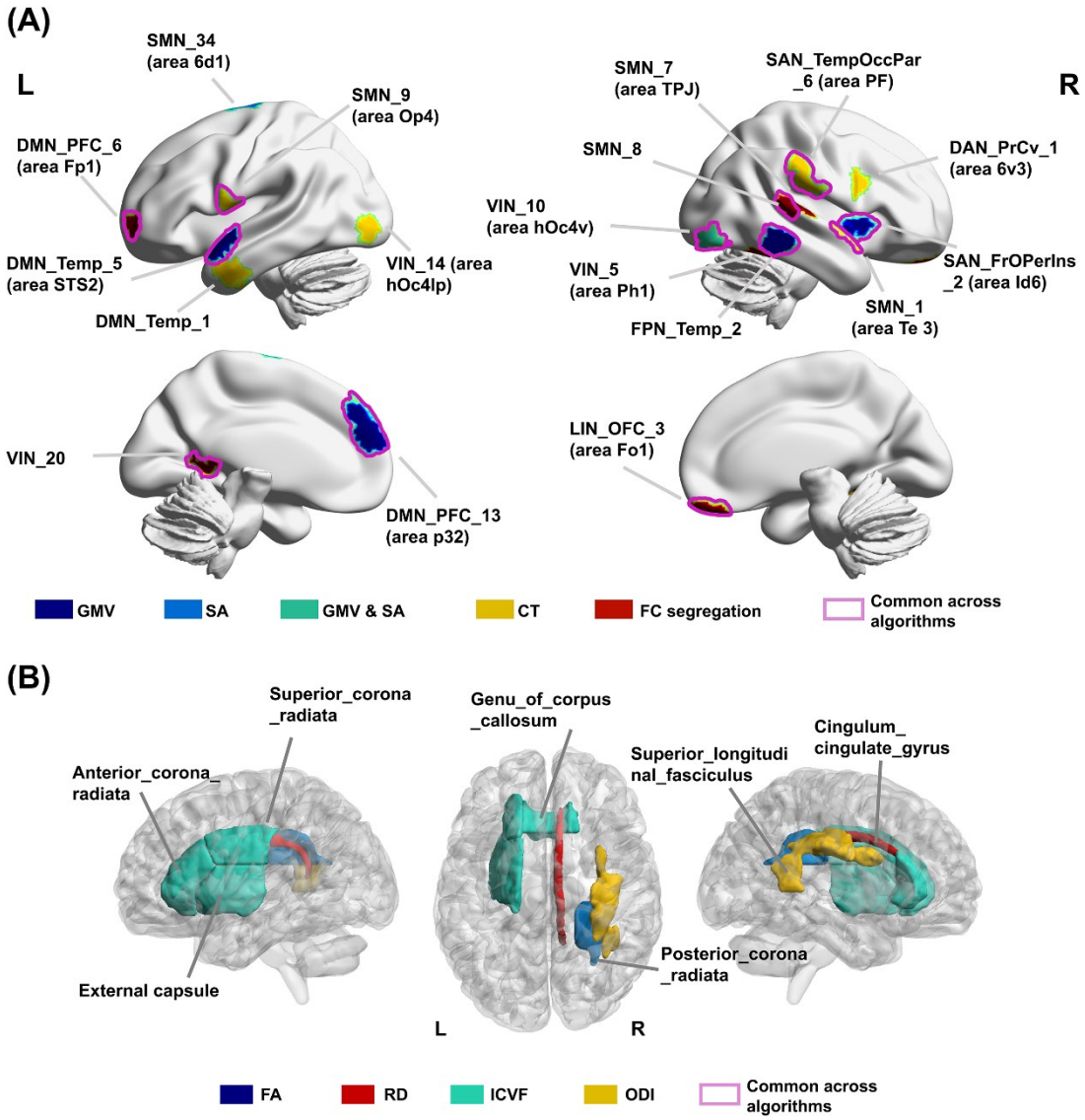

Figure 5.2.6 Feature importance in predicting figural memory using the BF-Life$_{multi}$ model (*k*=5) with elastic net regression. Projection of the most important features from gray **(A)** and white matter **(B)**. Brain regions marked with solid purple lines are consistently important across all five algorithms. Abbreviations: *k*, cluster number; BF-Life$_{multi}$, multiple lifestyle-informed brain features; L/R, left/right hemisphere

The top 30% of features (SHAP values ranging from 0.042–0.243) are presented in Figure 5.2.6 and together account for 81.27% of the total contribution for BF-Life$_{multi}$. Features that also appeared in the top 30% of any of the other four machine learning algorithms are highlighted (see also Table 5.2.6). The most predictive features were primarily located in the SAN, VIN, DMN, and SMN. The top three contributors were: (i) GMV in a cluster spanning the right insula and frontal operculum

(SAN_FrOperIns_2 [area Id6]; (ii) CT in the right temporo-parietal junction (SAN_TempOccPar_6 [area PF]; (iii) SA in the right visual network [VIN_10; area hOc4v]. Other highly ranked features included GMV and CT in several cortical regions, as well as node-wise FC segregation in multiple networks.

Specifically, GMV contribution was observed in the left superior temporal sulcus (DMN_Temp_5 [area STS2]) and left medial prefrontal cortex (DMN_PFC_13 [area p32]), while CT contribution was observed in the right superior temporal gyrus (SMN_1 [area Te3]) and left frontal operculum (SMN_9 [area Op4]). Contributions of node-wise FC segregation were mainly derived from the left visual network (VIN_20), the right superior temporal gyrus (SMN_8), and the right orbitofrontal cortex of the limbic network (LIN_OFC_3 [area Fo1]).

Comparing the top 30% of features for each of the four BF-Life$_{\mathbf{single}}$ models with those of the BF-Life$_{\mathbf{multi}}$ model (Figure 5.2.7), we found that four features were shared between the SMO and the BF-Life$_{\mathbf{multi}}$ model (right SMN_1 [area Te3], left SMN_9 [area Op4], left DMN_Temp_5 [area STS2], and left DMN_PFC_13 [area p32]), two shared between the PA and BF-Life$_{\mathbf{multi}}$ model (right SAN_TempOccPar_6 [area PF] and right SAN_TempOccPar_5), and one shared between the SI and BF-Life$_{\mathbf{multi}}$ model (right SMN_8), but none between the ALC model and BF-Life$_{\mathbf{multi}}$ model.

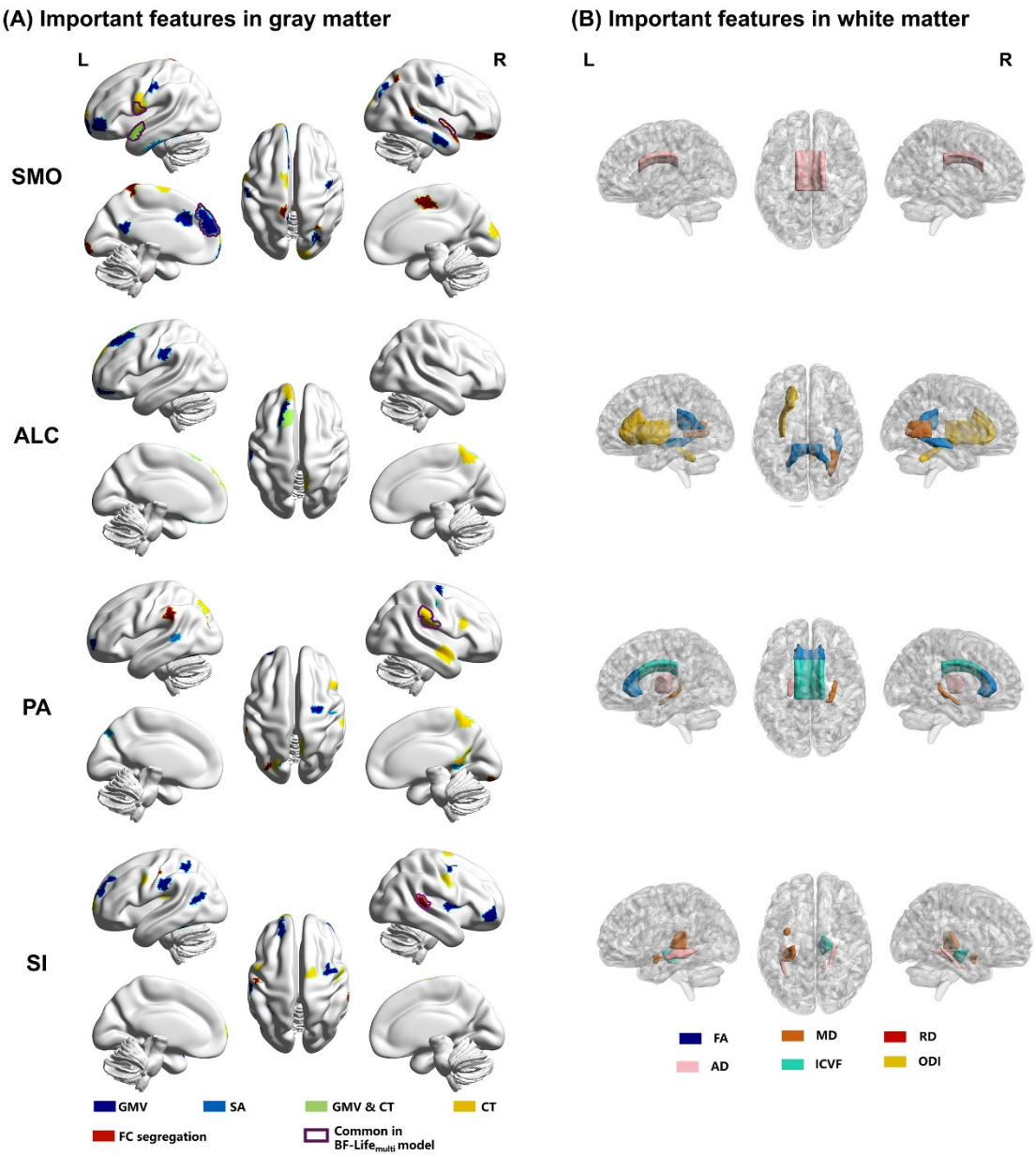

Figure 5.2.7 BF-Life$_{single}$ models: Feature importance in predicting figural memory using elastic net regression. Projection of the most important features from gray **(A)** and white matter **(B)**. The brain regions marked by solid purple lines are important brain regions common to the BF-Life$_{multi}$ model. Abbreviations: SHAP, SHapley Additive exPlanations; SMO/ALC/PA/SI, smoking-/alcohol-/physical activity-/social integration-informed brain features; L/R, left/right hemisphere

Table 5.2.6 Top 30% features in the BF-Life$_{multi}$ model in predicting figural memory using ENR and SHAP analysis.

Parameters	Labels	Network/fiber type	Mean |SHAP| value	Harvard-Oxford Cortical Structural Atlas	AAL3	Brodmann	Julich Brain Atlas
GMV	**SAN_FrOperIns_2 (R)**	SAN	0.24	Insular Cortex (R), 92.84%	Insula (R), 80.44%	BA48 (R), 90.53%	Area Id6 (Insula), 42.29%
GMV	**DMN_Temp_5 (L)**	DMN	0.14	Temporal Pole (L), 66.64%	Temporal_Pole_Sup (L), 54.13%	BA38 (L), 44.95%	Area STS2 (STS), 17.96%
GMV	**DMN_PFC_13 (L)**	DMN	0.09	Superior Frontal Gyrus (L), 28.91%	Frontal_Sup_Medial (L), 97.33%	BA10 (L), 32.46%	Area p32 (pACC), 35.13%
GMV	**FPN_Temp_2 (R)**	FPN	0.05	Middle Temporal Gyrus, temporooccipital part (R), 42.31%	Temporal_Mid (R), 63.16%	BA20 (R), 51.70%	Temporal-to-Parietal (GapMap), 88.10%
GMV	**VIN_10 (R)**	VIN	0.04	Lateral Occipital Cortex, inferior division (R), 90.46%	Frontal_Inf_Oper (R), 64.87%	BA19 (R), 80.40%	Area hOc4v (LingG), 35.80%
CT	**SAN_TempOccPar_6 (R)**	SAN	0.21	Supramarginal Gyrus, anterior division (R), 82.32%	SupraMarginal (R), 87.10%	BA2 (R), 52.37%	Area PF (IPL), 59.05%
CT	**SMN_1 (R)**	SMN	0.14	Planum Polare (R), 39.56%	Temporal_Pole_Sup (R), 35.11%	BA48 (R), 38.26%	Area Te 3 (STG), 29.40%
CT	**SMN_9 (L)**	SMN	0.09	Precentral Gyrus (L), 54.16%	Rolandic_Oper (L), 60.00%	BA48 (L), 70.45%	Area Op4 (POperc), 28.55%
CT	DAN_PrCv_1 (R)	DAN	0.07	Precentral Gyrus (R), 59.60%	Frontal_Inf_Oper (R), 64.87%	BA44 (R), 47.06%	Area 6v3 (PreCG), 20.39%
CT	VIN_14 (L)	VIN	0.06	Lateral Occipital Cortex, inferior division (L), 86.17%	Occipital_Mid (L), 51.34%	BA19 (L), 42.99%	Area hOc4lp (LOC), 41.21%
CT	DMN_Temp_1 (L)	DMN	0.05	Middle Temporal Gyrus, anterior division (L), 38.12%	Temporal_Mid (L), 51.35%	BA20 (L), 52.39%	Temporal-to-Parietal (GapMap), 55.18%
CT	SAN_TempOccPar_5 (R)	SAN	0.04	Supramarginal Gyrus, anterior division (R), 36.67%	SupraMarginal (R), 69.97%	BA48 (R), 66.94%	Frontal-to-Occipital (GapMap), 26.5035% CA1 (Hippocampus), 22.85% (551)
SA	**VIN_10 (R)**	VIN	0.15	Lateral Occipital Cortex, inferior division (R), 90.46%	Frontal_Inf_Oper (R), 64.87%	BA19 (R), 80.40%	Area hOc4v (LingG), 35.80%
SA	SMN_34 (L)	SMN	0.04	Superior Frontal Gyrus (L), 42.70%	Precentral (L), 32.57%	BA6 (L), 91.18%	Area 6d1 (PreCG), 60.24%
node FC	**VIN_20 (L)**	VIN	0.12	Cingulate Gyrus, posterior division (L), 40.90%	Calcarine (L), 51.42%	BA17 (L), 31.23%	Frontal-to-Occipital (GapMap), 78.23%
node FC	**SMN_8 (R)**	SMN	0.08	Superior Temporal Gyrus, posterior division (R), 59.20%	Temporal_Sup (R), 95.29%	BA22 (R), 63.16%	Temporal-to-Parietal (GapMap), 32.92%
node FC	**LIN_OFC_3 (R)**	LIN	0.07	Frontal Pole (R), 48.26%	Rectus (R), 54.86%		Area Fo1 (OFC), 53.58%
node FC	VIN_5 (R)	VIN	0.07	Lingual Gyrus (R), 62.57%	Lingual (R), 46.60%	BA37 (R), 65.61%	Area Ph1 (PhG), 44.02%
node FC	**DMN_PFC_6 (L)**	DMN	0.06	Frontal Pole (L), 99.25%	Frontal_Sup_2 (L), 78.57%	BA11 (L), 60.22%	Area Fp1 (FPole), 59.35%
node FC	VIN_3 (R)	VIN	0.05	Temporal Occipital Fusiform Cortex (R), 92.31%	Fusiform (R), 96.44%	BA37 (R), 89.85%	Area FG4 (FusG), 34.18%
node FC	SMN_7 (R)	SMN	0.04	Planum Temporale (R), 63.56%	Temporal_Sup (R), 91.40%	BA22 (R), 54.24%	Area TPJ (STG, SMG), 31.58%
net FC	**DMN_w**	DMN	0.05	/	/	/	/

FA	Posterior_corona_radiata (R)	Projection	0.10	/	/	/	/
RD	Cingulum_cingulate (R)	Association	0.06	/	/	/	/
ICVF	Superior_corona_radiata (L)	Projection	0.08	/	/	/	/
ICVF	Anterior_corona_radiata (L)	Projection	0.06	/	/	/	/
ICVF	Genu_of_corpus_callosum	Commissural	0.05	/	/	/	/
ICVF	External_capsule (L)	Association	0.05	/	/	/	/
ODI	Superior_longitudinal_fasciculus (R)	Association	0.08	/	/	/	/

Note: The row with blue color represents the common feature across all five algorithms. We determined the location of a region in the four atlases and the percentage of overlap. Abbreviations: L/R, left/right hemisphere

5.2.5 Supplementary Analyses

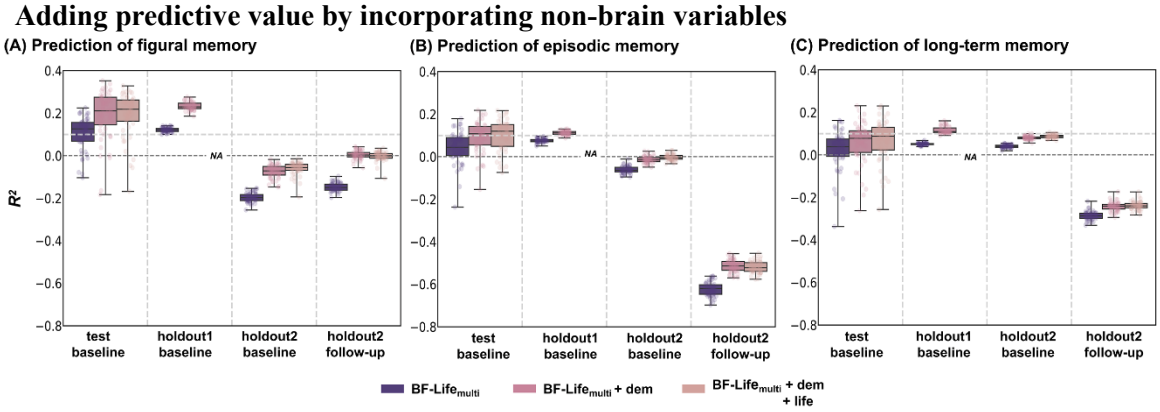

Figure 5.2.8 Performance of models incorporating non-brain data in predicting figural (A), episodic (B), and long-term memory (C). The combined model (BF-Life$_{multi}$ + demographics + lifestyle, *NA*) was not available in Holdout1 due to the lack of available lifestyle data. A light gray dashed line marks R^2 = 0.10 as a reference. Abbreviations: *k*, cluster number; BF-Life$_{multi}$, multiple lifestyle-informed brain features; +dem, includes demographic data

We extended the BF-Life$_{multi}$ model by incorporating demographic variables (i.e., age, sex, and education; BF-Life$_{multi}$ +dem), as well as the original eight continuous lifestyle variables (BF-Life$_{multi}$ +dem+life), to assess the added predictive value of these non-brain variables. Although the same eight lifestyle variables, recoded as categorical variables, were used initially for participants clustering, they were not included in the brain feature selection process and were added in the extended model only as independent predictors (see Figure 5.2.8 and Table 5.2.4).

Predictive performance of the BF-Life$_{multi}$ models with different cluster numbers

Varying the number of clusters (k = 2–5) yielded largely comparable BF-Life$_{multi}$ performance across memory domains. For figural memory, performance peaked at k = 5 in the test set and Holdout1. Episodic and long-term memory showed similar performance across all k values in these datasets. None of the models generalized to Holdout2 (see Figure 5.2.9 and Table 5.2.4).

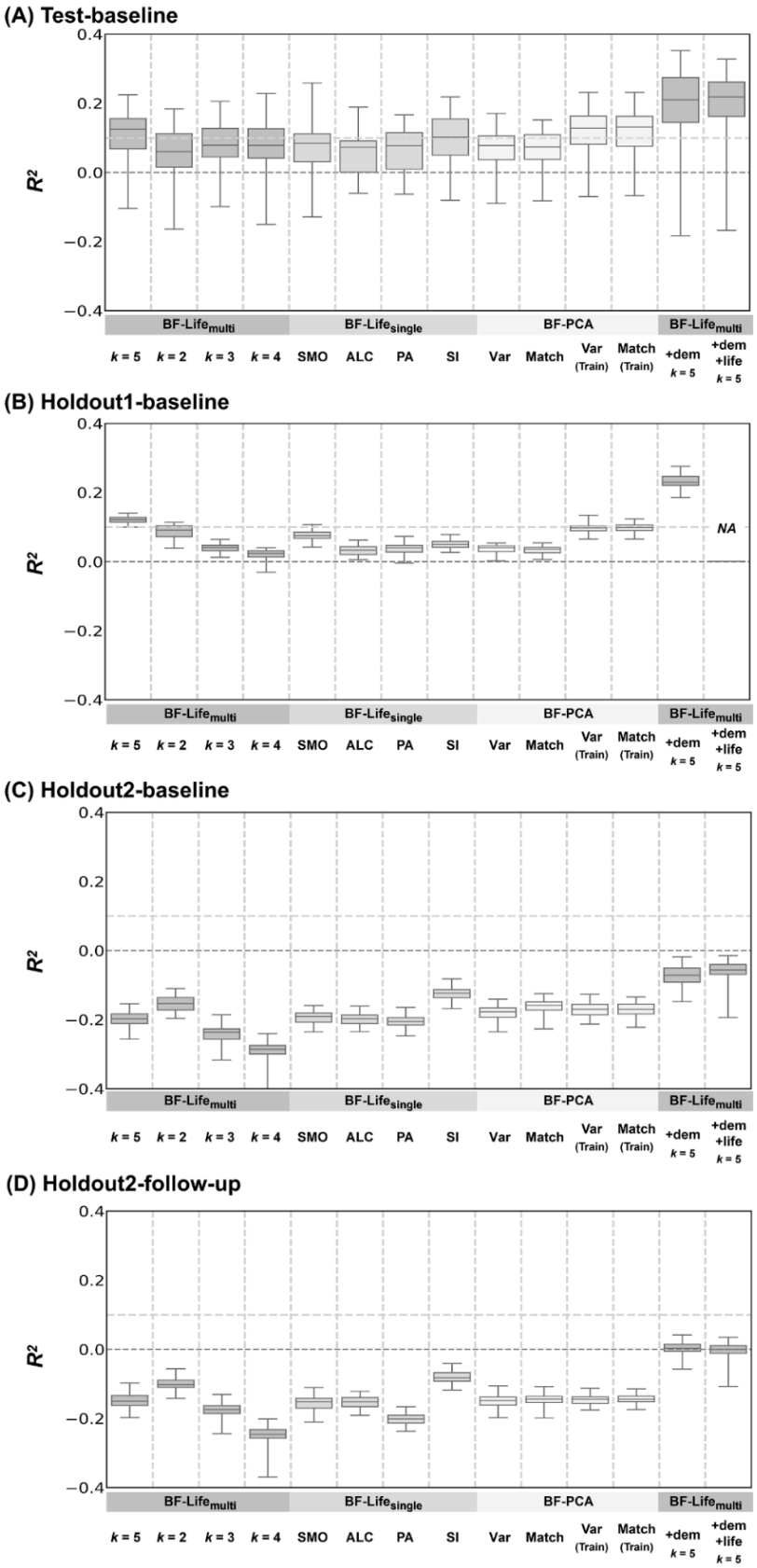

Figure 5.2.9 Predictive performance of various models for figural memory using elastic net regression. The model, which included multiple lifestyle-informed brain features, demographics, and lifestyle factors (BF-Life$_{multi}$ +dem+life), was not applied to the holdout1 set (**panel B**) due to missing lifestyle data and is marked as not available (NA). The light gray dashed line indicates an

R^2 value of 0.10. Abbreviations: R^2: Coefficient of determination; *k*: Cluster number; BF-Life$_{multi}$: multiple lifestyle factors-informed brain features; BF-Life$_{single}$, single lifestyle-informed brain features; SMO/ALC/PA/SI, smoking-/alcohol-/physical activity-/social integration-informed brain features; PCA, Principal component analysis; BF-PCAVar / PCAVar(Train), PCA brain features from the main /training set, components explaining 80% variance; BF-PCAMatch / PCAMatch(Train), PCA brain features from the main /training set, components matched to the BF-Life$_{multi}$ model; +dem, includes demographic data; +dem+life, includes demographic and lifestyle data

Prediction of the global cognitive component

The predictive performance of 14 ENR models for the global cognitive component is summarized in Figure 5.2.10 and Table 5.2.7. In the test set, BF-Life$_{multi}$ models (k = 2–5) showed comparable performance to BF-Life$_{single}$ models (explaining up to 13% of the variance), while fully data-driven models performed best (explained up to 17% of the variance); adding demographic and lifestyle data substantially improved the BF-Life$_{multi}$ model with k = 5 (explained up to 36% of the variance). In Holdout1, the BF-Life$_{multi}$ model with k = 5 (explained 17% of the variance) outperformed other BF-Life$_{multi}$ and BF-Life$_{single}$ models and matched the performance of fully data-driven models, with further gains when non-brain features were included (explained up to 36% of the variance). In Holdout2, only the BF-Life$_{multi}$ model with k = 2, the SI model, and data-driven models achieved positive median R^2 (explained up to 8% of the variance); the k = 5 model performed poorly with brain features alone but improved when demographic and lifestyle data were added (explained up to 19% of the variance).

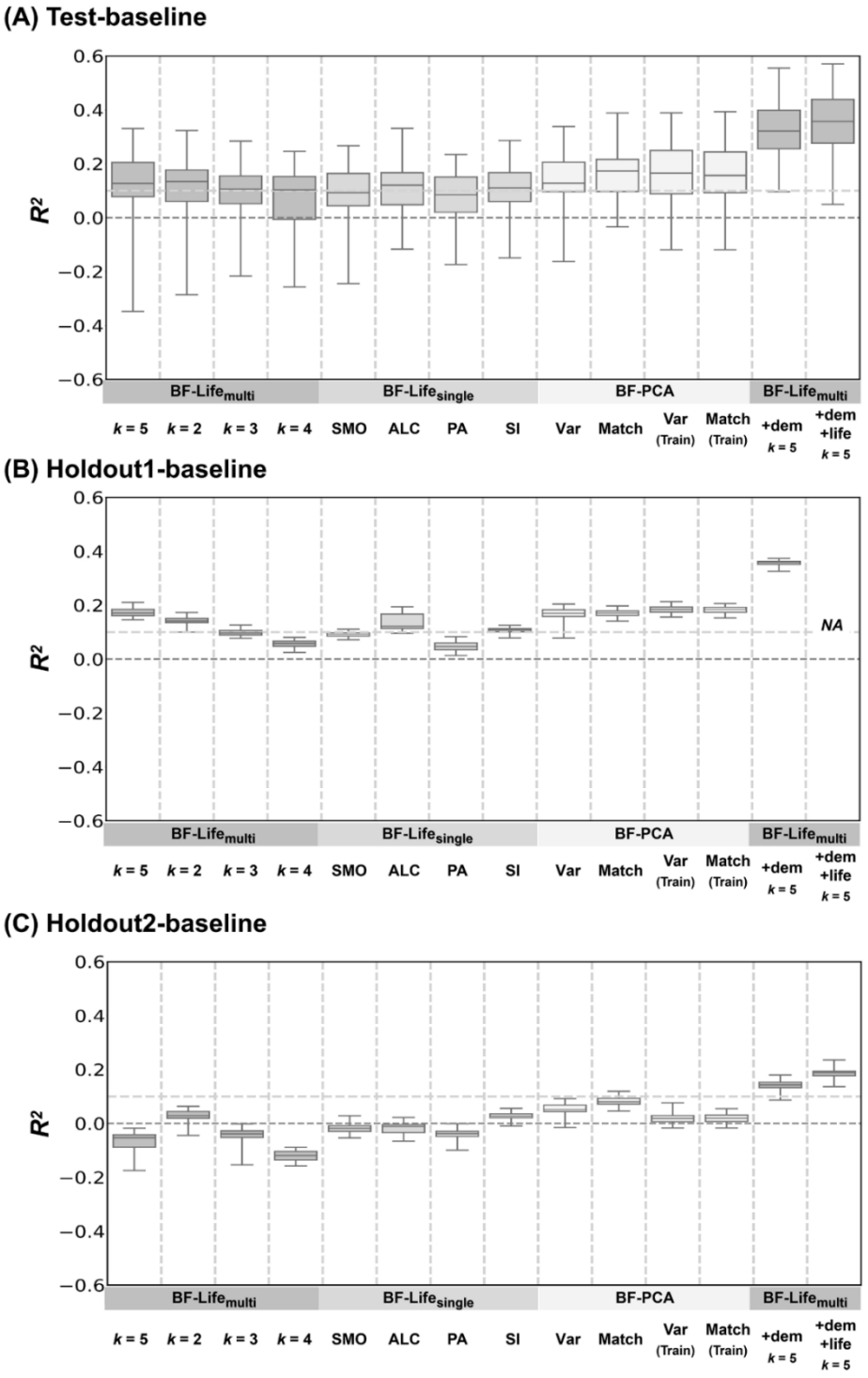

Figure 5.2.10 Predictive performance of various models for the global cognitive component using elastic net regression. The model, which included multiple lifestyle-informed brain features, demographics, and lifestyle factors (BF-Life$_{multi}$ +dem+life), was not applied to the holdout1 set (**panel B**) due to missing lifestyle data and is marked as not available (NA). The light gray dashed line indicates an R^2 value of 0.10. Abbreviations: R^2: Coefficient of determination; *k*: Cluster number; BF-Life$_{multi}$: multiple lifestyle factors-informed brain features; BF-Life$_{single}$, single lifestyle factor-informed brain features; SMO/ALC/PA/SI, smoking-/alcohol-/physical activity-/social integration-informed brain features; PCA, Principal component analysis; BF-PCAVar / PCAVar(Train), PCA brain features from the main /training set, components explaining 80% variance; BF-PCAMatch /

PCAMatch(Train), PCA brain features from the main /training set, components matched to the BF-Life$_{multi}$ model; +dem, includes demographic data

Table 5.2.7 Performance of 14 models using elastic net regression (ENR) on the global cognitive component.

Algorithm	Models	Median R^2			Median *MAE*		
		Test baseline	Holdout1 baseline	Holdout2 baseline	Test baseline	Holdout1 baseline	Holdout2 baseline
ENR	**BF-Life$_{multi}$ models**						
	k = 5	0.13	0.17	-0.05	1.66	1.67	1.61
	k = 2	0.13	0.14	0.03	1.65	1.71	1.56
	k = 3	0.11	0.10	-0.04	1.67	1.76	1.61
	k = 4	0.10	0.06	-0.12	1.72	1.77	1.67
	BF-Life$_{single}$ models						
	SMO	0.09	0.09	-0.02	1.68	1.76	1.60
	ALC	0.12	0.12	-0.01	1.65	1.73	1.58
	PA	0.08	0.05	-0.04	1.68	1.83	1.61
	SI	0.11	0.11	0.03	1.66	1.75	1.55
	Data-driven model						
	BF-PCAVar	0.13	0.17	0.05	1.61	1.71	1.50
	BF-PCAMatch	0.17	0.17	0.08	1.58	1.70	1.48
	BF-PCAVar(Train)	0.17	0.19	0.02	1.60	1.67	1.53
	BF-PCAMatch(Train)	0.16	0.19	0.02	1.61	1.67	1.53
	Incorporating non-brain data						
	BF-Life$_{multi}$ +dem: k=5	0.32	0.36	0.14	1.40	1.45	1.50
	BF-Life$_{multi}$ +dem+life: k=5	0.36	/	0.19	1.37	/	1.47

Abbreviations: k, cluster number; R^2, coefficient of determination; *MAE*, mean absolute error; BF-Life$_{multi}$, multiple lifestyle-informed brain features; BF-Life$_{single}$, single lifestyle-informed brain features; SMO/ALC/PA/SI, smoking-/alcohol-/physical activity-/social integration-informed brain features; PCA, Principal component analysis; BF-PCAVar / PCAVar(Train), PCA brain features from the main /training set, components explaining 80% variance; BF-PCAMatch / PCAMatch(Train), PCA brain features from the main /training set, components matched to the BF-Life$_{multi}$ model; +dem, includes demographic data; +dem+life, includes demographic and lifestyle data

Predictive performance of the models using target-dependent data-driven feature selection approaches

Using ENR, we compared the BF-Life$_{\mathbf{multi}}$ model (k = 5) with whole-brain models employing different feature selection approaches for figural memory prediction (Figure 5.2.11; Table 5.2.8). In the test set and Holdout1, the BF-Life$_{\mathbf{multi}}$ model showed performance comparable to or slightly better than mutual information and f_regression methods (explaining up to 13% and 11% the variance, respectively), and consistently outperformed ridge regression and hybrid approaches. None of the models generalized to Holdout2 at either baseline or follow-up.

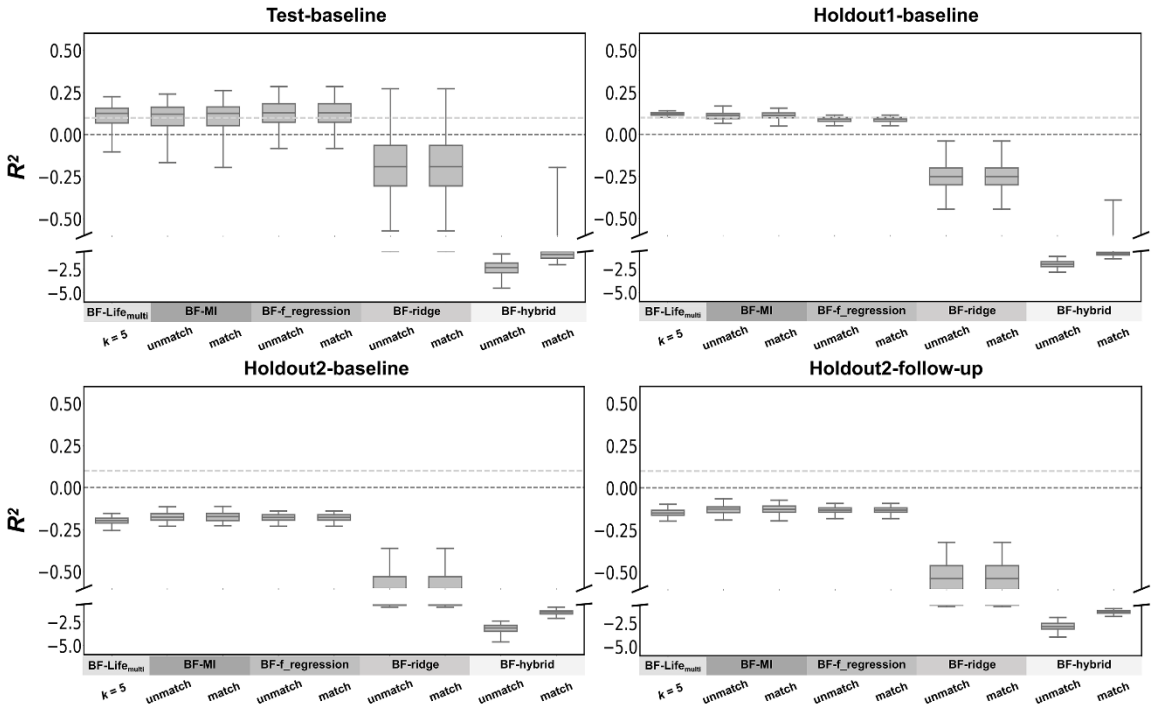

Figure 5.2.11 Comparison between the BF-Life$_{\mathbf{multi}}$ model and models with different target-dependent data-driven feature selection approaches using elastic net regression. The light gray horizontal dashed line represents the R^2 value of 0.10. Abbreviations: R^2, coefficient of determination; k, cluster number; MI_regression, mutual information regression feature selection method; f_regression, f_regression feature selection method; ridge_regression, ridge regression feature selection method; hybrid_regression, feature selection using both filter and wrapper strategies; unmatch, select the 193 features based on their respective rankings; match, select the 96 features based on their respective rankings to match the number of features in the BF-Life$_{\mathbf{multi}}$ model

Table 5.2.8 Comparison of target-dependent data-driven feature selection approaches using elastic net regression for predicting figural memory.

Models	median R^2				median *MAE*			
	Test baseline	Holdout1 baseline	Holdout2 baseline	Holdout2 follow-up	Test baseline	Holdout1 baseline	Holdout2 baseline	Holdout2 follow-up
BF-Life$_{\mathbf{multi}}$: k=5 [a]	0.13	0.12	-0.20	-0.15	3.16	3.35	3.30	3.32
BF-MI$_{\mathbf{unmatch}}$ [b]	0.12	0.11	-0.18	-0.13	3.18	3.36	3.27	3.33
BF-MI$_{\mathbf{match}}$ [b]	0.13	0.11	-0.17	-0.13	3.17	3.36	3.26	3.33
BF-f_regression$_{\mathbf{unmatch}}$ [b]	0.13	0.09	-0.18	-0.13	3.14	3.42	3.27	3.35
BF-f_regression$_{\mathbf{match}}$ [b]	0.13	0.09	-0.18	-0.13	3.14	3.42	3.27	3.35
BF-ridge$_{\mathbf{unmatch}}$ [b]	-0.19	-0.25	-0.63	-0.54	3.49	3.92	3.78	3.94
BF-ridge$_{\mathbf{match}}$ [b]	-0.19	-0.25	-0.63	-0.54	3.49	3.92	3.78	3.94
BF-hybrid$_{\mathbf{unmatch}}$ [b]	-2.31	-1.99	-3.14	-2.87	5.98	6.02	6.02	6.11
BF-hybrid$_{\mathbf{match}}$ [b]	-0.92	-0.89	-1.44	-1.31	4.45	4.77	4.69	4.80

Note: Model with multiple lifestyle-informed brain features showing here for a reference (BF-Life$_{\mathbf{multi}}$, marked in green); [a] feature selection performed in the main set (including training and test set); [b] feature selection strictly performed in the training set. Abbreviations: k, cluster number; R^2, coefficient of determination; *MAE*, mean absolute error; BF-MI, a model based on whole brain feature sets using mutual information regression feature selection method; BF-f_regression, a model based on whole brain feature sets using f_regression feature selection method; BF-ridge, a model based on whole brain feature sets using ridge regression feature selection method; BF-hybrid, a model based on whole brain feature sets using both filter and wrapper strategies; unmatch, select the 193 features based on their respective rankings; match, feature number (i.e., 96 features) match the number of features in the BF-Life$_{\mathbf{multi}}$ model

5.3 Discussion

We examined whether brain features reflecting composite lifestyle patterns improve the prediction of domain-specific cognitive functions relative to models based on individual lifestyle factors. Overall, integrating multiple lifestyle factors yielded modest gains in predictive performance, with the strongest effects observed for figural memory; however, it did not clearly outperform fully data-driven approaches. These findings suggest that lifestyle-informed brain differences contribute to cognitive prediction in a domain-specific manner, while highlighting the limited magnitude and generalizability of such effects.

5.3.1 Domain-Specific Predictive Performance of the BF-Life$_{multi}$ Model

Building on these results, we consider the domain-specific predictive pattern of the BF-Life$_{multi}$ model in relation to prior work. Prior studies in comparable aging cohorts using unimodal and multimodal neuroimaging approaches have reported explained variance of up to 12–14% for global cognitive performance (Jockwitz et al., 2024; Kramer et al., 2024). In this context, the BF-Life$_{multi}$ model showed its strongest predictive performance for figural memory and a global cognitive component, while demonstrating limited predictive sensitivity for other cognitive domains, including working memory, language-related functions, and executive control.

The BF-Life$_{multi}$ model did not achieve the higher levels of explained variance (e.g., >20%) reported in studies of young adults using task-based or resting-state FC to predict fluid and crystallized cognitive performance (Dhamala et al., 2021; Dubois et al., 2018; Gao et al., 2019). However, prediction of cognition in population-based samples across the adult lifespan has generally remained modest (MacDonald et al., 2011). For example, multimodal neuroimaging predicted visual working memory across the adult lifespan in Cam-CAN (~16.2% explained variance; N = 547, aged 18–88 years) (Xiao et al., 2021), while processing speed showed limited predictability using resting-state FC (~8–11%; N = 99, aged 62–71 years; Cam-CAN, N = 295, aged 25–80 years) (Gao et al., 2020). Consistently, a large-scale UK Biobank study reported that only a small proportion of the variance in fluid intelligence and neuroticism (~2–6%; N = 18,550, aged 44–80 years) was explained (Easley et al., 2023).

Although higher predictive performance has been reported in smaller or clinical samples, such as individuals with MCI or Alzheimer's disease (Avery et al., 2020; Kwak et al., 2021; Yu et

al., 2020), these findings are only partly comparable to population-based studies, given the more specific and pronounced neural changes in clinical cohorts and the increased risk of overfitting in smaller samples (Lee et al., 2024; Poldrack et al., 2017). In this context, the modest predictive performance observed here is broadly consistent with large-scale population studies such as the UK Biobank (Easley et al., 2023) and likely reflects realistic effect sizes in normal aging. Taken together, while the predictive performance of the BF-Life$_{\mathbf{multi}}$ model in older adults may appear modest compared to studies in young adults or clinical cohorts, its performance, particularly for figural memory and the global cognitive component, remains informative and broadly within the expected range in the context of age-related variability.

Nonetheless, within the present framework, the BF-Life$_{\mathbf{multi}}$ model outperformed the four models with single lifestyle-informed brain features (BF-Life$_{\mathbf{single}}$) in predicting figural memory. Specifically, in the test set, the BF-Life$_{\mathbf{multi}}$ model showed a statistically significant advantage over the alcohol-related (ALC) model. In Holdout1, the BF-Life$_{\mathbf{multi}}$ model showed a statistically significant advantage over the BF-Life$_{\mathbf{single}}$ models in predicting figural memory (Figure 5.2.4 A). Although the absolute effect sizes were small, integrating multiple lifestyle-informed brain features captured lifestyle-informed brain variance more comprehensively than modeling brain features based on individual lifestyle effects, supporting multivariate approaches in cognitive aging research.

Furthermore, the BF-Life$_{\mathbf{multi}}$ model outperformed fully data-driven models (without prior biological hypotheses) when both used the same feature-extraction procedure. In this procedure, features were selected or reduced from the main dataset before any model training. However, this advantage was conditional: the BF-Life$_{\mathbf{multi}}$ model did not outperform data-driven models when a more rigorous machine learning workflow was applied, in which PCA was performed separately within each training fold.

Importantly, the advantage of BF-Life$_{\mathbf{multi}}$ over both BF-Life$_{\mathbf{single}}$ and comparable data-driven models was sensitive to the granularity of the brain–lifestyle representation. When the cluster number was altered (k = 2–4), this advantage was no longer observed (Table 2 and Suppl. Figure 4), suggesting that the predictive performance of lifestyle-informed brain features depends on an appropriate level of representational granularity. In the present framework, the five-cluster solution captured a balance between aggregating shared lifestyle-informed variance and avoiding excessive fragmentation.

5.3.2 Predictive Insights from the BF-Life$_{multi}$ Model

Given the domain-specific advantage for figural memory, we next examined which brain features contributed most strongly to prediction. The BF-Life$_{multi}$ model ($k = 5$) showed its highest predictive performance for figural memory, which was primarily driven by features within the salience/ventral attention, default mode, and somatomotor networks, as well as node-wise functional segregation within the visual network. These networks are broadly associated with attentional control, internally directed cognition, and visual processing (Andrews-Hanna et al., 2010; Menon & Uddin, 2010; Spreng & Grady, 2010), suggesting that their involvement may indirectly support figural memory performance.

At the feature level, important contributors included gray-matter morphology in salience/ventral attention and visual regions (e.g., right insula and right lingual gyrus), node-wise functional segregation within the visual network (e.g., left calcarine fissure), and microstructural integrity of projection fibers such as the posterior and superior corona radiata. Several of these regions show structural sensitivity to lifestyle factors, including smoking (Durazzo et al., 2018), which may partly explain their relevance for figural memory prediction. The high contribution of node-wise functional network segregation within the visual network resonates with prior research on network dedifferentiation during aging (Deery et al., 2023; Diez et al., 2024), where reduced within-network specialization may compromise the fidelity of perceptual representations. While our feature-importance analysis does not establish directionality (i.e., higher vs lower segregation), it suggests that the balance between segregation and integration in visual systems is a candidate mechanism linking lifestyle-informed brain variance to figural memory. In addition, although the precise role of the integrity of projection-fiber tracts remains unclear, their inclusion suggests a potential contribution to this cognitive domain.

In contrast, BF-Life$_{single}$ models capture only partial aspects of lifestyle-informed neural variability by emphasizing specific modalities or network subsets in isolation. BF-Life$_{multi}$ integrates structural, functional, and microstructural features across multiple lifestyle domains, providing a more comprehensive representation than single-factor models. These observations are consistent with studies showing that multidomain lifestyle patterns are informative in predicting cognitive aging (Paolillo et al., 2023).

The predictive advantages of the BF-Life$_{multi}$ model were largely confined to figural

memory, with limited generalization to other cognitive domains. This pattern may reflect the specific brain networks engaged in figural memory, which involve higher-order visual regions, whereas episodic memory relies more on medial temporal lobe structures (Rolls & Treves, 2024), and verbal abilities depend on widely distributed language-specific networks (e.g., prefrontal, temporal, and subcortical regions) (Boerma et al., 2023). The limited prediction of verbal tasks may also reflect the relative stability of these abilities across aging (Harada et al., 2013), and they are strongly correlated with sociodemographic variables such as education and language exposure, which already encapsulate much of the neural information relevant to verbal performance (Stern, 2009). By contrast, approaches such as connectome-based predictive modeling, which use target-dependent feature selection to target specific networks, have successfully predicted verbal abilities (Dhamala et al., 2021), underscoring that prediction of different cognitive domains may benefit from tailoring feature selection and modeling approaches to the specific networks involved.

Interestingly, the BF-Life$_{\mathbf{multi}}$ model also showed relatively better predictive performance for the global cognitive component. This may partly reflect that global cognitive functions rely on widespread and distributed neural networks, which tend to show relatively consistent large-scale organization compared with highly localized, domain-specific processes and are therefore more amenable to multimodal characterization (Rasero et al., 2021). Although the variance explained is modest, these results may reflect associations between lifestyle-informed brain features and cognitive aging, especially for functions supported by distributed neural networks.

While the current study did not explicitly test aging frameworks, it exploratorily identified brain patterns—particularly in salience/ventral attention and visual networks—that may contribute to predicting specific cognitive domains. These brain patterns have not been directly examined in the context of established aging models in the current study, such as brain maintenance. This refers to the relative preservation of brain structure and function across the adult lifespan, which is associated with better cognitive outcomes in aging (Cabeza et al., 2018), and to STAC-R, which suggests that older adults recruit additional neural circuits to compensate for age-related declines (Prince et al., 2024). The present findings may nevertheless point to potential mechanisms through which multidomain lifestyle factors influence domain-specific cognitive performance. Future studies could further investigate these links, for example, by incorporating task-based functional measures or additional lifestyle variables to improve predictive performance.

Despite these brain-based insights, neuroimaging features alone accounted for only a limited proportion of the variance in cognitive performance. When demographic variables (age, sex, and education) were incorporated, predictive performance for figural memory improved substantially, consistent with prior findings that demographics capture a large share of explainable cognitive variance (e.g., Ashish & Turner, 2024; Bruno Hebling Vieira et al., 2022). By contrast, the incremental contribution of brain features remained modest, and adding individual-level lifestyle variables did not yield further gains. This pattern suggests that variance associated with lifestyle may already be partially reflected in demographic and brain measures, leaving limited additional predictive value for lifestyle variables themselves. Nevertheless, a substantial proportion of the variance in cognitive performance remained unexplained, indicating that future work may benefit from incorporating additional non-brain factors, such as socioeconomic status, physical health, cardiovascular risk, genetic predisposition, or social network characteristics.

5.3.3 Challenges to Generalization Across Samples

Despite the advantages in Holdout1, models showed limited robustness in the second holdout set. Neither BF-Life$_{\mathbf{multi}}$ nor the comparison models (BF-Life$_{\mathbf{single}}$ and data-driven models) showed meaningful predictive performance for figural memory at baseline or follow-up, even after incorporating demographic and lifestyle variables (Table 5.2.5). This consistent lack of performance across modeling approaches underscores the difficulty of predicting figural memory from brain features in this subgroup. Several factors may have contributed to this decline. Despite random assignment, Holdout2 differed from the training/test set and Holdout1 in key characteristics, including education level and baseline figural memory performance (Tables 5.2.1 and 5.2.2). In addition, the available training sample size may have been insufficient to learn patterns that generalize to a more distinct subgroup.

Together, these findings suggest that the associations captured by BF-Life$_{\mathbf{multi}}$, while informative in Holdout1, were not sufficiently stable to support reliable prediction across subsamples or follow-up assessments, likely to reflect sample heterogeneity and distributional differences rather than specific methodological flaws.

Furthermore, these findings point to several broader methodological limitations that warrant consideration. First, consistent with the sensitivity of model performance to clustering granularity, the separation of the identified lifestyle subgroups was relatively weak, as reflected by low

silhouette scores (Suppl. Table 4), highlighting the inherent difficulty of discretizing complex, multidimensional lifestyle behaviors. While clustering enabled the examination of broad lifestyle heterogeneity, future work could explore alternative methods and stability criteria to improve interpretability and robustness.

Second, between-group exploratory analyses were used to identify BF-Life$_{\mathbf{multi}}$ features without correcting for multiple comparisons across all brain variables, with correction applied only across lifestyle subgroups. Baseline health status or pre-existing disease may confound observed findings. In addition, the cross-sectional nature of neuroimaging and lifestyle data precludes conclusions about directionality between lifestyle factors and brain features. As such, these findings should be regarded as exploratory rather than conclusive and require cautious interpretation.

Third, although follow-up cognitive outcomes were examined, the lifestyle and neuroimaging data were cross-sectional, limiting inferences about cognitive change over time. Future research could further benefit from repeated behavioral and neural assessments over longer time spans to better characterize intra-individual differences in cognitive performance (Raz & Lindenberger, 2011).

5.4 Conclusions

In summary, this study shows that brain features reflecting composite lifestyle patterns carry modest but domain-specific predictive information for cognitive performance in older adults, with the clearest effects observed for figural memory. While these lifestyle-informed brain differences do not outperform fully data-driven approaches and exhibit limited generalizability, they highlight an information-guided representation of these brain differences that may complement existing predictive models. Future work integrating larger, more diverse samples and longitudinal measures may further clarify their relevance to cognitive aging.

Chapter 6: Cross-Study Discussion

6.1 Synthesis of Findings

Against the backdrop of accelerating global population aging, understanding why individuals exhibit markedly different cognitive trajectories during healthy aging has become an unavoidable question in cognitive neuroscience and aging research (Rothermund et al., 2023). Importantly, healthy aging is far from homogeneous: even in the absence of clinically diagnosed neurodegenerative diseases, older adults exhibit substantial inter-individual variability across cognitive functioning, brain network organization, and the maintenance of daily functional abilities (Stern et al., 2019). In this sense, uncovering the neural basis of heterogeneity in healthy aging is not merely a theoretical concern; it also has important implications for assessing, monitoring, and supporting cognitive maintenance and everyday functioning in later life.

Research on brain aging has often relied on group-level, cross-sectional comparisons to characterize typical age-related patterns, yet such approaches may overlook meaningful inter-individual variability in cognitive and neural aging trajectories (Patel et al., 2022; Persson et al., 2012). Current research indicates that the combined effects of biological factors (e.g., genetics) and non-biological factors (including social, cultural, life experiences, lifestyle, and psychosocial factors) shape an individual's distinct cognitive and brain patterns relative to peers (Castruita et al., 2022). Furthermore, cross-sectional evidence suggests that as individuals age, their cognitive and brain aging patterns become more "unique" (Nyberg, 2018; Nyberg & Lindenberger, 2020), though longitudinal studies suggest that within-subject variability does not necessarily increase with age (Grodem et al., 2025; Salthouse, 2012). However, treating interindividual heterogeneity in the brain as mere statistical noise may obscure critical information needed to understand the mechanisms underlying healthy aging.

Building on this perspective, the present dissertation places individual differences at the center of its research framework. Using multimodal neuroimaging, multivariate statistical approaches, and machine learning models, the dissertation addresses three interrelated questions: first, which lifestyle, psychosocial, and cognitive factors are associated with inter-individual

variability of connectivity; second, whether inter- and intra-individual variability of connectivity reflects large-scale brain network segregation, as a metric of network (re-)organization, and plays a role in the relationship between network segregation and cognitive function; and third, whether brain differences related to lifestyle and psychosocial factors provide additional helpful information for predicting cognitive performance. These questions are not independent but jointly serve a broader objective: to understand how external life experiences, internal brain network organization, and cognitive performance are interconnected at the individual level during healthy aging.

Study 1 addressed the first question. We identified a latent variable linking greater inter-individual variability of structural and functional connectivity patterns with less favorable lifestyle and psychosocial characteristics (e.g., lower social integration and heavier smoking), as well as poorer nonverbal cognitive performance, such as episodic memory and executive control. Moreover, different age groups exhibit sensitivity to distinct lifestyle/psychosocial factors. These findings contribute to a growing body of work indicating that inter-individual variability in brain connectivity reflects meaningful biological organization rather than random system noise (Huang et al., 2025; L. Li et al., 2021; Li et al., 2017; Mueller et al., 2013; T. Xu et al., 2019). Prior work has emphasized genetic, evolutionary, and developmental influences on inter-individual variability of functional connectivity, whereas inter-individual variability of structural connectivity has been shown to exhibit systematic spatial patterns that correlate with regional properties such as cortical structure and myelination. The present results further suggest that long-term lifestyle and psychosocial factors are associated with individual differences in connectivity patterns, indicating that such variability may arise from the combined influence of intrinsic neurobiological constraints and accumulated life experience. This interpretation is broadly consistent with the Scaffolding Theory of Aging and Cognition–revised (STAC-r), which emphasizes that cognitive maintenance depends on neural scaffolding resources. These resources are progressively formed and continuously adapted throughout the lifespan, shaped by life experiences and environmental exposures, and exhibit differential expression across individuals (Reuter-Lorenz & Park, 2014).

However, Study 1 focused particularly on the potential source of brain heterogeneity and its association with cognitive outcomes during aging, leaving unresolved the large-scale network organization underlying individual differences in brain connectomes. Relatively few studies have explored this perspective — namely, interpreting network reorganization during aging and its

relationship with executive control through the lens of individual differences in brain connectomes (Mueller et al., 2013). Therefore, Study 2 examined the role of inter- and intra-IV of connectivity in the relationship between network segregation and executive control.

The results of Study 2 indicate that the relationship between network segregation and executive control may not be fully captured at the mean level of segregation alone. Although direct associations were inconsistent, mediation analyses revealed a relatively coherent pattern: structural and, to a lesser extent, functional network segregation was linked to worse executive control through higher inter-individual variability of connectivity. Thus, inter-IV of connectivity—rather than network segregation per se—showed stable behavioral relevance. Across systems, changes in network segregation were accompanied by changes in inter-IV of connectivity, although the direction of these associations differed by brain system and imaging modality. In cortical networks, lower network segregation was generally associated with higher inter-IV of connectivity, a pattern broadly consistent with accounts of age-related functional dedifferentiation. In subcortical and cerebellar systems, however, segregation–variability associations varied across structural and functional domains, indicating that structural and functional segregation indices may reflect distinct organizational properties outside the cortex. Importantly, irrespective of direction, higher inter-IV of connectivity was consistently associated with poorer executive control.

Although inter-IV in structural and functional connectivity likely arises from partially distinct biological mechanisms (Huang et al., 2025; Mueller et al., 2013), both indices reflect reduced consistency of network organization across individuals. Aging has been associated with increased between-person heterogeneity in brain and cognition (Nyberg et al., 2012). When such between-person differences increase, similar levels of cognitive performance may be supported by more heterogeneous connectivity configurations, potentially reducing the stability of group-level brain–behavior associations (Dubois & Adolphs, 2016). In contrast, intra-IV of connectivity—capturing longitudinal changes within individuals—did not show consistent mediation effects within the present time window. This does not preclude a role for longitudinal brain reorganization; for example, the isolated mediation effect observed for intra-individual functional variability in specific networks may suggest that reduced long-term brain functional flexibility may not support executive control. However, compared to inter-IV of connectivity, these effects were unstable and context-dependent. In addition, age-moderated analyses further indicated that these mediation

pathways did not follow a monotonic age trend but instead varied across subgroups within older adulthood. Together, these findings highlight the importance of considering individual variability in understanding brain reorganization and cognitive outcomes during aging.

Building on these findings, a key next step is to examine whether heterogeneous brain differences can inform predictions of individual cognitive outcomes. In the context of the growing use of machine learning approaches in neuroimaging, developing such predictive models has become an important research objective. However, this goal remains challenging in healthy elderly populations—even with multimodal neuroimaging and complex modeling approaches, predictive efficacy often remains limited (e.g., Rasero et al., 2021; Schulz et al., 2024). A previous study suggests that distinct aging subtypes may exist among older adults due to differences in environmental and lifestyle exposures (Rodrigues et al., 2024). Building on insights from the first two studies regarding the sources of brain heterogeneity and their cognitive implications, we examined whether integrating lifestyle- and psychosocial-informed brain features could capture meaningful heterogeneity and improve the prediction of individual cognitive performance in healthy aging.

The findings of Study 3 revealed that while incorporating multimodal neuroimaging features related to lifestyle and psychosocial factors improves model performance in both test set and one internal unseen holdout set, overall predictive performance remains limited and does not obviously surpass findings in previous studies (Hilger et al., 2020; Jockwitz et al., 2024; Kramer et al., 2024; Rasero et al., 2021; Schulz et al., 2024). Nevertheless, Study 3 revealed that models integrating multiple lifestyle and psychosocial factors capture distinct brain differences compared with models that consider a single lifestyle/psychosocial factor. The former synthesizes more comprehensive and richer information, thereby accounting for greater variance in figural memory prediction. This finding may offer insights into further refining and developing personalized prediction models.

The limited predictive performance observed across BF-Life$_{\mathbf{multi}}$, BF-Life$_{\mathbf{single}}$, and fully data-driven models suggests that cognitive performance in healthy aging is unlikely to be determined by a single neural mechanism. Rather, it may reflect the combined influence of multiple neural, environmental, and demographic factors. This view is partly supported by the increase in explanatory power from 13% to 23% after incorporating demographic variables into the BF-Life$_{\mathbf{multi}}$

model. Against this backdrop, the limited predictive performance of models relying solely on neuroimaging features illustrates the inherent heterogeneity and multidimensional nature of healthy aging.

Taken together, the three studies systematically examined brain individual differences at associative, mechanistic, and predictive levels, demonstrating the important role of heterogeneity in understanding cognitive aging. Variability in the connectome reflects differences in large-scale brain network organization and provides a critical level for elucidating complex relationships among lifestyle and psychosocial factors and cognitive performance. This individual-differences-centered integrative perspective helps shift the study of healthy aging away from descriptions of "average trajectories" toward an understanding of diverse pathways of cognitive aging.

6.2 Methodological Considerations

The three studies included in this dissertation address individual differences in a distinct modeling framework. Studies 1 and 2 operate within an explanatory framework that models associations between variability in structural and functional connectivity and lifestyle/psychosocial, cognitive variables, and network organization characteristics. Study 2 further incorporates repeated measurements to estimate intra-individual variability in connectivity over time, thereby introducing a longitudinal component into the variability framework. In contrast, Study 3 adopts a predictive modeling strategy by constructing feature sets derived from lifestyle/psychosocial-informed brain differences and evaluating their added value to predict individual cognitive differences.

Across Studies 1 and 2, inter-individual differences in structural connectivity showed more stable and consistent effects across statistical models than those observed for functional connectivity. This discrepancy may partly reflect modality-specific measurement characteristics. Structural connectivity estimates reflect anatomical pathway configurations that are relatively stable across sessions (e.g., Buchanan et al.), whereas resting-state functional connectivity reflects temporally varying patterns of neural co-activation and may contain a larger state-related component (e.g., Noble et al., 2019). In cross-sectional analyses, such differences in variance composition may influence the stability of association estimates. Moreover, the linear modeling approaches applied in the present studies assume linear and additive relationships, which may not fully capture more complex or non-linear variance structures in functional connectivity (Smith et al., 2011), particularly given the coexistence of multiple mechanisms in brain function during aging (e.g., Cabeza et al., 2018). Accordingly, differences observed between structural and functional results should be interpreted with consideration of measurement reliability and analytical constraints inherent to each modality, rather than attributed solely to distinct underlying aging mechanisms.

Under the assumption of multi-subtype brain and cognitive aging, Study 3 adopts an intermediate methodological strategy situated between hypothesis-driven approaches (e.g., ROIs predefined based on theory or prior evidence) and fully data-driven predictive modeling, with embedded information-guided feature selection. We employed clustering and group-comparison statistical methods to capture brain differences related to lifestyle and psychosocial factors, thereby exploring multimodal brain features reflecting composite lifestyle and psychosocial patterns. This

approach reduces feature dimension and minimizes overfitting risk while maintaining flexibility to test the generalization of group-level behavior–brain associations to individual cognitive prediction (e.g., Mattoni et al., 2025; Yarkoni & Westfall, 2017). Although predictive performance remains limited, the primary value of this analysis lies in offering an initial methodological exploration of how explanatory and predictive perspectives might be bridged in cognitive aging research.

Several methodological limitations should be considered when interpreting the present findings. First, although all three studies are based primarily on a cross-sectional design, which reflects pragmatic trade-offs among sample size, age coverage, and feasibility, rather than a disregard for developmental inference. Even though Study 2 incorporated longitudinal data to estimate intra-individual variability, and Study 3 used baseline MRI measures to predict follow-up cognitive outcomes, the analytical framework does not permit strong conclusions regarding temporal ordering or causal mechanisms. As such, observed associations should be interpreted as age-related differences rather than within-person developmental trajectories (Raz & Lindenberger, 2011; Salthouse, 2011).

Second, IV of connectivity was operationalized using correlation-based dissimilarity metrics derived from Pearson correlations. While this method has been applied in studies of connectome similarity and individual differences due to its similarity and interpretability (e.g., Huang et al., 2025; Sun et al., 2022; Zhu & Qiu, 2022), it captures only a single statistical dimension of neural variability with a linear assumption, and fails to reflect the direction of the variance, such as whether relative groups exhibit positive or negative bias. Furthermore, inter-IV is a relative metric; its estimation must be interpreted within a group framework. For example, an individual aged 65 may exhibit significant inconsistencies between their inter-IV estimate within the 55-65 age group and their estimate within the 65-85 age group. Alternative approaches—including rank-based measures (e.g., Spearman correlation), angular similarity (e.g., cosine distance used in Karahan et al., 2022), variance-based indices, and generative modeling (Liu et al., 2020)—may reveal additional dimensions of inter- and intra-individual variability not accessible within the current framework.

Third, across the present set of studies, we primarily included age, sex, and education as covariates. Although these variables account for major demographic influences, other biological and contextual factors—such as genetic factors, socioeconomic context, baseline health status,

vascular and metabolic conditions, and medication use—may contribute to both neural and behavioral measures. In addition, imaging-related measurement confounds (e.g., head motion) may introduce systematic bias into brain metric estimates despite standard correction procedures. Therefore, a restricted covariate framework is insufficient to capture the multivariate complexity of brain–behavior associations, a limitation emphasized in large-scale methodological discussions (Genon et al., 2022). Future research incorporating broader biological, environmental, and methodological controls will be necessary to clarify the specificity and potential mechanisms underlying brain heterogeneity and cognitive aging.

Fourth, from the perspective of generalizability and reproducibility, the present findings should be interpreted cautiously. Differences in factors such as cohort characteristics, imaging parameters, preprocessing pipelines, white matter fiber tracking methodology, brain atlas, definition of brain connectivity, and cognitive assessments may introduce potential sources of system error or bias. Future work would benefit from replication in independent cohorts, cross-sample validation, and systematic assessments of methodological robustness to establish the stability of these effects across research contexts (Botvinik-Nezer & Wager, 2023; Dubois & Adolphs, 2016; Nath et al., 2020).

Fifth, measurement constraints apply to both cognitive and lifestyle/psychosocial variables. Executive control was assessed using a single behavioral measure derived from the Trail Making Test (TMT B–A). This measure is widely used and has been shown to be sensitive to age-related differences in executive control (Sanchez-Cubillo et al., 2009; Tsiakiri et al., 2024). However, it may not fully capture the multidimensional structure of executive control function. In addition, lifestyle and psychosocial variables were self-reported, which may introduce recall or social desirability bias (Franz et al., 2021; Licher et al., 2019); however, such measures are commonly used and have demonstrated acceptable validity and reliability (Del Boca & Darkes, 2003). Future work would benefit from multi-task cognitive batteries, latent-variable approaches, and objective behavioral assessments.

Finally, the sample consisted of a relatively homogeneous group of older German adults with respect to educational background, with a substantial proportion of participants holding a high school degree qualifying for university admission. While this homogeneity may reduce sociocultural confounding and increase statistical power, it limits generalizability to more diverse

populations (Lakes, 2013). Given the close association between education and cognition, future studies should examine the findings of the present study in educationally and culturally diverse cohorts (Zvonarev et al., 2020).

6.3 Summary

This dissertation advances a systems-level perspective on brain heterogeneity in cognitive aging by examining individual variability in brain connectivity and its associations with behavioral and cognitive factors, as well as network organization. It further evaluates the extent to which information-guided multimodal brain features contribute to individualized cognitive prediction.

Results indicate that greater inter-individual variability of connectivity is correlated with unfavorable lifestyle/psychosocial factors and is associated with poorer non-verbal cognitive performance. This association is more pronounced in structural connectivity and varies across age groups. These findings are consistent with the STAC-r framework, suggesting differential neural resource availability or scaffolding processes related to health risk factors during aging.

Furthermore, inter-individual variability in connectivity statistically accounted for part of the association between large-scale network segregation and executive control. This pattern was consistently observed across several cortical networks in structural connectivity and showed larger conditional effects at higher age values, whereas the corresponding effects in functional connectivity were less consistent. In contrast, intra-individual variability in functional connectivity showed only a weak and isolated association within the visual network. These findings are broadly consistent with the neural dedifferentiation framework and refine our understanding of how network organization relates to cognitive function in aging.

Finally, from a predictive perspective, an information-guided model using multimodal brain features reflecting a composite of lifestyle and psychosocial patterns demonstrated moderate and domain-specific predictive value, particularly for figural memory, but showed limited longitudinal generalizability and did not outperform fully data-driven models. This distinction between explanatory associations and predictive performance underscores the challenges of translating group-level findings on brain heterogeneity into reliable individualized prediction.

In summary, this dissertation highlights brain heterogeneity as a meaningful dimension of cognitive aging. The limited translation of explanatory findings into individualized prediction suggests that static cross-sectional measures may not fully capture the brain–cognition dynamic relationships, calling for more integrative and longitudinal research frameworks.

References

Abdi, H., & Williams, L. J. (2013). Partial least squares methods: Partial least squares correlation and partial least square regression. *Methods in Molecular Biology*, *930*, 549–579. https://doi.org/10.1007/978-1-62703-059-5_23

Ainsworth, B. E., Haskell, W. L., Whitt, M. C., Irwin, M. L., Swartz, A. M., Strath, S. J., O'Brien, W. L., Bassett, D. R., Jr., Schmitz, K. H., Emplaincourt, P. O., Jacobs, D. R., Jr., & Leon, A. S. (2000). Compendium of physical activities: An update of activity codes and MET intensities. *Medicine & Science in Sports & Exercise*, *32*(9 Suppl), S498–504. https://doi.org/10.1097/00005768-200009001-00009

Amunts, K., Mohlberg, H., Bludau, S., & Zilles, K. (2020). Julich-Brain: A 3D probabilistic atlas of the human brain's cytoarchitecture. *Science*, *369*(6506), 988–992. https://doi.org/10.1126/science.abb4588

Anaturk, M., Demnitz, N., Ebmeier, K. P., & Sexton, C. E. (2018). A systematic review and meta-analysis of structural magnetic resonance imaging studies investigating cognitive and social activity levels in older adults. *Neuroscience & Biobehavioral Reviews*, *93*, 71–84. https://doi.org/10.1016/j.neubiorev.2018.06.012

Andersson, J. L. R., Graham, M. S., Drobnjak, I., Zhang, H., Filippini, N., & Bastiani, M. (2017). Towards a comprehensive framework for movement and distortion correction of diffusion MR images: Within volume movement. *NeuroImage*, *152*, 450–466. https://doi.org/10.1016/j.neuroimage.2017.02.085

Andrews-Hanna, J. R., Reidler, J. S., Huang, C., & Buckner, R. L. (2010). Evidence for the default network's role in spontaneous cognition. *Journal of Neurophysiology*, *104*(1), 322–335. https://doi.org/10.1152/jn.00830.2009

Ansado, J., Marsolais, Y., Methqal, I., Alary, F., & Joanette, Y. (2013). The adaptive aging brain: Evidence from the preservation of communication abilities with age. *European Journal of Neuroscience*, *37*(12), 1887–1895. https://doi.org/10.1111/ejn.12252

Aschenbrenner, S., Tucha, O., & Lange, K. W. (2000). Der Regensburger Wortflüssigkeits-Test (RWT). *Göttingen: Hogrefe.*

Ashburner, J., & Friston, K. J. (2005). Unified segmentation. *NeuroImage*, *26*(3), 839–851. https://doi.org/10.1016/j.neuroimage.2005.02.018

Ashendorf, L., Jefferson, A. L., O'Connor, M. K., Chaisson, C., Green, R. C., & Stern, R. A. (2008). Trail Making Test errors in normal aging, mild cognitive impairment, and dementia. *Archives of Clinical Neuropsychology*, *23*(2), 129–137. https://doi.org/10.1016/j.acn.2007.11.005

Ashish, R. M., & Turner, J. A. (2024). Towards multimodal longitudinal analysis for predicting cognitive decline using neuroimaging biomarkers. *bioRxiv*. https://doi.org/10.1101/2024.11.18.624226

Avery, E. W., Yoo, K., Rosenberg, M. D., Greene, A. S., Gao, S., Na, D. L., Scheinost, D., Constable, T. R., & Chun, M. M. (2020). Distributed patterns of functional connectivity predict working memory performance in novel healthy and memory-impaired individuals. *Journal of Cognitive Neuroscience*, *32*(2), 241–255. https://doi.org/10.1162/jocn_a_01487

Babaeeghazvini, P., Rueda-Delgado, L. M., Gooijers, J., Swinnen, S. P., & Daffertshofer, A. (2021). Brain structural and functional connectivity: A review of combined works of diffusion magnetic resonance imaging and electro-encephalography. *Frontiers in Human Neuroscience*, *15*, 721206. https://doi.org/10.3389/fnhum.2021.721206

Bagarinao, E., Watanabe, H., Maesawa, S., Mori, D., Hara, K., Kawabata, K., Yoneyama, N., Ohdake, R.,

Imai, K., Masuda, M., Yokoi, T., Ogura, A., Taoka, T., Koyama, S., Tanabe, H. C., Katsuno, M., Wakabayashi, T., Kuzuya, M., Ozaki, N., …Sobue, G. (2019). Reorganization of brain networks and its association with general cognitive performance over the adult lifespan. *Scientific Reports*, *9*, 11352. https://doi.org/10.1038/s41598-019-47922-x

Bassett, D. S., Wymbs, N. F., Porter, M. A., Mucha, P. J., Carlson, J. M., & Grafton, S. T. (2011). Dynamic reconfiguration of human brain networks during learning. *PNAS*, *108*(18), 7641–7646. https://doi.org/10.1073/pnas.1018985108

Baum, G. L., Ciric, R., Roalf, D. R., Betzel, R. F., Moore, T. M., Shinohara, R. T., Kahn, A. E., Vandekar, S. N., Rupert, P. E., Quarmley, M., Cook, P. A., Elliott, M. A., Ruparel, K., Gur, R. E., Gur, R. C., Bassett, D. S., & Satterthwaite, T. D. (2017). Modular segregation of structural brain networks supports the development of executive function in youth. *Current Biology*, *27*(11), 1561–1572.e1568. https://doi.org/10.1016/j.cub.2017.04.051

Bautista, T., O'Muircheartaigh, J., Hajnal, J. V., & Tournier, J.-D. (2021). Removal of Gibbs ringing artefacts for 3D acquisitions using subvoxel shifts. In *Proceedings of the International Society for Magnetic Resonance in Medicine* (Vol. 29, pp. 3535). Mira Smart Conference.

Bender, A. R., Volkle, M. C., & Raz, N. (2016). Differential aging of cerebral white matter in middle-aged and older adults: A seven-year follow-up. *NeuroImage*, *125*, 74–83. https://doi.org/10.1016/j.neuroimage.2015.10.030

Benjamini, Y., & Hochberg, Y. (1995). Controlling the false discovery rate: A practical and powerful approach to multiple testing. *Journal of the Royal Statistical Society: Series B (Methodological)*, *57*(1), 289–300. https://doi.org/10.1111/j.2517-6161.1995.tb02031.x

Bennett, I. J., & Madden, D. J. (2014). Disconnected aging: Cerebral white matter integrity and age-related differences in cognition. *Neuroscience*, *276*, 187–205. https://doi.org/10.1016/j.neuroscience.2013.11.026

Benton, A. L., Benton-Sivan, A., Spreen, O., & Streck, P. (2009). Der Benton-Test. *Göttingen: Verlag Hans Huber.*

Beretta, L., & Santaniello, A. (2016). Nearest neighbor imputation algorithms: A critical evaluation. *BMC Medical Informatics and Decision Making*, *16 Suppl 3*(Suppl 3), 74. https://doi.org/10.1186/s12911-016-0318-z

Berkman, L. F., Melchior, M., Chastang, J. F., Niedhammer, I., Leclerc, A., & Goldberg, M. (2004). Social integration and mortality: A prospective study of French employees of Electricity of France-Gas of France: the GAZEL Cohort. *American Journal of Epidemiology*, *159*(2), 167–174. https://doi.org/10.1093/aje/kwh020

Birn, R. M., Molloy, E. K., Patriat, R., Parker, T., Meier, T. B., Kirk, G. R., Nair, V. A., Meyerand, M. E., & Prabhakaran, V. (2013). The effect of scan length on the reliability of resting-state fMRI connectivity estimates. *NeuroImage*, *83*, 550–558. https://doi.org/10.1016/j.neuroimage.2013.05.099

Bittner, N., Jockwitz, C., Franke, K., Gaser, C., Moebus, S., Bayen, U. J., Amunts, K., & Caspers, S. (2021). When your brain looks older than expected: Combined lifestyle risk and BrainAGE. *Brain Structure and Function*, *226*(3), 621–645. https://doi.org/10.1007/s00429-020-02184-6

Bittner, N., Jockwitz, C., Muhleisen, T. W., Hoffstaedter, F., Eickhoff, S. B., Moebus, S., Bayen, U. J., Cichon, S., Zilles, K., Amunts, K., & Caspers, S. (2019). Combining lifestyle risks to disentangle brain structure and functional connectivity differences in older adults. *Nature Communications*, *10*(1), 621. https://doi.org/10.1038/s41467-019-08500-x

Boerma, T., Ter Haar, S., Ganga, R., Wijnen, F., Blom, E., & Wierenga, C. J. (2023). What risk factors for Developmental Language Disorder can tell us about the neurobiological mechanisms of language

development. *Neuroscience & Biobehavioral Reviews*, *154*, 105398. https://doi.org/10.1016/j.neubiorev.2023.105398

Botvinik-Nezer, R., & Wager, T. D. (2023). Reproducibility in neuroimaging analysis: Challenges and solutions. *Biological Psychiatry: Cognitive Neuroscience and Neuroimaging*, *8*(8), 780–788. https://doi.org/10.1016/j.bpsc.2022.12.006

Brown, J. W., & Jaffe, J. (1975). Hypothesis on cerebral dominance. *Neuropsychologia*, *13*(1), 107–110.

Buckner, R. L. (2004). Memory and executive function in aging and AD: Multiple factors that cause decline and reserve factors that compensate. *Neuron*, *44*(1), 195–208. https://doi.org/10.1016/j.neuron.2004.09.006

Buckner, R. L., Krienen, F. M., Castellanos, A., Diaz, J. C., & Yeo, B. T. (2011). The organization of the human cerebellum estimated by intrinsic functional connectivity. *Journal of Neurophysiology*, *106*(5), 2322–2345. https://doi.org/10.1152/jn.00339.2011

Cabeza, R. (2002). Hemispheric asymmetry reduction in older adults: the HAROLD model. *Psychology and Aging*, *17*(1), 85.

Cabeza, R., Albert, M., Belleville, S., Craik, F. I. M., Duarte, A., Grady, C. L., Lindenberger, U., Nyberg, L., Park, D. C., Reuter-Lorenz, P. A., Rugg, M. D., Steffener, J., & Rajah, M. N. (2018). Maintenance, reserve and compensation: the cognitive neuroscience of healthy ageing. *Nature Reviews Neuroscience*, *19*(11), 701–710. https://doi.org/10.1038/s41583-018-0068-2

Cabeza, R., & Dennis, N. A. (2012). Frontal lobes and aging: Deterioration and compensation. In D. T. Stuss & R. T. Knight (Eds.), *Principles of frontal lobe function* (pp. 628–652). Oxford University Press. https://doi.org/10.1093/med/9780199837755.003.0044

Cao, F., Liang, J., & Bai, L. (2009). A new initialization method for categorical data clustering. *Expert Systems with Applications*, *36*(7), 10223–10228. https://doi.org/10.1016/j.eswa.2009.01.060

Caspers, S., Moebus, S., Lux, S., Pundt, N., Schutz, H., Muhleisen, T. W., Gras, V., Eickhoff, S. B., Romanzetti, S., Stocker, T., Stirnberg, R., Kirlangic, M. E., Minnerop, M., Pieperhoff, P., Modder, U., Das, S., Evans, A. C., Jockel, K. H., Erbel, R., …Amunts, K. (2014). Studying variability in human brain aging in a population-based German cohort-rationale and design of 1000BRAINS. *Frontiers in Aging Neuroscience*, *6*, 149. https://doi.org/10.3389/fnagi.2014.00149

Castruita, P. A., Pina-Escudero, S. D., Renteria, M. E., & Yokoyama, J. S. (2022). Genetic, social, and lifestyle drivers of healthy aging and longevity. *Current Genetic Medicine Reports*, *10*(3), 25–34. https://doi.org/10.1007/s40142-022-00205-w

Chamberland, M., Girard, G., Bernier, M., Fortin, D., Descoteaux, M., & Whittingstall, K. (2017). On the origin of individual functional connectivity variability: The role of white matter architecture. *Brain Connectivity*, *7*(8), 491–503. https://doi.org/10.1089/brain.2017.0539

Chan, M. Y., Park, D. C., Savalia, N. K., Petersen, S. E., & Wig, G. S. (2014). Decreased segregation of brain systems across the healthy adult lifespan. *PNAS*, *111*(46), E4997–5006. https://doi.org/10.1073/pnas.1415122111

Choi, H., & Feng, J. (2015). General Slowing Hypothesis. In S. K. Whitbourne (Ed.), *The Encyclopedia of Adulthood and Aging* (pp. 1–4). https://doi.org/10.1002/9781118521373.wbeaa198

Chong, J. S. X., Ng, K. K., Tandi, J., Wang, C., Poh, J. H., Lo, J. C., Chee, M. W. L., & Zhou, J. H. (2019). Longitudinal changes in the cerebral cortex functional organization of healthy elderly. *Journal of Neuroscience*, *39*(28), 5534–5550. https://doi.org/10.1523/JNEUROSCI.1451-18.2019

Ciric, R., Wolf, D. H., Power, J. D., Roalf, D. R., Baum, G. L., Ruparel, K., Shinohara, R. T., Elliott, M. A., Eickhoff, S. B., Davatzikos, C., Gur, R. C., Gur, R. E., Bassett, D. S., & Satterthwaite, T. D. (2017). Benchmarking of participant-level confound regression strategies for the control of motion artifact

in studies of functional connectivity. *NeuroImage*, *154*, 174–187. https://doi.org/10.1016/j.neuroimage.2017.03.020

Coelho, A., Fernandes, H. M., Magalhaes, R., Moreira, P. S., Marques, P., Soares, J. M., Amorim, L., Portugal-Nunes, C., Castanho, T., Santos, N. C., & Sousa, N. (2021). Reorganization of brain structural networks in aging: A longitudinal study. *Journal of Neuroscience Research*, *99*(5), 1354–1376. https://doi.org/10.1002/jnr.24795

Conrad, B. N., Pollack, C., Yeo, D. J., & Price, G. R. (2023). Structural and functional connectivity of the inferior temporal numeral area. *Cerebral Cortex*, *33*(10), 6152–6170. https://doi.org/10.1093/cercor/bhac492

Cox, S. R. (2024). Neurocognitive aging. *Annual Review of Developmental Psychology*, *6*(1), 505–527. https://doi.org/10.1146/annurev-devpsych-010923-102441

Craik, F. I., & Salthouse, T. A. (2011). *The handbook of aging and cognition* (3rd ed.). Psychology Press.

Damoiseaux, J. S. (2017). Effects of aging on functional and structural brain connectivity. *NeuroImage*, *160*, 32–40. https://doi.org/10.1016/j.neuroimage.2017.01.077

Davies, D. L., & Bouldin, D. W. (1979). A cluster separation measure. *IEEE Transactions on Pattern Analysis and Machine Intelligence*, *PAMI-1*(2), 224–227. https://doi.org/10.1109/tpami.1979.4766909

Davis, S. W., Dennis, N. A., Daselaar, S. M., Fleck, M. S., & Cabeza, R. (2008). Que PASA? The posterior-anterior shift in aging. *Cerebral Cortex*, *18*(5), 1201–1209. https://doi.org/10.1093/cercor/bhm155

De Benedictis, A., Rossi-Espagnet, M. C., de Palma, L., Carai, A., & Marras, C. E. (2022). Networking of the human cerebellum: From anatomo-functional development to neurosurgical implications. *Frontiers in Neurology*, *13*, 806298. https://doi.org/10.3389/fneur.2022.806298

Deary, I. J., Corley, J., Gow, A. J., Harris, S. E., Houlihan, L. M., Marioni, R. E., Penke, L., Rafnsson, S. B., & Starr, J. M. (2009). Age-associated cognitive decline. *British Medical Bulletin*, *92*, 135–152. https://doi.org/10.1093/bmb/ldp033

Deery, H. A., Di Paolo, R., Moran, C., Egan, G. F., & Jamadar, S. D. (2023). The older adult brain is less modular, more integrated, and less efficient at rest: A systematic review of large-scale resting-state functional brain networks in aging. *Psychophysiology*, *60*(1), e14159. https://doi.org/10.1111/psyp.14159

Del Boca, F. K., & Darkes, J. (2003). The validity of self-reports of alcohol consumption: state of the science and challenges for research. *Addiction*, *98*, 1–12. https://doi.org/10.1046/j.1359-6357.2003.00586.x

Deligianni, F., Carmichael, D. W., Zhang, G. H., Clark, C. A., & Clayden, J. D. (2016). NODDI and tensor-based microstructural indices as predictors of functional connectivity. *PLoS ONE*, *11*(4), e0153404. https://doi.org/10.1371/journal.pone.0153404

Dhamala, E., Jamison, K. W., Jaywant, A., Dennis, S., & Kuceyeski, A. (2021). Distinct functional and structural connections predict crystallised and fluid cognition in healthy adults. *Human Brain Mapping*, *42*(10), 3102–3118. https://doi.org/10.1002/hbm.25420

Diez, I., Troyas, C., Bauer, C. M., Sepulcre, J., & Merabet, L. B. (2024). Reorganization of integration and segregation networks in brain-based visual impairment. *NeuroImage: Clinical*, *44*, 103688. https://doi.org/10.1016/j.nicl.2024.103688

Dohmatob, E., Varoquaux, G., & Thirion, B. (2018). Inter-subject registration of functional images: Do we need anatomical images? *Frontiers in Neuroscience*, *12*, 64. https://doi.org/10.3389/fnins.2018.00064

Dolcos, F., Rice, H. J., & Cabeza, R. (2002). Hemispheric asymmetry and aging: right hemisphere decline or asymmetry reduction. *Neuroscience & Biobehavioral Reviews*, *26*(7), 819–825. https://doi.org/10.1016/s0149-7634(02)00068-4

Dubois, J., & Adolphs, R. (2016). Building a science of individual differences from fMRI. *Trends in Cognitive Sciences*, *20*(6), 425–443. https://doi.org/10.1016/j.tics.2016.03.014

Dubois, J., Galdi, P., Paul, L. K., & Adolphs, R. (2018). A distributed brain network predicts general intelligence from resting-state human neuroimaging data. *Philosophical Transactions of the Royal Society B: Biological Sciences*, *373*(1756). https://doi.org/10.1098/rstb.2017.0284

DuPre, E., & Spreng, R. N. (2017). Structural covariance networks across the life span, from 6 to 94 years of age. *Network Neuroscience*, *1*(3), 302–323. https://doi.org/10.1162/NETN_a_00016

Durazzo, T. C., Meyerhoff, D. J., & Yoder, K. K. (2018). Cigarette smoking is associated with cortical thinning in anterior frontal regions, insula and regions showing atrophy in early Alzheimer's Disease. *Drug and Alcohol Dependence*, *192*, 277–284. https://doi.org/10.1016/j.drugalcdep.2018.08.009

Duriez, Q., Crivello, F., & Mazoyer, B. (2014). Sex-related and tissue-specific effects of tobacco smoking on brain atrophy: assessment in a large longitudinal cohort of healthy elderly. *Frontiers in Aging Neuroscience*, *6*, 299. https://doi.org/10.3389/fnagi.2014.00299

Easley, T., Chen, R., Hannon, K., Dutt, R., & Bijsterbosch, J. (2023). Population modeling with machine learning can enhance measures of mental health - Open-data replication. *NeuroImage: Reports*, *3*(2), 100163. https://doi.org/10.1016/j.ynirp.2023.100163

Erickson, K. I., Voss, M. W., Prakash, R. S., Basak, C., Szabo, A., Chaddock, L., Kim, J. S., Heo, S., Alves, H., White, S. M., Wojcicki, T. R., Mailey, E., Vieira, V. J., Martin, S. A., Pence, B. D., Woods, J. A., McAuley, E., & Kramer, A. F. (2011). Exercise training increases size of hippocampus and improves memory. *PNAS*, *108*(7), 3017–3022. https://doi.org/10.1073/pnas.1015950108

Felix, C., Rosano, C., Zhu, X., Flatt, J. D., & Rosso, A. L. (2021). Greater social engagement and greater gray matter microstructural integrity in brain regions relevant to dementia. *The Journals of Gerontology, Series B: Psychological Sciences and Social Sciences*, *76*(6), 1027–1035. https://doi.org/10.1093/geronb/gbaa173

Ferreira, L. K., & Busatto, G. F. (2013). Resting-state functional connectivity in normal brain aging. *Neuroscience & Biobehavioral Reviews*, *37*(3), 384–400. https://doi.org/10.1016/j.neubiorev.2013.01.017

Finn, E. S., Shen, X., Scheinost, D., Rosenberg, M. D., Huang, J., Chun, M. M., Papademetris, X., & Constable, R. T. (2015). Functional connectome fingerprinting: identifying individuals using patterns of brain connectivity. *Nature Neuroscience*, *18*(11), 1664–1671. https://doi.org/10.1038/nn.4135

Fjell, A. M., & Walhovd, K. B. (2010). Structural brain changes in aging: courses, causes and cognitive consequences. *Reviews in the Neurosciences*, *21*(3), 187–221. https://doi.org/10.1515/revneuro.2010.21.3.187

Franz, C. E., Hatton, S. N., Elman, J. A., Warren, T., Gillespie, N. A., Whitsel, N. A., Puckett, O. K., Dale, A. M., Eyler, L. T., Fennema-Notestine, C., Hagler, D. J., Jr., Hauger, R. L., McKenzie, R., Neale, M. C., Panizzon, M. S., Pearce, R. C., Reynolds, C. A., Sanderson-Cimino, M., Toomey, R., …Kremen, W. S. (2021). Lifestyle and the aging brain: interactive effects of modifiable lifestyle behaviors and cognitive ability in men from midlife to old age. *Neurobiology of Aging*, *108*, 80–89. https://doi.org/10.1016/j.neurobiolaging.2021.08.007

Friedman, N. P., & Miyake, A. (2017). Unity and diversity of executive functions: Individual differences as a window on cognitive structure. *Cortex*, *86*, 186–204. https://doi.org/10.1016/j.cortex.2016.04.023

Fu, Z., Liu, J., Salman, M. S., Sui, J., & Calhoun, V. D. (2023). Functional connectivity uniqueness and variability? Linkages with cognitive and psychiatric problems in children. *Nature Mental Health*, *1*(12), 956–970. https://doi.org/10.1038/s44220-023-00151-8

Funk-White, M., Wing, D., Eyler, L. T., Moore, A. A., Reas, E. T., & McEvoy, L. (2023). Neuroimaging-

derived predicted brain age and alcohol use among community-dwelling older adults. *The American Journal of Geriatric Psychiatry*, *31*(9), 669–678. https://doi.org/10.1016/j.jagp.2023.02.043

Gallen, C. L., Turner, G. R., Adnan, A., & D'Esposito, M. (2016). Reconfiguration of brain network architecture to support executive control in aging. *Neurobiology of Aging*, *44*, 42–52. https://doi.org/10.1016/j.neurobiolaging.2016.04.003

Gao, M., Wong, C. H. Y., Huang, H., Shao, R., Huang, R., Chan, C. C. H., & Lee, T. M. C. (2020). Connectome-based models can predict processing speed in older adults. *NeuroImage*, *223*, 117290. https://doi.org/10.1016/j.neuroimage.2020.117290

Gao, S., Greene, A. S., Constable, R. T., & Scheinost, D. (2019). Combining multiple connectomes improves predictive modeling of phenotypic measures. *NeuroImage*, *201*, 116038. https://doi.org/10.1016/j.neuroimage.2019.116038

Gao, W., Elton, A., Zhu, H., Alcauter, S., Smith, J. K., Gilmore, J. H., & Lin, W. (2014). Intersubject variability of and genetic effects on the brain's functional connectivity during infancy. *Journal of Neuroscience*, *34*(34), 11288–11296. https://doi.org/10.1523/JNEUROSCI.5072-13.2014

Garrett, D. D., Kovacevic, N., McIntosh, A. R., & Grady, C. L. (2013). The modulation of BOLD variability between cognitive states varies by age and processing speed. *Cerebral Cortex*, *23*(3), 684–693. https://doi.org/10.1093/cercor/bhs055

Garrett, D. D., Samanez-Larkin, G. R., MacDonald, S. W., Lindenberger, U., McIntosh, A. R., & Grady, C. L. (2013). Moment-to-moment brain signal variability: a next frontier in human brain mapping? *Neuroscience & Biobehavioral Reviews*, *37*(4), 610–624. https://doi.org/10.1016/j.neubiorev.2013.02.015

Gaser, C., Dahnke, R., Thompson, P. M., Kurth, F., Luders, E., & The Alzheimer's Disease Neuroimaging, I. (2024). CAT: a computational anatomy toolbox for the analysis of structural MRI data. *Gigascience*, *13*, giae049. https://doi.org/10.1093/gigascience/giae049

Geerligs, L., Maurits, N. M., Renken, R. J., & Lorist, M. M. (2014). Reduced specificity of functional connectivity in the aging brain during task performance. *Human Brain Mapping*, *35*(1), 319–330. https://doi.org/10.1002/hbm.22175

Geerligs, L., Renken, R. J., Saliasi, E., Maurits, N. M., & Lorist, M. M. (2015). A brain-wide study of age-related changes in functional connectivity. *Cerebral Cortex*, *25*(7), 1987–1999. https://doi.org/10.1093/cercor/bhu012

Geerligs, L., Tsvetanov, K. A., Cam, C., & Henson, R. N. (2017). Challenges in measuring individual differences in functional connectivity using fMRI: The case of healthy aging. *Human Brain Mapping*, *38*(8), 4125–4156. https://doi.org/10.1002/hbm.23653

Genon, S., Eickhoff, S. B., & Kharabian, S. (2022). Linking interindividual variability in brain structure to behaviour. *Nature Reviews Neuroscience*, *23*(5), 307–318. https://doi.org/10.1038/s41583-022-00584-7

Ghosal, A. M., & Chandrasekaran, B. (2024). Stair-climbing interventions on cardio-metabolic outcomes in adults: A scoping review. *Journal of Taibah University Medical Sciences*, *19*(1), 136–150. https://doi.org/10.1016/j.jtumed.2023.10.003

Glasser, M. F., Sotiropoulos, S. N., Wilson, J. A., Coalson, T. S., Fischl, B., Andersson, J. L., Xu, J., Jbabdi, S., Webster, M., Polimeni, J. R., Van Essen, D. C., Jenkinson, M., & Consortium, W. U.-M. H. (2013). The minimal preprocessing pipelines for the Human Connectome Project. *NeuroImage*, *80*, 105–124. https://doi.org/10.1016/j.neuroimage.2013.04.127

Glaubitz, L., Stumme, J., Lucht, S., Moebus, S., Schramm, S., Jockwitz, C., Hoffmann, B., & Caspers, S. (2022). Association between long-term air pollution, chronic traffic noise, and resting-state

functional connectivity in the 1000BRAINS study. *Environmental Health Perspectives*, *130*(9). https://doi.org/10.1289/ehp9737

Goh, J. O., & Park, D. C. (2009). Neuroplasticity and cognitive aging: the scaffolding theory of aging and cognition. *Restorative Neurology and Neuroscience*, *27*(5), 391–403. https://doi.org/10.3233/RNN-2009-0493

Goh, Y. K., Iqbal, M., Sofyan, H., Usman, T., Marzuki, M., & Sim, H. S. (2024). Determination of characteristics of stunting risk families in Subulussalam, Aceh in 2022 using k-modes cluster analysis. *ITM Web of Conferences*, *67*. https://doi.org/10.1051/itmconf/20246701038

Gong, G., Rosa-Neto, P., Carbonell, F., Chen, Z. J., He, Y., & Evans, A. C. (2009). Age- and gender-related differences in the cortical anatomical network. *Journal of Neuroscience*, *29*(50), 15684–15693. https://doi.org/10.1523/JNEUROSCI.2308-09.2009

Gons, R. A. R., van Norden, A. G. W., de Laat, K. F., van Oudheusden, L. J. B., van Uden, I. W. M., Zwiers, M. P., Norris, D. G., & de Leeuw, F.-E. (2011). Cigarette smoking is associated with reduced microstructural integrity of cerebral white matter. *Brain*, *134*(7), 2116–2124. https://doi.org/10.1093/brain/awr145

Goodman, Z. T., Nomi, J. S., Kornfeld, S., Bolt, T., Saumure, R. A., Romero, C., Bainter, S. A., & Uddin, L. Q. (2024). Brain signal variability and executive functions across the life span. *Network Neuroscience*, *8*(1), 226–240. https://doi.org/10.1162/netn_a_00347

Grady, C. L., Maisog, J. M., Horwitz, B., Ungerleider, L. G., Mentis, M. J., Salerno, J. A., Pietrini, P., Wagner, E., & Haxby, J. V. (1994). Age-related changes in cortical blood flow activation during visual processing of faces and location. *Journal of Neuroscience*, *14*(3 Pt 2), 1450–1462. https://doi.org/10.1523/JNEUROSCI.14-03-01450.1994

Gratton, C., Sun, H., & Petersen, S. E. (2018). Control networks and hubs. *Psychophysiology*, *55*(3), e13032. https://doi.org/10.1111/psyp.13032

Greenwood, P. M. (2000). The frontal aging hypothesis evaluated. *Journal of the International Neuropsychological Society*, *6*(6), 705–726. https://doi.org/10.1017/s1355617700666092

Grodem, E. O. S., Vidal-Pineiro, D., Sorensen, O., Bartres-Faz, D., Brandmaier, A. M., Cattaneo, G., Garrido, P. F., Henson, R. N., Kuhn, S., Lindenberger, U., MacIntosh, B. J., Nyberg, L., Pascual-Leone, A., Smith, S. M., Sole-Padulles, C., Solana-Sanchez, J., Watne, L. O., Walhovd, K. B., Bjornerud, A., & Fjell, A. M. (2025). Distinguishing lifelong individual differences from divergent aging trajectories of adult brain volumes. *bioRxiv*. https://doi.org/10.1101/2025.05.26.655710

Groh, J., & Simons, M. (2025). White matter aging and its impact on brain function. *Neuron*, *113*(1), 127–139. https://doi.org/10.1016/j.neuron.2024.10.019

Grundy, J. G., Anderson, J. A. E., & Bialystok, E. (2017). Neural correlates of cognitive processing in monolinguals and bilinguals. *Annals of the New York Academy of Sciences*, *1396*(1), 183–201. https://doi.org/10.1111/nyas.13333

Halassa, M. M., & Kastner, S. (2017). Thalamic functions in distributed cognitive control. *Nature Neuroscience*, *20*(12), 1669–1679. https://doi.org/10.1038/s41593-017-0020-1

Han, L., & Jia, J. (2021). Long-term effects of alcohol consumption on cognitive function in seniors: a cohort study in China. *BMC Geriatrics*, *21*(1), 699. https://doi.org/10.1186/s12877-021-02606-y

Harada, C. N., Natelson Love, M. C., & Triebel, K. L. (2013). Normal cognitive aging. *Clinics in Geriatric Medicine*, *29*(4), 737–752. https://doi.org/10.1016/j.cger.2013.07.002

Harrison, O. K., Guell, X., Klein-Flugge, M. C., & Barry, R. L. (2021). Structural and resting state functional connectivity beyond the cortex. *NeuroImage*, *240*, 118379. https://doi.org/10.1016/j.neuroimage.2021.118379

Hasher, L., & Zacks, R. T. (1988). Working memory, comprehension, and aging: A review and a new view. In G. H. Bower (Ed.), *Psychology of Learning and Motivation* (Vol. 22, pp. 193–225). Academic Press. https://doi.org/10.1016/S0079-7421(08)60041-9

Hassing, L. B. (2018). Light alcohol consumption does not protect cognitive function: A longitudinal prospective study. *Frontiers in Aging Neuroscience*, *10*, 81. https://doi.org/10.3389/fnagi.2018.00081

Hausman, H. K., Hardcastle, C., Albizu, A., Kraft, J. N., Evangelista, N. D., Boutzoukas, E. M., Langer, K., O'Shea, A., Van Etten, E. J., Bharadwaj, P. K., Song, H., Smith, S. G., Porges, E., DeKosky, S. T., Hishaw, G. A., Wu, S., Marsiske, M., Cohen, R., Alexander, G. E., & Woods, A. J. (2022). Cingulo-opercular and frontoparietal control network connectivity and executive functioning in older adults. *Geroscience*, *44*(2), 847–866. https://doi.org/10.1007/s11357-021-00503-1

Hayes, A. F. (2017). Partial, conditional, and moderated moderated mediation: Quantification, inference, and interpretation. *Communication Monographs*, *85*(1), 4–40. https://doi.org/10.1080/03637751.2017.1352100

He, Y., & Evans, A. (2010). Graph theoretical modeling of brain connectivity. *Current Opinion in Neurology*, *23*(4), 341–350. https://doi.org/10.1097/WCO.0b013e32833aa567

Hebling Vieira, B., Liem, F., Dadi, K., Engemann, D. A., Gramfort, A., Bellec, P., Craddock, R. C., Damoiseaux, J. S., Steele, C. J., Yarkoni, T., Langer, N., Margulies, D. S., & Varoquaux, G. (2022). Predicting future cognitive decline from non-brain and multimodal brain imaging data in healthy and pathological aging. *Neurobiology of Aging*, *118*, 55–65. https://doi.org/10.1016/j.neurobiolaging.2022.06.008

Hedden, T., & Gabrieli, J. D. (2004). Insights into the ageing mind: a view from cognitive neuroscience. *Nature Reviews Neuroscience*, *5*(2), 87–96. https://doi.org/10.1038/nrn1323

Hennig, C. (2015). What are the true clusters? *Pattern Recognition Letters*, *64*, 53–62. https://doi.org/10.1016/j.patrec.2015.04.009

Heyder, K., Suchan, B., & Daum, I. (2004). Cortico-subcortical contributions to executive control. *Acta Psychologica*, *115*(2-3), 271–289. https://doi.org/10.1016/j.actpsy.2003.12.010

Hilger, K., Winter, N. R., Leenings, R., Sassenhagen, J., Hahn, T., Basten, U., & Fiebach, C. J. (2020). Predicting intelligence from brain gray matter volume. *Brain Structure and Function*, *225*(7), 2111–2129. https://doi.org/10.1007/s00429-020-02113-7

Hoagey, D. A., Rieck, J. R., Rodrigue, K. M., & Kennedy, K. M. (2019). Joint contributions of cortical morphometry and white matter microstructure in healthy brain aging: A partial least squares correlation analysis. *Human Brain Mapping*, *40*(18), 5315–5329. https://doi.org/10.1002/HBM.24774

Hodson, T. O. (2022). Root-mean-square error (RMSE) or mean absolute error (MAE): When to use them or not. *Geoscientific Model Development*, *15*(14), 5481–5487. https://doi.org/10.5194/gmd-15-5481-2022

Honey, C. J., Sporns, O., Cammoun, L., Gigandet, X., Thiran, J. P., Meuli, R., & Hagmann, P. (2009). Predicting human resting-state functional connectivity from structural connectivity. *PNAS*, *106*(6), 2035–2040. https://doi.org/10.1073/pnas.0811168106

Huang, W., Chen, H., Liu, Z., Dong, X., Feng, G., Liu, G., Yang, A., Zhang, Z., Shmuel, A., Su, L., Ma, G., & Shu, N. (2025). Individual variability in the structural connectivity architecture of the human brain. *Journal of Neuroscience*, *45*(5), e2139232024. https://doi.org/10.1523/JNEUROSCI.2139-23.2024

Huang, Z. (1998). Extensions to the k-means algorithm for clustering large data sets with categorical values. *Data Mining and Knowledge Discovery*, *2*(3), 283–304. https://doi.org/10.1023/a:1009769707641

Jahangiri, M., Kazemnejad, A., Goldfeld, K. S., Daneshpour, M. S., Mostafaei, S., Khalili, D., Moghadas, M. R., & Akbarzadeh, M. (2023). A wide range of missing imputation approaches in longitudinal data: a simulation study and real data analysis. *BMC Medical Research Methodology*, *23*(1), 161. https://doi.org/10.1186/s12874-023-01968-8

Jamadar, S. D. (2020). The CRUNCH model does not account for load-dependent changes in visuospatial working memory in older adults. *Neuropsychologia*, *142*, 107446. https://doi.org/10.1016/j.neuropsychologia.2020.107446

James, B. D., Glass, T. A., Caffo, B., Bobb, J. F., Davatzikos, C., Yousem, D., & Schwartz, B. S. (2012). Association of social engagement with brain volumes assessed by structural MRI. *Journal of Aging Research*, *2012*, 512714. https://doi.org/10.1155/2012/512714

Jauny, G., Mijalkov, M., Canal-Garcia, A., Volpe, G., Pereira, J., Eustache, F., & Hinault, T. (2024). Linking structural and functional changes during aging using multilayer brain network analysis. *Communications Biology*, *7*(1), 239. https://doi.org/10.1038/s42003-024-05927-x

Jeurissen, B., Tournier, J. D., Dhollander, T., Connelly, A., & Sijbers, J. (2014). Multi-tissue constrained spherical deconvolution for improved analysis of multi-shell diffusion MRI data. *NeuroImage*, *103*, 411–426. https://doi.org/10.1016/j.neuroimage.2014.07.061

Jirsaraie, R. J., Gorelik, A. J., Gatavins, M. M., Engemann, D. A., Bogdan, R., Barch, D. M., & Sotiras, A. (2023). A systematic review of multimodal brain age studies: Uncovering a divergence between model accuracy and utility. *Patterns (N Y)*, *4*(4), 100712. https://doi.org/10.1016/j.patter.2023.100712

Jockwitz, C., & Caspers, S. (2021). Resting-state networks in the course of aging-differential insights from studies across the lifespan vs. amongst the old. *Pflügers Archiv - European Journal of Physiology*, *473*(5), 793–803. https://doi.org/10.1007/s00424-021-02520-7

Jockwitz, C., Kramer, C., Dellani, P., & Caspers, S. (2024). Differential predictability of cognitive profiles from brain structure in older males and females. *Geroscience*, *46*(2), 1713–1730. https://doi.org/10.1007/s11357-023-00934-y

Kalbe, E., Kessler, J., Calabrese, P., Smith, R., Passmore, A. P., Brand, M., & Bullock, R. (2004). DemTect: a new, sensitive cognitive screening test to support the diagnosis of mild cognitive impairment and early dementia. *International Journal of Geriatric Psychiatry*, *19*(2), 136–143. https://doi.org/10.1002/gps.1042

Kamalov, F., Sulieman, H., Alzaatreh, A., Emarly, M., Chamlal, H., & Safaraliev, M. (2025). Mathematical methods in feature selection: A review. *Mathematics*, *13*(6). https://doi.org/10.3390/math13060996

Kang, W., Wang, J., & Malvaso, A. (2021). Inhibitory control in aging: the compensation-related utilization of neural circuits hypothesis. *Frontiers in Aging Neuroscience*, *13*, 771885. https://doi.org/10.3389/fnagi.2021.771885

Karahan, E., Tait, L., Si, R., Ozkan, A., Szul, M. J., Graham, K. S., Lawrence, A. D., & Zhang, J. (2022). The interindividual variability of multimodal brain connectivity maintains spatial heterogeneity and relates to tissue microstructure. *Communications Biology*, *5*(1), 1007. https://doi.org/10.1038/s42003-022-03974-w

Kellner, E., Dhital, B., Kiselev, V. G., & Reisert, M. (2016). Gibbs-ringing artifact removal based on local subvoxel-shifts. *agnetic Resonance in Medicine*, *76*(5), 1574–1581. https://doi.org/10.1002/mrm.26054

Khalilian, M., Toba, M. N., Roussel, M., Tasseel-Ponche, S., Godefroy, O., & Aarabi, A. (2024). Age-related differences in structural and resting-state functional brain network organization across the adult lifespan: A cross-sectional study. *Aging Brain*, *5*, 100105.

https://doi.org/10.1016/j.nbas.2023.100105

Kivipelto, M., Helkala, E. L., Laakso, M. P., Hanninen, T., Hallikainen, M., Alhainen, K., Soininen, H., Tuomilehto, J., & Nissinen, A. (2001). Midlife vascular risk factors and Alzheimer's disease in later life: Longitudinal, population based study. *BMJ*, *322*(7300), 1447–1451. https://doi.org/10.1136/bmj.322.7300.1447

Koen, J. D., & Rugg, M. D. (2019). Neural dedifferentiation in the aging brain. *Trends in Cognitive Sciences*, *23*(7), 547–559. https://doi.org/10.1016/j.tics.2019.04.012

Koen, J. D., Srokova, S., & Rugg, M. D. (2020). Age-related neural dedifferentiation and cognition. *Current Opinion in Behavioral Sciences*, *32*, 7–14. https://doi.org/10.1016/j.cobeha.2020.01.006

Kramer, C., Stumme, J., da Costa Campos, L., Dellani, P., Rubbert, C., Caspers, J., Caspers, S., & Jockwitz, C. (2024). Prediction of cognitive performance differences in older age from multimodal neuroimaging data. *Geroscience*, *46*(1), 283–308. https://doi.org/10.1007/s11357-023-00831-4

Kramer, C., Stumme, J., da Costa Campos, L., Rubbert, C., Caspers, J., Caspers, S., & Jockwitz, C. (2023). Classification and prediction of cognitive performance differences in older age based on brain network patterns using a machine learning approach. *Network Neuroscience*, *7*(1), 122–147. https://doi.org/10.1162/netn_a_00275

Kraskov, A., Stögbauer, H., & Grassberger, P. (2004). Estimating mutual information. *Physical Review E—Statistical, Nonlinear, and Soft Matter Physics*, *69*(6), 066138.

Krishnan, A., Williams, L. J., McIntosh, A. R., & Abdi, H. (2011). Partial Least Squares (PLS) methods for neuroimaging: A tutorial and review. *NeuroImage*, *56*(2), 455–475. https://doi.org/10.1016/j.neuroimage.2010.07.034

Kwak, S., Kim, H., Kim, H., Youm, Y., & Chey, J. (2021). Distributed functional connectivity predicts neuropsychological test performance among older adults. *Human Brain Mapping*, *42*(10), 3305–3325. https://doi.org/10.1002/hbm.25436

Lacreuse, A., Raz, N., Schmidtke, D., Hopkins, W. D., & Herndon, J. G. (2020). Age-related decline in executive function as a hallmark of cognitive ageing in primates: an overview of cognitive and neurobiological studies. *Philosophical Transactions of the Royal Society B: Biological Sciences*, *375*(1811), 20190618. https://doi.org/10.1098/rstb.2019.0618

Lakes, K. D. (2013). Restricted sample variance reduces generalizability. *Psychological Assessment*, *25*(2), 643–650. https://doi.org/10.1037/a0030912

Lavanga, M., Stumme, J., Yalcinkaya, B. H., Fousek, J., Jockwitz, C., Sheheitli, H., Bittner, N., Hashemi, M., Petkoski, S., Caspers, S., & Jirsa, V. (2023). The virtual aging brain: Causal inference supports interhemispheric dedifferentiation in healthy aging. *NeuroImage*, *283*, 120403. https://doi.org/10.1016/j.neuroimage.2023.120403

Lee, W. K., Hinrichs, C., Chen, Y. L., Wang, P. S., Guo, W. Y., & Wu, Y. T. (2024). Analysis of the difference between Alzheimer's disease, mild cognitive impairment and normal people by using fractal dimensions and small-world network. *Progress in Brain Research*, *290*, 179–190. https://doi.org/10.1016/bs.pbr.2024.07.005

Li, J., Wu, G. R., Li, B., Fan, F., Zhao, X., Meng, Y., Zhong, P., Yang, S., Biswal, B. B., Chen, H., & Liao, W. (2021). Transcriptomic and macroscopic architectures of intersubject functional variability in human brain white-matter. *Communications Biology*, *4*(1), 1417. https://doi.org/10.1038/s42003-021-02952-y

Li, L., Wei, Y., Zhang, J., Ma, J., Yi, Y., Gu, Y., Li, L. M. W., Lin, Y., & Dai, Z. (2021). Gene expression associated with individual variability in intrinsic functional connectivity. *NeuroImage*, *245*, 118743. https://doi.org/10.1016/j.neuroimage.2021.118743

Li, R., Yin, S., Zhu, X., Ren, W., Yu, J., Wang, P., Zheng, Z., Niu, Y. N., Huang, X., & Li, J. (2017). Linking inter-individual variability in functional brain connectivity to cognitive ability in elderly individuals. *Frontiers in Aging Neuroscience*, *9*, 385. https://doi.org/10.3389/fnagi.2017.00385

Li, S. C., Lindenberger, U., & Sikstrom, S. (2001). Aging cognition: from neuromodulation to representation. *Trends in Cognitive Sciences*, *5*(11), 479–486. https://doi.org/10.1016/s1364-6613(00)01769-1

Li, X., Wang, Y., Wang, W., Huang, W., Chen, K., Xu, K., Zhang, J., Chen, Y., Li, H., Wei, D., Shu, N., & Zhang, Z. (2020). Age-related decline in the topological efficiency of the brain structural connectome and cognitive aging. *Cerebral Cortex*, *30*(8), 4651–4661. https://doi.org/10.1093/cercor/bhaa066

Licher, S., Ahmad, S., Karamujic-Comic, H., Voortman, T., Leening, M. J. G., Ikram, M. A., & Ikram, M. K. (2019). Genetic predisposition, modifiable-risk-factor profile and long-term dementia risk in the general population. *Nature Medicine*, *25*(9), 1364–1369. https://doi.org/10.1038/s41591-019-0547-7

Liegeois, R., Li, J., Kong, R., Orban, C., Van De Ville, D., Ge, T., Sabuncu, M. R., & Yeo, B. T. T. (2019). Resting brain dynamics at different timescales capture distinct aspects of human behavior. *Nature Communications*, *10*(1), 2317. https://doi.org/10.1038/s41467-019-10317-7

Linli, Z., Rolls, E. T., Zhao, W., Kang, J., Feng, J., & Guo, S. (2023). Smoking is associated with lower brain volume and cognitive differences: A large population analysis based on the UK Biobank. *Progress in Neuro-Psychopharmacology & Biological Psychiatry*, *123*, 110698. https://doi.org/10.1016/j.pnpbp.2022.110698

Listabarth, S., Groemer, M., Waldhoer, T., Vyssoki, B., Pruckner, N., Vyssoki, S., Glahn, A., Konig-Castillo, D. M., & Konig, D. (2022). Cognitive decline and alcohol consumption in the aging population-a longitudinal analysis of the survey of health, ageing and retirement in Europe. *European Psychiatry*, *65*(1), e83. https://doi.org/10.1192/j.eurpsy.2022.2344

Liu, R., Subakan, C., Balwani, A. H., Whitesell, J., Harris, J., Koyejo, S., & Dyer, E. L. (2020). A generative modeling approach for interpreting population-level variability in brain structure. In *Medical Image Computing and Computer-Assisted Intervention – MICCAI 2020* (pp. 257–266). Springer. https://doi.org/10.1007/978-3-030-59722-1_25

Livingston, G., Huntley, J., Sommerlad, A., Ames, D., Ballard, C., Banerjee, S., Brayne, C., Burns, A., Cohen-Mansfield, J., Cooper, C., Costafreda, S. G., Dias, A., Fox, N., Gitlin, L. N., Howard, R., Kales, H. C., Kivimaki, M., Larson, E. B., Ogunniyi, A., …Mukadam, N. (2020). Dementia prevention, intervention, and care: 2020 report of the Lancet Commission. *Lancet*, *396*(10248), 413–446. https://doi.org/10.1016/S0140-6736(20)30367-6

Lundberg, S. M., & Lee, S.-I. (2017). A unified approach to interpreting model predictions. In *Advances in Neural Information Processing Systems* (Vol. 30).

Lux, S., Hartje, W., Reich, C., & Nagel, C. (2012). VGT: Verbaler Gedächtnistest: Bielefelder Kategorielle Wortlisten. *Göttingen: Verlag Hans Huber*.

Ma, C., Liu, A., Liu, J., Wang, X., Cong, F., Li, Y., & Liu, J. (2025). A window into the brain: Multimodal MRI assessment of vascular cognitive impairment. *Frontiers in Neuroscience*, *19*, 1526897. https://doi.org/10.3389/fnins.2025.1526897

Ma, L., Tian, L., Hu, T., Jiang, T., & Zuo, N. (2021). Development of individual variability in brain functional connectivity and capability across the adult lifespan. *Cerebral Cortex*, *31*(8), 3925–3938. https://doi.org/10.1093/cercor/bhab059

MacDonald, M. E., & Pike, G. B. (2021). MRI of healthy brain aging: A review. *NMR in Biomedicine*, *34*(9), e4564. https://doi.org/10.1002/nbm.4564

MacDonald, S. W., DeCarlo, C. A., & Dixon, R. A. (2011). Linking biological and cognitive aging: toward

improving characterizations of developmental time. *The Journals of Gerontology, Series B: Psychological Sciences and Social Sciences*, *66 Suppl 1*(Suppl 1), i59–70. https://doi.org/10.1093/geronb/gbr039

MacKinnon, D. P. (2012). *Introduction to statistical mediation analysis* (1st ed.). Routledge. https://doi.org/10.4324/9780203809556

Madden, D. J., Bennett, I. J., & Song, A. W. (2009). Cerebral white matter integrity and cognitive aging: contributions from diffusion tensor imaging. *Neuropsychology Review*, *19*(4), 415–435. https://doi.org/10.1007/s11065-009-9113-2

Madden, D. J., Jain, S., Monge, Z. A., Cook, A. D., Lee, A., Huang, H., Howard, C. M., & Cohen, J. R. (2020). Influence of structural and functional brain connectivity on age-related differences in fluid cognition. *Neurobiology of Aging*, *96*, 205–222. https://doi.org/10.1016/j.neurobiolaging.2020.09.010

Martin, S., Williams, K. A., Saur, D., & Hartwigsen, G. (2023). Age-related reorganization of functional network architecture in semantic cognition. *Cerebral Cortex*, *33*(8), 4886–4903. https://doi.org/10.1093/cercor/bhac387

Mattoni, M., Fisher, A. J., Gates, K. M., Chein, J., & Olino, T. M. (2025). Group-to-individual generalizability and individual-level inferences in cognitive neuroscience. *Neuroscience & Biobehavioral Reviews*, *169*, 106024. https://doi.org/10.1016/j.neubiorev.2025.106024

Mattoni, M., Smith, D. V., Chein, J., & Olino, T. M. (2025). Functional connectivity heterogeneity and consequences for clinical and cognitive prediction: Stage 2 registered report. *Imaging Neuroscience*, *3*. https://doi.org/10.1162/IMAG.a.107

Matyi, M. A., Radhakrishnan, H., Olm, C. A., Phillips, J. S., Cook, P. A., Rhodes, E., Gee, J. C., Irwin, D. J., McMillan, C. T., & Massimo, L. (2025). Executive dysfunction relates to salience network desegregation in behavioural variant frontotemporal dementia. *NeuroImage: Clinical*, *48*, 103853. https://doi.org/10.1016/j.nicl.2025.103853

McDonough, I. M., Nolin, S. A., & Visscher, K. M. (2022). 25 years of neurocognitive aging theories: what have we learned? *Frontiers in Aging Neuroscience*, *14*, 1002096. https://doi.org/10.3389/fnagi.2022.1002096

McDowd, J. M. (1997). Inhibition in attention and aging. *The Journals of Gerontology, Series B: Psychological Sciences and Social Sciences*, *52*(6), P265–273. https://doi.org/10.1093/geronb/52b.6.p265

Mendez Colmenares, A., Prytherch, B., Thomas, M. L., & Burzynska, A. Z. (2023). Within-person changes in the aging white matter microstructure and their modifiers: A meta-analysis and systematic review of longitudinal diffusion tensor imaging studies. *Imaging Neuroscience*, *1*. https://doi.org/10.1162/imag_a_00045

Menon, V., & Uddin, L. Q. (2010). Saliency, switching, attention and control: a network model of insula function. *Brain Structure and Function*, *214*(5-6), 655–667. https://doi.org/10.1007/s00429-010-0262-0

Mihalik, A., Chapman, J., Adams, R. A., Winter, N. R., Ferreira, F. S., Shawe-Taylor, J., & Mourão-Miranda, J. (2022). Canonical correlation analysis and partial least squares for identifying brain–behavior associations: A tutorial and a comparative study. *Biological Psychiatry: Cognitive Neuroscience and Neuroimaging*, *7*(11), 1055–1067. https://doi.org/10.1016/j.bpsc.2022.07.012

Mori, S., Oishi, K., Jiang, H., Jiang, L., Li, X., Akhter, K., Hua, K., Faria, A. V., Mahmood, A., Woods, R., Toga, A. W., Pike, G. B., Neto, P. R., Evans, A., Zhang, J., Huang, H., Miller, M. I., van Zijl, P., & Mazziotta, J. (2008). Stereotaxic white matter atlas based on diffusion tensor imaging in an ICBM template. *NeuroImage*, *40*(2), 570–582. https://doi.org/10.1016/j.neuroimage.2007.12.035

Morris, J. C., Heyman, A., Mohs, R. C., Hughes, J. P., van Belle, G., Fillenbaum, G., Mellits, E. D., & Clark, C. (1989). The consortium to establish a registry for Alzheimer's Disease (CERAD). Part I. Clinical and neuropsychological assessment of Alzheimer's disease. *Neurology*, *39*(9), 1159–1165. https://doi.org/10.1212/wnl.39.9.1159

Mortimer, J. A., Ding, D., Borenstein, A. R., DeCarli, C., Guo, Q., Wu, Y., Zhao, Q., & Chu, S. (2012). Changes in brain volume and cognition in a randomized trial of exercise and social interaction in a community-based sample of non-demented Chinese elders. *Journal of Alzheimer's Disease*, *30*(4), 757–766. https://doi.org/10.3233/JAD-2012-120079

Mueller, S., Wang, D., Fox, M. D., Pan, R., Lu, J., Li, K., Sun, W., Buckner, R. L., & Liu, H. (2015). Reliability correction for functional connectivity: Theory and implementation. *Human Brain Mapping*, *36*(11), 4664–4680. https://doi.org/10.1002/hbm.22947

Mueller, S., Wang, D., Fox, M. D., Yeo, B. T., Sepulcre, J., Sabuncu, M. R., Shafee, R., Lu, J., & Liu, H. (2013). Individual variability in functional connectivity architecture of the human brain. *Neuron*, *77*(3), 586–595. https://doi.org/10.1016/j.neuron.2012.12.028

Mulugeta, A., Navale, S. S., Lumsden, A. L., Llewellyn, D. J., & Hypponen, E. (2022). Healthy lifestyle, genetic risk and brain health: A gene-environment interaction study in the UK Biobank. *Nutrients*, *14*(19), 3907. https://doi.org/10.3390/nu14193907

Mungas, D., Beckett, L., Harvey, D., Farias, S. T., Reed, B., Carmichael, O., Olichney, J., Miller, J., & DeCarli, C. (2010). Heterogeneity of cognitive trajectories in diverse older persons. *Psychol Aging*, *25*(3), 606–619. https://doi.org/10.1037/a0019502

Mwangi, B., Tian, T. S., & Soares, J. C. (2014). A review of feature reduction techniques in neuroimaging. *Neuroinformatics*, *12*(2), 229–244. https://doi.org/10.1007/s12021-013-9204-3

Nakuci, J., Wasylyshyn, N., Cieslak, M., Elliott, J. C., Bansal, K., Giesbrecht, B., Grafton, S. T., Vettel, J. M., Garcia, J. O., & Muldoon, S. F. (2023). Within-subject reproducibility varies in multi-modal, longitudinal brain networks. *Scientific Reports*, *13*(1), 6699. https://doi.org/10.1038/s41598-023-33441-3

Nath, V., Schilling, K. G., Parvathaneni, P., Huo, Y., Blaber, J. A., Hainline, A. E., Barakovic, M., Romascano, D., Rafael-Patino, J., Frigo, M., Girard, G., Thiran, J. P., Daducci, A., Rowe, M., Rodrigues, P., Prckovska, V., Aydogan, D. B., Sun, W., Shi, Y., …Landman, B. A. (2020). Tractography reproducibility challenge with empirical data (TraCED): The 2017 ISMRM diffusion study group challenge. *Journal of Magnetic Resonance Imaging*, *51*(1), 234–249. https://doi.org/10.1002/jmri.26794

Nelson, M. C., Royer, J., Lu, W. D., Leppert, I. R., Campbell, J. S. W., Schiavi, S., Jin, H., Tavakol, S., Vos de Wael, R., Rodriguez-Cruces, R., Pike, G. B., Bernhardt, B. C., Daducci, A., Misic, B., & Tardif, C. L. (2023). The human brain connectome weighted by the myelin content and total intra-axonal cross-sectional area of white matter tracts. *Network Neuroscience*, *7*(4), 1363–1388. https://doi.org/10.1162/netn_a_00330

Ng, K. K., Lo, J. C., Lim, J. K. W., Chee, M. W. L., & Zhou, J. (2016). Reduced functional segregation between the default mode network and the executive control network in healthy older adults: A longitudinal study. *NeuroImage*, *133*, 321–330. https://doi.org/10.1016/j.neuroimage.2016.03.029

Noble, S., Scheinost, D., & Constable, R. T. (2019). A decade of test-retest reliability of functional connectivity: A systematic review and meta-analysis. *NeuroImage*, *203*, 116157. https://doi.org/10.1016/j.neuroimage.2019.116157

Nolin, S. A., Faulkner, M. E., Stewart, P., Fleming, L. L., Merritt, S., Rezaei, R. F., Bharadwaj, P. K., Franchetti, M. K., Raichlen, D. A., Jessup, C. J., Edwards, L., Hishaw, G. A., Van Etten, E. J., Trouard, T. P.,

Geldmacher, D., Wadley, V. G., Alperin, N., Porges, E. S., Woods, A. J., …Visscher, K. M. (2025). Network segregation is associated with processing speed in the cognitively healthy oldest-old. *eLife*, *14*. https://doi.org/10.7554/eLife.78076

Nomi, J. S., Bolt, T. S., Ezie, C. E. C., Uddin, L. Q., & Heller, A. S. (2017). Moment-to-moment BOLD signal variability reflects regional changes in neural flexibility across the lifespan. *Journal of Neuroscience*, *37*(22), 5539–5548. https://doi.org/10.1523/JNEUROSCI.3408-16.2017

Nyberg, L. (2017). Functional brain imaging of episodic memory decline in ageing. *Journal of Internal Medicine*, *281*(1), 65–74. https://doi.org/10.1111/joim.12533

Nyberg, L. (2018). Cognitive control in the prefrontal cortex: a central or distributed executive? *Scandinavian Journal of Psychology*, *59*(1), 62–65. https://doi.org/10.1111/sjop.12409

Nyberg, L., & Lindenberger, U. (2020). Brain maintenance and cognition in old age. In David Poeppel, George R. Mangun, & M. S. Gazzaniga (Eds.), *The cognitive neurosciences* (6th ed., pp. 81–89). The MIT Press. https://doi.org/10.7551/mitpress/11442.001.0001

Nyberg, L., Lovden, M., Riklund, K., Lindenberger, U., & Backman, L. (2012). Memory aging and brain maintenance. *Trends in Cognitive Sciences*, *16*(5), 292–305. https://doi.org/10.1016/j.tics.2012.04.005

O'Sullivan, M., Jones, D. K., Summers, P. E., Morris, R. G., Williams, S. C., & Markus, H. S. (2001). Evidence for cortical "disconnection" as a mechanism of age-related cognitive decline. *Neurology*, *57*(4), 632–638. https://doi.org/10.1212/wnl.57.4.632

Oswald, W. D., & Fleischmann, U. M. (1997). Nürnberger-Alters-Inventar (NAI). *Göttingen: Hogrefe.*

Pagnotta, M. F., Riddle, J., & D'Esposito, M. (2024). Multimodal neuroimaging of hierarchical cognitive control. *Biological Psychology*, *193*, 108896. https://doi.org/10.1016/j.biopsycho.2024.108896

Panizzon, M. S., Fennema-Notestine, C., Eyler, L. T., Jernigan, T. L., Prom-Wormley, E., Neale, M., Jacobson, K., Lyons, M. J., Grant, M. D., Franz, C. E., Xian, H., Tsuang, M., Fischl, B., Seidman, L., Dale, A., & Kremen, W. S. (2009). Distinct genetic influences on cortical surface area and cortical thickness. *Cerebral Cortex*, *19*(11), 2728–2735. https://doi.org/10.1093/cercor/bhp026

Paolillo, E. W., Saloner, R., VandeBunte, A., Lee, S., Bennett, D. A., & Casaletto, K. B. (2023). Multimodal lifestyle engagement patterns support cognitive stability beyond neuropathological burden. *Alzheimer's Research & Therapy*, *15*(1), 221. https://doi.org/10.1186/s13195-023-01365-9

Parkes, L., Fulcher, B., Yucel, M., & Fornito, A. (2018). An evaluation of the efficacy, reliability, and sensitivity of motion correction strategies for resting-state functional MRI. *NeuroImage*, *171*, 415–436. https://doi.org/10.1016/j.neuroimage.2017.12.073

Patel, R., Mackay, C. E., Jansen, M. G., Devenyi, G. A., O'Donoghue, M. C., Kivimaki, M., Singh-Manoux, A., Zsoldos, E., Ebmeier, K. P., Chakravarty, M. M., & Suri, S. (2022). Inter- and intra-individual variation in brain structural-cognition relationships in aging. *NeuroImage*, *257*, 119254. https://doi.org/10.1016/j.neuroimage.2022.119254

Peng, P., Li, M., Liu, H., Tian, Y. R., Chu, S. L., Van Halm-Lutterodt, N., Jing, B., & Jiang, T. (2018). Brain structure alterations in respect to tobacco consumption and nicotine dependence: a comparative voxel-based morphometry study. *Frontiers in Neuroanatomy*, *12*, 43. https://doi.org/10.3389/fnana.2018.00043

Perez, D. C., Hernandez, J. J., Wulfekuhle, G., & Gratton, C. (2025). Variation in brain aging: A review and perspective on the utility of individualized approaches to the study of functional networks in aging. *Neurobiology of Aging*, *147*, 68–87. https://doi.org/10.1016/j.neurobiolaging.2024.11.010

Perinelli, A., Assecondi, S., Tagliabue, C. F., & Mazza, V. (2022). Power shift and connectivity changes in healthy aging during resting-state EEG. *NeuroImage*, *256*, 119247.

https://doi.org/10.1016/j.neuroimage.2022.119247

Persson, J., Pudas, S., Lind, J., Kauppi, K., Nilsson, L.-G., & Nyberg, L. (2012). Longitudinal structure–function correlates in elderly reveal MTL dysfunction with cognitive decline. *Cerebral Cortex*, *22*(10), 2297–2304.

Petersen, M., Hoffstaedter, F., Nagele, F. L., Mayer, C., Schell, M., Rimmele, D. L., Zyriax, B. C., Zeller, T., Kuhn, S., Gallinat, J., Fiehler, J., Twerenbold, R., Omidvarnia, A., Patil, K. R., Eickhoff, S. B., Thomalla, G., & Cheng, B. (2024). A latent clinical-anatomical dimension relating metabolic syndrome to brain structure and cognition. *eLife*, *12*, RP93246. https://doi.org/10.7554/eLife.93246.2.sa2

Poldrack, R. A., Baker, C. I., Durnez, J., Gorgolewski, K. J., Matthews, P. M., Munafo, M. R., Nichols, T. E., Poline, J. B., Vul, E., & Yarkoni, T. (2017). Scanning the horizon: towards transparent and reproducible neuroimaging research. *Nature Reviews Neuroscience*, *18*(2), 115–126. https://doi.org/10.1038/nrn.2016.167

Poulakis, K., Reid, R. I., Przybelski, S. A., Knopman, D. S., Graff-Radford, J., Lowe, V. J., Mielke, M. M., Machulda, M. M., Jack, C. R., Jr., Petersen, R. C., Westman, E., & Vemuri, P. (2021). Longitudinal deterioration of white-matter integrity: heterogeneity in the ageing population. *Brain Commun*, *3*(1), fcaa238. https://doi.org/10.1093/braincomms/fcaa238

Prince, J. B., Davis, H. L., Tan, J., Muller-Townsend, K., Markovic, S., Lewis, D. M. G., Hastie, B., Thompson, M. B., Drummond, P. D., Fujiyama, H., & Sohrabi, H. R. (2024). Cognitive and neuroscientific perspectives of healthy ageing. *Neuroscience & Biobehavioral Reviews*, *161*, 105649. https://doi.org/10.1016/j.neubiorev.2024.105649

Pruitt, P. J., Lahna, D., Schwartz, D. L., Peltier, S., Silbert, L. C., & Dodge, H. H. (2022). Social engagement intervention increases dorsal attention network functional connectivity in socially-isolated older-old adults: I-CONECT. *Alzheimer's & Dementia*, *18*(S11). https://doi.org/10.1002/alz.059653

Puxeddu, M. G., Faskowitz, J., Betzel, R. F., Petti, M., Astolfi, L., & Sporns, O. (2020). The modular organization of brain cortical connectivity across the human lifespan. *NeuroImage*, *218*, 116974. https://doi.org/10.1016/j.neuroimage.2020.116974

Rae, G. (1985). Quade's nonparametric analysis of covariance by matching. *Behavior Research Methods, Instruments, & Computers*, *17*(3), 421–422. https://doi.org/10.3758/bf03200959

Ranasinghe, P. V. N. N., & Mapa, M. S. T. (2024). Functional connectivity and cognitive decline: A review of rs-fMRI, EEG, MEG, and graph theory approaches in aging and dementia. *Exploration of Medicine*, 797–821. https://doi.org/10.37349/emed.2024.00256

Raschka, S. (2018). MLxtend: Providing machine learning and data science utilities and extensions to Python's scientific computing stack. *Journal of Open Source Software*, *3*(24). https://doi.org/10.21105/joss.00638

Rasero, J., Sentis, A. I., Yeh, F. C., & Verstynen, T. (2021). Integrating across neuroimaging modalities boosts prediction accuracy of cognitive ability. *PLoS Computational Biology*, *17*(3), e1008347. https://doi.org/10.1371/journal.pcbi.1008347

Raz, N., & Lindenberger, U. (2011). Only time will tell: cross-sectional studies offer no solution to the age-brain-cognition triangle: comment on Salthouse (2011). *Psychological Bulletin*, *137*(5), 790–795. https://doi.org/10.1037/a0024503

Reitan, R. M. (1958). Validity of the trail making test as an indicator of organic brain damage. *Perceptual and Motor Skills*, *8*(7). https://doi.org/10.2466/pms.8.7.271-276

Reuter-Lorenz, P. A., & Cappell, K. A. (2008). Neurocognitive aging and the compensation hypothesis. *Current Directions in Psychological Science*, *17*(3), 177–182.

Reuter-Lorenz, P. A., & Park, D. C. (2014). How does it STAC up? Revisiting the scaffolding theory of aging and cognition. *Neuropsychology Review*, *24*(3), 355–370. https://doi.org/10.1007/s11065-014-9270-9

Reuter-Lorenz, P. A., & Park, D. C. (2024). Cognitive aging and the life course: A new look at the Scaffolding theory. *Current Opinion in Psychology*, *56*, 101781. https://doi.org/10.1016/j.copsyc.2023.101781

Ribeiro, M., Yordanova, Y. N., Noblet, V., Herbet, G., & Ricard, D. (2024). White matter tracts and executive functions: a review of causal and correlation evidence. *Brain*, *147*(2), 352–371. https://doi.org/10.1093/brain/awad308

Rodrigues, E. A., Christie, G. J., Cosco, T., Farzan, F., Sixsmith, A., & Moreno, S. (2024). A subtype perspective on cognitive trajectories in healthy aging. *Brain Sciences*, *14*(4). https://doi.org/10.3390/brainsci14040351

Rodriguez-Nieto, G., Seer, C., Adab, H. Z., Jimenez-Marin, A., Chalavi, S., Rasooli, A., Cortes, J. M., Sunaert, S., & Swinnen, S. P. (2025). Efficiency of structural brain networks mediates age-associated differences in executive functioning in older adults. *Frontiers in Aging Neuroscience*, *17*, 1593868. https://doi.org/10.3389/fnagi.2025.1593868

Rolls, E. T., Feng, R., & Feng, J. (2023). Lifestyle risks associated with brain functional connectivity and structure. *Human Brain Mapping*, *44*(6), 2479–2492. https://doi.org/10.1002/hbm.26225

Rolls, E. T., & Treves, A. (2024). A theory of hippocampal function: New developments. *Progress in Neurobiology*, *238*, 102636. https://doi.org/10.1016/j.pneurobio.2024.102636

Ross, B. C. (2014). Mutual information between discrete and continuous data sets. *PLoS ONE*, *9*(2), e87357. https://doi.org/10.1371/journal.pone.0087357

Rothermund, K., Englert, C., & Gerstorf, D. (2023). Explaining variation in individual aging, its sources, and consequences: A comprehensive conceptual model of human aging. *Gerontology*, *69*(12), 1437–1447. https://doi.org/10.1159/000534324

Rousseeuw, P. J. (1987). Silhouettes: A graphical aid to the interpretation and validation of cluster analysis. *Journal of Computational and Applied Mathematics*, *20*, 53–65. https://doi.org/10.1016/0377-0427(87)90125-7

Rubinov, M., & Sporns, O. (2010). Complex network measures of brain connectivity: Uses and interpretations. *NeuroImage*, *52*(3), 1059–1069. https://doi.org/10.1016/j.neuroimage.2009.10.003

Sabia, S., Elbaz, A., Britton, A., Bell, S., Dugravot, A., Shipley, M., Kivimaki, M., & Singh-Manoux, A. (2014). Alcohol consumption and cognitive decline in early old age. *Neurology*, *82*(4), 332–339. https://doi.org/10.1212/WNL.0000000000000063

Sabia, S., Fayosse, A., Dumurgier, J., Schnitzler, A., Empana, J. P., Ebmeier, K. P., Dugravot, A., Kivimaki, M., & Singh-Manoux, A. (2019). Association of ideal cardiovascular health at age 50 with incidence of dementia: 25 year follow-up of Whitehall II cohort study. *BMJ*, *366*, l4414. https://doi.org/10.1136/bmj.l4414

Sala-Llonch, R., Bartres-Faz, D., & Junque, C. (2015). Reorganization of brain networks in aging: A review of functional connectivity studies. *Frontiers in Psychology*, *6*, 663. https://doi.org/10.3389/fpsyg.2015.00663

Salthouse, T. A. (1996). The processing-speed theory of adult age differences in cognition. *Psychological Review*, *103*(3), 403–428. https://doi.org/10.1037/0033-295x.103.3.403

Salthouse, T. A. (2004). What and when of cognitive aging. *Current Directions in Psychological Science*, *13*(4), 140–144. https://doi.org/10.1111/j.0963-7214.2004.00293.x

Salthouse, T. A. (2011). Neuroanatomical substrates of age-related cognitive decline. *Psychological Bulletin*, *137*(5), 753–784. https://doi.org/10.1037/a0023262

Salthouse, T. A. (2012). Are individual differences in rates of aging greater at older ages? *Neurobiology of Aging*, *33*(10), 2373–2381. https://doi.org/10.1016/j.neurobiolaging.2011.10.018

Sanchez-Cubillo, I., Perianez, J. A., Adrover-Roig, D., Rodriguez-Sanchez, J. M., Rios-Lago, M., Tirapu, J., & Barcelo, F. (2009). Construct validity of the Trail Making Test: Role of task-switching, working memory, inhibition/interference control, and visuomotor abilities. *Journal of the International Neuropsychological Society*, *15*(3), 438–450. https://doi.org/10.1017/S1355617709090626

Schaefer, A., Kong, R., Gordon, E. M., Laumann, T. O., Zuo, X. N., Holmes, A. J., Eickhoff, S. B., & Yeo, B. T. T. (2018). Local-global parcellation of the human cerebral cortex from intrinsic functional connectivity MRI. *Cerebral Cortex*, *28*(9), 3095–3114. https://doi.org/10.1093/cercor/bhx179

Schelling, D. (1997). Block-Tapping-Test. *Frankfurt: Swets Test Services*.

Schmermund, A., Mohlenkamp, S., Stang, A., Gronemeyer, D., Seibel, R., Hirche, H., Mann, K., Siffert, W., Lauterbach, K., Siegrist, J., Jockel, K. H., & Erbel, R. (2002). Assessment of clinically silent atherosclerotic disease and established and novel risk factors for predicting myocardial infarction and cardiac death in healthy middle-aged subjects: rationale and design of the Heinz Nixdorf RECALL Study. Risk Factors, Evaluation of Coronary Calcium and Lifestyle. *Am Heart J*, *144*(2), 212–218. https://doi.org/10.1067/mhj.2002.123579

Schmidt, K. H., & Metzler, P. (1992). Wst-Wortschatztest. *Göttingen: Beltz Test*, *16*.

Schulz, M. A., Bzdok, D., Haufe, S., Haynes, J. D., & Ritter, K. (2024). Performance reserves in brain-imaging-based phenotype prediction. *Cell Reports*, *43*(1), 113597. https://doi.org/10.1016/j.celrep.2023.113597

Schurz, M., Uddin, L. Q., Kanske, P., Lamm, C., Sallet, J., Bernhardt, B. C., Mars, R. B., & Bzdok, D. (2021). Variability in brain structure and function reflects lack of peer support. *Cerebral Cortex*, *31*(10), 4612–4627. https://doi.org/10.1093/cercor/bhab109

Shen, H. H. (2015). Core concept: Resting-state connectivity. *PNAS*, *112*(46), 14115–14116. https://doi.org/10.1073/pnas.1518785112

Slavin, R., & Smith, D. (2009). The relationship between sample sizes and effect sizes in systematic reviews in education. *Educational Evaluation and Policy Analysis*, *31*(4), 500–506. https://doi.org/10.3102/0162373709352369

Smith, D. M., Kraus, B. T., Dworetsky, A., Gordon, E. M., & Gratton, C. (2023). Brain hubs defined in the group do not overlap with regions of high inter-individual variability. *NeuroImage*, *277*, 120195. https://doi.org/10.1016/j.neuroimage.2023.120195

Smith, J. F., Pillai, A., Chen, K., & Horwitz, B. (2011). Effective connectivity modeling for fMRI: six issues and possible solutions using linear dynamic systems. *Frontiers in Systems Neuroscience*, *5*, 104. https://doi.org/10.3389/fnsys.2011.00104

Smith, R. E., Tournier, J. D., Calamante, F., & Connelly, A. (2015). SIFT2: Enabling dense quantitative assessment of brain white matter connectivity using streamlines tractography. *NeuroImage*, *119*, 338–351. https://doi.org/10.1016/j.neuroimage.2015.06.092

Smith, S. M., Elliott, L. T., Alfaro-Almagro, F., McCarthy, P., Nichols, T. E., Douaud, G., & Miller, K. L. (2020). Brain aging comprises many modes of structural and functional change with distinct genetic and biophysical associations. *eLife*, *9*, e52677. https://doi.org/10.7554/eLife.52677

Sofyan, H., Iqbal, M., Marzuki, M., & Muhammad, M. (2021). The comparison of k-modes clustering and ROCK clustering to the poverty indicator in Samadua Subdistrict, South Aceh. *IOP Conference Series: Materials Science and Engineering*, *1087*(1). https://doi.org/10.1088/1757-899x/1087/1/012085

Spreng, R. N., & Grady, C. L. (2010). Patterns of brain activity supporting autobiographical memory,

prospection, and theory of mind, and their relationship to the default mode network. *Journal of Cognitive Neuroscience*, *22*(6), 1112–1123. https://doi.org/10.1162/jocn.2009.21282

Spreng, R. N., & Turner, G. R. (2019). The shifting architecture of cognition and brain function in older adulthood. *Perspectives on Psychological Science*, *14*(4), 523–542. https://doi.org/10.1177/1745691619827511

Steffener, J., Habeck, C., O'Shea, D., Razlighi, Q., Bherer, L., & Stern, Y. (2016). Differences between chronological and brain age are related to education and self-reported physical activity. *Neurobiology of Aging*, *40*, 138–144. https://doi.org/10.1016/j.neurobiolaging.2016.01.014

Stern, Y. (2002). What is cognitive reserve? Theory and research application of the reserve concept. *Journal of the International Neuropsychological Society*, *8*(3), 448–460. https://doi.org/10.1017/S1355617702813248

Stern, Y. (2009). Cognitive reserve. *Neuropsychologia*, *47*(10), 2015–2028. https://doi.org/10.1016/j.neuropsychologia.2009.03.004

Stern, Y. (2012). Cognitive reserve in ageing and Alzheimer's disease. *The Lancet Neurology*, *11*(11), 1006–1012. https://doi.org/10.1016/S1474-4422(12)70191-6

Stern, Y., Barnes, C. A., Grady, C., Jones, R. N., & Raz, N. (2019). Brain reserve, cognitive reserve, compensation, and maintenance: operationalization, validity, and mechanisms of cognitive resilience. *Neurobiology of Aging*, *83*, 124–129. https://doi.org/10.1016/j.neurobiolaging.2019.03.022

Stoecklein, S., Hilgendorff, A., Li, M., Förster, K., Flemmer, A. W., Galiè, F., Wunderlich, S., Wang, D., Stein, S., Ehrhardt, H., Dietrich, O., Zou, Q., Zhou, S., Ertl-Wagner, B., & Liu, H. (2020). Variable functional connectivity architecture of the preterm human brain: Impact of developmental cortical expansion and maturation. *PNAS*, *117*(2), 1201–1206. https://doi.org/10.1073/pnas.1907892117

Stumme, J., Jockwitz, C., Hoffstaedter, F., Amunts, K., & Caspers, S. (2020). Functional network reorganization in older adults: Graph-theoretical analyses of age, cognition and sex. *NeuroImage*, *214*, 116756. https://doi.org/10.1016/j.neuroimage.2020.116756

Stumme, J., Kramer, C., Miller, T., Schreiber, J., Caspers, S., & Jockwitz, C. (2022). Interrelating differences in structural and functional connectivity in the older adult's brain. *Human Brain Mapping*, *43*(18), 5543–5561. https://doi.org/10.1002/hbm.26030

Sui, J., Jiang, R., Bustillo, J., & Calhoun, V. (2020). Neuroimaging-based individualized prediction of cognition and behavior for mental disorders and health: methods and promises. *Biological Psychiatry*, *88*(11), 818–828. https://doi.org/10.1016/j.biopsych.2020.02.016

Sun, L., Liang, X., Duan, D., Liu, J., Chen, Y., Wang, X., Liao, X., Xia, M., Zhao, T., & He, Y. (2022). Structural insight into the individual variability architecture of the functional brain connectome. *NeuroImage*, *259*, 119387. https://doi.org/10.1016/j.neuroimage.2022.119387

Sun, X., Liu, J., Ma, Q., Duan, J., Wang, X., Xu, Y., Xu, Z., Xu, K., Wang, F., Tang, Y., He, Y., & Xia, M. (2021). Disrupted intersubject variability architecture in functional connectomes in schizophrenia. *Schizophrenia Bulletin*, *47*(3), 837–848. https://doi.org/10.1093/schbul/sbaa155

Thovinakere, N., Ai, M., Colina, A. N. d. l., Walker, C., Baracchini, G., Tremblay-Mercier, J., Villeneuve, S., Spreng, N., & Geddes, M. R. (2024). Ventromedial frontoinsular connectivity is associated with long-term smoking behavior change in aging. *Imaging Neuroscience*, *2*, 1–20. https://doi.org/10.1162/imag_a_00142

Topiwala, A., Allan, C. L., Valkanova, V., Zsoldos, E., Filippini, N., Sexton, C., Mahmood, A., Fooks, P., Singh-Manoux, A., Mackay, C. E., Kivimaki, M., & Ebmeier, K. P. (2017). Moderate alcohol consumption as risk factor for adverse brain outcomes and cognitive decline: longitudinal cohort study. *BMJ*, *357*, j2353. https://doi.org/10.1136/bmj.j2353

Topiwala, A., Ebmeier, K. P., Maullin-Sapey, T., & Nichols, T. E. (2022). Alcohol consumption and MRI markers of brain structure and function: Cohort study of 25,378 UK Biobank participants. *NeuroImage: Clinical*, *35*, 103066. https://doi.org/10.1016/j.nicl.2022.103066

Tournier, J. D., Calamante, F., & Connelly, A. (2012). MRtrix: diffusion tractography in crossing fiber regions. *International Journal of Imaging Systems and Technology*, *22*(1), 53–66. https://doi.org/10.1002/ima.22005

Tsiakiri, A., Christidi, F., Tsiptsios, D., Vlotinou, P., Kitmeridou, S., Bebeletsi, P., Kokkotis, C., Serdari, A., Tsamakis, K., Aggelousis, N., & Vadikolias, K. (2024). Processing speed and attentional shift/mental flexibility in patients with stroke: a comprehensive review on the trail making test in stroke studies. *Neurology International*, *16*(1), 210–225. https://doi.org/10.3390/neurolint16010014

van der Velpen, I. F., Melis, R. J. F., Perry, M., Vernooij-Dassen, M. J. F., Ikram, M. A., & Vernooij, M. W. (2022). Social health is associated with structural brain changes in older adults: the Rotterdam study. *Biological Psychiatry: Cognitive Neuroscience and Neuroimaging*, *7*(7), 659–668. https://doi.org/10.1016/j.bpsc.2021.01.009

Van Horn, J. D., Grafton, S. T., & Miller, M. B. (2008). Individual variability in brain activity: A nuisance or an opportunity? *Brain Imaging and Behavior*, *2*(4), 327–334. https://doi.org/10.1007/s11682-008-9049-9

Vik, A., Hodneland, E., Haasz, J., Ystad, M., Lundervold, A. J., & Lundervold, A. (2015). Fractional anisotropy shows differential reduction in frontal-subcortical fiber bundles-a longitudinal MRI study of 76 middle-aged and older adults. *Frontiers in Aging Neuroscience*, *7*, 81. https://doi.org/10.3389/fnagi.2015.00081

Waggestad, T. H., Kirsebom, B. E., Strobel, C., Wallin, A., Eckerstrom, M., Fladby, T., & Egeland, J. (2023). Improving validity of the trail making test with alphabet support. *Frontiers in Psychology*, *14*, 1227578. https://doi.org/10.3389/fpsyg.2023.1227578

Wallace, J. E., Krauter, E. E., & Campbell, B. A. (1980). Motor and reflexive behavior in the aging rat. *Journal of Gerontology*, *35*(3), 364–370.

Wang, R., Liu, M., Cheng, X., Wu, Y., Hildebrandt, A., & Zhou, C. (2021). Segregation, integration, and balance of large-scale resting brain networks configure different cognitive abilities. *PNAS*, *118*(23). https://doi.org/10.1073/pnas.2022288118

Wang, Y., Rheault, F., Schilling, K. G., Beason-Held, L. L., Shafer, A. T., Resnick, S. M., & Landman, B. A. (2022). Longitudinal changes of connectomes and graph theory measures in aging. *Proceedings of SPIE--the International Society for Optical Engineering*, *12032*. https://doi.org/10.1117/12.2611845

Wani, A. A. (2025). Comprehensive review of dimensionality reduction algorithms: Challenges, limitations, and innovative solutions. *PeerJ Computer Science*, *11*, e3025. https://doi.org/10.7717/peerj-cs.3025

West, R. L. (1996). An application of prefrontal cortex function theory to cognitive aging. *Psychological Bulletin*, *120*(2), 272.

Whalley, L. J., Deary, I. J., Appleton, C. L., & Starr, J. M. (2004). Cognitive reserve and the neurobiology of cognitive aging. *Ageing Research Reviews*, *3*(4), 369–382. https://doi.org/10.1016/j.arr.2004.05.001

Whitsel, N., Reynolds, C. A., Buchholz, E. J., Pahlen, S., Pearce, R. C., Hatton, S. N., Elman, J. A., Gillespie, N. A., Gustavson, D. E., Puckett, O. K., Dale, A. M., Eyler, L. T., Fennema-Notestine, C., Hagler, D. J., Jr., Hauger, R. L., McEvoy, L. K., McKenzie, R., Neale, M. C., Panizzon, M. S., …Franz, C. E. (2022). Long-term associations of cigarette smoking in early mid-life with predicted brain aging from mid- to late life. *Addiction*, *117*(4), 1049–1059. https://doi.org/10.1111/add.15710

Wig, G. S. (2017). Segregated systems of human brain networks. *Trends in Cognitive Sciences*, *21*(12), 981–996. https://doi.org/10.1016/j.tics.2017.09.006

Wise, T., Marwood, L., Perkins, A. M., Herane-Vives, A., Joules, R., Lythgoe, D. J., Luh, W. M., Williams, S. C. R., Young, A. H., Cleare, A. J., & Arnone, D. (2017). Instability of default mode network connectivity in major depression: A two-sample confirmation study. *Transl Psychiatry*, *7*(4), e1105. https://doi.org/10.1038/tp.2017.40

Wu, J., Li, J., Eickhoff, S. B., Scheinost, D., & Genon, S. (2023). The challenges and prospects of brain-based prediction of behaviour. *Nature Human Behaviour*, *7*(8), 1255–1264. https://doi.org/10.1038/s41562-023-01670-1

Xia, H., He, Q., & Chen, A. (2022). Understanding cognitive control in aging: a brain network perspective. *Frontiers in Aging Neuroscience*, *14*, 1038756. https://doi.org/10.3389/fnagi.2022.1038756

Xia, H., Hou, Y., Li, Q., & Chen, A. (2024). A meta-analysis of cognitive flexibility in aging: Perspective from functional network and lateralization. *Human Brain Mapping*, *45*(14), e70031. https://doi.org/10.1002/hbm.70031

Xiao, Y., Lin, Y., Ma, J., Qian, J., Ke, Z., Li, L., Yi, Y., Zhang, J., Cam, C. A. N., & Dai, Z. (2021). Predicting visual working memory with multimodal magnetic resonance imaging. *Human Brain Mapping*, *42*(5), 1446–1462. https://doi.org/10.1002/hbm.25305

Xu, T., Sturgeon, D., Ramirez, J. S. B., Froudist-Walsh, S., Margulies, D. S., Schroeder, C. E., Fair, D. A., & Milham, M. P. (2019). Interindividual variability of functional connectivity in awake and anesthetized rhesus macaque monkeys. *Biological Psychiatry: Cognitive Neuroscience and Neuroimaging*, *4*(6), 543–553. https://doi.org/10.1016/j.bpsc.2019.02.005

Xu, Y., Cao, M., Liao, X., Xia, M., Wang, X., Jeon, T., Ouyang, M., Chalak, L., Rollins, N., Huang, H., & He, Y. (2019). Development and emergence of individual variability in the functional connectivity architecture of the preterm human brain. *Cerebral Cortex*, *29*(10), 4208–4222. https://doi.org/10.1093/cercor/bhy302

Yang, H., Wu, G., Li, Y., Xu, X., Cong, J., Xu, H., Ma, Y., Li, Y., Chen, R., Pines, A., Xu, T., Sydnor, V. J., Satterthwaite, T. D., & Cui, Z. (2025). Connectional axis of individual functional variability: Patterns, structural correlates, and relevance for development and cognition. *PNAS*, *122*(12), e2420228122. https://doi.org/10.1073/pnas.2420228122

Yarkoni, T., & Westfall, J. (2017). Choosing prediction over explanation in psychology: Lessons from machine learning. *Perspectives on Psychological Science*, *12*(6), 1100–1122. https://doi.org/10.1177/1745691617693393

Yeo, B. T., Krienen, F. M., Sepulcre, J., Sabuncu, M. R., Lashkari, D., Hollinshead, M., Roffman, J. L., Smoller, J. W., Zollei, L., Polimeni, J. R., Fischl, B., Liu, H., & Buckner, R. L. (2011). The organization of the human cerebral cortex estimated by intrinsic functional connectivity. *Journal of Neurophysiology*, *106*(3), 1125–1165. https://doi.org/10.1152/jn.00338.2011

Yu, J., Rawtaer, I., Fam, J., Feng, L., Kua, E. H., & Mahendran, R. (2020). The individualized prediction of cognitive test scores in mild cognitive impairment using structural and functional connectivity features. *Neuroimage*, *223*, 117310. https://doi.org/10.1016/j.neuroimage.2020.117310

Zalesky, A., Fornito, A., & Bullmore, E. (2012). On the use of correlation as a measure of network connectivity. *NeuroImage*, *60*(4), 2096–2106. https://doi.org/10.1016/j.neuroimage.2012.02.001

Zhang, F., Daducci, A., He, Y., Schiavi, S., Seguin, C., Smith, R. E., Yeh, C. H., Zhao, T., & O'Donnell, L. J. (2022). Quantitative mapping of the brain's structural connectivity using diffusion MRI tractography: A review. *NeuroImage*, *249*, 118870. https://doi.org/10.1016/j.neuroimage.2021.118870

Zhang, H., Lee, A., & Qiu, A. (2017). A posterior-to-anterior shift of brain functional dynamics in aging. *Brain Structure and Function*, *222*(8), 3665–3676. https://doi.org/10.1007/s00429-017-1425-z

Zhang, M., Moebus, S., Dragano, N., Bittner, N., & Caspers, S. (2025). Linking individual variability of multi-

modal connectivity, lifestyle, psycho-social factors and cognition in older adults. *aging and disease*, *17*(5). https://doi.org/10.14336/AD.2025.0428

Zhao, T., Cao, M., Niu, H., Zuo, X. N., Evans, A., He, Y., Dong, Q., & Shu, N. (2015). Age-related changes in the topological organization of the white matter structural connectome across the human lifespan. *Human Brain Mapping*, *36*(10), 3777–3792. https://doi.org/10.1002/hbm.22877

Zhu, J., & Qiu, A. (2022). Interindividual variability in functional connectivity discovers differential development of cognition and transdiagnostic dimensions of psychopathology in youth. *NeuroImage*, *260*, 119482. https://doi.org/10.1016/j.neuroimage.2022.119482

Zijlmans, J. L., Lamballais, S., Vernooij, M. W., Ikram, M. A., & Luik, A. I. (2022). Sociodemographic, lifestyle, physical, and psychosocial determinants of cognitive reserve. *Journal of Alzheimer's Disease*, *85*(2), 701–713. https://doi.org/10.3233/JAD-215122

Zvonarev, V., Mamtani, S., Yadav, S., Sharazi, K., Syed, H., Giri, A., Rodas, A., Tregubenko, P., & Kotler, D. (2020). Neurocognitive performance of African Americans and Hispanic adults in relation to diet and physical activity: A literature review. *Journal of Neurology Research*, *10*(3), 56–68. https://doi.org/10.14740/jnr594

List of Publications

Paper

Zhang, M., Moebus, S., Dragano, N., Bittner, N., & Caspers, S. (2025). Linking individual variability of multi-modal connectivity, lifestyle, psycho-social factors and cognition in older adults. *Aging and Disease, 17*(5). https://doi.org/10.14336/AD.2025.0428.

Poster

Zhang, M., et al. (2025). *Leveraging lifestyle clusters and multimodal brain features to enhance cognitive prediction models in healthy older adults***.** 8th International Conference on Aging & Cognition (EUCAS), University of Pavia, Italy.

Zhang, M., et al. (2024). *Linking individual variability in multi-modal connectivity, lifestyles, and cognition in older adults*. Poster presented at the Society for Neuroscience Annual Meeting, Chicago, USA.

Acknowledgements

I would like to express my sincere gratitude to my supervisor, **Prof. Dr. Dr. Svenja Caspers**, for giving me the opportunity to pursue my doctoral research in her group and for proposing a challenging and inspiring dissertation topic. Throughout my doctoral studies, I have greatly benefited from her continuous support, insightful comments, and critical feedback. Her guidance and encouragement have shaped both the scientific quality of this work and my development as an independent researcher. I am also grateful for the opportunities she provided to participate in international conferences and advanced training programs, which broadened my perspective and enriched my scientific experience.

My deepest appreciation goes to **Dr. rer. nat. Nora Bittner** for her exceptional supervision and unwavering support throughout my doctoral journey. Her thoughtful guidance in addressing scientific questions, methodological challenges, and statistical analyses was invaluable for this dissertation. Beyond her academic mentorship, her kindness, patience, and encouragement meant a great deal to me during my time as an international student far from home. Her support helped me navigate not only the scientific complexities of this work but also the personal challenges that inevitably accompany such a journey.

I would also like to thank **Prof. Dr. Nico Dragano** and **Prof. Dr. Susanne Moebus** for their valuable support, helpful comments, and suggestions throughout this work.

Many colleagues have contributed to this work in different ways, and I am sincerely grateful for their help. In particular, I thank Dr. Paulo R. Dellani for his technical support with the JURECA supercomputer and MRI preprocessing, Dr. Johanna Stumme for her early work on fMRI preprocessing, Dr. Camilla Mendl-Heinisch and Tatiana Miller for their guidance in machine learning and clustering methods, and Dr. Christiane Jockwitz for providing cognitive data and valuable suggestions. I also thank all members of the Connectivity Group for creating a warm and inclusive academic environment and for many fruitful discussions, including, among others, **Dr. Christiane Jockwitz, Dr. Katharina Peitz, Natalia Zhukova, Yuanyuan Yang, Tatiana Miller, and Daniel Kröz**. My thanks also go to colleagues at the Institute of Neuroscience and Medicine (INM-1) for contributing to a supportive and inspiring research environment.

I am also grateful to all those in Germany who have helped me along the way, even though I cannot name everyone individually.

This research was conducted within the framework of the 1000BRAINS study at Forschungszentrum Jülich. I gratefully acknowledge the Heinz Nixdorf Foundation, the EBRAINS 2.0 project, and JARA for their generous support, as well as the Jülich Supercomputing Centre for providing the computing resources that made this work possible.

I sincerely thank the China Scholarship Council for supporting my doctoral studies. I feel fortunate to have had the opportunity to take part in an international academic community, and even more fortunate to have met such inspiring mentors, colleagues, and friends during my time in Germany.

Finally, I am deeply grateful to my friends and family in Germany and China. Your encouragement, patience, and unwavering belief in me have accompanied me throughout this journey.

Time seems to have passed both quickly and slowly during these years. A few years are hardly enough to fully understand a research question, and the more I learned, the more I realized how much remains unknown. There were moments of doubt and uncertainty along the way, yet they were also part of the process of learning and discovery. Looking back on these years, I can only hope that I have done the best I could. Above all, I hope that these efforts may eventually contribute, even in a small way, to our understanding of cognitive aging.

Erklärung zur Datenaufbewahrung

Erklärung § 5 Abs. 1 zur Datenaufbewahrung

Hiermit erkläre ich, dass die dieser Dissertation zu Grunde liegenden Originaldaten in dem **Institut für Neurowissenschaft und Medizin -1 des Forschungszentrums Jülich**

hinterlegt sind.

Mingxian Zhang